The use of stable isotopes to assess the controls on pelagic carbon basal resources in Canadian Shield lakes

by

Emily Josephine Barber

A thesis
presented to the University of Waterloo
in fulfillment of the
thesis requirement for the degree of

Master of Science
in
Earth Sciences (Water)

Waterloo, Ontario, Canada, 2021

Author's Declaration

I hereby declare that I am the sole author of this thesis. This is a true copy of the thesis, including any required final revisions, as accepted by my examiners.

I understand that my thesis may be made electronically available to the public.

Abstract

Freshwater lakes are often natural sources of greenhouse gases (GHGs) such as carbon dioxide (CO_2) and methane (CH_4) to the atmosphere, and therefore it is important to examine carbon and nutrient cycling in these complex ecosystems. Stable isotopes of carbon, nitrogen, and hydrogen are incredibly useful tools for providing information on lake processes. The overarching objective of this thesis is to use stable isotopes to examine how carbon, in its many forms, is partitioned between the atmosphere, sediments, and the pelagic zone of small, oligotrophic, Canadian Shield lakes.

Lakes receive large external, terrestrial inputs of organic matter (OM). These OM inputs alter and change the physical and chemical parameters of lakes and exist in both the dissolved (DOC) and particulate (POM) forms. In order to examine the ways in which OM inputs can affect lake ecosystems, I took monthly samples during the ice-free season of a suite of stable isotope and biogeochemical parameters in a series of nine lakes along DOC gradient. The DOC gradient represents varying inputs of terrestrial OM. There is seasonality in terms of DIC concentrations, pCO_2 values, and δ^{13}C-DIC values, across the DOC gradient. Across the suite of lakes, higher DOC concentrations show more negative δ^{13}C-DIC values. This may indicate that in lakes with higher inputs of terrestrial OM that these inputs exert control over the values of δ^{13}C-DIC and δ^{13}C-CO_2, and therefore lake POM and surficial sediments.

Terrestrial OM can also control the relationships between DOC, DIC, POM, and lake sediments. I examined the terrestrial contamination of POM using two different methods. I first corrected for the terrestrial fraction of POM using C:N ratios and estimated δ^{13}C and δ^{15}N values for phytoplankton. Bulk, uncorrected δ^{13}C and δ^{15}N-POM values are more positive than values corrected using this method. I also physically size separated POM. For each method, two different terrestrial end members were used- DOC and terrestrial vegetation. No significant differences were found between size fractions. However, in terms of C:N ratios, the C:N ratio of the $10<x<20$ μm fraction was significantly higher (one-way ANOVA, $p= 1.62 \times 10^{-5}$, $F= 13.99$) than the other size fractions, perhaps due to a higher number of terrestrial particles falling into the size range.

There can be confounding issues when using δ^{13}C values to parse allochthonous and autochthonous sources in lake ecosystems due to seasonal changes in pH, DIC

concentration, shifts in phytoplankton species composition, and the carbon species used in photosynthesis (CO_2, HCO_3^-). It can be advantageous to use additional isotopes, such as stable hydrogen isotopes (δ^2H). I measured δ^2H-DOM values in a subset of six lakes and four headwater boreal streams. DOM in both streams and lakes does not reflect the autochthonous OM but is also substantially modified from terrestrial vegetation. Therefore, there are ultimately issues with this approach as neither terrestrial endmember is accurately represented by δ^2H-DOM values.

I also used stable carbon and hydrogen isotopes to examine dissolved CH_4 in boreal lakes. Most lake studies measure $\delta^{13}C$-CH_4 alone, and in those that do measure δ^2H-CH_4, the values are much different from the small, soft water, oligotrophic lakes studied in this thesis. I took samples of $\delta^{13}C$-CH_4 and δ^2H-CH_4 throughout the water column in fourteen different lakes. These values show that lake CH_4 above the thermocline does not originate from the atmosphere. The sampled CH_4 does not clearly fall into the suggested diagnostic ranges for either methanogenesis pathway, and is isotopically different from literature values. The range in hypolimnion CH_4 isotopic values was found to be much more constrained compared to epilimnion values, particularly in terms of δ^2H-CH_4 values. Therefore, there is a need for further research on other CH_4 processes, such as anaerobic CH_4 oxidation.

The data presented in this thesis demonstrates the complex nature of the lake carbon cycle. There is a need to better define terrestrial endmembers, and current methods may not be sufficient to determine allochthonous and autochthonous OM inputs. Further, isotopic values of CH_4 illustrate the need for further investigation of lake CH_4 dynamics.

Acknowledgements

I would like to thank Dr. Scott Higgins, Dr. Thai Phan, Dr. Jason Venkiteswaran, and Dr. Sherry Schiff for being on my committee and for all of their invaluable and thoughtful feedback on my research.

This thesis would not have been possible without the mentorship and guidance of my supervisor, Dr. Sherry Schiff. I am forever grateful for the amazing opportunities presented me throughout my time at the Environmental Geochemistry Laboratory, and I am so appreciative of Sherry's advice and patience. Sherry pushed me to excel and allowed me to realize my full potential as a scientist.

Thank you to Dr. Jason Venkiteswaran, for always being available for a tea and a chat, whether it was about science, life, or sometimes both. To Richard Elgood, for the incredible laboratory, logistical, technical, scientific, and emotional support provided throughout this degree. Without Jason and Richard's time and encouragement, this thesis would not have been completed.

Thank you to Rachel Henderson, for going on this journey of stable carbon isotopes with me. Whether in the field or in the lab, Rachel is so knowledgeable, and has taught me so much. She has made me not only a better scientist, but also a better person. To Jordyn Atkins, for continuously being there for me, her GIS expertise and assistance, for making sure I always have a manicure, and for pushing me to be the best that I can be. Without Rachel and Jordyn's constant support and friendship this thesis would not have been possible. Thank you to Puru Shah, for always being willing to grab a coffee and for digging through freezers on countless occasions. Having you three as friends and lab mates throughout our time as master's students was a true joy.

Thank you to Jenn Mead for showing me the ropes at the Environmental Geochemistry Lab and for always letting me cry in the office, either from laughing or from stress, or sometimes both at the same time. Thank you to Sarah Sine, for keeping me caffeinated, for all of your help with DOC data, for being a great field partner and an even better friend. There is no one else I would rather laugh and eat field lunch in the pouring rain with. Thank you to Eric McQuay, for your help in the lab and for brightening my mornings with our daily coffee runs, it was much needed, and much appreciated.

I am privileged to have met so many people throughout my time in grad school who generously took the time to assist me. Firstly, thank you to Dr. Megan Larsen and Dr. Kateri Salk for teaching the ins and outs of programming in R. Thank you to Dr.

Jackson Tsuji, for talking all things methane with me, and for editing my thesis proposal. Thank you to Dr. Pieter Aukes for his kind, constructive, and meticulous edits on my methane chapter. As well, thank you to Bill Mark and Rhys Gwynne of the Environmental Isotope Lab for analyzing my numerous samples and answering all of my questions about data.

A special thank you to everyone who makes our research group so great: Paul Dainard, Dr. Ryan Hutchins, Jeremy Leathers, Kai Liu, and Mackenzie Schultz. I am also incredibly thankful for the hard work of the Environmental Geochemistry Laboratory's co-op students- Thomas Cornell, Bethany Gruber, Kimberley Tran, Emma Jewett, Phillip Wright, Matthew Soares-Paquin, Holden Little, and Aaron Spoelstra.

I was fortunate enough to have the chance to conduct my field work at the International Institute for Sustainable Development Experimental Lakes Area (IISD-ELA). I am so thankful for all of the amazing staff and students that helped me along the way.

I have such amazing friends and a great support system in Matt Abramson, Fatema Adamji, Tali Barclay, Julia Bergevin, Bryce Claughton, Maankrit Dua, Shaumi Kulendran, Angie Le Chat, Melissa Mark, Steph Mirtisch, and Kaitlin Thompson. Friends are truly one's chosen family. Thank you for cheering me on countless times throughout this degree.

Thank you to my André E. Lalonde AMS Lab supervisors Carley Crann and Sarah Murseli for turning a nervous undergraduate student into a competent lab technician, for providing me with the scientific skills I needed to dive head first into this degree, for their mentorship throughout the past several years, and for their support in the completion of this thesis.

I would also like to thank my wonderful in-laws, Doug and Heather Allen for graciously allowing me to take over their kitchen island with my writing setup for several months. Thank you for all of your love, patience, and kindness.

Thank you to my mom and dad, Linda and Bill Barber, for fostering my love of the outdoors and the Canadian Shield. You provided me with everything I needed to succeed throughout my education-from my passion for reading and writing to boat driving. I am so grateful for all of your love and support. To my sister, Sophie, thank you for being my person. I am so lucky to have a sister and a best friend all in one.

To my wonderful fiancé Michael, for believing in me even when I didn't believe in myself. What a whirlwind three years it has been. Whether it was across an ocean, across the country, or across the kitchen table, you were always there for me. I can't wait to see what is next for us. I love you.

Table of Contents

List of Figures

List of Tables

List of Equations

Chapter 1. Introduction

1.1 Carbon Cycle

Carbon is an essential element to all life on earth. The global carbon cycle characterizes the exchange of carbon through the atmosphere, ocean, and terrestrial environment (Cole et al. 2007). Carbon dioxide (CO_2) and methane (CH_4) are naturally produced through both abiotic and biotic reactions. However, due to anthropogenic disturbances such as combustion of fossil fuels and land use change, there has been drastic increases in both CO_2 and CH_4 over the last 200 years (Dlugokencky et al. 1994, Falkowski et al. 2000). Atmospheric concentrations of CO_2 are currently greater than 400 ppm, far above pre-industrial revolution concentrations of 280 ppm (National Oceanic and Atmospheric Administration 2019a). CH_4 concentrations have risen from 0.72 ppm to 1.86 ppm today (Intergovernmental Panel on Climate Change 2014, National Oceanic and Atmospheric Administration 2019b). As climate change continues to alter global carbon dynamics, there is a need for investigation of how these changes will affect the environment.

In addition to the aforementioned major global carbon reservoirs, inland freshwaters also play a significant role in the global carbon cycle (Cole et al. 2007, Battin et al. 2009, Tranvik et al. 2009). It has been estimated that at a minimum 1.9 Pg C y^{-1} is transferred from land to freshwater (Cole et al. 2007). This carbon flux cannot be ignored; therefore, freshwaters need to be considered a major source in the global carbon cycle.

The world's surface area consists of approximately 1 % freshwater. Freshwater occupies about 9 % of Canada's total area (Natural Resources Canada 2005, Battin et al. 2009). Canada's vast water resources therefore play a significant role in the global carbon cycle.

This thesis will focus on small Canadian shield lakes. Small lakes are innumerable on the Canadian shield and physically and biogeochemically differ from large lakes (Downing 2010). Globally, these small but mighty ecosystems are essential for biogeochemical cycling and are key players in the carbon cycle, despite their size (Cole et al. 2007, Read and Rose 2013).

1.2 Aquatic carbon

1.2.1 Organic matter and dissolved organic carbon

Organic matter (OM) greatly influences lake metabolism (De Kluijver et al. 2014). Lakes receive OM inputs from their terrestrial surroundings, profoundly affecting these freshwater ecosystems. OM is a driver of ecosystem function and exists in both particulate and dissolved fractions (Cole et al. 2006, Bartels et al. 2012). Inputs of OM from terrestrial systems can change the function of lakes by darkening or "browning" water (Craig et al. 2017) and subsidize food webs by providing nutrients to the system (Cole et al. 2006). When OM inputs are altered, lakes are susceptible to both physical and chemical changes, such as changes in the depth of the mixed layer, temperature, and light penetration. These changes result in fundamental alterations in lakes, therefore affecting not only aquatic ecosystems as a whole, but also aquatic organisms and biogeochemical cycles (Steinberg et al. 2006)

OM inputs are controlled by catchment hydrology, wetland area, and soil characteristics (Findlay and Sinsabaugh 2003). The drainage ratio of a lake has been shown to have a positive relationship with lake colour in boreal lakes (i.e. terrestrial OM input) (Schindler 1971, Rasmussen et al. 1989), illustrating that water residence time and catchment characteristics are key controls on OM in lakes.

Terrestrial OM originates from plant tissues and is processed by soil microbes before entering lakes (Solomon et al. 2015). Due to the variations in its original material and soil conditions during processing, OM consists of numerous and diverse compounds and is difficult to concisely define (Solomon et al. 2015). Forms of OM are commonly defined by filtration through a 0.45 μm filter (Evans et al. 2005). In the filtration process, the filtrate is the dissolved fraction of OM (DOM), whereas the solid material collected on the filter is the particulate organic matter (POM) (Kennedy et al. 1974, Danielsson 1982, Liu et al. 2007, Mostofa et al. 2009). Typically, DOC is the element of DOM that is measured (Evans et al. 2005, Solomon et al. 2015). It is composed of complex organic molecules with a large range in molecular weights, ranging from less than 100 Daltons to greater than 300,000 Daltons (Thurman 1985). These complex compounds attenuate UV-A, UV-B, and visible light leading to brown or tea-coloured water (Jones 1992, Solomon et al. 2015). Thus, lakes with higher OM concentrations have increased light attenuation (Stubbins et al. 2014), which provides less water volume for photosynthesis to take place (Solomon et al. 2015, Creed et al. 2018). Lakes with higher concentrations of terrestrial

OM have different thermal structures than lakes with lower concentrations, because light does not penetrate as deeply into the water column (Solomon et al. 2015). This prevents hypolimnion waters from increasing in temperature (Creed et al. 2018).

In addition to terrestrial inputs of OM, OM is derived from in-lake primary production. The production of autochthonous OM occurs through photosynthesis, and can be conducted by phytoplankton communities, macrophytes, or periphyton communities at the base of aquatic food webs (Likens 1975, Rantakari and Kortelainen 2008). POM can be used as a proxy to represent autochthonous OM (algae) (Gu et al. 2011). Allochthonous OM inputs have also been shown to be important for nutrient and energy flow (Cole et al. 2011, Bartels et al. 2012, Karlsson et al. 2012, Tanentzap et al. 2017). The concentration of DOM in boreal lake systems is one determinant of productivity (Solomon et al. 2015).

1.2.2 Dissolved inorganic carbon

The main forms of dissolved inorganic carbon (DIC) in small Canadian shield lakes are CO_2, bicarbonate (HCO_3^-), and carbonate (CO_3^{2-}) **(Equation 1.1.1).** The dominant form of DIC depends on lake pH values, lake temperature, and lake pressure **(Figure 1.2).**

Equation 1.1 $$[DIC]= [CO_2] + [HCO_3^-] + [CO_3^{2-}]$$

The main sources of DIC to freshwaters are diffusion from the atmosphere ($CO_{2\,(g)}$) and carbonate minerals (Wetzel 2001a, Cole 2013a). However, the Canadian shield is widely composed of metamorphosed granite and as such does not have high amounts of calcium carbonate minerals (Renwick 2009). This low calcium content leads to the Canadian shield's characteristic softwater, oligotrophic lakes (Renwick 2009). Thus, carbonate minerals are not a significant source of DIC to Canadian shield lakes. Many processes in the aquatic carbon cycle transform DIC **(Figure 1.1).** For instance, DIC can be formed through photodegradation of DOC (Mostofa et al. 2013). DIC can also be transformed to POC or DOC via photosynthesis, respiration, and degradation (Herczeg 1987).

1.2.3 Sediments

Sediments are a critical component of the lake carbon cycle. Lakes emit greenhouse gases (GHGs), such as CH_4 and CO_2, to the atmosphere. These GHGs are cycled back into the biosphere on a relatively short time scale (Mendonça et al. 2017). In comparison, through sequestration, a significant amount of carbon (approximately 0.6 Pg C yr^{-1}) is stored in lake sediments (Battin et al. 2009, Tranvik et al. 2009). The carbon captured in lake sediments is effectively removed from this shorter atmospheric cycle, and while stored in sediments becomes a part of the carbon cycle at geological time scales (Kortelainen et al. 2004, Mendonça et al. 2017). In this way, lake sediments act as a significant carbon sink.

Once OM reaches lake sediments, it has one of two fates. It can be utilized by microbes and mineralized to CO_2 or CH_4, or it can be buried (Sobek et al. 2009, Chmiel et al. 2016). Thus, lake sediments do not only store carbon, but also contribute to lake metabolism (Guillemette et al. 2017). One factor that influences the fate of OM is its origin (allochthonous or autochthonous). Allochthonous OM inputs represent the main source of OM to lake sediments (Meyers and Ishiwatari 1993, Guillemette et al. 2017). This is likely because autochthonous OM is more readily metabolized by microbes (Wetzel 1995), In lakes with higher terrestrial OM inputs (i.e. a higher DOC concentration), there will be a greater proportion of terrestrial carbon captured in sediments (Mendonça et al. 2017).

1.2.4 Methane

CH_4, a powerful GHG, is a key form of carbon in both global and lake carbon cycles. Lakes are a natural source of CH_4 to the atmosphere, contributing 6-16 % of all natural CH_4 emissions (Borrel et al. 2011). CH_4 production, or methanogenesis, in lakes is mediated by anoxia, temperature, and type of substrate (Rudd and Hamilton 1978, Strayer and Tiedje 1978, Liikanen et al. 2003).

Methanogenesis takes place in anoxic waters and is a process by which organic matter is decomposed (Grey 2016). It was previously thought that methanogenesis and methanotrophy (CH_4 consumption) did not play a significant role in the carbon cycle (Grey 2016). However, research has shown that CH_4 can be a carbon source in lakes for both planktonic and benthic organisms (Deines et al. 2009). Through CH_4 production and consumption, CH_4 can support lacustrine food webs (Cole 2013b), and has been produced

both in the oxic water column of lakes (Bogard et al. 2014) and under oxic laboratory conditions in several cyanobacteria strains (Bižić et al. 2020). CH_4 and carbon derived from CH_4 present an important link between the pelagic zone, benthic zone, and lake sediments (Deines et al. 2009, Bogard et al. 2014, Grey 2016).

1.3 Food webs and basal resources

A food web is a representation of the transfer of energy and nutrients among trophic levels (Lindeman 1942). Food webs are a key concept in ecology, and are highly complex due to the spatial variability of their components: nutrients, detritus, and organisms (Polis et al. 1997) (**Figure 1.3)**. Primary producers, or photoautotrophs, fix CO_2 to produce complex organic molecules via photosynthesis (Lindeman 1942). This primary production in ecosystems provides nutrients to organisms at higher trophic levels (Post 2002). The base of the food web (i.e. basal resources) can be defined as the combined primary production in a system and is where organisms acquire their nutrients (Post 2002, Karlsson et al. 2012). In order to understand organisms at higher trophic levels, like fishes, there is a need to understand the processes at the base of the food web.

In addition to photosynthesis producing autochthonous carbon, terrestrial organic matter inputs in the form of DOC also play an important role in lake food webs. This is because in most lakes, respiration exceeds primary production, meaning that they are net heterotrophic (del Giorgio and Williams 2007). Heterotrophic microbes are able to use allochthonous carbon as an energy source (Guillemette et al. 2016). Bacterial respiration of allochthonous carbon could act as a "dead end" for this carbon due to the fact that it becomes part of the microbial loop, and thus does not reach organisms at higher trophic levels (Tranvik 1992). While this respired allochthonous carbon may not be incorporated into the food web by higher consumers, microbes are able to use it as a carbon source, thus allochthonous carbon can support heterotrophic production in lakes.

DOC also affects food webs due to its physical properties. As previously discussed, dark, tea-coloured lakes attenuates both visible and ultraviolet radiation differently than clear water lakes and as such less photosynthetically active radiation (PAR) can penetrate the water column (Jones 1992, Schindler et al. 1997). Due to this, DOC is a key control on primary production (Karlsson et al. 2009). Changes in the amount of photosynthesis occurring in a lake affect the food web because if less photosynthesis is taking place, less autochthonous OM will be produced, affecting the food web.

Since DOC absorbs visible and ultraviolet radiation, this can change the vertical thermal structure of the water column (Fee et al. 1996). Light is extinguished at shallower depths in high DOC lakes, leading to shallower thermocline depths (Solomon et al. 2015). This stratification is often quite stable (Read and Rose 2013, Palmer et al. 2014), reducing the degree to which vertical mixing can occur (Imberger 1998, MacIntyre et al. 2006). Changes in light and heat penetration affect food webs further due to changes in availability of suitable habitat (Solomon et al. 2015).

1.4 International Institute for Sustainable Development Experimental Lakes Area

The International Institute for Sustainable Development Experimental Lakes Area (IISD-ELA) is located in southeast of Kenora in Northwestern Ontario (49°400 N 93°450 W), Canada on the Canadian Shield. IISD-ELA is an ideal location to investigate the role of the base of the food web on the lake carbon cycle. Aquatic research at IISD-ELA allows for the study of scientific questions at a whole ecosystem level without the limitations of laboratory studies (Johnson and Vallentyne 1971).

The climate at IISD-ELA is continental, with a mean annual air temperature of 2.2°C and mean annual precipitation of 689 mm (McCullough and Campbell 1993). Soils are topped with *Sphagnum* or *Polytrichum* moss species (Venkiteswaran 2008). While *Sphagnum* moss can reach depths greater than 0.5 m in low relief areas, rocky uplands are often bare, with exposed granite bedrock or forested islands (Schindler et al. 1996, Lamontagne et al. 2000). Wetlands are typically ombrotrophic bogs or fens containing peat which can be more than 10 m deep (Schindler et al. 1996). Typical vegetation includes Labrador tea (*Ledum groenlandicum*), leather leaf (*Chamaedaphne calyculata*), jack pine (*Pinus banskiana*), trembling aspen (*Populus tremuloides*), white birch (*Betula papyrifera*), black spruce (*Picea mariana*), balsam fir (*Abies balsamea*), and red pine (*Pinus resinosa*) (Mead 2017). Refer to Brunskill and Schindler (1971) for more information regarding the geography of IISD-ELA.

This project is part of a larger study at IISD-ELA called Photons to Fish (PHISH). The PHISH project is aimed at determining drivers of fish productivity. In order to understand what controls fish productivity in ecosystems, it is imperative to understand the base of the food web supporting higher consumers.

1.5 Stable isotope analysis

Stable isotopes are a powerful tool used to trace ecosystem processes. An isotope is an atom of an element with a different number of neutrons but the same number of protons. For example, stable isotopes of carbon, nitrogen, and hydrogen are ^{12}C, ^{13}C, ^{14}N, ^{15}N, ^{1}H, and ^{2}H **(Table 1.1)**.

These differences in atomic mass cause changes in the vibrational energy of the nucleus, therefore affecting both bond strength and reaction rate (Sulzman 2020). Due to this, two isotopes of the same element are quantitatively different and therefore are in different pools, or molecules, during chemical reactions (Sulzman 2020).

Rates of reactions are different for each isotope, and variations in the ratio between heavy and light isotopes (e.g. $^{2}H/^{1}H$) result in isotope effects, or fractionation (Farquhar et al. 1989). Typically, the lighter and more abundant isotope (^{12}C, ^{14}N, ^{1}H) is favoured during reactions. An isotopic ratio mass spectrometer (IRMS) measures the isotopic ratio of a sample. This ratio is reported relative to a standard in delta (δ) notation in permil units (‰) **(Equation 1.2).**

Equation 1.2

$$\delta = \left[\frac{R_{sample}}{R_{standard}} - 1\right]$$

These slight, naturally occurring differences in stable isotope ratios from fractionation can be measured and used in both biogeochemical and ecological applications (Middelburg 2014). For instance, carbon and nitrogen stable isotopes ($\delta^{13}C$ and $\delta^{15}N$) are used widely in food web studies to trace feeding and energy flow pathways ($\delta^{13}C$; Perkins et al. 2014) and to determine the trophic position of organisms ($\delta^{15}N$; Post 2002). This is because an organism's diet is reflected in its isotopic ratio (DeNiro and Epstein 1978, 1981).

However, in order to interpret stable isotope values in food web studies, it is imperative to accurately measure the isotopic values of the base of the food web (Woodland et al. 2012). Information regarding an organism's trophic level or carbon source cannot be gained by solely measuring its $\delta^{13}C$ and $\delta^{15}N$ values (Post 2002), due to seasonal fluctuations in the $\delta^{13}C$ and $\delta^{15}N$ values of basal resources (Zohary et al. 1994, Cabana and Rasmussen 1996). Therefore, without the context provided by baseline

isotopic values, any variation in $\delta^{13}C$ and $\delta^{15}N$ values of consumers cannot be distinguished between temporal changes in the $\delta^{13}C$ and $\delta^{15}N$ values of the base of the food web or changes in trophic level and carbon source (Post 2002). The stable isotopic values at the base of the food web incorporate the isotopic values of various carbon sources, and these values are transferred up the food web **(Figure 1.4)**.

Using additional isotopes alongside $\delta^{13}C$ and $\delta^{15}N$ can further explain food web processes and dynamics in aquatic ecosystems. For instance, stable hydrogen isotopes ($\delta^{2}H$) provide information regarding allochthonous versus autochthonous energy sources (Doucett et al. 2007, Karlsson et al. 2012), methanogenesis pathways (Whiticar 1999), and CH_4 subsidies in food webs (Deines et al. 2009, Vander Zanden et al. 2016). Hydrogen incorporated into the OM of aquatic vegetation and algae originates from environmental water (Hondula et al. 2014). Typically, $\delta^{2}H$ values for aquatic photoautotrophs are 160-170 ‰ more negative than the surrounding water (Doucett et al. 2007, Solomon et al. 2011). In terrestrial plants, it has been observed that $\delta^{2}H$ values are more similar to environmental water $\delta^{2}H$ values (Hondula et al. 2014). This is due to transpiration, wherein evapotranspiration causes plant ^{2}H to be preferentially retained in plant OM over ^{1}H, yielding more positive $\delta^{2}H$ values (Roden and Ehleringer 1999). $\delta^{2}H$ values can therefore be used in a variety of ecological applications due to the large differences in $\delta^{2}H$ values between aquatic and terrestrial photosynthesis.

$\delta^{2}H$ values are also advantageous when used in conjunction with $\delta^{13}C$ to determine the role of CH_4 in the lake carbon cycle. Biogenically produced CH_4 has more negative $\delta^{13}C$ and $\delta^{2}H$ values with respect to carbon dioxide, plant material, and environmental water (Woltemate et al. 1984, Peterson and Fry 1987). These distinctly negative values are characteristic of biogenic CH_4, and therefore can be used to determine if CH_4 has been consumed and thus contributes to aquatic food webs (Deines et al. 2009, Jones and Grey 2011, Grey 2016). $\delta^{2}H$ and $\delta^{13}C$ values of CH_4 can also be used to track CH_4 production and consumption and these isotopic values can identify the pathway of CH_4 formation (CO_2 reduction or acetate fermentation) (Whiticar 1999). CH_4 and carbon derived from CH_4 can therefore be easily traced through ecosystems because it is intrinsically labelled by characteristically negative $\delta^{13}C$ and $\delta^{2}H$ values compared to other basal resources.

1.6 Thesis objectives

In order to improve understanding of biogeochemical cycles and their role in aquatic ecosystem functioning, continued work is required in the areas of both carbon and nutrient flows into ecosystems and through food webs (Middelburg 2014). By determining the respective contributions of terrestrial and aquatic carbon to the food web, the ways in which nutrients are transferred throughout food webs and support consumers at higher trophic levels will be better understood. This project will focus on the dynamics of the isotopic values at the base of the pelagic food web in a suite of boreal lakes, their seasonal variations, and the drivers of these changes in both particulate and dissolved fractions of OM.

The goal of my thesis is to examine and assess the controls on the isotopic values that are captured by the base of the food web and sediments in small, oligotrophic Canadian Shield lakes across a DOC gradient of 3.3- 12 mg/L. This goal will be achieved via the following objectives:

1. Examine the seasonal trends of DIC concentration, pCO_2, δ^{13}C-DIC, and δ^{13}C-CO_2 values and their relationship with and control on the isotopic values of pelagic carbon basal resources (POM) across a lake DOC gradient **(Chapter 2)**.
2. Assess the terrestrial contamination of lake surface POM across a lake DOC gradient using two different methods: (1) estimating the δ^{13}C and δ^{15}N values of phytoplankton by correcting for the terrestrial fraction of POM using C:N ratios, (2) the physical size separation of POM **(Chapter 2)**.
3. Determine the relationship between the δ^{13}C and δ^{15}N values of lake surface POM and those of surficial lake sediments across a lake DOC gradient **(Chapter 2)**.
4. Examine the δ^{2}H-DOM values in a series of Canadian Shield lakes and streams in comparison to the allochthonous and autochthonous end members **(Chapter 3)**.
5. Evaluate the use of δ^{2}H-DOM values as a method for separating allochthonous and autochthonous inputs to food webs **(Chapter 3)**.

6. Examine and define the range of $\delta^{13}C\text{-}CH_4$ and $\delta^{2}H\text{-}CH_4$ in fourteen boreal lakes, over four broad categories: deep anoxic bottom lakes, shallow anoxic bottom lakes, majority oxic lakes, and polymictic lakes **(Chapter 4)**.
7. Compare the observed $\delta^{2}H\text{-}CH_4$ and $\delta^{13}C\text{-}CH_4$ values to atmospheric values and predictions of sources based on literature values for both surface and deeper water column CH_4 **(Chapter 4)**.
8. Assess the potential roles of methanogenic pathway and CH_4 oxidation in controlling CH_4 isotopes **(Chapter 4)**.

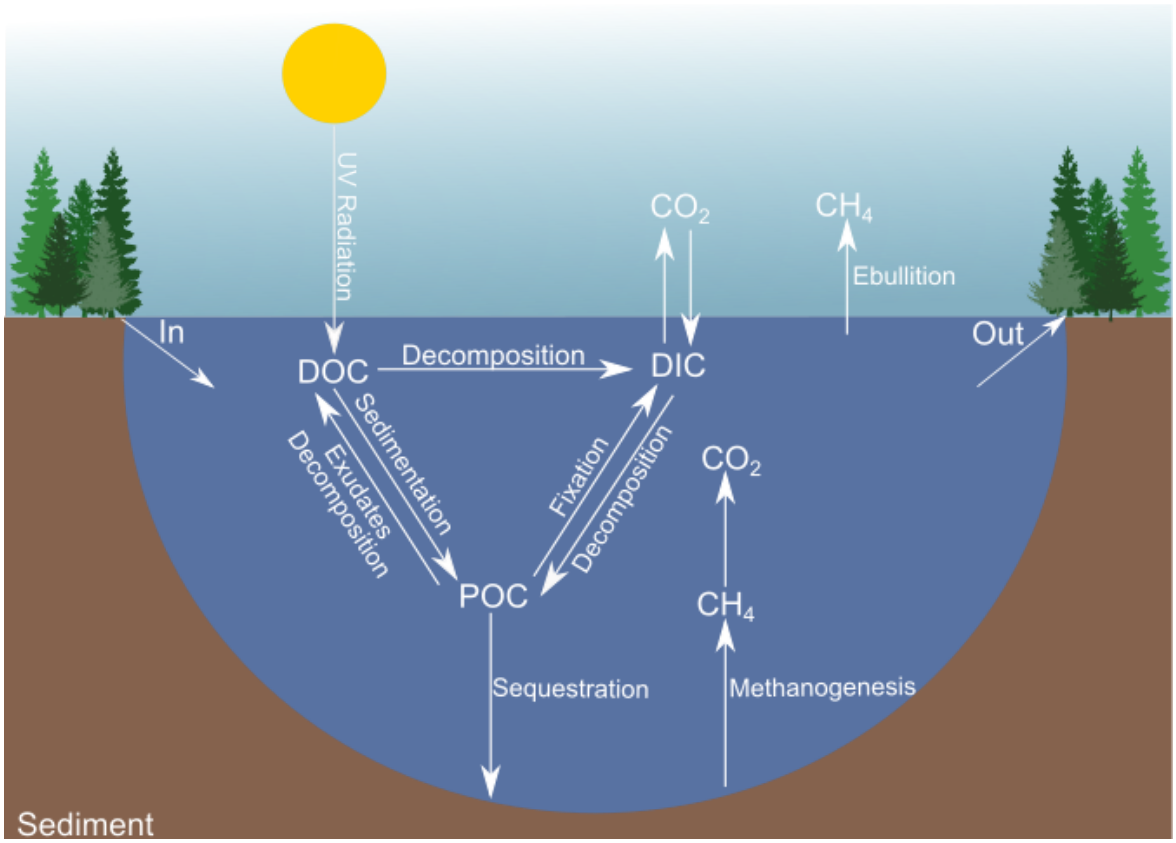

Figure 1.1 Simplified lake carbon cycle. Adapted from (Schiff, unpublished, Bastviken et al. 2004).

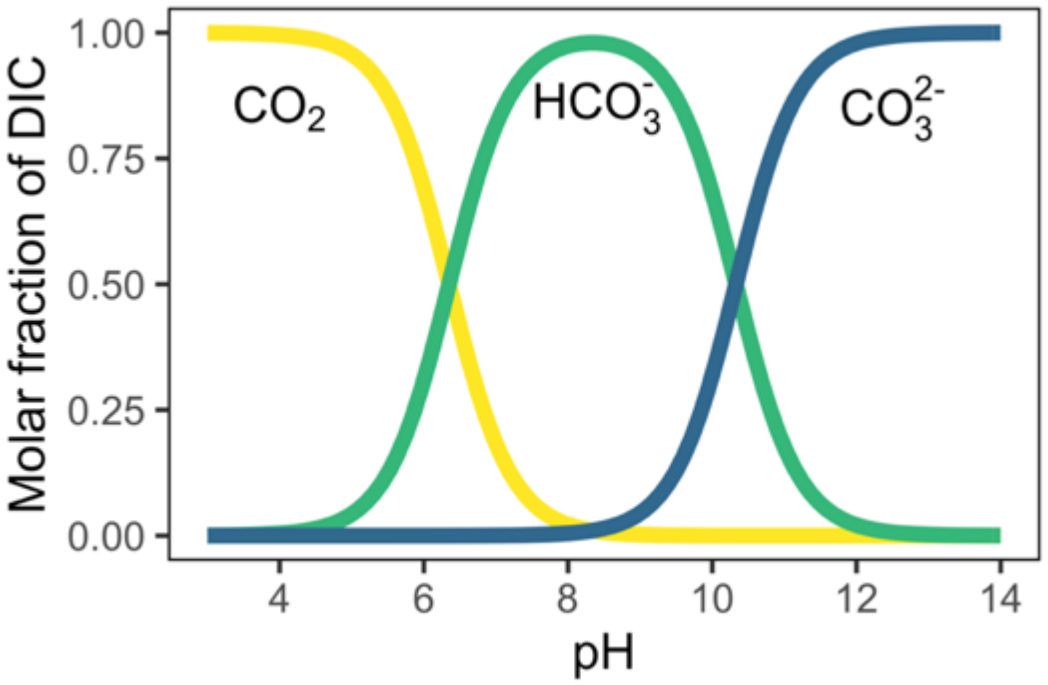

Figure 1.2 Bjerrum plot of the carbonate system at 25°C.

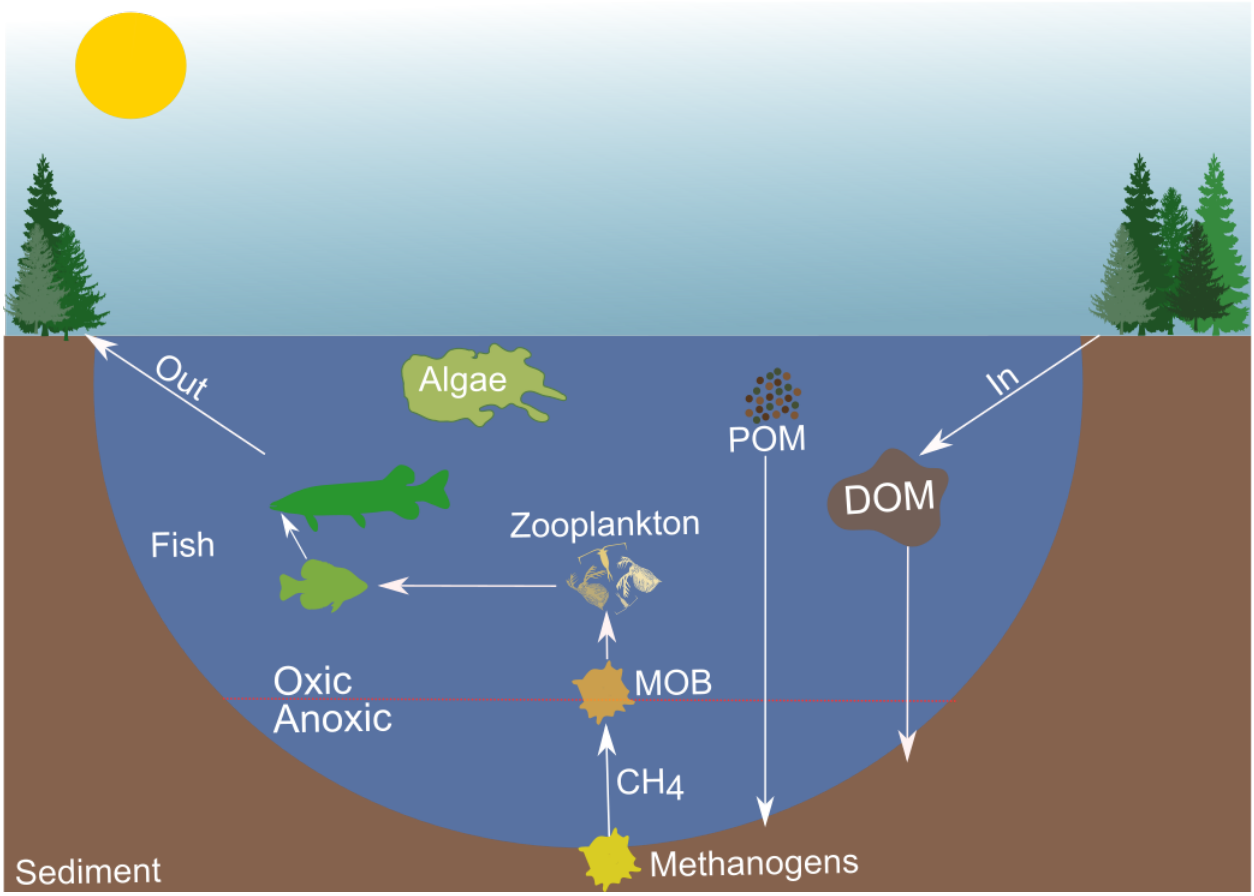

Figure 1.3 Simplified lake food web. Methane oxidizing bacteria= MOB.

Table 1.1 Abundances of carbon, nitrogen, and hydrogen stable isotopes.

Element	**Isotope**	**Abundance**
Carbon	^{12}C	98.9 %
	^{13}C	1.1 %
Nitrogen	^{14}N	99.6 %
	^{15}N	0.4 %
Hydrogen	^{1}H	99.9 %
	^{2}H	0.02 %

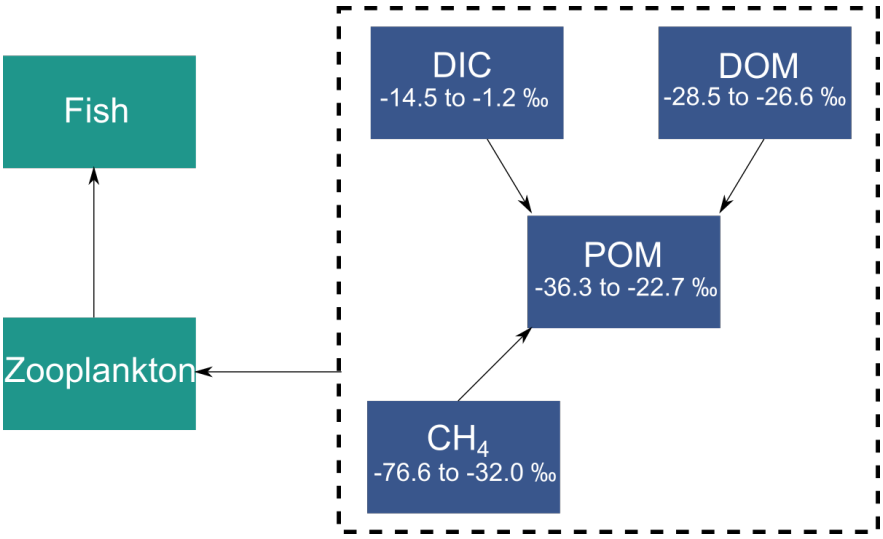

Figure 1.4 Ranges in $\delta^{13}C$ values in the base of the food web measured in this thesis. These values are an assimilation of $\delta^{13}C$-DIC, $\delta^{13}C$-DOM, $\delta^{13}C$-CH_4, and $\delta^{13}C$-POM values and are transferred up the food web to higher consumers.

Chapter 2. The control of terrestrial organic matter on lake carbon cycling along a DOC gradient

2.1 Introduction

A food web is a representation of the transfer of energy and nutrients among trophic levels (Lindeman 1942). Food webs are composed of organisms ranging from primary producers and bacteria, to higher consumers and predators. It can be challenging to analyze and disentangle these complicated relationships, particularly at the basal level. The base of the food web (i.e. basal resources) is defined as combined bacterial and primary production in an ecosystem (Karlsson et al. 2012) that supplies nutrients (e.g. carbon, nitrogen) for organisms at higher trophic levels (Post 2002). This chapter will examine how terrestrial organic matter inputs exert control over lake basal resources using stable isotope analysis.

As a direct consequence of concerns about the effects of climate change and land use change on watersheds, there is growing scientific interest about whether inputs from the terrestrial environment or lake primary productivity drive the function and production of freshwater ecosystems (Cole et al. 2002, Jansson et al. 2007, Rantakari and Kortelainen 2008, Seekell et al. 2015). The view that terrestrial carbon inputs of organic matter (OM) could support food webs in aquatic ecosystems has been subject to debate (Cole 2013b, Finstad et al. 2014, Tanentzap et al. 2017, Jones et al. 2018).

Physical characteristics of lakes and their catchments regulate DOC concentrations. For instance, catchment area:lake area (drainage ratio), proportion of wetlands, proportion of upstream lakes, watershed slope, and lake area (Rasmussen et al. 1989, Kortelainen 1993, Xenopoulos et al. 2003). Terrestrial OM is washed into lakes as water moves from the landscape, through vegetation, and finally infiltrates the soil (Findlay and Sinsabaugh 2003). DOC that reaches lakes is typically recalcitrant, having been thoroughly processed by soil bacteria during transport (Brett et al. 2009, Guillemette et al. 2016), and thus it is not as easily metabolized compared to autochthonous carbon. Terrestrial OM inputs can be larger than autochthonous production in lakes (Cole et al. 2002, 2011, Pace et al. 2011, Karlsson et al. 2015), and accordingly, allochthonous carbon tends to make up a larger proportion of the lake DOC pool than autochthonous carbon. This is especially the case in small, oligotrophic lakes such as those on the Canadian shield (Tranvik et al. 2009).

Microbes may also preferentially metabolize autochthonous carbon over allochthonous carbon (Guillemette et al. 2016). In some cases, where microbes utilize

terrestrial carbon, this carbon does not move up the food web to other consumers (Cole et al. 2002, Jones et al. 2012). Terrestrial OM also lacks important nutrients and fatty acids (Tanentzap et al. 2017). For these reasons, terrestrial OM may not provide meaningful support for lake food webs due to being of lower quality compared to autochthonous carbon (Brett et al. 2017).

Conversely, terrestrial OM may be beneficial to lake production and function. Allochthonous carbon can support heterotrophic production in lake ecosystems (Bartels et al. 2012, Karlsson et al. 2015). In cases where lakes are net heterotrophic, there must be some utilization of external inputs to the system (i.e. terrestrial OM) in order for there to be more respiration than primary production (Jones et al. 1999, Cole et al. 2011). Solomon et al. (2011) found that 20-80 % of lake zooplankton biomass was supported by terrestrial resources across four lakes with varying DOC concentrations and light regimes, suggesting that terrestrial carbon is a nutrient subsidy. A nutrient subsidy is a donor-controlled resource (e.g. terrestrial OM) from one habitat that increases the productivity of a recipient habitat (Polis et al. 1997). Therefore, terrestrial OM may subsidize aquatic food webs.

The positive effects of DOC concentration (shielding organisms from harmful UV rays, energy source) may outweigh the negative effects (decreased photosynthetically active radiation, changes in thermal structure) until a threshold concentration is reached (Finstad et al. 2014). It has been suggested that such a threshold concentration would be approximately 10 – 14 mg/L (Solomon et al. 2015). There are conflicting results as to whether the role of terrestrial OM is beneficial or harmful, and therefore further research is needed to elucidate the role of allochthonous carbon in freshwater lake food webs.

$\delta^{13}C$ and $\delta^{15}N$ are extensively used in stable isotope analysis, particularly in food web studies (Post 2002, Middelburg 2014, Vander Zanden et al. 2016). Measuring $\delta^{13}C$ values not only provides information about energy flows in food webs, but also allows researchers to examine changes and fluxes in lake carbon cycles and in both inorganic and organic carbon pools (De Kluijver et al. 2014). In order to understand and interpret the $\delta^{13}C$ and $\delta^{15}N$ values of higher consumers, there is a need to understand the processes at the base of the food web. However, because of the seasonal variability of $\delta^{13}C$ and $\delta^{15}N$ values in aquatic ecosystems, these values can be difficult to determine. POM is typically used as a proxy for algae (i.e. the base of the food web) (Gu et al. 2011). However, POM

is not solely composed to algal material, and is a combination of terrestrial material, bacteria, detritus, etc. (Mostofa et al. 2009). One solution to this problem is to physically separate the algal material from bulk POM in order to isolate a more representative sample of basal resources (Zohary et al. 1994, Bade et al. 2006).

$\delta^{13}C$ values are useful because primary producers take up ^{12}C preferentially over ^{13}C during photosynthesis, so primary producers (e.g. algae) will have a lower $\delta^{13}C$ value compared to the inorganic carbon source (Bade et al. 2006). This is because $^{12}CO_2$ is fixed slightly faster than $^{13}CO_2$. There are also differences between the $\delta^{13}C$ values of aquatic and terrestrial vegetation. The $\delta^{13}C$ values of aquatic primary producers are dependent on the $\delta^{13}C$-DIC values. $\delta^{13}C$-DIC values are variable, and the equilibrium fractionation between the two dominant forms of DIC in lakes (HCO_3^- and CO_2) is about -9 ‰ (O'Leary 1988). Therefore, the isotopic value of carbon fixed through photosynthesis reflects the isotopic value of the carbon source, and its associated transformations. Due to this, terrestrial vegetation (C3) $\delta^{13}C$ are typically between -28 to -26 ‰ (Peterson and Fry 1987), whereas algal $\delta^{13}C$ values lie between -35 and-25 ‰ (Grey et al. 2000).

There are three potential destinations for organic carbon inputs to lakes: storage, mineralization, or transport (Hanson et al. 2011). This chapter uses stable isotopes to examine these reservoirs of organic carbon across a gradient of DOC concentrations. DOC concentrations (terrestrial OM) in some European and North American freshwaters have increased in recent years, and are likely to continue to do so (Evans et al. 2005, Monteith et al. 2007). Proposed reasons for rising DOC concentrations in surface waters include reduced acid deposition, increasing temperatures, and land use change (Evans et al. 2005, Mattsson et al. 2005, Monteith et al. 2007). As temperatures continues to rise with climate change, this raises the question; how will increasing DOC concentrations affect our lakes, and in particular small Canadian shield lakes?

There are over 1,000,000 lakes on the Canadian shield, providing critical ecosystem services to Canadians. In order to preserve these valuable freshwater ecosystems, it is imperative to continue to research the interaction between terrestrial and aquatic environments. Therefore, the objectives of this chapter are as follows:

1. Examine the seasonal trends of DIC concentration, pCO_2, $\delta^{13}C$-DIC, and $\delta^{13}C$-CO_2 values and their relationship with and control on the isotopic

values of pelagic carbon basal resources (POM) across a lake DOC gradient.

2. Assess the terrestrial contamination of lake surface POM across a lake DOC gradient using two different methods: (1) estimating the $\delta^{13}C$ and $\delta^{15}N$ values of phytoplankton by correcting for the terrestrial fraction of POM using C:N ratios, (2) the physical size separation of POM.
3. Determine the relationship between the $\delta^{13}C$ and $\delta^{15}N$ values of lake surface POM and those of surficial lake sediments across a lake DOC gradient.

2.2 Material and methods

2.2.1 Study Sites

This project is part of a larger study at IISD-ELA called Photons to Fish (PHISH), which is aimed at determining factors affecting fish productivity along a DOC gradient (3.3 – 12 mg/L) in nine lakes (**Figure 2.2**). This DOC gradient is partly a result of differing quantities of terrestrial OM. Fourteen lakes and four streams were sampled for this thesis across the 2018 and 2019 field seasons **(Figure 2.1)**. A summary of physical and chemical parameters of the study lakes can be found in **(Table 2.1)**.

2.2.2 Field sampling

Throughout the 2018 field season (May-September), water column profiles of PHISH lakes were sampled using a gear pump on a monthly basis for a suite of water chemistry and stable isotope parameters. Samples were taken at 2-5 m intervals throughout the water column.

Samples for DIC concentration and $\delta^{13}C$-DIC analysis were collected in 12 mL exetainers with no headspace and were preserved by injecting a saturated solution of $ZnCl_2$. DOC concentration samples were filtered using a Whatman 0.45 μm syringe tip filter and collected in 40 mL amber glass vials and stored at 4°C. For POM isotope analysis, 1 L of water was collected and filtered through a Whatman QM-A quartz filter (pore size 2.2 μm) using a vacuum pump. Filters were frozen and subsequently shipped to the University of Waterloo for analysis. pH samples were collected in 15 mL PET containers with a Hach HQ40d meter and IntelliCAL™ PH301 probe.

$\delta^{13}C$-DOM and $\delta^{15}N$-DOM samples were filtered using Whatman 0.45 μm syringe tip filters, collected in 250 mL glass serum bottles with a small headspace, capped with rubber stoppers, and acidified using 6 mol/L HCl at the IISD-ELA field station in order to lower the pH to approximately 3.

In March of 2018, L223 and L224 were freeze cored to collect sediment from the hypolimnion. All remaining lakes were cored at the deepest depth in July and August of 2018 using a gravity corer. Sediment cores were sectioned in the field, then frozen and shipped to the University of Waterloo for analysis.

2.2.3 Laboratory and stable isotope analysis

Isotopic analysis for stable C and N isotopes was conducted at the University of Waterloo Environmental Isotope Laboratory. δ^{13}C-sediment and δ^{15}N-sediment analysis was conducted by first freeze drying sediments, then homogenizing the sediment using a ball mill, then weighed into Elemental Microanalysis D1002 tin sample cups (Elemental Analysis Ltd., UK). ^{13}C-POM and δ^{15}N-POM analysis was conducted by drying the frozen Whatman QM-A quartz filters (pore size 2.2 μm), then folded into Elemental Microanalysis D1002 tin sample cups (Elemental Analysis Ltd., UK). δ^{13}C-DOM and δ^{15}N-DOM samples were freeze dried and weighed into Elemental Microanalysis D1002 tin sample cup (Elemental Analysis Ltd., UK).

δ^{13}C-POM, δ^{15}N-POM, δ^{13}C-DOM, δ^{15}N-DOM, δ^{13}C-sediment and δ^{15}N-sediment samples were analyzed by EA-CF-IRMS using a Carlo Erba Elemental Analyzer and folding into an Elemental Microanalysis D1002 tin sample cup (Elemental Analysis Ltd., UK) (CHNS-O EA1108) coupled with a Delta Plus (Thermo) IRMS (δ^{13}C precision ± 0.2‰, δ^{15}N precision ± 0.3‰).

DIC concentration and stable isotope samples were prepared by acidifying, then equilibrating the headspace. Samples were then analyzed by GC-CF-IRMS using an Agilent 6890 GC coupled to an Isochrom isotope ratio mass spectrometer (IRMS: Micromass UK) (δ^{13}C precision ± 0.3‰). DOC concentration analysis was conducted using a Shimadzu Total Organic Carbon (TOC-L) analyzer (precision ± 0.3 mg C/L).

2.2.4 Estimating the δ^{13}C and δ^{15}N values of phytoplankton by correcting for the terrestrial fraction of POM

Estimations of algal δ^{13}C and δ^{15}N values ($\delta^{13}C_A$, $\delta^{15}N_A$) were calculated by correcting for the terrestrial fraction (ϕ_T) of POM. ϕ_T was calculated using the C:N ratio of POM, algae, and a terrestrial end member **(Equation 2.1)**, as outlined in (Francis et al.

2011, Yang et al. 2014, Tonin 2019). ϕ_T, $\delta^{13}C_A$, and $\delta^{15}N_A$ was estimated for each lake using mean seasonal C:N ratio, δ^{13}C-POM, and δ^{15}N-POM values.

Equation 2.1

$$\phi_T = \frac{(C{:}N_{POM} - C{:}N_A)}{(C{:}N_T - C{:}N_A)}$$

$C{:}N_{POM}$ was measured directly from surface bulk POM samples. $C{:}N_A$ represents the C:N ratio of phytoplankton. A $C{:}N_A$ of 6.8 was used (Vuorio et al. 2006, Yang et al. 2014, Tonin 2019). Two terrestrial end member values were used for the terrestrial C:N value ($C{:}N_T$) **(Table 2.2).** Firstly, the C:N of DOC (measured directly) was used as the $C{:}N_T$. The C:N of terrestrial vegetation at IISD-ELA was also used as the $C{:}N_T$ (Boudreau 2000).

Using the two calculated ϕ_T values, two different estimations of phytoplankton δ^{13}C and δ^{15}N values were determined using **Equation 2.2** and **Equation 2.3** (Francis et al. 2011, Yang et al. 2014). Both the stable isotopic values of DOC (measured directly) and terrestrial vegetation (values from Tonin (2019)) were used for the $\delta^{13}C_T$ and $\delta^{15}N_T$ values.

Equation 2.2

$$\delta^{13}C_A = \frac{\delta^{13}C_{POM} - (\phi_T \times \delta^{13}C_T)}{(1 - \phi_T)}$$

Equation 2.3

$$\delta^{15}N_A = \frac{\delta^{15}N_{POM} - (\phi_T \times \delta^{15}N_T \times 0.3)}{(1 - \phi_T \times 0.3)}$$

In addition to the calculation of ϕ_T, $\delta^{13}C_A$, and $\delta^{15}N_A$ from bulk POM samples, the same methodology was applied to each of the size fractions for the size separated POM samples.

2.2.5 Size separation of POM

In order to attempt to isolate a solely algal sample of POM, physical size separation of POM was conducted. Lake surface water (approximately 0.25 m) was filtered through Nitex mesh sieves in descending order of mesh size **(Table 2.3)**. These methods are based on those in Zohary et al. (1994) and Bade et al. (2006). The size fractions were selected according to Zohary et al. (1994) and Bade et al. (2006), as well as with examining IISD-ELA phytoplankton community data (Dr. Megan L. Larsen, personal communication). Size separation was conducted in July 2019 in L626, L239, L304, and L470 to represent a

subset of the DOC gradient, and thus varying degrees of terrestrial OM inputs (5.1 – 12 mg/L).

In the field, 20 L of surface water was pumped through stackable 100 μm, 53 μm, and 20 μm sieves into a carboy. The 100 μm sieve pre-screened for any large terrestrial detritus and zooplankton, so material captured on this sieve was discarded. Material on the 53 μm and 20 μm sieves was collected by gently rinsing sieves with RO water from a wash bottle into clean 250 mL Nalgene bottles. A separate 1 L sample of bulk water was reserved and sieved through the 100 μm screen, then onto a QM-A filter via a vacuum pump.

The 20 L carboy sieved to 20 μm was brought back to the IISD-ELA station and the 53<x<100 μm and 20<x<53 μm size fractions were collected on a QM-A filter (2.2 μm) using a vacuum pump. From the carboy, water was filtered through a 10 μm sieve to capture the 10<x<20 μm fraction, then collected on a QM-A filter (2.2 μm) via a vacuum pump.

Using a gear pump, the 20 μm carboy water was pumped through a high capacity 10 μm disposable filter capsule (Geotech, USA), then filtered through a QM-A filter using a vacuum pump. The filtrate from the 2.2<x<10 μm size fraction was then filtered through a Whatman GF/F glass microfibre filter to capture the 0.7<x<2.2 100 μm fraction. Once filtration on each size fraction was complete, samples were frozen and shipped to the University of Waterloo for δ^{13}C-POM and δ^{15}N-POM analysis (methods outlined above). For the L304 0.7<x<2.2 μm size fraction, not enough material was recovered on the filter for stable isotope analysis.

2.2.6 Calculating the percentage of DOC composed of algal material

The percentage of DOC composed of algal, or autochthonous material, was calculated using the methodology and empirical relationships outlined in Bade et al. (2007) **(Equation 2.4)**. Bade et. al (2007) suppose an exponential relationship between the percentage of algal DOC and the ratio of colour at 440 nm to chlorophyll *a* (chl *a*) concentration. This equation assumes that as chl *a* concentrations decrease and colour increases, a smaller proportion of DOC would be composed of algal material (Bade et al. 2007).

Chl *a* measurements were conducted at the IISD-ELA field station. Samples were collected on Whatman GF/C filters (pore size 1.2 μm), frozen, and analyzed fluorometrically. Colour is expressed as the absorbance coefficient at 440 nm wavelength (a_{440}), and is a measure of lake DOC concentration, and therefore also allochthonous carbon availability (Carpenter et al. 2005, Pace et al. 2011). Chl *a* is an indicator of lake primary productivity and thus also an indicator of autochthonous carbon (Carpenter et al. 2005, Pace et al. 2011).

Equation 2.4 $\%$ algal DOC = $56.36 \times e^{(-3.73 \times [\text{colour:chl } a])}$

Spectral absorbance (A_γ) samples were collected alongside monthly DOC concentration samples in 40 mL amber glass vials. Spectral absorbance was measured using a Cary 100 UV-Vis spectrophotometer. In a 1 cm quartz cuvette, samples were scanned at 5nm intervals from 200-800 nm. Samples were then corrected based on the absorbance of NANOpure water (≥ 18.2mΩ-cm). Using **(Equation 2.5)** (Xiao et al. 2013), absorbance spectra were normalized to absorbance coefficients (m^{-1}) (a_γ). Monthly a_{440} values for each PHISH lake were averaged to provide a seasonal colour value for each lake's surface water.

Equation 2.5 $$a_\gamma = \frac{2.303 A_\gamma}{0.01}$$

2.2.7 Statistical analysis and calculations

Linear mixed-effects models were calculated using the "lme4" package version 1.1-21 (Bates et al. 2015). Partial pressure of CO_2 (pCO_2) and $\delta^{13}C$-CO_2 values were calculated using the "isocalc" package version 1 using measured values for water temperature, pH, and DIC concentration (Henderson, 2018). Drainage ratio was calculated by dividing the whole catchment area (km^2) by the area of open water in the catchment (km^2).

2.3 Results

2.3.1 Seasonal trends in δ^{13}C-DIC, calculated δ^{13}C-CO2, δ^{13}C-POM, and δ^{15}N-POM values

In the PHISH lakes, DIC concentration is highest earliest in the season for all lakes except L164, and L470 **(Figure 2.3).** L164 and L470 have high DOC concentrations. It appears that DIC concentrations stabilize in the ice-free season. This pattern can also be observed in surface pCO_2 values **(Figure 2.4**), wherein the highest pCO_2 values are observed in May. pCO_2 values are also above atmospheric equilibrium for most lakes, indicating that these lakes are supersaturated **(Figure 2.4**). Calculated δ^{13}C-CO_2 values **(Figure 2.5)** show that all lakes, regardless of DOC concentration, are out of equilibrium with the atmosphere in terms of δ^{13}C-CO_2 values. These values ranged between -10.6 ‰ to -21.5 ‰. Surface δ^{13}C-CO_2 values are more negative earlier in the ice-free season. No relationship was found between the percent saturation of CO_2 in the surface water of the PHISH lakes and the calculated δ^{13}C-CO_2 values (R^2= -0.028, p= 0.7005) (**Figure 2.6**).

In terms of δ^{13}C-DIC, the most negative values are observed earliest in the season **(Figure 2.7)**. There is seasonality in the DIC concentrations, pCO_2 values, and δ^{13}C-DIC values in the PHISH lakes. Across lakes, δ^{13}C-DIC values vary by 14.2 ‰ over the ice-free season **(Figure 2.7)**. Further, lakes with lower DIC concentrations and lower pCO_2 values have higher DOC concentrations. δ^{13}C-DIC values are negatively correlated with DOC concentrations **(Figure 2.8**) (R^2= 0.73, p= 0.0020).

A large range (9.4 ‰) in δ^{15}N-POM was observed **(Figure 2.9A)**. The most negative δ^{13}C-POM values **(Figure 2.9B)** are observed earlier in the summer, similar to δ^{13}C-DIC. δ^{13}C-POM values follow the same trend as δ^{13}C-DIC values because POM consists partly of algae, and thus the isotopic values of POM reflect the carbon source used in photosynthesis. However, the opposite trend is observed in L470, the lake highest on the DOC gradient **(Figure 2.9B)**. Over the course of the 2018 ice-free season, δ^{13}C-POM values across the PHISH lakes varied by 8 ‰ **(Figure 2.9B)**. The C:N ratios of POM in the PHISH lakes ranged between 8.2 to 16.3 over the 2018 field season **(Figure 2.10)**. The lakes in May have a C:N ratio of approximately 10, with the exception of L470.

2.3.2 Relationship between δ^{13}C-POM, δ^{13}C-CO_2 and DOC concentration

POM is a mixture of terrestrial OM and autochthonous OM. Because of this, it is expected that the isotopic signal of POM is controlled both by pCO_2 (and thus the

photosynthetic fractionation factor, ε_C) and terrestrial contamination (e.g. DOC concentration). However, the degree to which each variable controls the POM signal, depends on the physical and chemical characteristics of lakes, as well as phytoplankton growth dynamics.

δ^{13}C-POM values are weakly and negatively correlated with surface pCO_2 values **(Figure 2.11)**. δ^{13}C-CO_2 values and δ^{13}C-POM values have a significant and positive relationship (R^2=0.377, p= 8.55 x 10^{-5}) **(Figure 2.112C**). No correlation was found between DOC concentration and pCO_2 (R^2= 0.029, p= 0.158) **(Figure 2.12A).** There was also a significant negative relationship between DOC concentration and δ^{13}C-CO_2 values (**Figure 2.12B**). Further, as DOC concentration increases, the C:N ratio of POM decreases (R^2= 0.74, p= 0.0038) (**Figure 2.13**).

2.3.3 Estimating the terrestrial fraction of POM and calculating $\delta^{13}C$ and $\delta^{15}N$ values of phytoplankton

Using **Equation *2.1***, ϕ_T was estimated using two different end members commonly used as proxies for allochthonous carbon- DOC and terrestrial vegetation **(Table 2.2)**. For each lake, when DOC was utilized to calculate ϕ_T of POM, ϕ_T was higher than when terrestrial vegetation was used **(Figure 2.14)**. L373 had the highest estimated ϕ_T out of all the lakes, for both end member corrections. Further, the two different end members used to calculate ϕ_T values for the PHISH lakes are significantly different (Welch's two sample t-test, df=10.8, t= 7.22, p= 1.90*10^{-5}).

Using the calculated ϕ_T of POM, the δ^{13}C and δ^{15}N values of phytoplankton ($\delta^{13}C_A$, $\delta^{15}N_A$) were estimated from **Equation 2.2** and **Equation 2.3**. $\delta^{13}C_A$ and $\delta^{15}N_A$ values with no end member correction are the mean, surface, bulk POM values for each lake. Uncorrected, bulk POM values are more negative than each of the corrected values, with the exception of L626 **(Figure 2.15)**. It appears that when using terrestrial vegetation to estimate $\delta^{13}C_A$ and $\delta^{15}N_A$, δ^{15}N values are slightly more positive when compared to bulk POM **(Figure 2.15)**. When DOC was used as an end member, the δ^{13}C values are more negative when compared to bulk POM **(Figure 2.15)**. DOC has δ^{13}C and δ^{15}N values more similar to calculated $\delta^{13}C_A$ and $\delta^{15}N_A$ values for each lake. The stable isotopic values for

terrestrial vegetation are much more negative than those of the PHISH lakes with respect to $\delta^{15}N$ values. L626 has very positive calculated $\delta^{13}C_A$ and $\delta^{15}N_A$ values **(Figure 2.15)**.

The relationship between the estimated $\delta^{13}C_A$ values and calculated $\delta^{13}C\text{-}CO_2$ values was examined **(Figure 2.16)**. For the most part, higher DOC lakes have more negative calculated $\delta^{13}C\text{-}CO_2$ values. The estimated $\delta^{13}C_A$ values are more negative than the two terrestrial end members (DOC, terrestrial vegetation), with the exception of L626. These estimated values for phytoplankton fall within a range of reported ε_C values (ε_C= 10, ε_C=15, ε_C= 20) (Bade et al. 2006, Mohamed and Taylor 2009, Wilkinson et al. 2013b), even those of L626 which are considerably more positive than the other PHISH lakes.

2.3.4 Size separation of POM

In order to determine the degree to which terrestrial contamination occurs in bulk POM, POM was size separated. The goal of physically size separating POM is to examine the differences between bulk POM and subsequently smaller size fractions. Most algal species present in unamended IISD-ELA lakes should fall into the 2.2<x<10 μm and the 10<x<20 μm size fractions. The size separated POM from L626 had the most positive $\delta^{15}N$ and $\delta^{13}C$ values across all size fractions with the exception of the $\delta^{15}N$ value for the 2.2<x<10 μm size fraction **(Figure 2.18)**. The POM C:N ratios of the 10<x<20 μm size fraction are markedly higher than the remaining size fraction for all lakes **(Figure 2.19)**. No significant differences were found between size fraction classes for $\delta^{13}C$ or $\delta^{15}N$ values **(Figure 2.18)** (one-way ANOVA, p>0.05). However, there were significant differences in between size fractions for C:N ratios (one-way ANOVA, p= 1.62 x 10^{-5}, F= 13.99) **(Figure 2.19**). A Tukey's post-hoc test was conducted to determine pairwise differences between the size fractions, and showed that the mean C:N ratio for the 10<x<20 μm size fraction for all lakes is significantly different from all other size fractions (**Figure 2.20**).

The ϕ_T of POM for each size fraction was also calculated using **Equation 2.1** with two different terrestrial end members- lake DOC and terrestrial vegetation **(Table 2.2)**. Similar to the estimates of ϕ_T in bulk POM, the use of DOC as an end member estimates a higher ϕ_T. This is the case for each size fraction **(Figure 2.21)**. In each lake, the 10<x<20 μm size fraction has the highest estimated ϕ_T, for both end members **(Figure 2.21)**. Using

these estimations of ϕ_T, the $\delta^{13}C_A$ and $\delta^{15}N_A$ values were calculated. The end member corrections did not greatly alter the $\delta^{13}C_A$ or $\delta^{15}N_A$ values of each size fraction.

2.3.5 Calculating percent algal DOC

Another important aspect to examine is what parameters set the "signal" of DOC. DOC can be composed of autochthonous and allochthonous OM, however the amount of terrestrial or in-lake material that makes up DOC can change. Since DOC can be allochthonous or autochthonous, the $\delta^{13}C$ values of various types of OM at IISD-ELA across various terrain classifications (lake, soil, upland streams, vegetation, wetland streams, wetland pond) **(Figure 2.23)** were examined. Of all classifications, vegetation $\delta^{13}C$ values have the largest range (9.8 ‰).

The percentage of DOC comprised of algal material was calculated by using an empirical equation (**Equation 2.4**) from Bade et al. (2007). This equation is derived from the exponential equation fit to empirical spectral absorbance (a_{440}), chl *a*, and DOC concentration data from 32 lakes in the Northern Highland Lake District (Bade et al. 2007).

Overall, the calculated percent algal DOC in the PHISH lakes ranged from 0.02 % to 28.2 % (**Figure 2.24A**). For the most part, the calculated lower percent algal DOC values were found in lakes with higher DOC concentrations (**Figure 2.24A**). This trend also applies to DOC concentration, because higher DOC lakes have a higher a_{440} value due to their dark colour, and therefore a larger colour:chl *a* ratio. According to this empirical relationship, lakes with higher DOC concentrations (L470, L164, L658) have the lowest percentage of autochthonous material comprising DOC (**Figure 2.24A**).

There is no apparent relationship between $\delta^{13}C$-DOM values and calculated algal DOC content **(Figure 2.24B)**. (R^2= -0.092, p= 0.47). There is a small range in surface water $\delta^{13}C$-DOM values, ranging from -26.7 ‰ to -28.5 ‰.

In contrast, there is a slight positive relationship between $\delta^{13}C$-POM values and calculated algal DOC **(Figure 2.24C)**. (R^2=0.37, p= 0.048). The average seasonal surface water $\delta^{13}C$-POM values occupy a larger range of -26.9 ‰ to -31.9 ‰. As the average surface $\delta^{13}C$-POM values increased, so did the percentage of algal DOC **(Figure 2.24C)**.

2.3.6 Relationship between DOC concentration and lake drainage ratio

One characteristic of lakes that sets the signal of DOC is residence time. Since not all of the PHISH lakes are headwater lakes (**Table 2.1**), lake drainage ratio was used instead of water residence time. No relationship was found between either drainage ratio and DOC concentration (R^2= 0.126, p= 0.168) **(Figure 2.25A**) and drainage ratio and δ^{13}C-DOM values (R^2= -0.0552, p= 0.471) **(Figure 2.25B**).

2.3.7 δ^{13}C values, δ^{15}N values, and C:N ratios of surficial sediments

Another important relationship is that of surficial sediments and POM, and it is important to investigate how this relationship changes across a DOC gradient. Sediment from deeper core sections have more positive δ^{15}N and δ^{13}C values than those shallower in the sediment core. δ^{13}C-sediment values ranged by 6.5 ‰ and δ^{15}N sediment values ranged by 3.7 ‰ across all lakes and sediment cores **(Figure 2.26)**. For both δ^{15}N and δ^{13}C values, the sediment core from L303 are consistently more positive than the other lakes **(Figure 2.27)**. Using a linear mixed-effects model, the effect of DOC on the δ^{13}C-sediment values at depth within the sediment core was examined. There was no significant effect shown (p = 0.53) **(Figure 2.28)**. There was also no significant relationship between the surface sediment δ^{13}C values and δ^{13}C-POM values (R^2= -0.0612, p=0.532) **(Figure 2.29A)** or between the C:N ratios of POM and surface sediments **(Figure 2.29B)**. Across the sediment cores, C:N ratios ranged from 11.5-16.9, with higher C:N ratios observed in deeper core sections **(Figure 2.30)**.

2.4 Discussion

2.4.1 Seasonal trends of DIC concentration, pCO_2, δ^{13}C-DIC, and δ^{13}C-CO_2 values and their relationship with and control on the isotopic values of POM

DIC concentration is highest earliest in the season for all lakes with the exception of L164 and L470 **(Figure 2.3)**. Processes taking place under ice, such as decomposition and respiration, cause DIC to accumulate (Striegl et al. 2001). After ice-off, the trapped DIC will equilibrate with the atmosphere. This causes the pattern observed in the data, where the highest DIC concentrations occur in May, then decrease, and subsequently level off over the season.

Surface pCO_2 values are also highest earlier in the year and most lakes are consistently above atmospheric saturation **(Figure 2.4)**. The lakes are also out of equilibrium with the atmosphere in terms of their calculated surface $\delta^{13}C\text{-}CO_2$ values **(Figure 2.5**), and no relationship was found between percent saturation of CO_2 in the surface water of the PHISH lakes and the $\delta^{13}C\text{-}CO_2$ values (R^2= -0.028, p= 0.7005) (**Figure 2.6**).

Lakes tend to be sources of CO_2 to the atmosphere (Cole et al. 1994, Tranvik et al. 2009), due to the respiration of allochthonous carbon by bacteria (Jansson et al. 2012). Supersaturated waters may then indicate a commensal relationship between heterotrophic microbes and phytoplankton (Jansson et al. 2012). In fact, DOC, and therefore terrestrial OM, has been shown to be a significant control on lake pCO_2 (Sobek et al. 2005). However, no significant relationship was found between DOC concentration and pCO_2 in the PHISH lakes. This may be due to differences in lake catchment characteristics, such as residence time, as observed by Whitfield et al. (2009).

Both $\delta^{13}C$-DIC and calculated $\delta^{13}C\text{-}CO_2$ values show that earlier in the season, values are more negative **(Figure 2.5) (Figure 2.7)**. After ice-off, due to equilibration with the atmosphere the lighter isotope (^{12}C) will be lost first, thus increasing the $\delta^{13}C$-DIC and $\delta^{13}C\text{-}CO_2$ values. $\delta^{13}C$-DIC values also ranged by 14.2 ‰. This is a smaller range than reported in Finnish lakes (27.3 ‰) (Striegl et al. 2001) or the Northern Highlands Lake District (29.0 ‰) (Bade et al. 2004). These ranging values in $\delta^{13}C$-DIC show the intricacy of the reactions within the lake carbon cycle, and how due to differences in lake hydrology, these reactions can vary greatly (Striegl et al. 2001).

For the PHISH lakes, lakes with more negative $\delta^{13}C$-DIC values have higher DOC concentrations (R^2= 0.77, p=0.0011) **(Figure 2.8)**. Therefore, there are processes occurring in lakes with higher DOC concentrations that cause the $\delta^{13}C$ of the DIC to be more negative. For instance, CO_2 produced from the respiration of allochthonous OM (DOC) has a $\delta^{13}C$ value similar to its source (Chomicki 2009). As DOC is respired, CO_2 is produced, thereby increasing the DIC concentration. The $\delta^{13}C\text{-}CO_2$ produced from respiration will be lower than the atmospheric $\delta^{13}C\text{-}CO_2$ value of -8.4 ‰(Chomicki 2009, Keeling et al. 2017). Therefore, with higher DOC concentrations, more respiration can occur, making $\delta^{13}C$-DIC values more negative **(Figure 2.8)**.

Over the course of the 2018 ice-free season, δ^{13}C-POM **(Figure 2.9B)** values vary up to 8 ‰, illustrating that the use of a single POM value in food web studies is unrealistic. This variation is due to changes in the carbon source used in photosynthesis. As primary productivity increases in the summer, phytoplankton deplete ^{12}C-DIC, leading to more positive δ^{13}C-POM values. However, as previously discussed, POM is not solely composed of algal material. A weak negative correlation was found between δ^{13}C-POM and pCO_2 **(Figure 2.11)**. The pCO_2 of surface waters is the carbon source that algae (a component of POM) are using for photosynthesis.

The δ^{15}N values of small, freshwater organisms at low trophic levels have been shown to vary considerably (Cabana and Rasmussen 1996, Syväranta et al. 2008). δ^{15}N values of phytoplankton, and therefore POM, should relatively indicate the inorganic nitrogen source (Syväranta et al. 2008). δ^{15}N-POM varied by approximately 9 ‰ in the PHISH lakes **(Figure 2.9A)**, again exemplifying the breadth of seasonal variations at the base of the food web. This is in the upper end of the range of seasonal δ^{15}N-POM values (1.5 ‰ to 8.5 ‰) in oligotrophic lakes presented by Gu (2009). Higher ranges in seasonal δ^{15}N-POM has been found in eutrophic lakes, where POM is mostly algal material, and therefore can reflect changes in the environment (Gu 2009). Conversely, smaller ranges can be observed in oligotrophic lakes because in these environments POM consists more of allochthonous material (i.e. non-living) (Gu 2009).

The C:N ratios of the POM in the PHISH lakes varied seasonally. The C:N ratio of algae has previously been reported as 6.8 (Vuorio et al. 2006, Yang et al. 2014), and the C:N ratio of terrestrial OM is typically >20 (Meyers 1994). The POM C:N ratio in various IISD-ELA lakes have been reported to range between 11.8-16.0 (Hecky et al. 1993, Turner et al. 1994). The POM ratios of the PHISH lakes vary between 8.2 and 16.3. This perhaps indicates that the surface POM is a mixture of algal and terrestrial OM.

The mean surface DOC concentration is negatively correlated with the mean molar C:N ratio of POM **(Figure 2.13)**. As previously mentioned, the C:N ratio of terrestrial material is >20, and algae have a C:N ratio between 4-10 (Meyers 1994), and it has been reported in freshwater as 6.8 (Vuorio et al. 2006, Yang et al. 2014). Therefore, it is expected that in lakes with higher terrestrial OM inputs (i.e. a higher DOC concentration), the POM would have a higher C:N ratio. However, as DOC is photolyzed, the C:N ratio decreases

(Chomicki 2009). This may be why decreasing C:N ratios are observed with increasing DOC concentrations **(Figure 2.13)**. If there were no allochthonous OM contribution to POM, then the C:N ratio of POM would only reflect that of autochthonous material. L470 was not included in the linear regression between mean surface DOC concentration and mean C:N ratio of POM, as it is an outlier. L470 likely does not follow this relationship because of its very short residence time (**Table 2.1)**.

The calculated pCO_2 values of the PHISH lakes have no significant relationship with DOC concentrations (R^2= 0.029, p= 0.158) **(Figure 2.12A)**. However, there is a significant, negative relationship between DOC concentrations and calculated $\delta^{13}C\text{-}CO_2$ values (R^2= 0.175, p=8.99 x 10^{-3}) **(Figure 2.12B)**. As surface DOC concentrations increase, the $\delta^{13}C\text{-}CO_2$ values become increasingly negative. This indicates that the PHISH lakes with higher DOC concentrations are more depleted in their $\delta^{13}C\text{-}CO_2$ values.

δ^{13}C-POM values are weakly and negatively correlated with surface pCO_2 values **(Figure 2.11)**. There is also a significant, positive relationship between calculated $\delta^{13}C\text{-}CO_2$ values and δ^{13}C-POM values (R^2=0.377, p= 8.55 x 10^{-5}) **(Figure 2.12C**). Since algae is a component of POM, the isotopic values of the carbon source used in photosynthesis should be reflected in the values of POM, depending on the degree to which algal material comprises POM.

2.4.2 Assessing the terrestrial contamination of lake surface POM

The ϕ_T of POM was calculated using **Equation 2.1** using either DOC or terrestrial vegetation as terrestrial end members **(Table 2.2)**. Two different end members were used in these calculations because terrestrial vegetation and DOC are both commonly used as terrestrial end members (terrestrial vegetation: (Cole et al. 2002, Pace et al. 2004, Caraco et al. 2010, Wilkinson et al. 2013a, 2013b, Guillemette et al. 2016); DOC: (Kritzberg et al. 2004, Bade et al. 2007, Guillemette and del Giorgio 2012)). In addition, DOC and terrestrial vegetation are sometimes assumed to be the same (Grosbois et al. 2020).

For each PHISH lake, the ϕ_T was estimated to be higher when DOC was used as the end member correction **(Figure 2.14)**. These estimations are calculated using an algebraic mixing model which calculates ϕ_T from the C:N ratios of bulk POM, phytoplankton, and terrestrial organic matter **(Equation 2.1)**. Estimating the ϕ_T of POM allows for the correction of terrestrial POM, which has a large C:N ratio **(Table 2.2)**. The

ϕ_T values calculated using DOC and terrestrial vegetation as terrestrial end members are significantly different (Welch's two sample t-test, df=10.8, t= 7.22, p= $1.90*10^{-5}$). Differences in these estimations are likely due to the large differences between the C:N ratios of DOC and terrestrial vegetation **(Table 2.2)**. This is because terrestrial primary producers are nutrient starved, and therefore terrestrial plant tissues have been shown to have C:N ratios three times higher than lake particulate matter (Elser et al. 2000). The C:N ratio of terrestrial vegetation at IISD-ELA used in this thesis is approximately twice that of the C:N ratio of DOC **(Table 2.2)**.

Once ϕ_T was calculated for each lake, this value was used to calculate an estimation of the $\delta^{13}C$ and $\delta^{15}N$ values of phytoplankton ($\delta^{13}C_A$, $\delta^{15}N_A$) that are corrected for ϕ_T. POM is a mixture of autochthonous and allochthonous material, therefore by calculating ϕ_T, an approximation for $\delta^{13}C_A$ and $\delta^{15}N_A$ can be determined. This was done using the two different estimations for ϕ_T (DOC and terrestrial vegetation). The $\delta^{13}C_A$ and $\delta^{15}N_A$ values with no end member correction are the mean, surface, bulk POM values for each lake **(Figure 2.15)**.

With the exception of L626, each lake has more negative $\delta^{13}C_A$ and $\delta^{15}N_A$values when an end member correction is applied. The positive calculated $\delta^{13}C_A$ and $\delta^{15}N_A$ values for L626 can be attributed to the fact that its uncorrected POM value is more positive than the end member values of both DOC and terrestrial vegetation **(Figure 2.15)**. The estimated $\delta^{13}C_A$ and $\delta 15N_A$ values are an attempt to correct bulk POM for the large C:N ratio of terrestrial organic matter, whether terrestrial vegetation or DOC is used as an end member. When DOC is used for the end member correction, $\delta^{13}C_A$ values are more negative than the uncorrected values, as well as those corrected with the terrestrial vegetation end member. This is because the $\delta^{13}C$ of DOC is more positive than phytoplankton **(Figure 2.15)**. Therefore, using this method removes the influence of DOC and results in $\delta^{13}C_A$ values that are more negative than the bulk POM.

The relationship between calculated $\delta^{13}C$-CO_2 values and estimated $\delta^{13}C_A$ was examined **(Figure 2.16)**. When the $\delta^{13}C_A$ values are estimated using DOC as the terrestrial end member, the values are more negative. All of the calculated $\delta^{13}C_A$ values (both uncorrected and corrected) fall between a range of literature ε_C values (Bade et al. 2006,

Mohamed and Taylor 2009, Wilkinson et al. 2013b) and the mean $\delta^{13}C$ values for terrestrial vegetation and DOC. This suggests that the POM is a mixture of both allochthonous and autochthonous material.

The $\delta^{15}N_A$ values are generally mixed and cluster around the $\delta^{15}N$ value of DOC **(Figure 2.15)**. However, the $\delta^{15}N$ of terrestrial vegetation is much more negative than that of DOC. Consequently, when using terrestrial vegetation as the terrestrial end member, the $\delta^{15}N_A$ values are shifted to be more positive **(Figure 2.15)**. Both of these terrestrial end members are commonly used in literature and are sometimes assumed to have the same isotopic values. While these assumptions may hold for the $\delta^{13}C$ values of terrestrial end members (approximately -27 ‰), this is not the case for the $\delta^{15}N$ values **(Figure 2.15, Figure 2.17)**. The mean value of $\delta^{15}N$-DOC is 2.0 ‰ compared to the mean $\delta^{15}N$ value of terrestrial vegetation, -5.5 ‰ **(Table 2.2).**

The $\delta^{15}N$ values of terrestrial vegetation are more negative compared to the $\delta^{15}N$ values of DOC **(Figure 2.17)**. This is because of nitrogen limitation in the boreal forest (Maynard et al. 2014). While DOC originates from the terrestrial environment and therefore represents an allochthonous carbon source to lacustrine ecosystems, it is altered through reactions in the stream and lake carbon cycle (photolysis, microbially degradation, sedimentation). DOC is also already altered before reaching the lake. Due to these transformations, DOC is a mix between autochthonous and allochthonous material, and it is more similar to lake POM in terms of C:N ratios , $\delta^{13}C$ values, and $\delta^{15}N$ values **(Table 2.2, Figure 2.15)**.

Size separation of POM was undertaken in order to examine the stable isotopic values of POM at various size fractions. By isolating POM into different sizes **(Figure 2.18)**, the goal is to obtain a more accurate algal sample and to determine the role of contamination by terrestrial OM in POM. However, no significant differences were found in terms of $\delta^{13}C$ (one-way ANOVA, p= 0.979, F= 0.144) and $\delta^{15}N$ values (one-way ANOVA, p= 0.459, F= 0.978) between the different size fractions **(Figure 2.18)**. As stated in Marty and Planas (2008), while physical separation of algae from bulk POM may be the ideal method, in many ecosystems using smaller and smaller mesh sizes means that particles of various sizes that are not of interest may attach themselves to algae, confounding isotopic values. This was also a concern in Bade et al. (2006). Problems may

also arise if algal communities are diverse, which most communities are (Marty and Planas 2008). Zohary et al. (1994) showed that bulk POM samples were not sufficient in providing in depth insight into the $\delta^{13}C$ values at the base of the pelagic food web, due to seasonal changes in phytoplankton species, demonstrating that size separation of POM to obtain algal $\delta^{13}C$ values is viable in cases where a less complex view of a food web is needed.

However, there are significant differences in size fractions for C:N ratios (one-way ANOVA, p= 1.62 x 10^{-5}, F= 13.99) **(Figure 2.19)**. A post-hoc Tukey test showed that between size fractions for all lakes, the mean C:N ratio for the 10<x<20 μm size fraction is significantly different from all other size fractions **(Figure 2.20)**.

One potential reason for the increase in C:N ratios for the 10<x<20 μm size fraction **(Figure 2.19, Figure 2.20)** is that pollen also falls between 10 and 20 μm. As previously stated, The C:N ratio of algae has been shown to be 6.8 (Vuorio et al. 2006, Yang et al. 2014), and the C:N ratio of POM and IISD-ELA has been reported in the range of 11.8-16.0 (Hecky et al. 1993, Turner et al. 1994), whereas the C:N ratio of terrestrial OM is typically >20 (Meyers 1994). Therefore, since a higher C:N ratio was observed, it is plausible that there may be a higher degree of terrestrial contamination in the 10<x<20 μm size fraction.

Typical terrestrial vegetation at IISD-ELA includes Labrador tea (*Ledum groenlandicum*), leather leaf (*Chamaedaphne calyculata*), jack pine (*Pinus banskiana*), trembling aspen (*Populus tremuloides*), white birch (*Betula papyrifera*), black spruce (*Picea mariana*), balsam fir (*Abies balsamea*), and red pine (*Pinus resinosa*). Coniferous trees such as jack pine, black spruce, balsam fir, and red pine have pollen grains that average approximately 58 μm, 89 μm, 119 μm, and 63 μm in diameter respectively (Bassett et al. 1978). However, deciduous trees and shrubs such as white birch, Labrador tea, leather leaf, and trembling aspen have pollen grains that average 28 μm, 28.4 μm, 32.6 μm, and 27.5 μm respectively (Bassett et al. 1978, Crompton and Wojtas 1993, Sawara 2007). As the pore sizes on the mesh sieves used are nominal, it is plausible that some of the deciduous and shrub pollen is captured in the 10<x<20 μm size fraction, thereby increasing the C:N ratio of this fraction **(Figure 2.19**).

Further, Preston et al. (2008) showed that in an oligotrophic temperate lake in Wisconsin, USA, 55 % of aerial terrestrial particulate organic carbon deposition input occurred far from shore (>12m), and 39 % of total terrestrial particulate carbon deposited was less than 153 μm (Preston et al. 2008). These particles also had a similar range in C:N ratios (6-22) as observed in this thesis (7.6-17.9) (**Figure 2.19)**, indicating that perhaps some material captured in size separation is deposited airborne terrestrial particulate organic carbon (Preston et al. 2008).

Similarly to the mean bulk POM of each PHISH lake, the ϕ_T for each of the size separation fractions was calculated **(Equation 2.1)**. For each size fraction, when DOC was utilized as the terrestrial end member, ϕ_T was estimated to be much larger **(Figure 2.21).** For all lakes and both terrestrial end members, the $10<x<20$ size fraction has the highest estimated ϕ_T **(Figure 2.21)**. Alongside the significant differences in C:N ratios **(Figure 2.19, Figure 2.20)**, this may also illustrate that this size fraction has some terrestrial contamination.

$\delta^{13}C_A$ and $\delta^{15}N_A$ values were then calculated using ϕ_T **(Equation 2.2) (Equation 2.3**) **(Figure 2.22)**. Upon correcting the size separated POM with the terrestrial end members, the $\delta^{13}C_A$ and $\delta^{15}N_A$ values are not changed drastically. Perhaps this is because due to the size separation of POM, the samples were already physically "corrected" for terrestrial contamination.

A $\delta^{13}C$ value of -27 ‰ is commonly used to represent terrestrial plants (Marshall et al. 2008). While DOC is of terrestrial origin, it is heavily processed before finally reaching lakes. Therefore, the stable isotope values of DOC do not equate to that of terrestrial material as is sometimes assumed (Grosbois et al. 2020). The $\delta^{13}C$ range for terrestrial vegetation is also quite large compared to that of the $\delta^{13}C$ values for DOC in lakes **(Figure 2.23).**

As previously discussed, the percentage of DOC comprised of autochthonous material (algae) was estimated using **Equation 2.4** from Bade et al. 2007. This equation supposes that colour:chl *a* ratio and percent algal DOC have a positive relationship, and is derived from the empirical relationships observed in 32 lakes located in the Northern Highlands Lake District by Bade et al. (2007).

Higher a_{440} values are associated with higher DOC concentrations (Cuthbert and del Giorgio 1992). Allochthonous DOC is typically darker in colour than autochthonous DOC due to humic compounds (Meili 1992). In addition to being associated with darker water colour, high DOC concentrations have also been shown to decrease primary production (Ask et al. 2012), and with lower primary production, it is expected that chl *a* concentrations should also decrease. Therefore, it follows that as a_{440} values increase, so should colour:chl *a* ratios.

According to **Equation 2.4**, the higher DOC lakes (L470, L164, L658) have a much lower calculated percentage of algal material than the low DOC lakes **(Figure 2.24A)**, likely because higher DOC concentrations can indicate a higher proportion of terrestrial OM. Allochthonous carbon constitutes a larger proportion of surface water DOC in the PHISH lakes with higher DOC concentrations. Similarly, in humic and polyhumic Swedish boreal lakes, which are dark in colour, it has been shown that the majority of the organic carbon consists of allochthonous material (Meili 1992).

There was no relationship shown between δ^{13}C-DOM values and calculated percent algal DOC **(Figure 2.24B)**. One potential reason for this is that there is a large range of water residence times present in the PHISH lakes **(Table 2.1) (Figure 2.3)**, perhaps altering the δ^{13}C-DOM values.

It is then unexpected that there is a slight positive relationship between δ^{13}C-POM values and calculated percent algal DOC **(Figure 2.24A)** (R^2=0.37, p<0.05). As the calculated percentage of DOC comprised of algal material increased, so did δ^{13}C-POM. Surface DOC concentration also increased along this trend. In higher DOC lakes, δ^{13}C-POM values are more negative and algal material comprises a negligible percentage of total DOC. Wilkinson et al. (2013b) show using δ^{13}C values of POM and DOM that DOM is composed of allochthonous material, whereas POM is composed of a mixture of autochthonous and allochthonous material.

In contrast, lower DOC lakes have more positive δ^{13}C-POM values, and a much higher proportion of their DOC is made up of autochthonous material. Previous studies have shown that phytoplankton δ^{13}C values can range from -35.2 ‰ to -18.4 ‰ in a series of 24 lakes across the United Kingdom (Grey et al. 2000), and from -34.9 ‰ to -19.6 ‰ in 10 lakes in the Northern Highlands Lake District, USA (Wilkinson et al. 2013b, Yang et

al. 2014). One may expect that lakes on the low end of the DOC gradient would demonstrate a high proportion of algal material in their DOC and have a δ^{13}C-POM value closer to that of the end member. However, the entire range of δ^{13}C-POM shown in **Figure 2.9** encompasses the previously established range of δ^{13}C values of phytoplankton.

The PHISH lakes did not have a significant relationship between either drainage ratio and DOC concentration or drainage ratio and δ^{13}C-DOM **(Figure 2.25)**. Drainage ratio takes into account upstream lakes within each catchment, as opposed to water residence time. DOC loading should increase alongside drainage ratio, because lakes with larger drainage ratios have more upstream lakes in their catchments. Further, it is expected that lakes with large drainage ratios have higher flushing rates, lower loss of DOC, and thus higher concentrations of DOC (Sobek et al. 2007). However, as previously mentioned, no relationships were found between drainage ratio and DOC concentration or δ^{13}C-DOM values. Similarly, in a global survey of 7500 lakes, drainage ratio was not an important predictor of DOC concentration (Sobek et al. 2007). Xenopolous et al. (2003) expected that drainage ratio would be a key predictor of DOC concentration, however, did not find this to be the case. In contrast, Schindler (1971) found that drainage ratio was significantly related to water colour (i.e. DOC concentration) in 14 IISD-ELA lakes. This relationship was also expected because lake colour, and thus DOC concentration should be proportional to the area of terrestrial drainage per unit of lake area, or drainage ratio (Schindler 1971). Perhaps these relationships do not apply in this case because the PHISH lakes are not all headwater lakes **(Table 2.1)**.

2.4.3 The relationship between the δ^{13}C-POM and δ^{15}N-POM values and δ^{13}C-sediment and δ^{15}N-sediment values

Terrestrial OM is the main source of OM to lake sediments (Hall et al. 2018), and this material can act as an energy source for microbes (Meyers and Ishiwatari 1993). As sediments undergo diagenesis, the δ^{13}C and δ^{15}N values are altered, and therefore will be distinct from those of the original OM (Meyers and Ishiwatari 1993). For most lakes in this study, deeper sediment core sections have more positive δ^{13}C and δ^{15}N values **(Figure 2.26)**. One reason for the heavier δ^{13}C values deeper in the cores is diagenesis, which preferentially loses ^{12}C (Flinn 2012). As OM is degraded, residual OM is enriched in the heavier isotopes, increasing δ^{13}C and δ^{15}N (Meyers and Ishiwatari 1993). Since OM is more

easily degraded in oxic conditions than in anoxic conditions, oxygen concentration affects the isotopic values of sediments (Lehmann et al. 2002). If OM undergoes a greater degree of diagenesis within the water column, then $\delta^{13}C$ and $\delta^{15}N$ values once the OM reaches the sediment will be affected (Teranes and Bernasconi 2000).

No relationship was found between $\delta^{13}C$-POM values and surface $\delta^{13}C$-sediment values (R^2= -0.0612, p= 0.532) (**Figure 2.29A)**. The $\delta^{13}C$ values of OM buried in sediment is dictated by the quantities of allochthonous and autochthonous OM, the $\delta^{13}C$-DIC values, primary production rates, and respiration rates (Meyers and Teranes 2001). Many processes can affect the $\delta^{13}C$ values of OM between its source and its burial, however, the main process is degradation as the particles settle to the sediment surface (Meyers and Ishiwatari 1993). Once the OM has reached the sediment surface, it is further oxidized and degraded as a carbon source for microbes (Meyers and Ishiwatari 1993). Therefore, while one may expect that pelagic $\delta^{13}C$-POM values should be correlated with $\delta^{13}C$-sediment values, this is not the case due to degradation of OM during burial and settling. Similarly, there was no relationship between the C:N ratio of POM and surficial sediments (**Figure 2.29B)**. Like $\delta^{13}C$ and $\delta^{15}N$ values, C:N ratios of sediment are altered by deposition (Gälman et al. 2009).

There are two important considerations in interpreting the C:N ratios of sediments, firstly, the C:N ratio of the material being deposited, as well as the proportions of allochthonous and autochthonous material being deposited. Meyers et al. (1995) showed that the C:N ratios of white spruce (*Picae glauca*) that had undergone diagenesis differed from that of unburied wood, however that these differences were not enough to negate the contrast between the high C:N ratio of terrestrial OM and the lower ratio of aquatic OM. In all cores, the deeper sections have higher C:N ratios **(Figure 2.30)**. OM that is more nitrogen-rich is of algal origin and is lost first in freshly deposited material, affecting C:N ratios (Herczeg 1988). As previously stated, the C:N ratio of algae is approximately 6 and can range between 4-10, compared to that of terrestrial OM which is >20 (Meyers 1994, Vuorio et al. 2006, Yang et al. 2014). The POM C:N ratio in IISD-ELA lakes is in the range of 11.8- 16.0 (Hecky et al. 1993, Turner et al. 1994). The lowest C:N ratio shown at the sediment water interface (0-0.5) from the cored lakes is 11.5 in L626 (a low DOC lake), and the highest C:N ratio is from L222 and is 15.9 (a high DOC lake).

As terrestrial inputs increase with increasing DOC concentration, we may expect to see a more terrestrial "signal" in the $\delta^{13}C$ values of lake sediments. In order to investigate this, a linear mixed effects model was used. This model investigated the effect of DOC on $\delta^{13}C$-sediment values at depth within sediment cores at each lake sampled. However, no significant effect was shown (p= 0.18) **(Figure 2.28)**. Variation can be observed within the sediment cores for each lake, as opposed to across the DOC gradient **(Figure 2.28)**.

One potential issue with this approach is that as diagenesis occurs, the $\delta^{13}C$ values of sediments change (Meyers and Ishiwatari 1993), and therefore it may be difficult to gain insight into whether the source of the sediment OM is autochthonous or allochthonous. It may be expected that at depth, the ratio of preserved algae:DOC would be preserved in the sediment, and that this ratio would change with DOC concentration in oligotrophic lakes. For instance, Tonin (2019) showed that at higher DOC concentrations, the basal production that occurs is conducted to a greater degree by heterotrophic bacteria respiring terrestrial OM, as opposed to autotrophic primary production. Therefore, with increasing DOC concentration, more terrestrial OM should be preserved in the sediment, and at lower DOC concentrations, more algal material should be preserved, relative to each other. However, this was not observed **(Figure 2.28)**.

Some studies have shown the importance of terrestrial OM to lake sediments. For instance, Hall and collegaues (2018) found that at IISD-ELA, over a 40-year period in L239, more DOC was buried in sediments than was evaded as CO_2 or lost via the outflow. In regard to autochthonous OM, it has been shown that in surficial sediments in a suite of Florida lakes, $\delta^{13}C$ values were a function of primary production (chl *a*) (Gu et al. 1996). These studies show that autochthonous settling particles are preferentially degraded in lake sediments.

2.5 Conclusions

Upon examination of the seasonal trends in the basal carbon resources of the pelagic zone in the PHISH lakes at IISD-ELA, it is clear that there is seasonality in terms of DIC concentrations, pCO_2 values, and $\delta^{13}C$-DIC values across the DOC gradient. Surface DIC concentrations and pCO_2 values are higher earlier in the year due to off-

gassing to the atmosphere after ice-off. Subsequently, the PHISH lakes were above atmospheric saturation for the duration of the summer. High DOC lakes (L164, L470) behave somewhat differently than lower DOC lakes. This may be due to their shorter residence times. Due to higher amounts of OM there may be more respiration occurring producing $\delta^{13}C$- CO_2 values that are more negative than the atmosphere (Chomicki 2009).

Due to these seasonal variations in pCO_2 and DIC concentrations, there are concomitant variations in $\delta^{13}C$-CO_2 and $\delta^{13}C$-DIC, which thus alter $\delta^{13}C$-POM and $\delta^{15}N$-POM values seasonally. The C:N ratios of POM in the PHISH lakes also varied seasonally and showed that the surface water POM is likely a mix of allochthonous and autochthonous material. Lower POM C:N ratios were observed in higher DOC lakes. This is unexpected due to the high ratios of terrestrial material (Meyers 1994). This unexpected trend may be due to the photolysis of DOC, which reduces the C:N ratio (Chomicki 2009).

Two different methods were used to assess terrestrial contamination of surface water POM. First, the ϕ_T values of POM were calculated and corrected for using two common different terrestrial end members- lake DOC and terrestrial vegetation. By using DOC as the terrestrial end member, the ϕ_T of POM was consistently estimated to be higher than when using terrestrial vegetation. Through using the calculated ϕ_T values, phytoplankton $\delta^{15}N$ and $\delta^{13}C$ ($\delta^{15}N_A$ and $\delta^{13}C_A$) were estimated. When DOC is corrected for, the $\delta^{13}C_A$ values are more negative compared to bulk POM values by an average of 0.489 ‰. When terrestrial vegetation is used, the $\delta^{13}C_A$ values decrease by 0.0497 ‰ on average. These small changes in $\delta^{13}C_A$ values show that the correction for the terrestrial fraction of POM may not in fact be necessary.

The physical size separation of POM showed no significant differences between size fractions for $\delta^{13}C$ and $\delta^{15}N$ values. However, there were significant differences shown in terms of C:N values between size fractions, perhaps due to airborne inputs of terrestrial particulate matter. Further, the $10<x<20$ μm size fraction was shown to be significantly different (one-way ANOVA, $p= 1.62 \times 10^{-5}$, $F= 13.99$) from the remaining size fractions, as well as having the highest calculated ϕ_T values. While in theory the physical isolation of solely algal carbon is the best way to determine the $\delta^{13}C$ value of algae, it is not always viable, as shown in this chapter. Due to the time-consuming nature of the physical separation of POM and lack of conclusive results, perhaps other methods of isolating

algal $\delta^{13}C$ values are more appropriate. However, in order to exclude large terrestrial debris and zooplankton, it may be worthwhile to undertake bulk POM pre-screening using a sieve of approximately 100 μm.

According to the calculated percentage of algal material composing DOC **(Equation 2.1)**, the DOC in high DOC lakes may be composed of less algal material than in low DOC lakes due to higher colour, and therefore likely higher inputs of terrestrial OM. Additional work could be conducted in regard to DOC composition and dynamics using further absorbance and fluorescence analysis (Fellman et al. 2010).

In this chapter, $\delta^{15}N$ and $\delta^{13}C$ values of surficial sediments and their respective C:N ratios are shown. Deeper core sections have more positive $\delta^{15}N$ and $\delta^{13}C$ values and higher C:N ratios indicating the effects of diagenesis on deposited OM. No relationship was found between the surface $\delta^{13}C$ values of sediment and lake DOC concentrations. This is unexpected since it has been shown that there is a higher degree of basal production conducted by heterotrophic bacteria respiring terrestrial OM. As such, with increasing DOC concentration, there should be more terrestrial OM preserved in surface sediments.

One limitation to this study is that I examine only pelagic carbon resources, thereby not considering any benthic production. However, the research presented in this chapter could also be used as baseline stable isotope data for studies concentrating on larger consumers at IISD-ELA. In the future, the reactions within the lake carbon cycle must be considered when looking at the implications of climate change on freshwater ecosystems.

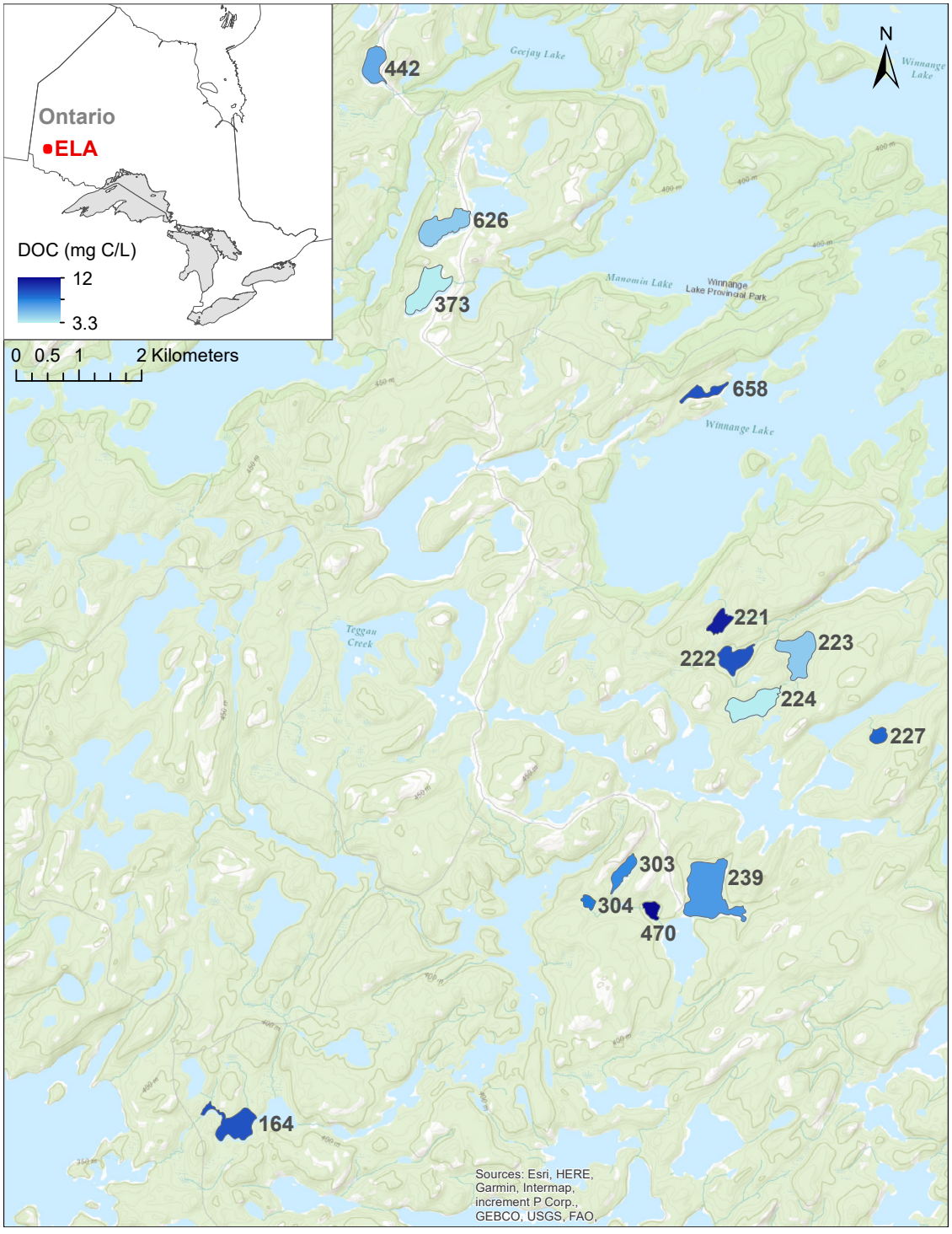

Figure 2.1 Map of IISD-ELA showing the fourteen lakes sampled as part of this research project. PHISH project lakes: L164, L223, L224, L239, L373, L442, L470, L626, L658. Size separation lakes: L626, L239, L304, L470. δ^2H-DOM lakes sampled: L373, L239, L222, L221, L227. δ^2H-DOM streams sampled: U8, NWIF, EIF, NEIF.

Table 2.1 Summary of mean physical and chemical parameters of sampled lakes, including lake order, lake area, lake volume, maximum depth (Z_{max}), residence time, DOC concentration, and whether the lake is sampled as part of the PHISH project. Residence time calculated as the average theoretical water renewal time (years) by dividing lake volume (m^3) by estimated outflow (m^3).

Lake	DOC (mg/L)	Lake order	Lake Area (ha)	Lake Volume (m^3)	Z_{max} (m)	Estimated Outflow (m^3)	Residence time (years)	PHISH lake?
L224	3.3	2	25.9	3005000	27.4	239899	12.5	Yes
L373	3.9	1	27.3	2941000	21	198316	14.8	Yes
L223	4.7	3	27.3	1951000	14.4	639730	3.0	Yes
L626	5.1	4	25.9	1772000	11.3	954674	1.9	Yes
L442	6.2	2	16	1303000	16	396141	3.3	Yes
L239	7.0	1	56.1	5910000	30.4	967813	6.1	Yes
L303	7.6	1	9.9	150000	2.5	133113	1.1	No
L304	7.9	1	3.6	115000	6.7	64957	1.8	No
L227	8.3	1	34.4	221000	10	84641	2.6	No
L658	8.9	1	8.4	546473	13.5	140249	3.9	Yes
L222	9.4	1	16.4	600000	5.8	502680	1.2	No
L164	9.2	32	20.3	1002000	7	12174554	0.2	Yes
L221	11	2	9	189100	5.7	201761	0.9	No
L470	12	4	6	33000	2	412626	0.1	Yes

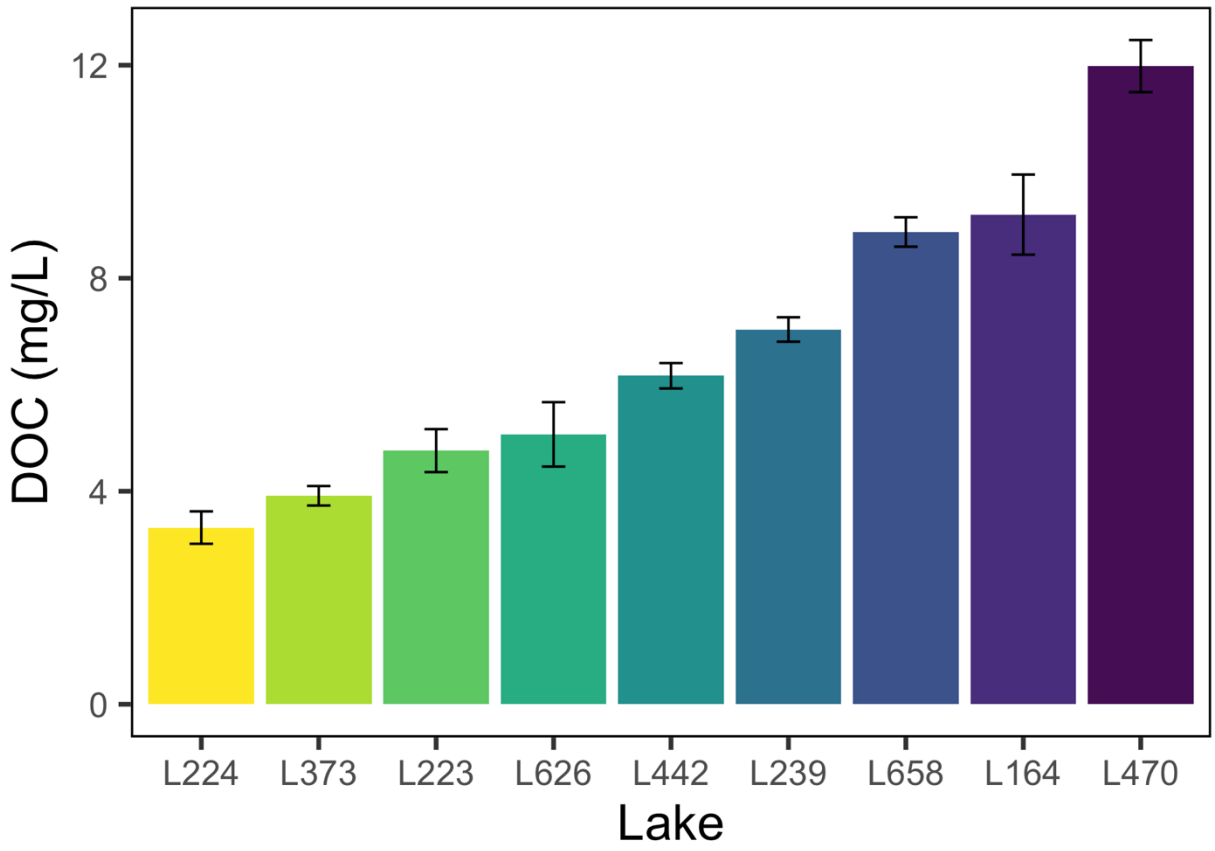

Figure 2.2 DOC gradient (3.3 – 12 mg/L) present in the nine PHISH lakes. DOC concentrations represent the mean surface DOC concentration (n= 52) over the 2018 field season (May-September). Error bars represent +/- one standard deviation. Lakes in this figure and in all preceding figures are presented in order of ascending DOC concentration.

Table 2.2 End members used to correct for the terrestrial fraction of POM and calculate the $\delta^{13}C$ and $\delta^{15}N$ values of phytoplankton.

End member	C:N ratio	$\delta^{13}C$	$\delta^{15}N$
Terrestrial vegetation	62.0 ± 24.2 (n=25)[a]	-29.7 ± 1.03 (n=27)[b]	-5.5 ± 1.6 (n=27)[b]
DOC[c]	30.2 ± 7.3 (n=13)[c]	-27.9 ± 0.39 (n=13)[c]	2.0 ± 1.3 (n=13)[c]

[a] Mean C:N ratio of terrestrial vegetation at IISD-ELA (Boudreau 2000).

[b] Mean $\delta^{13}C$ and $\delta^{15}N$ values of terrestrial vegetation (Tonin 2019).

[c] Mean DOC C:N ratio, $\delta^{13}C$, and $\delta^{15}N$ values from surface water values of 13 IISD-ELA lakes (this thesis).

Table 2.3 Summary of size fraction, rationale, and filter used to capture material for size separation.

Size fraction (μm)	**Rationale**	**Filter (pore size μm)**
x< 100	By pre-screening with 100 μm mesh, zooplankton and other large particles will be excluded.	QM-A (2.2)
53< x < 100	Collect material on 53 μm mesh.	QM-A (2.2)
20< x < 53	Collect material on 20 μm mesh. Collect water screened through 20 μm mesh in a carboy.	QM-A (2.2)
10< x <20	Collect material on 10 μm mesh.	QM-A (2.2)
2.2< x <10	Using large capacity capsule filter, pump the carboy of water sieved to 20 μm down to 10 μm. Filter water sieved to 10 μm through a QM-A filter.	QM-A (2.2)
0.7< x <2.2	Capture bacterial portion/ picoplankton by using filtrate from previous size fraction and filtering through a GF/F.	GF/F (0.7)

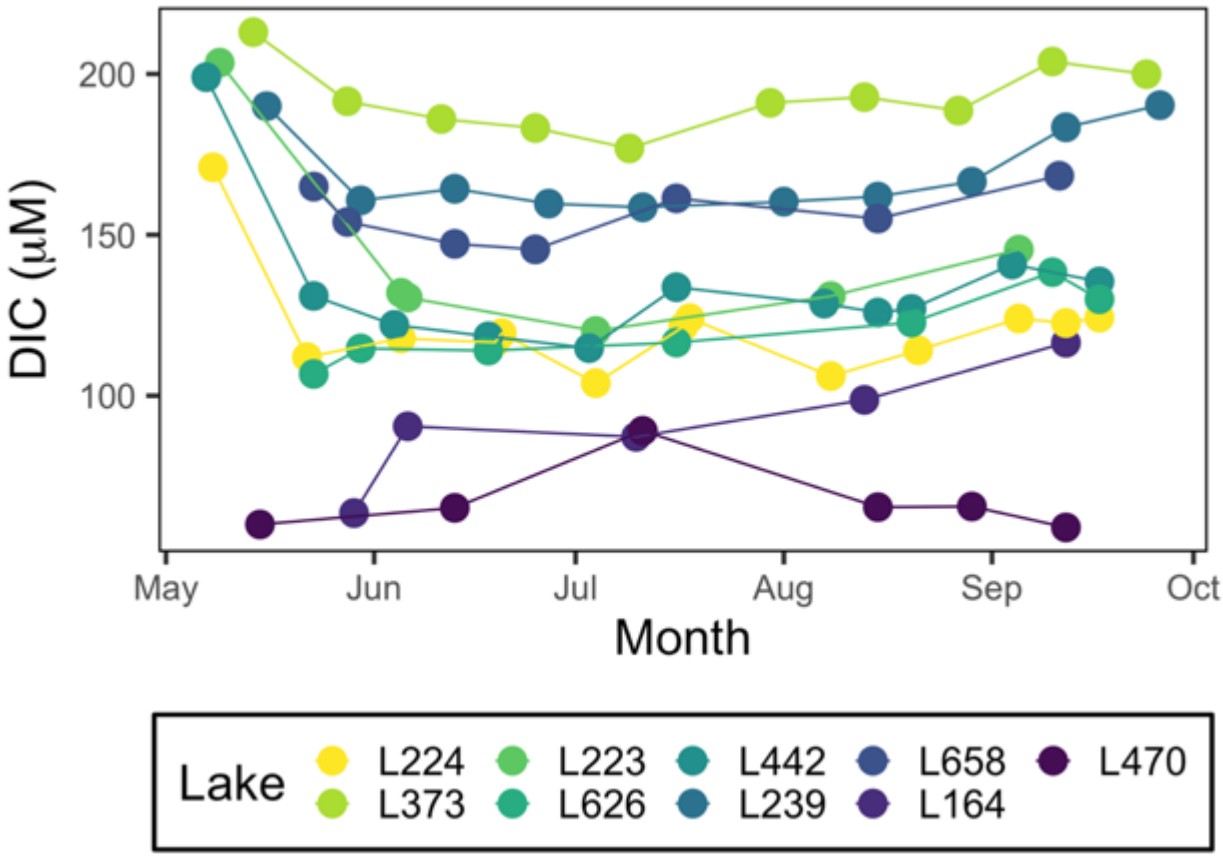

Figure 2.3 Surface DIC concentration (µM) in the PHISH lakes over the 2018 ice free season.

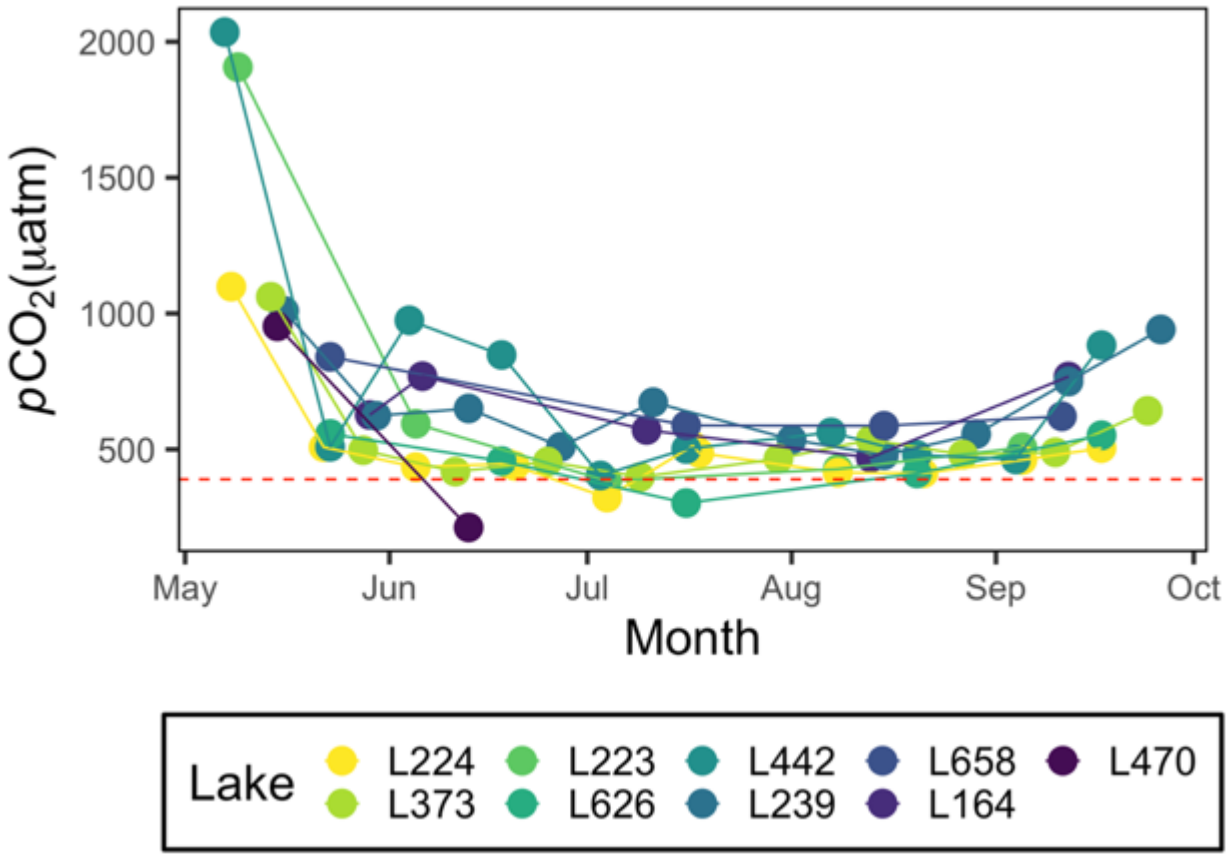

Figure 2.4 Calculated surface pCO_2 values (µatm) in the surface of the PHISH lakes over the 2018 ice free season. Red dashed line indicates atmospheric equilibrium (370 µatm).

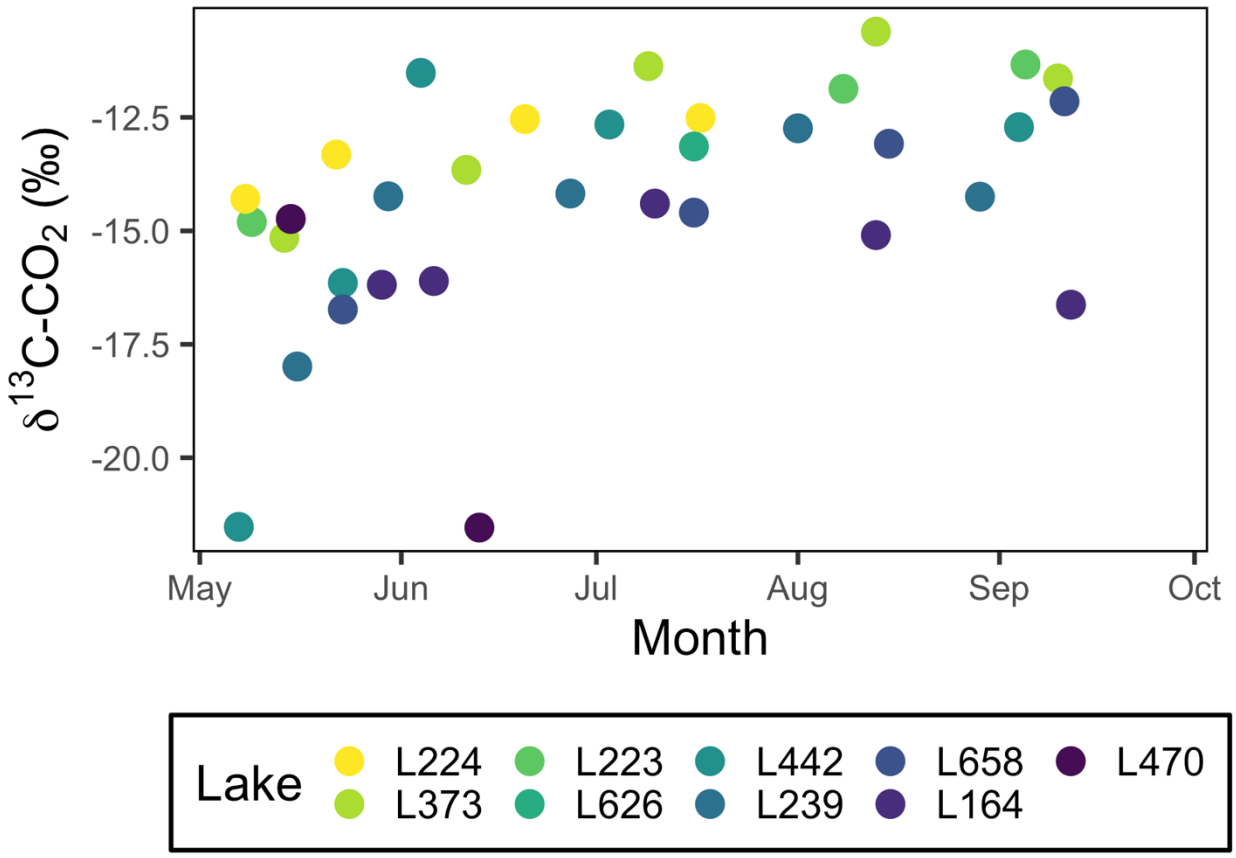

Figure 2.5 Calculated $\delta^{13}C\text{-}CO_2$ values for the PHISH lakes throughout the 2018 ice free season.

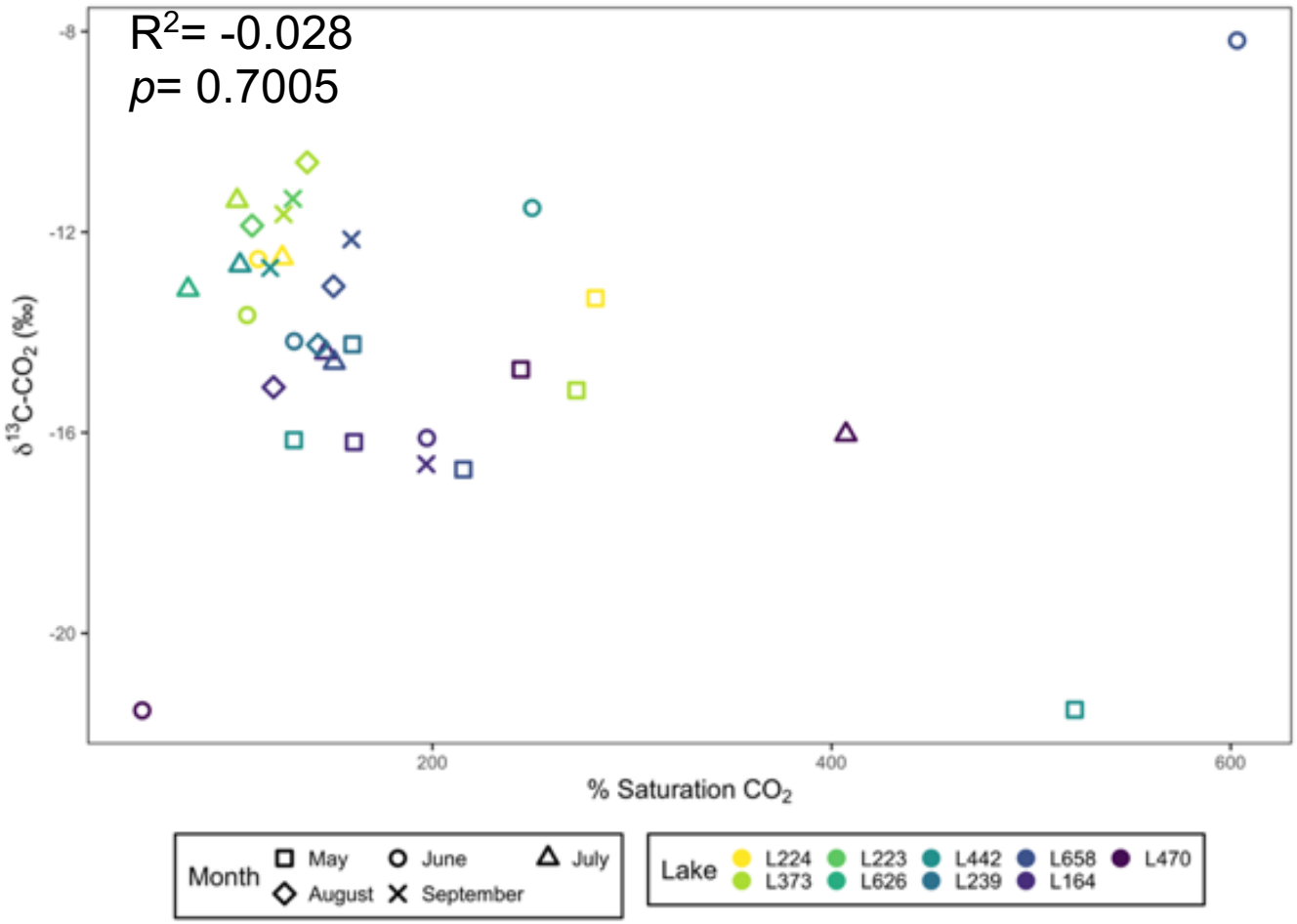

Figure 2.6 Relationship between percent saturation of surface water CO_2 and calculated surface $\delta^{13}C$-CO_2 values in the PHISH lakes.

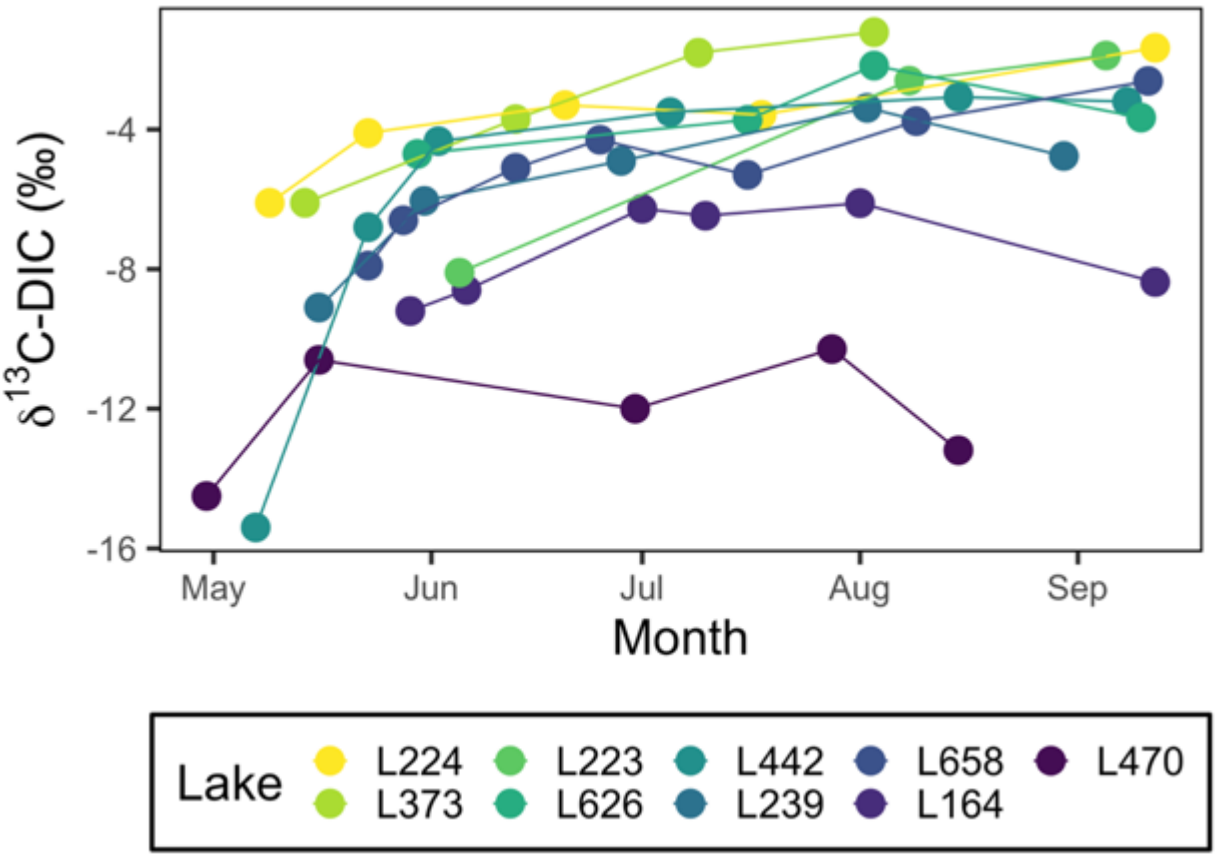

Figure 2.7 Surface δ^{13}C-DIC values for the PHISH lakes throughout the 2018 ice-free season.

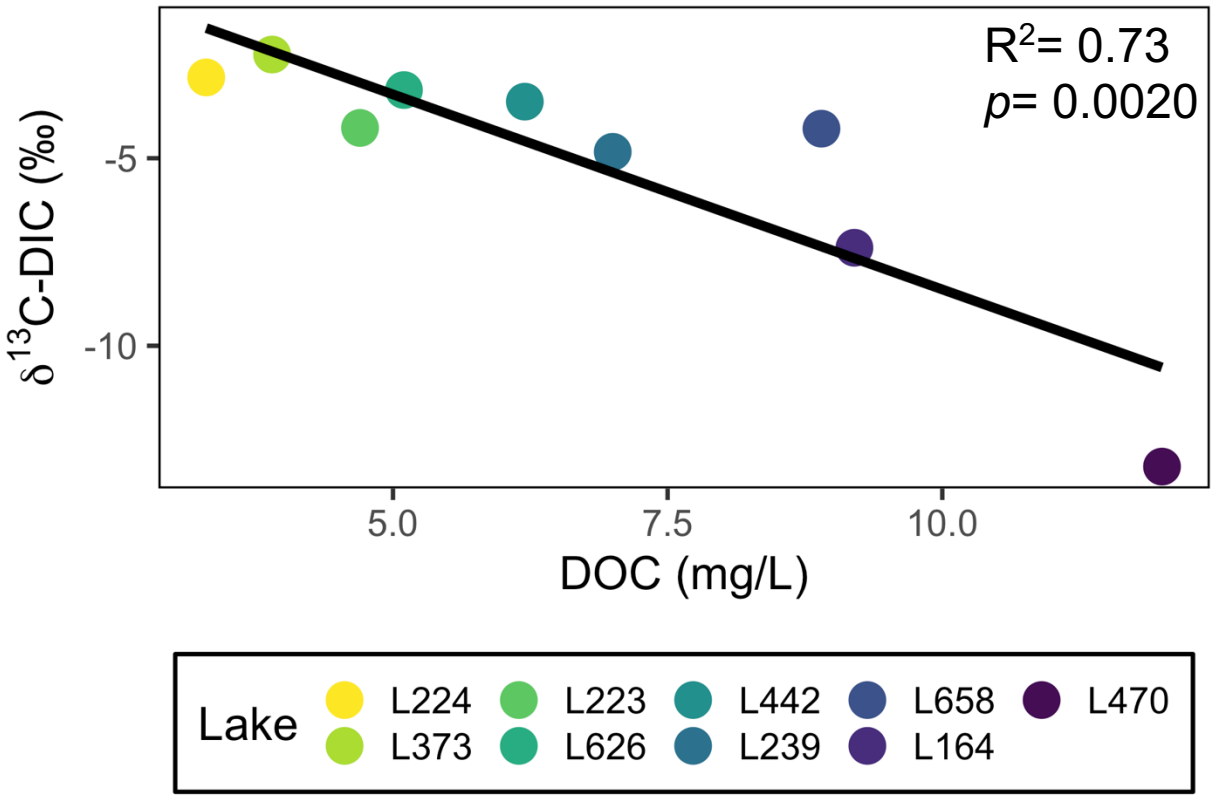

Figure 2.8 Relationship between the mean summer (June-September) surface δ^{13}C-DIC values and mean summer (June-September) surface DOC concentration (mg/L) of the PHISH lakes in the 2018 ice-free season.

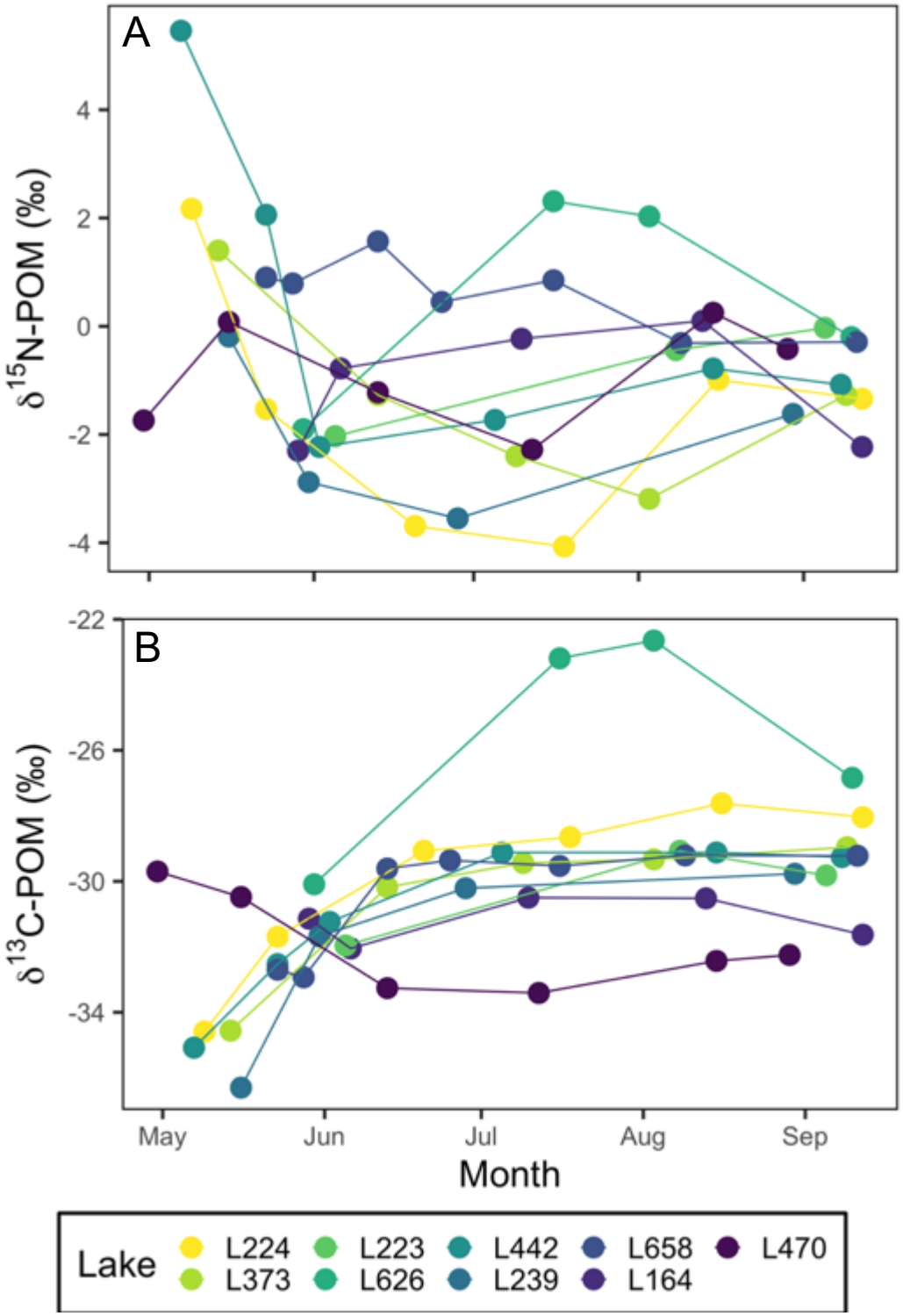

Figure 2.9 A. Surface δ^{15}N-POM values for the PHISH lakes throughout the 2018 ice-free season. **B.** Surface δ^{13}C-POM values for the PHISH lakes throughout the 2018 ice-free season.

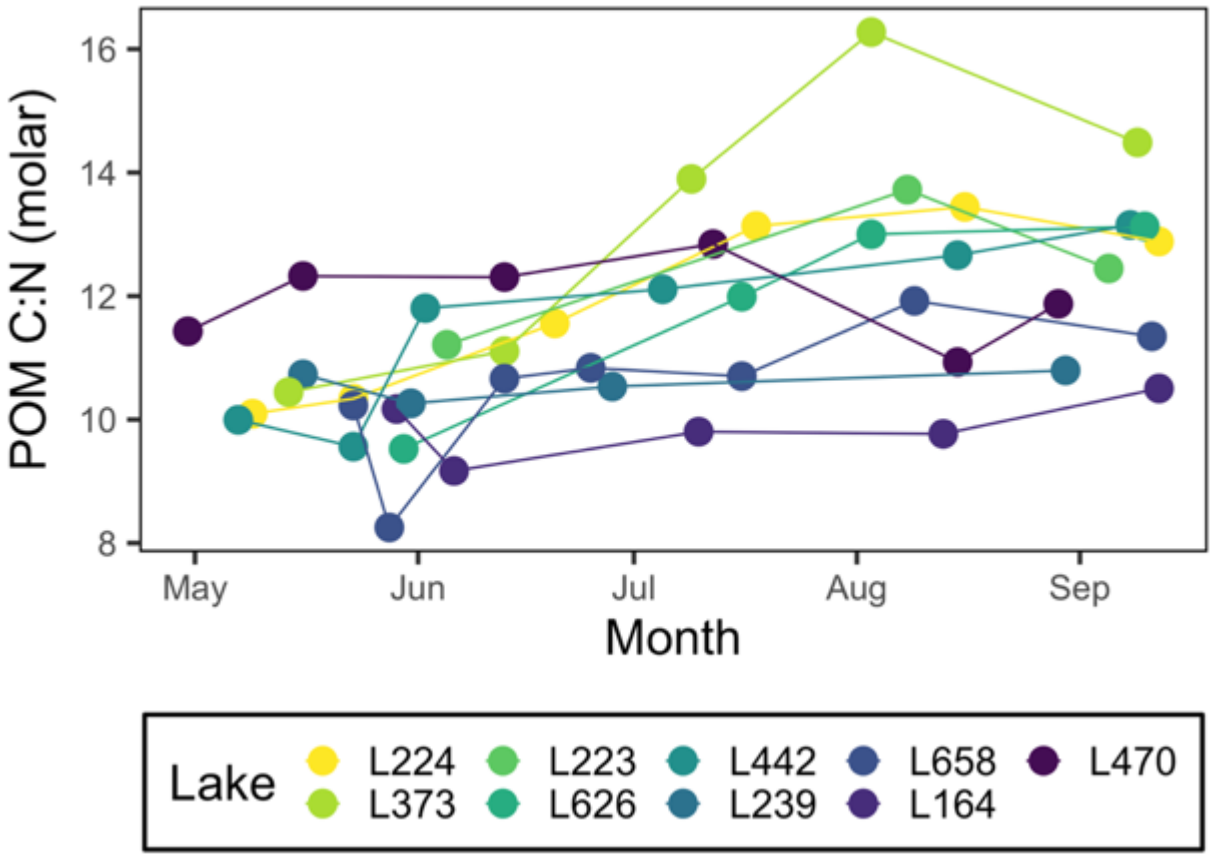

Figure 2.10 Surface molar POM C:N ratios for the PHISH lakes throughout the 2018 field season.

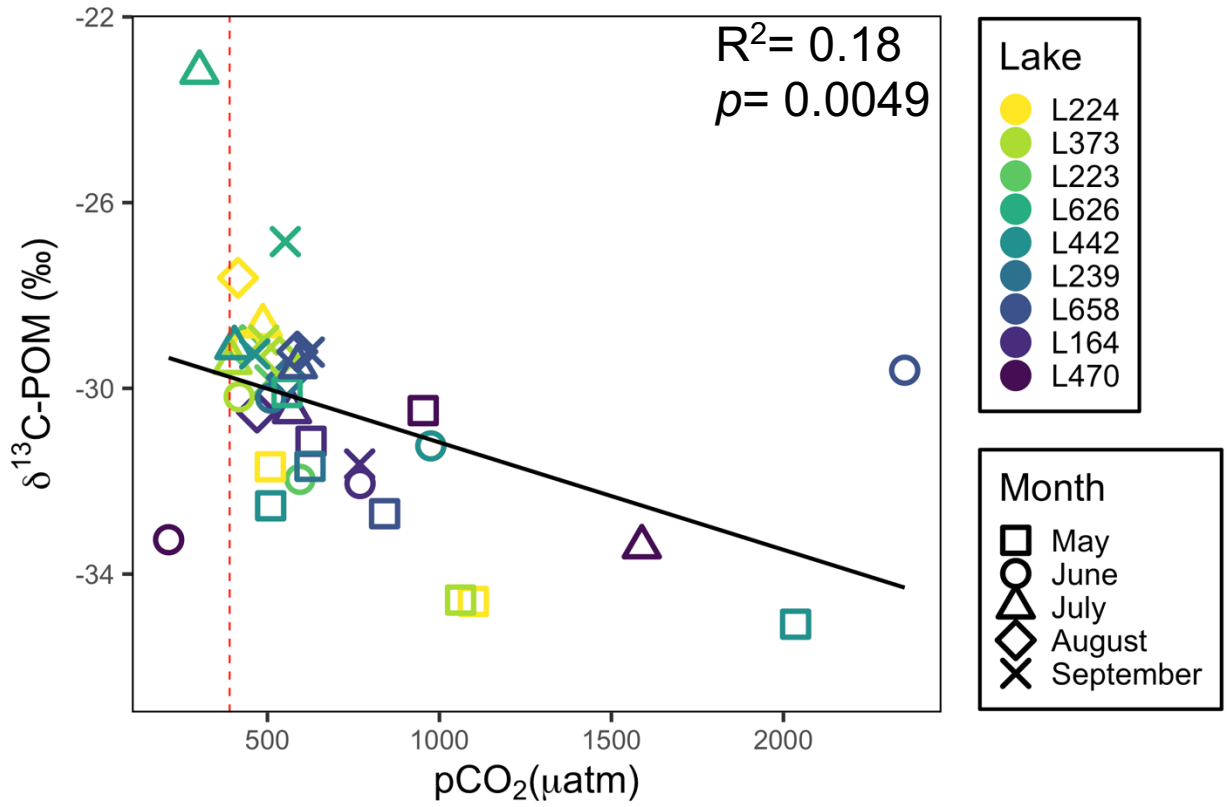

Figure 2.11 Relationship between calculated surface pCO_2 values and surface δ^{13}C-POM values in the 2018 ice-free season. Dashed red line indicates atmospheric equilibrium.

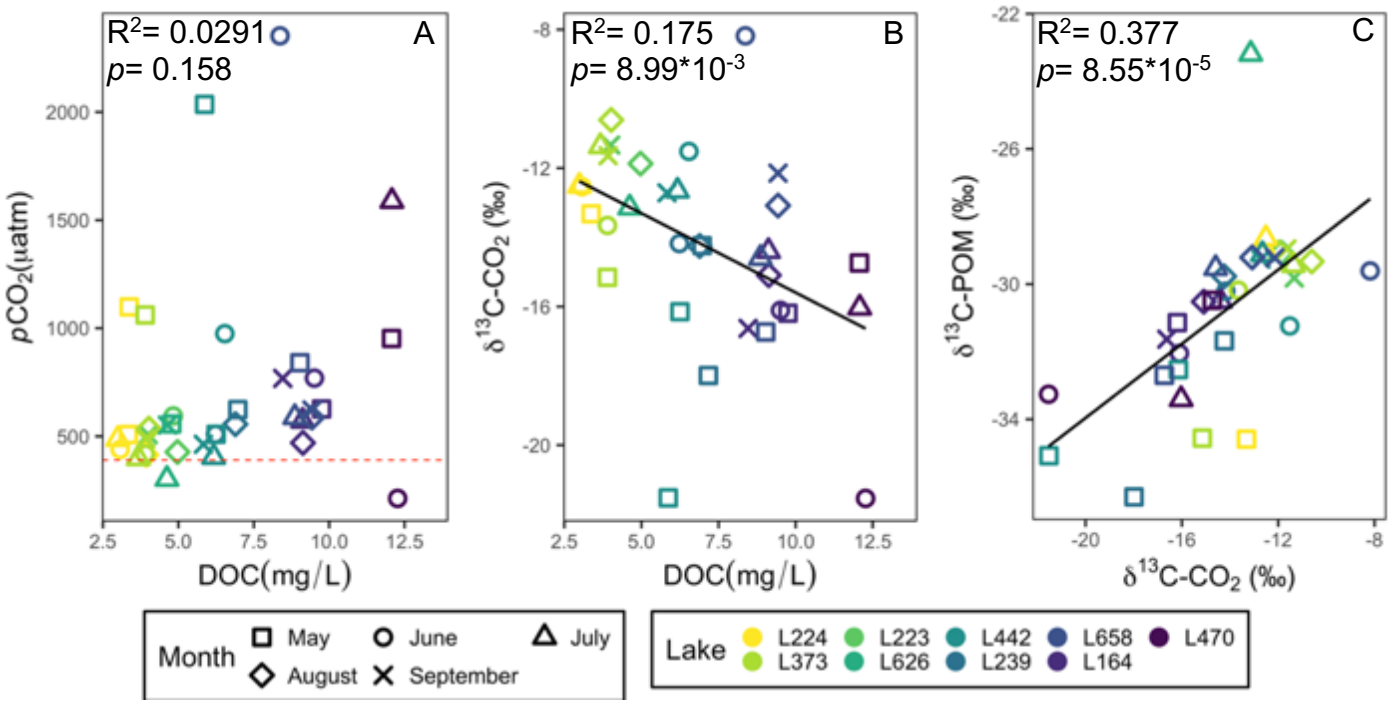

Figure 2.12 A. Relationship between pCO_2 and DOC concentration (mg/L) in the 2018 ice-free season. Dashed red line indicates atmospheric equilibrium. **B.** Relationship between $\delta^{13}C\text{-}CO_2$ and DOC concentration (mg/L) values in the PHISH lakes in the 2018 ice free season. **C.** Relationship between $\delta^{13}C\text{-}CO_2$ values and $\delta^{13}C$-POM values in the PHISH lakes in the 2018 ice-free season.

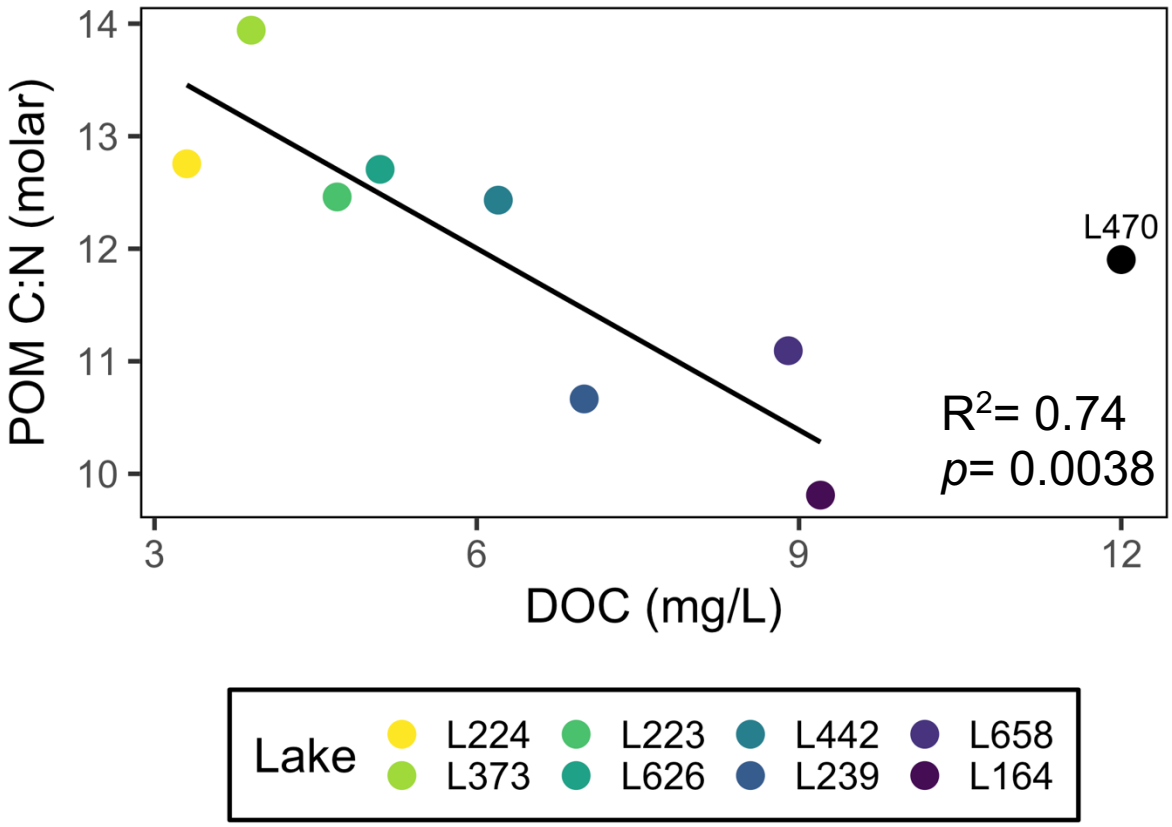

Figure 2.13 Relationship between surface mean summer (June-September) molar C:N ratio of POM and surface mean summer (June-September) DOC concentration (mg/L) in the PHISH lakes in the ice-free season in 2018. L470 was not included in the linear regression.

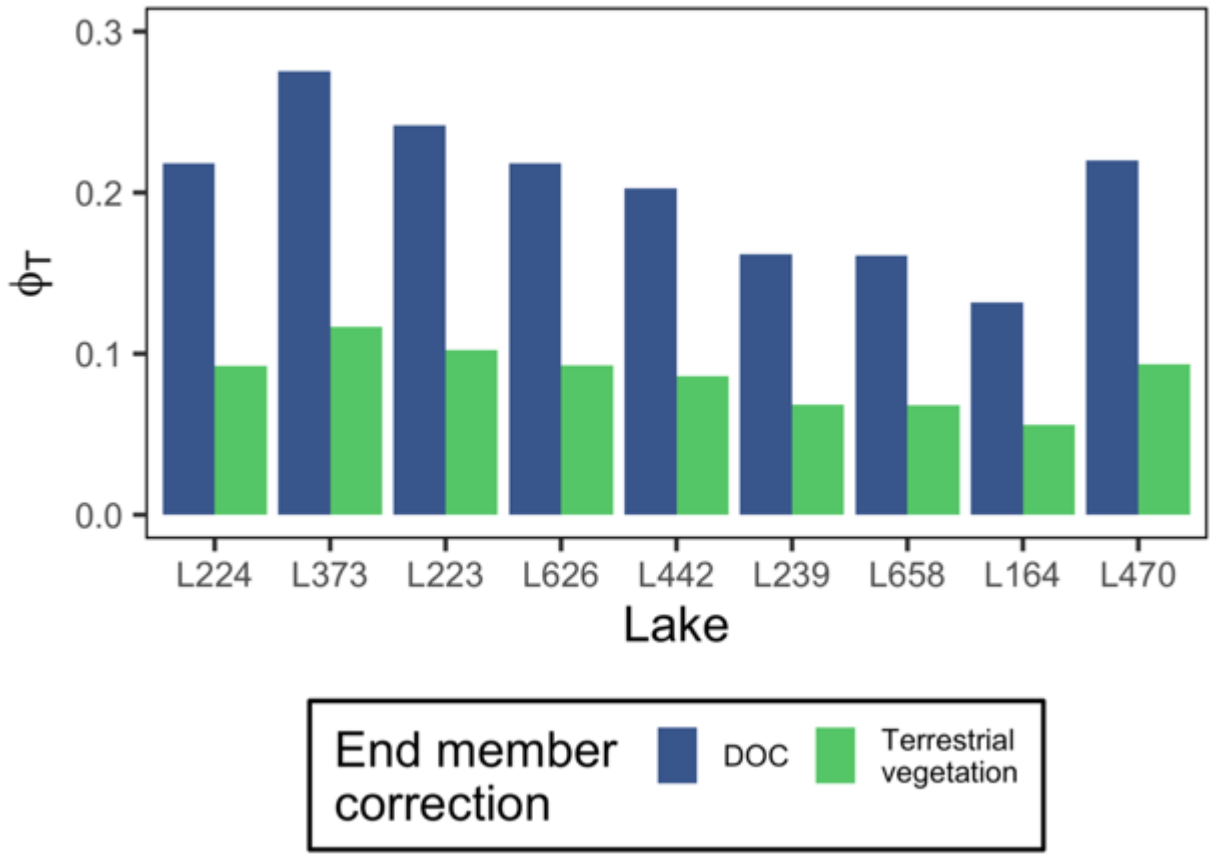

Figure 2.14 Estimated terrestrial fraction (ϕ_T) in mean, surface, bulk POM from the ice-free season for the PHISH lakes calculated from **Equation 2.1** ($\phi_T = \frac{(C{:}N_{POM} - C{:}N_A)}{(C{:}N_T - C{:}N_A)}$).

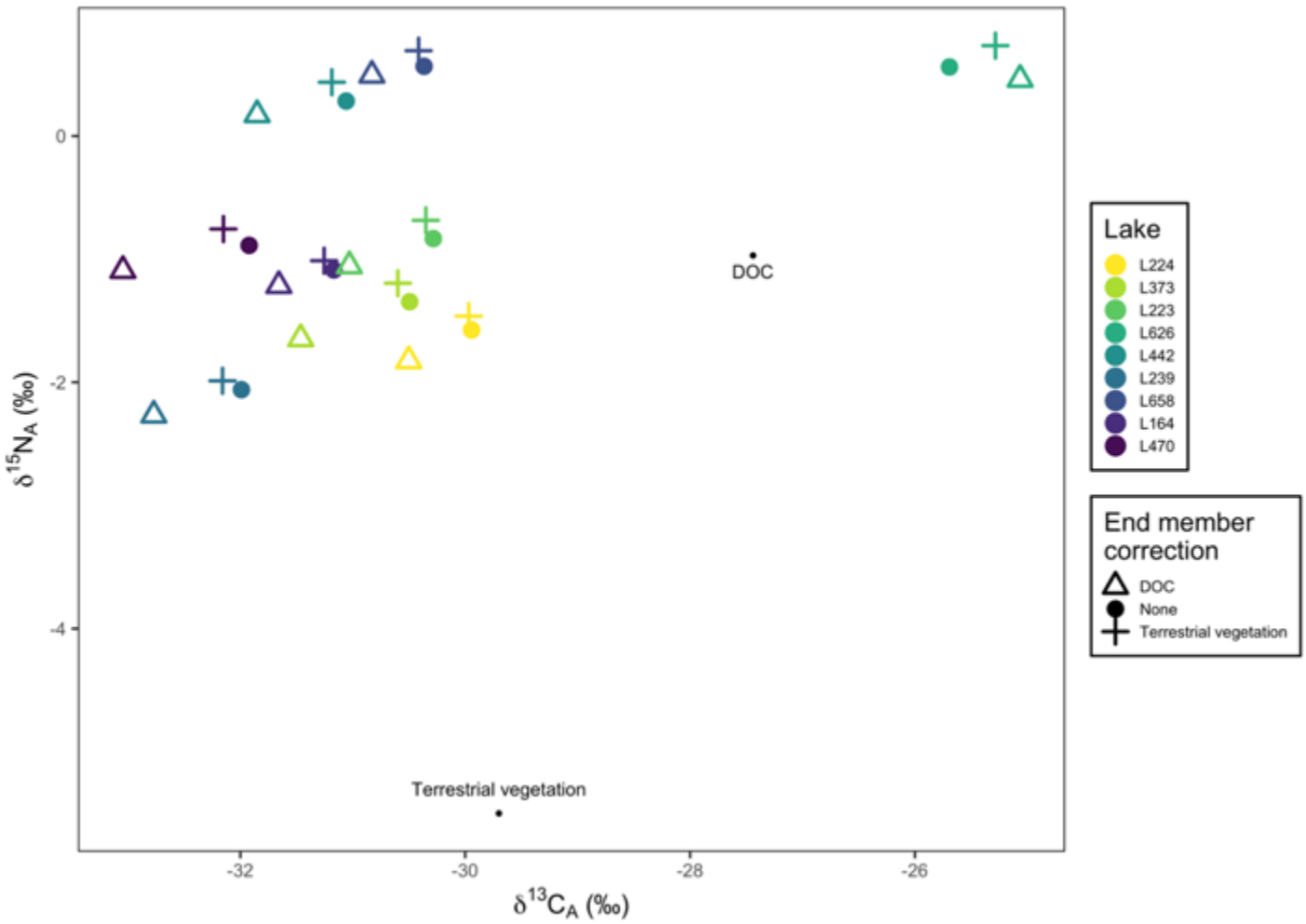

Figure 2.15 Estimated surface $\delta^{13}C$ and $\delta^{15}N$ values of phytoplankton ($\delta^{13}C_A$, $\delta^{15}N_A$) calculated from **Equation 2.2** ($\delta^{13}C_A = \frac{\delta^{13}C_{POM} - (\phi_T \times \delta^{13}C_T)}{(1 - \phi_T)}$) and **Equation 2.3** ($\delta^{15}N_A = \frac{\delta^{15}N_{POM} - (\phi_T \times \delta^{15}N_T \times 0.3)}{(1 - \phi_T \times 0.3)}$) respectively. Values where no end member correction is applied represent mean, surface, bulk POM samples for each lake from the 2018 ice-free season.

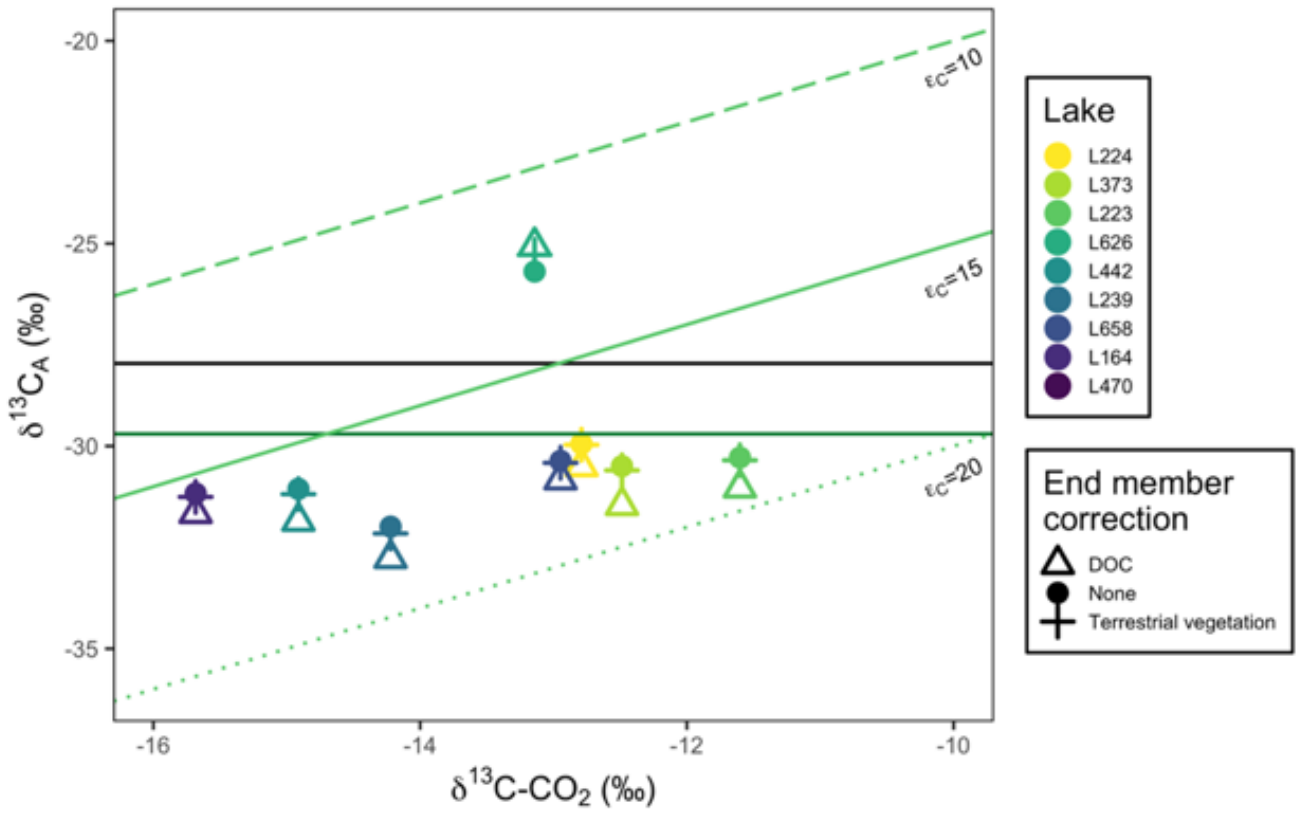

Figure 2.16 Relationship between the mean calculated $\delta^{13}CO_2$ values for the 2018 ice-free season and estimated $\delta^{13}C$ values of phytoplankton ($\delta^{13}C_A$). $\delta^{13}C_A$ values were calculated from **Equation 2.2** ($\delta^{13}C_A = \frac{\delta^{13}C_{POM} - (\phi_T \times \delta^{13}C_T)}{(1 - \phi_T)}$) and **Equation 2.3** ($\delta^{15}N_A = \frac{\delta^{15}N_{POM} - (\phi_T \times \delta^{15}N_T \times 0.3)}{(1 - \phi_T \times 0.3)}$) respectively. Values where no end member correction is applied represent mean, bulk POM samples for each lake. The solid black line represents mean of $\delta^{13}C$ value of DOC in the sampled lakes. The solid, horizontal dark green line represents the stable isotopic values of terrestrial vegetation (Boudreau 2000, Tonin 2019). The ε_C values used are the same as those utilized by Wilkinson et al. (2013b) and are based on various reported ε_C in (Bade et al. 2006, Mohamed and Taylor, 2009).

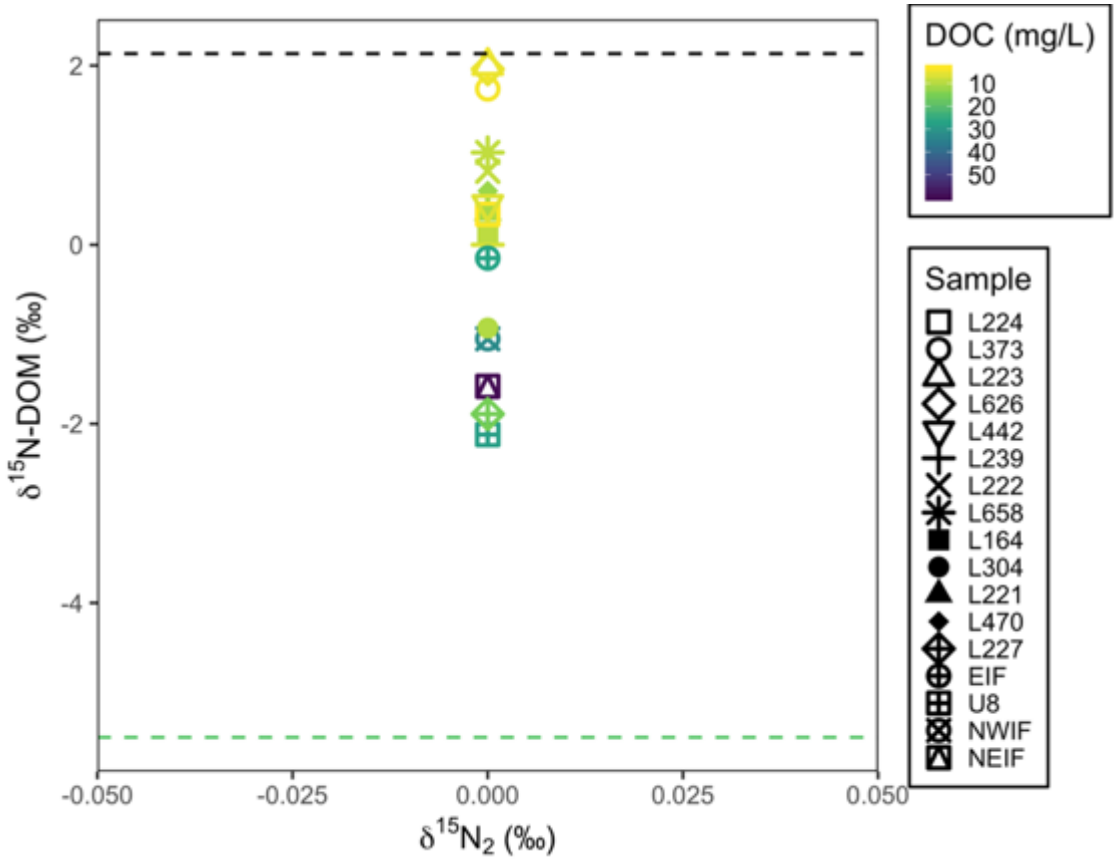

Figure 2.17 Relationship between surface $\delta^{15}N_2$ and $\delta^{15}N$-DOM values of sampled lakes and streams. The black dashed line represents the mean surface $\delta^{5}N$ value of DOC in the sampled lakes. The green dashed line represents the mean $\delta^{5}N$ of terrestrial vegetation (Boudreau 2000, Tonin 2019).

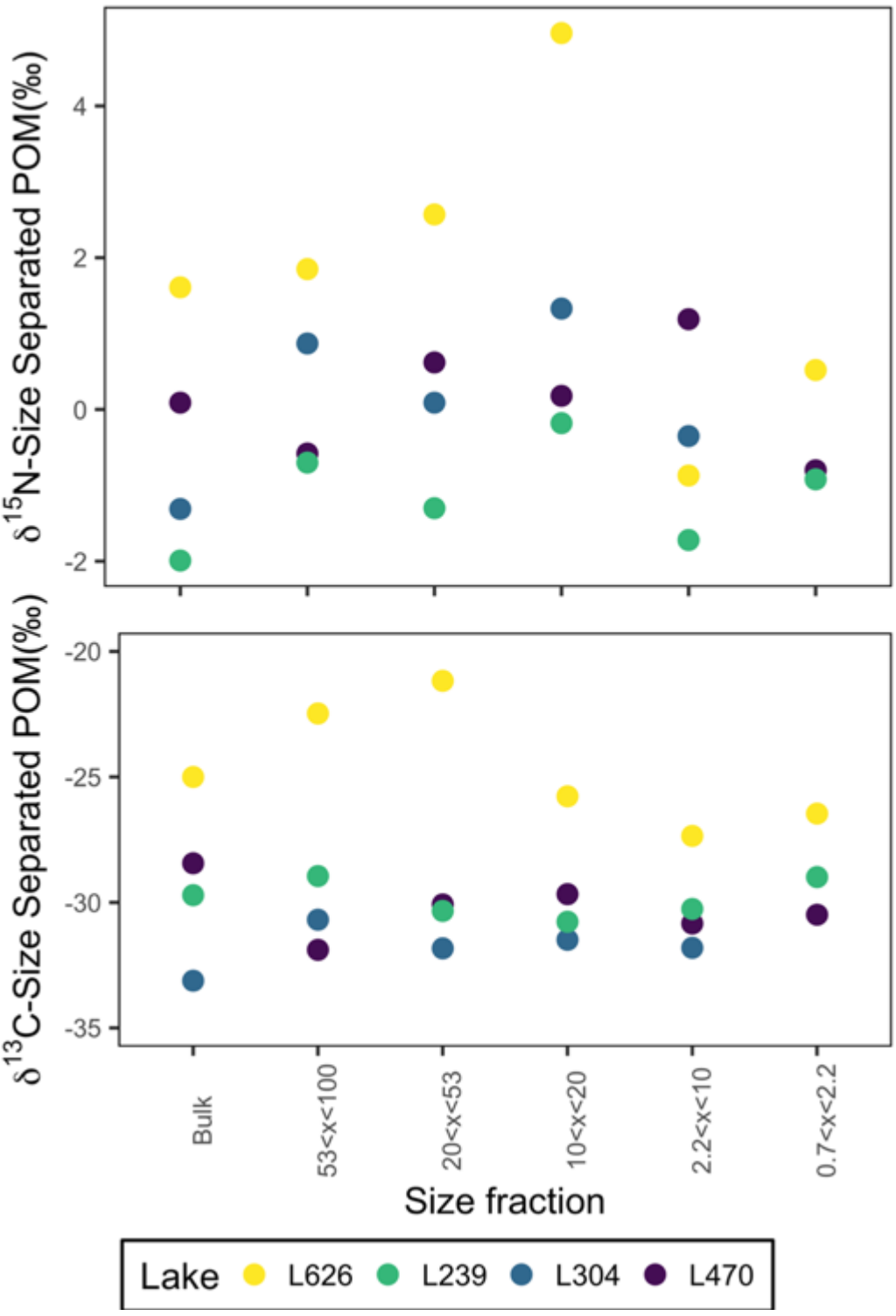

Figure 2.18 A. Surface $\delta^{15}N$ values for size separated (μm) POM. **B.** Surface $\delta^{13}C$ values for size separated (μm) POM. For this figure and all preceding size separation figures, size fractions are presented in descending order.

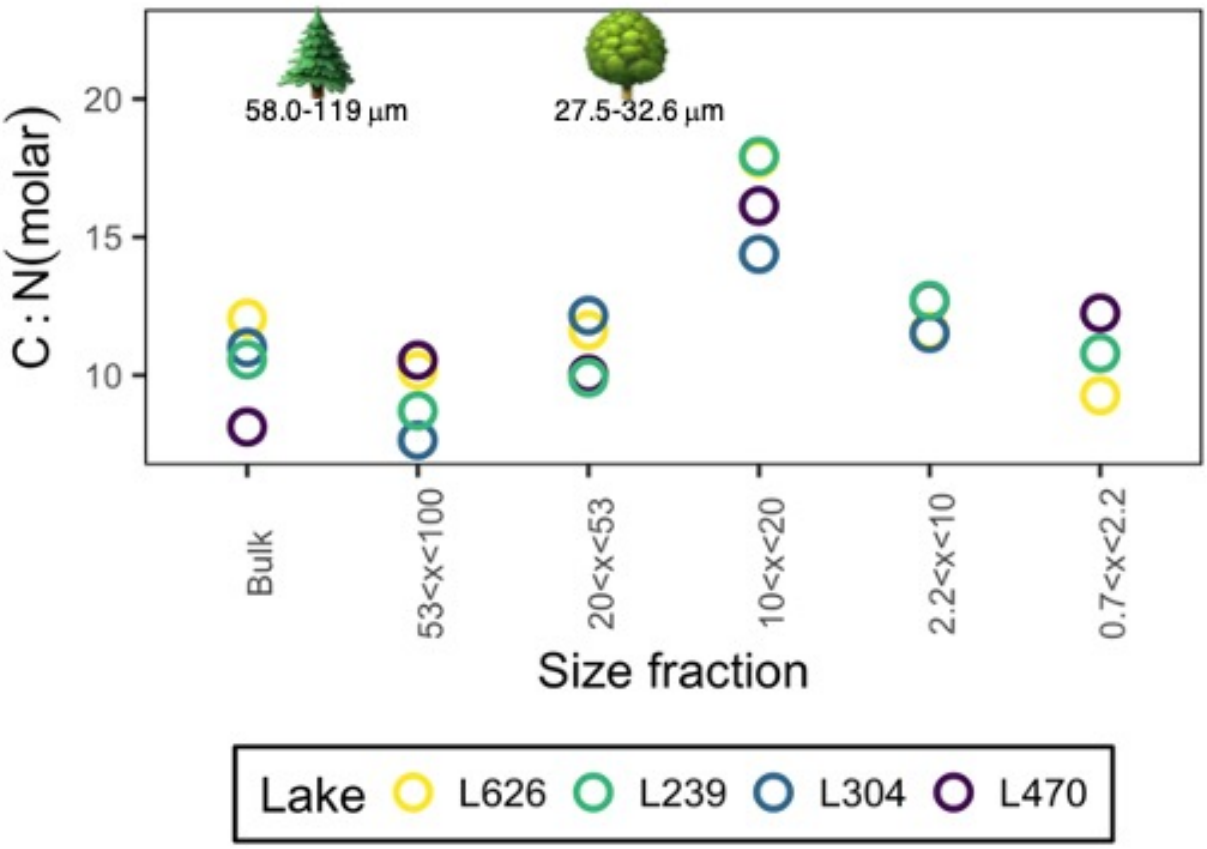

Figure 2.19 C:N ratios (molar) for surface size separated (µm) POM. Ranges for pollen grains of typical coniferous (Bassett et al. 1978) and deciduous (Bassett et al. 1978, Crompton and Wojtas 1993, Sawara 2007) species present at IISD-ELA. Terrestrial material typically has a C:N ratio >20 (Meyers 1994).

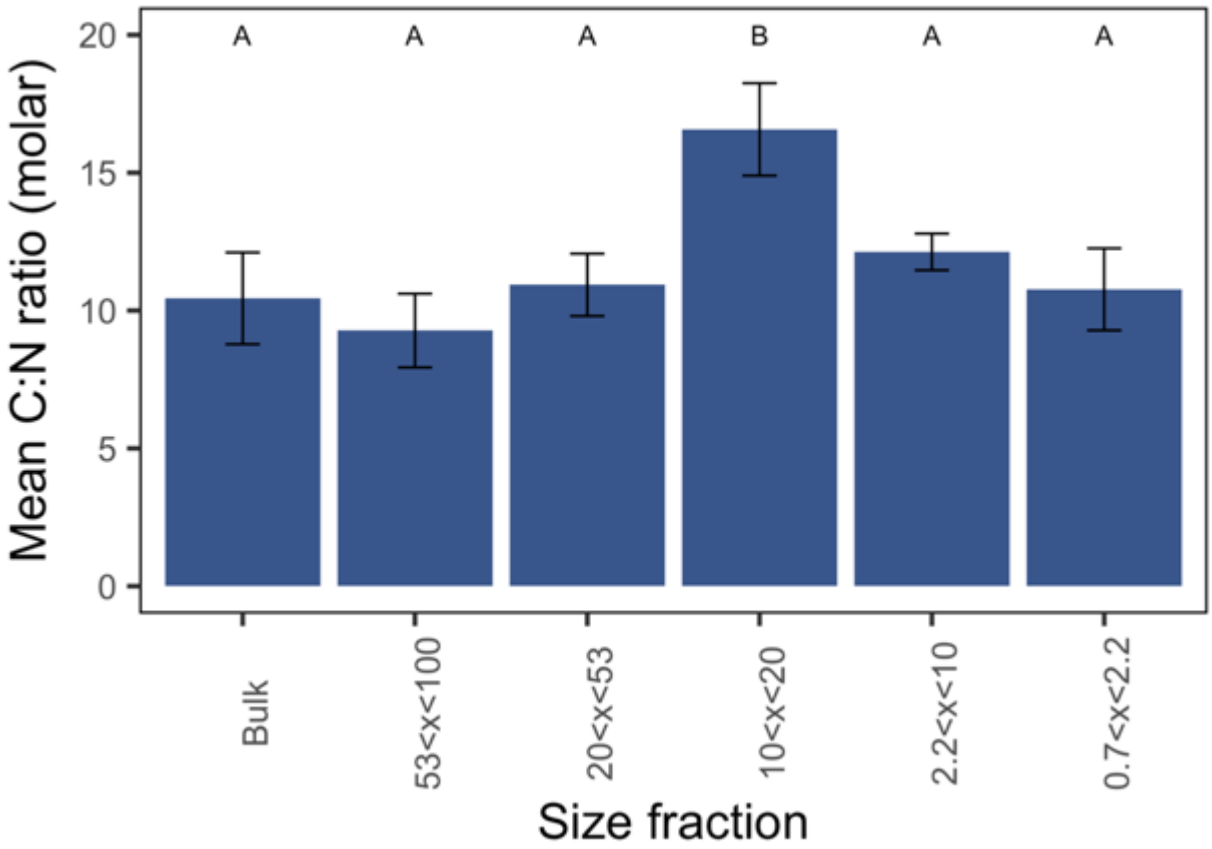

Figure 2.20 Pairwise differences between mean surface C:N ratios for each size fraction (μm). Lakes are combined for each size fraction. Letters A and B indicate that there is no statistical significance in molar C:N ratios within the group, but there are statistically differences between letter groups. Error bars represent +/- one standard deviation.

Table 2.4 Ranges of $\delta^{13}C$, $\delta^{15}N$, and C:N ratio in size separated POM.

Size fraction (μm)	$\delta^{13}C$ value range	$\delta^{15}N$ value range	C:N ratio (molar) range
x< 100 (Bulk)	8.12	3.60	3.35
53< x < 100	9.42	2.43	2.53
20< x < 53	10.66	3.87	2.25
10< x <20	5.72	5.14	7.89
2.2< x <10	4.46	2.91	1.20
0.7< x <2.2	4.03	1.44	2.98

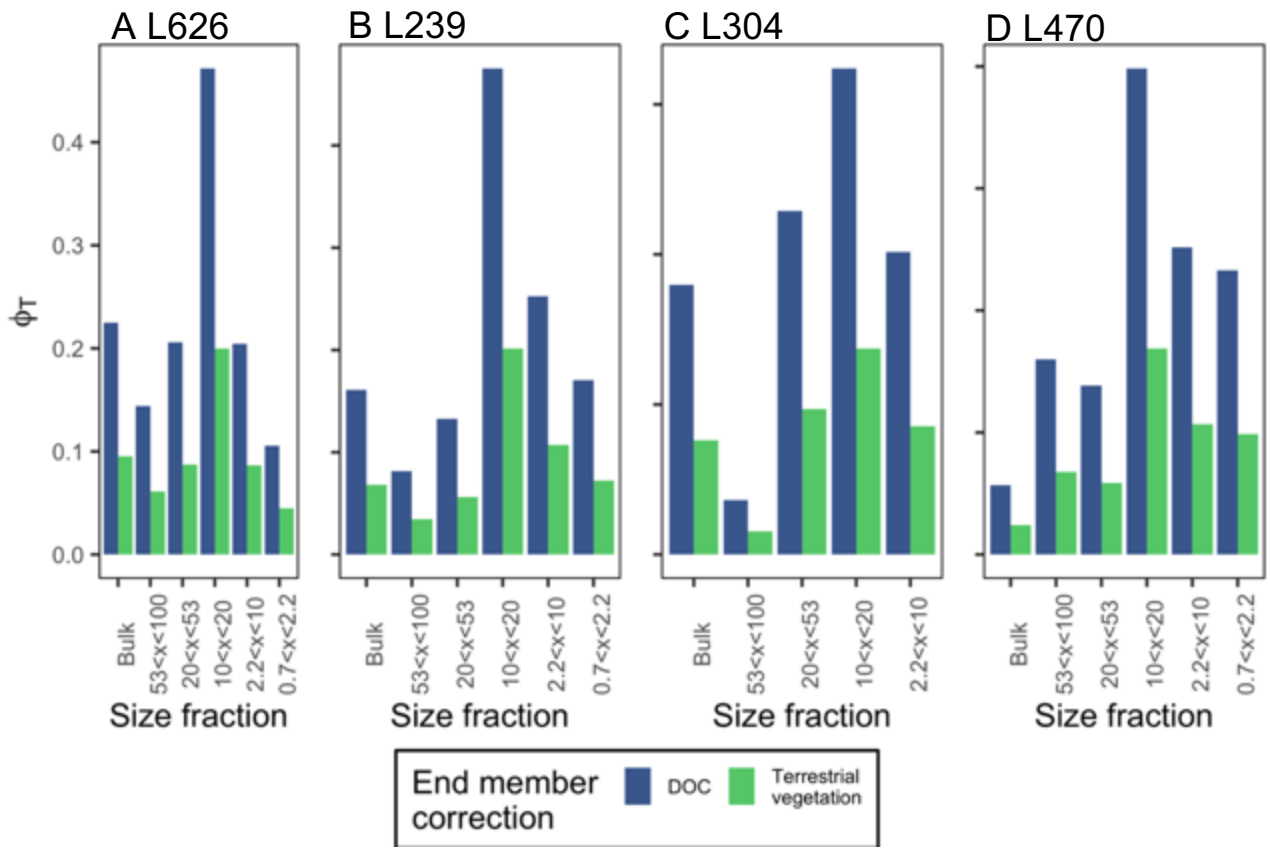

Figure 2.21 Estimated terrestrial fraction (ϕ_T) in surface size separated POM for A. L626, B. L239, C. L304, D. L470, calculated from **Equation 2.1** ($\phi_T = \frac{(C{:}N_{POM} - C{:}N_A)}{(C{:}N_T - C{:}N_A)}$).

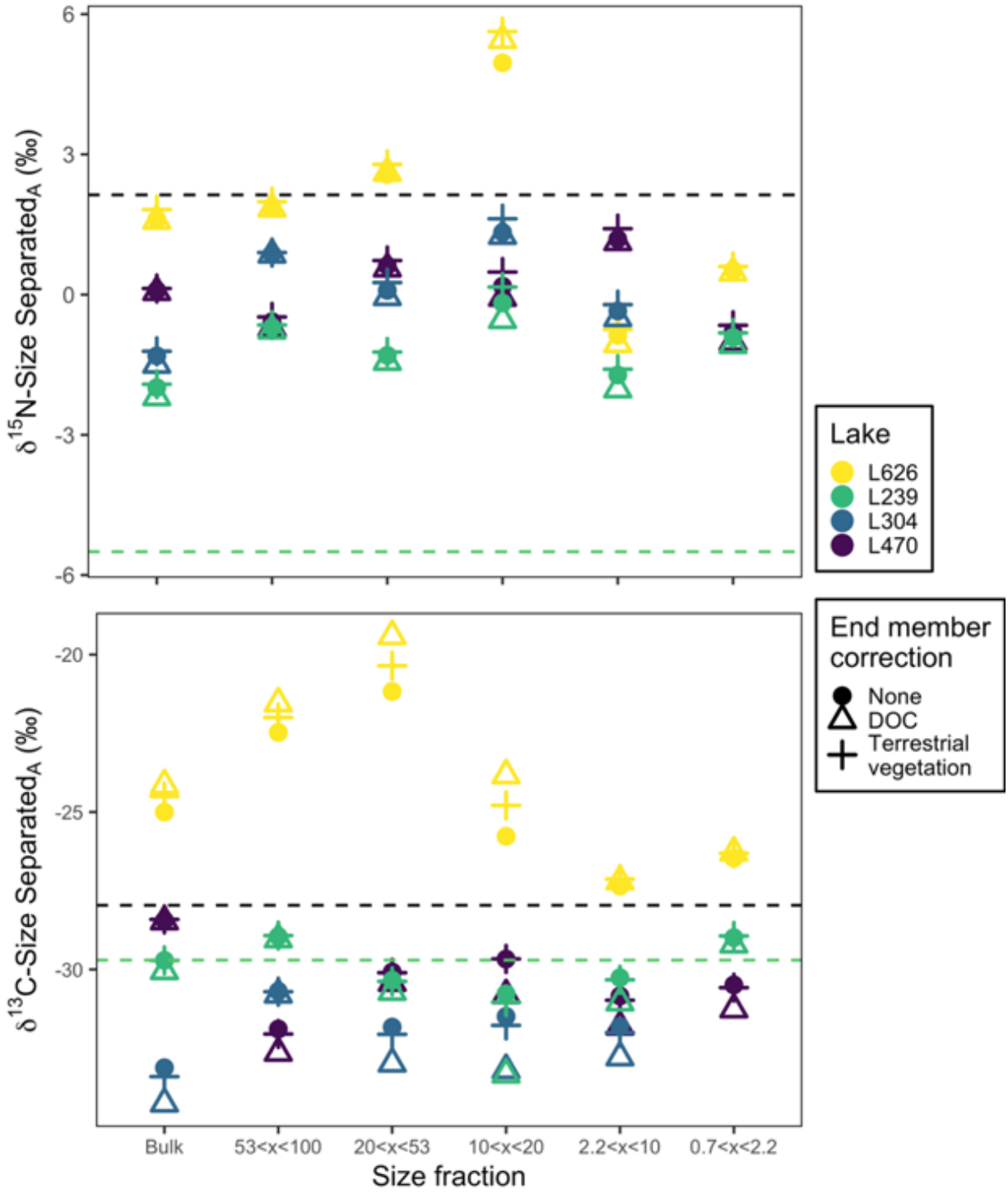

Figure 2.22 Estimated $\delta^{13}C$ and $\delta^{15}N$ values of surface phytoplankton ($\delta^{13}C_A$, $\delta^{15}N_A$) for size separated POM, calculated from **Equation 2.2** ($\delta^{13}C_A = \frac{\delta^{13}C_{POM} - (\phi_T \times \delta^{13}C_T)}{(1 - \phi_T)}$) and **Equation 2.3** ($\delta^{15}N_A = \frac{\delta^{15}N_{POM} - (\phi_T \times \delta^{15}N_T \times 0.3)}{(1 - \phi_T \times 0.3)}$) respectively.. The black dashed line represents the stable isotopic values of surface DOC. The green dashed line represents the stable isotopic values of terrestrial vegetation (Boudreau 2000, Tonin 2019).

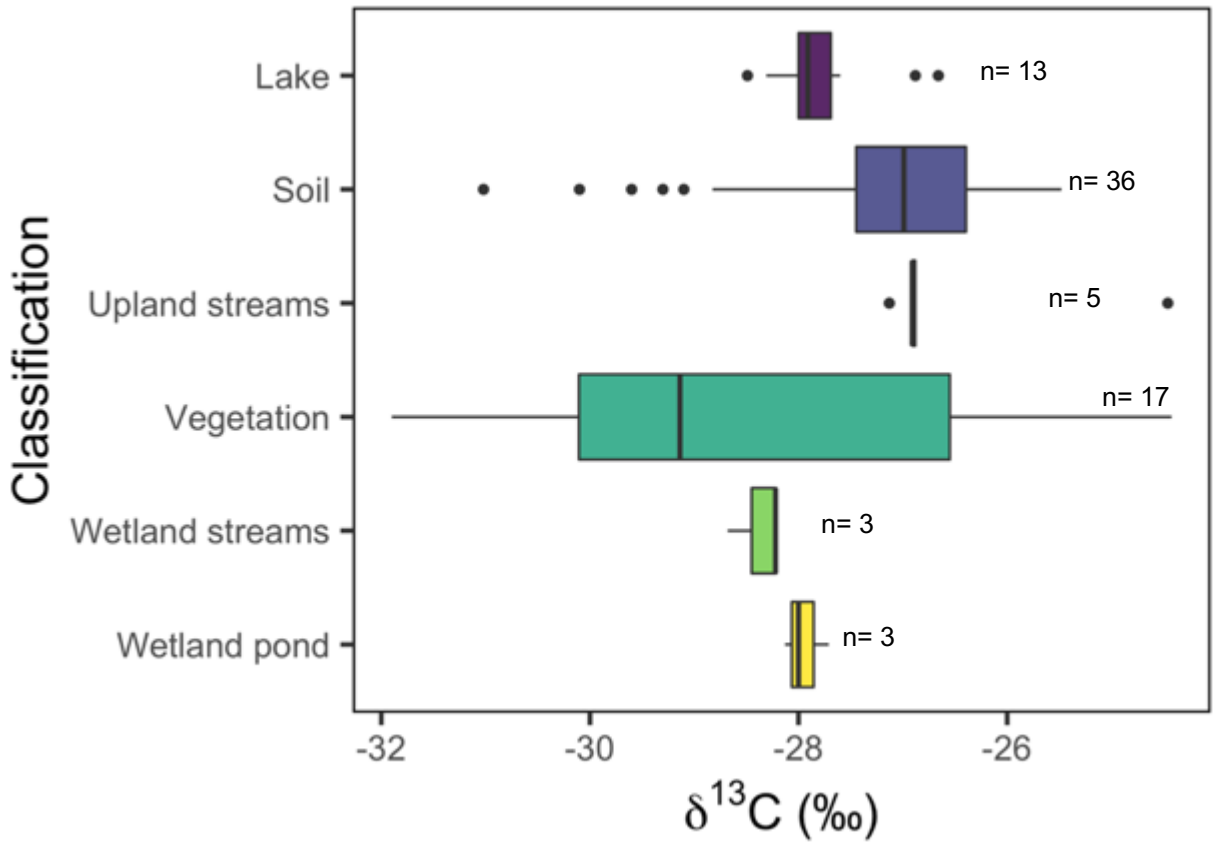

Figure 2.23 Historical ranges of δ^{13}C-DOM across different terrain classifications at IISD-ELA. Lake, wetland stream, and wetland pond data was taken from surface water. Soil data represents the range of δ^{13}C values across soil layers at IISD-ELA. Vegetation data encompasses a range of species typical at IISD-ELA. Additional data for soil, upland streams, vegetation, wetland streams, and wetland ponds from (Boudreau 2000, Ferguson 2000, Baril 2001, Venkiteswaran 2008).

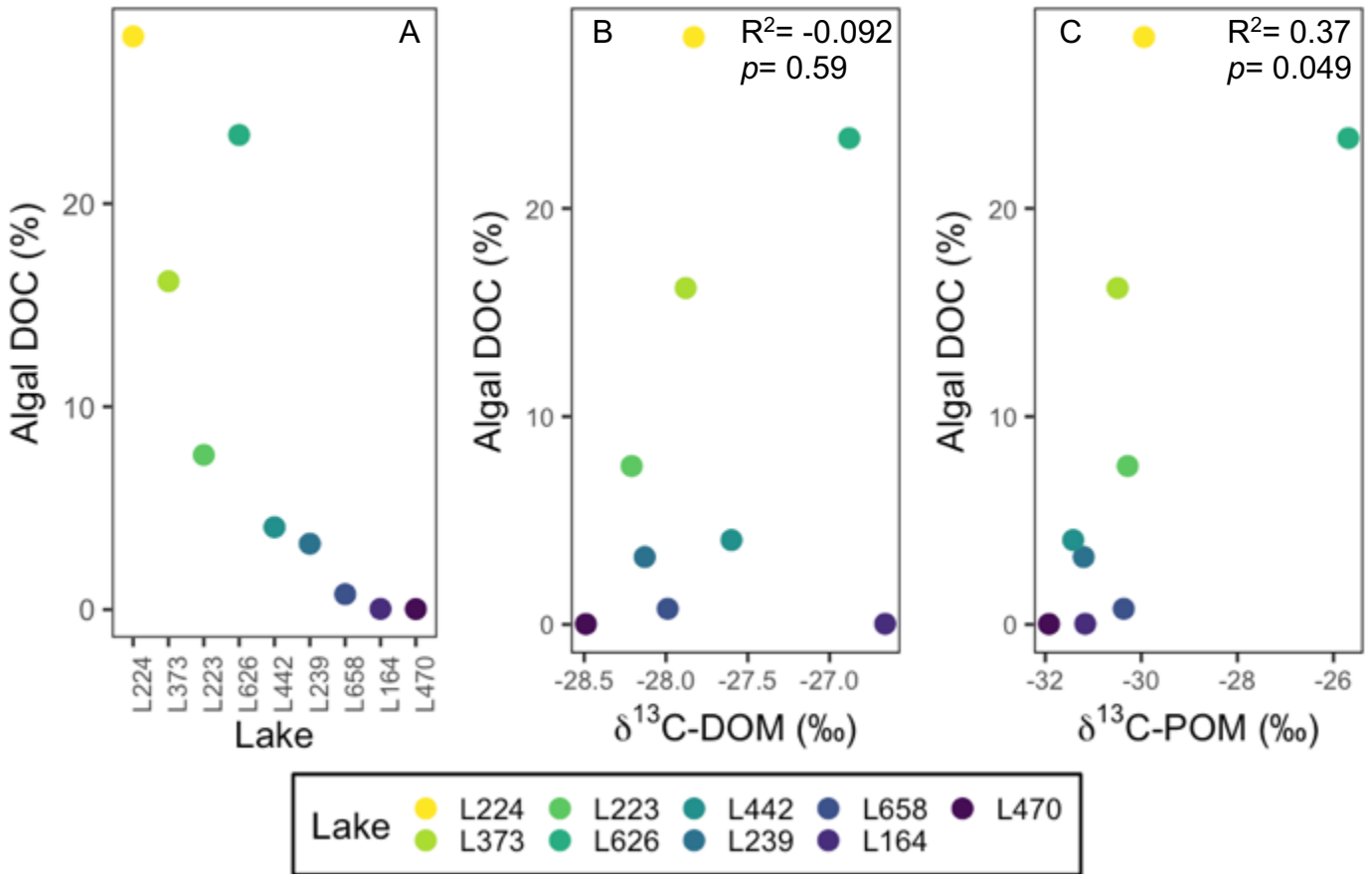

Figure 2.24 A. Percent of DOC comprised of algal material as calculated by **Equation 2.4** (% algal DOC = 56.36 x $e^{(-3.73 \times [colour:chl\ a])}$). **B.** Relationship between the calculated percentage of algal DOC and δ^{13}C-DOM values in PHISH lake surface water. **C.** Relationship between the calculated percentage of algal DOC and δ^{13}C-POM values in PHISH lake surface water.

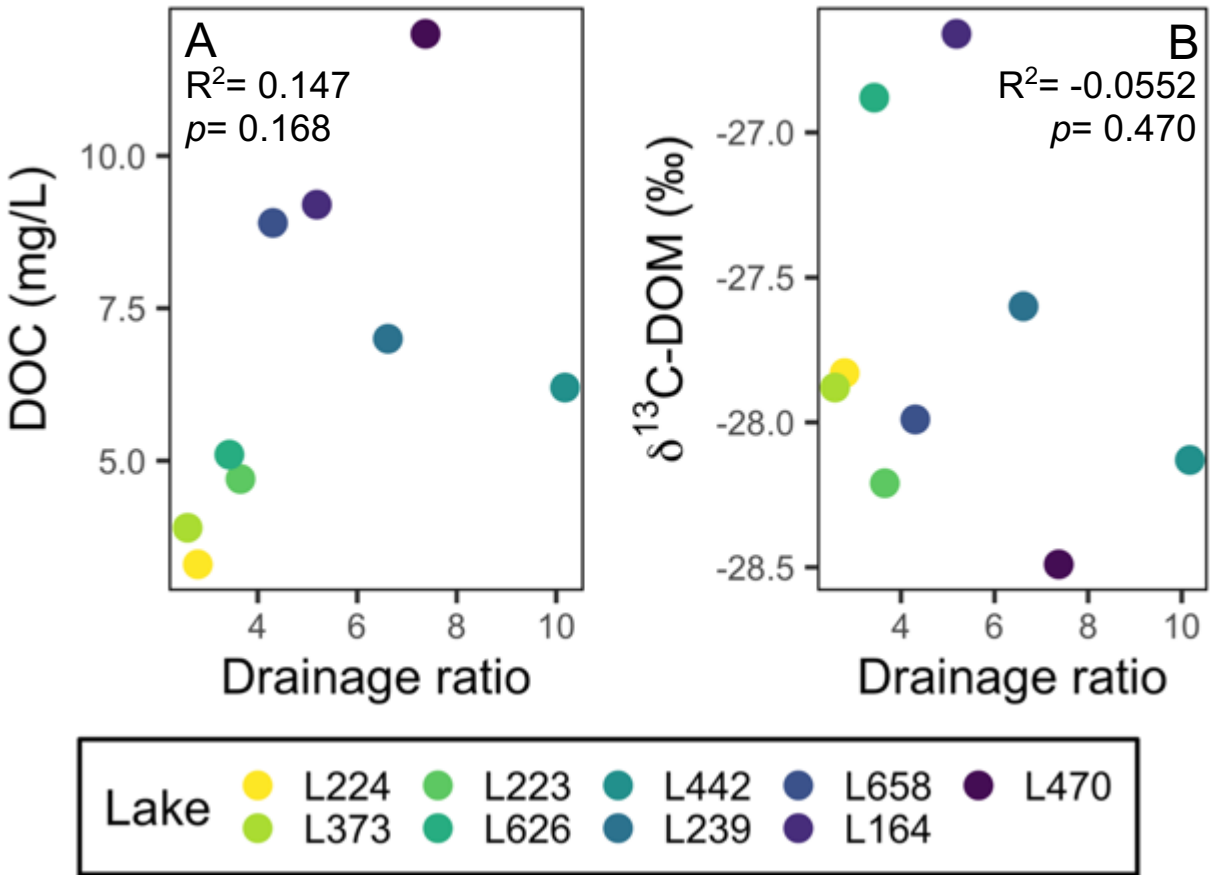

Figure 2.25 A. Relationship between DOC concentration (mg/L) and drainage ratio in the PHISH lakes. **B.** Relationship between surface δ^{13}C-DOM values and drainage ratio in the PHISH lakes.

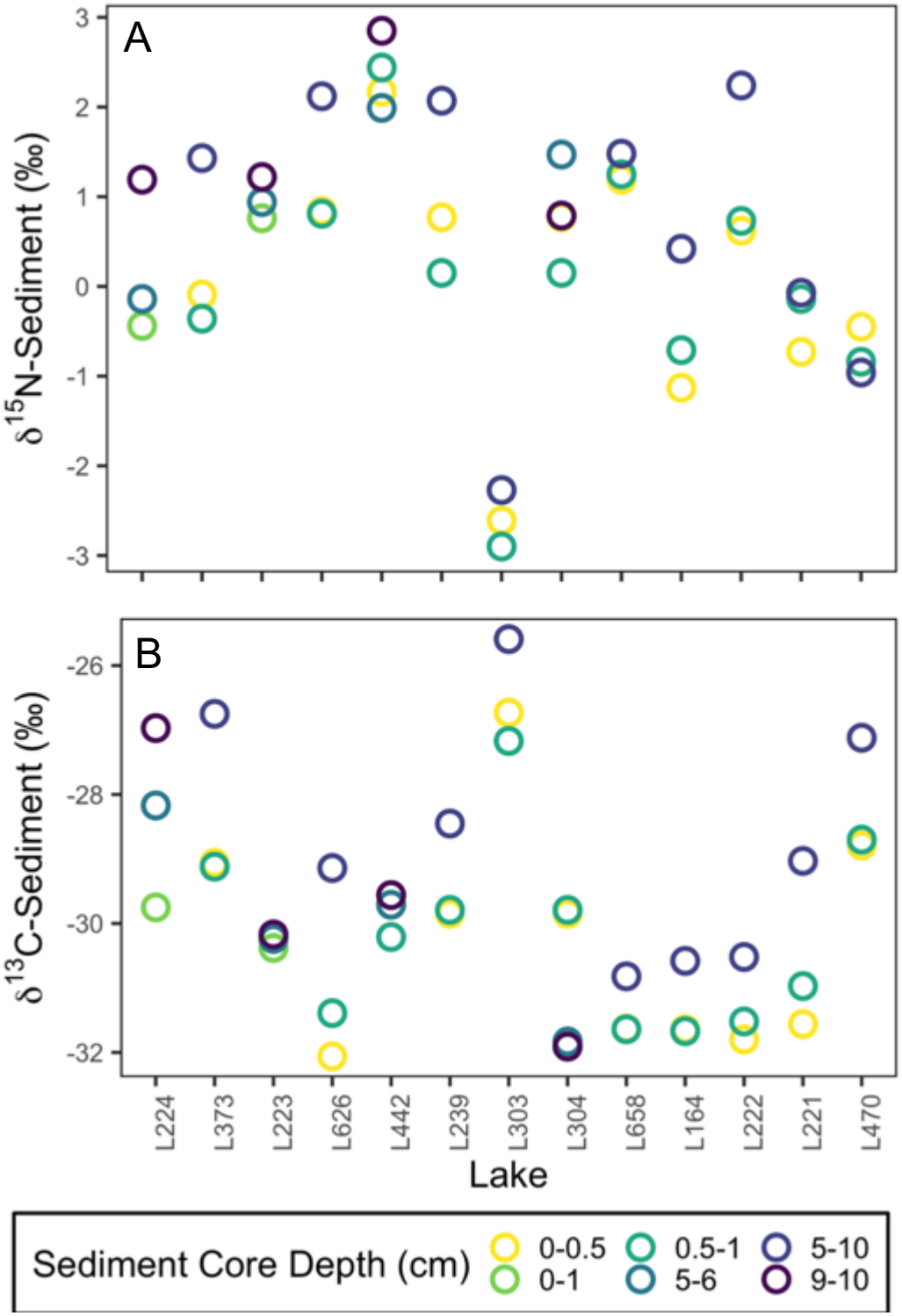

Figure 2.26 A. δ^{15}N-sediment values. **B.** δ^{13}C-sediment values. For this figure and all preceding sediment figures, darker colours indicate deeper core sections.

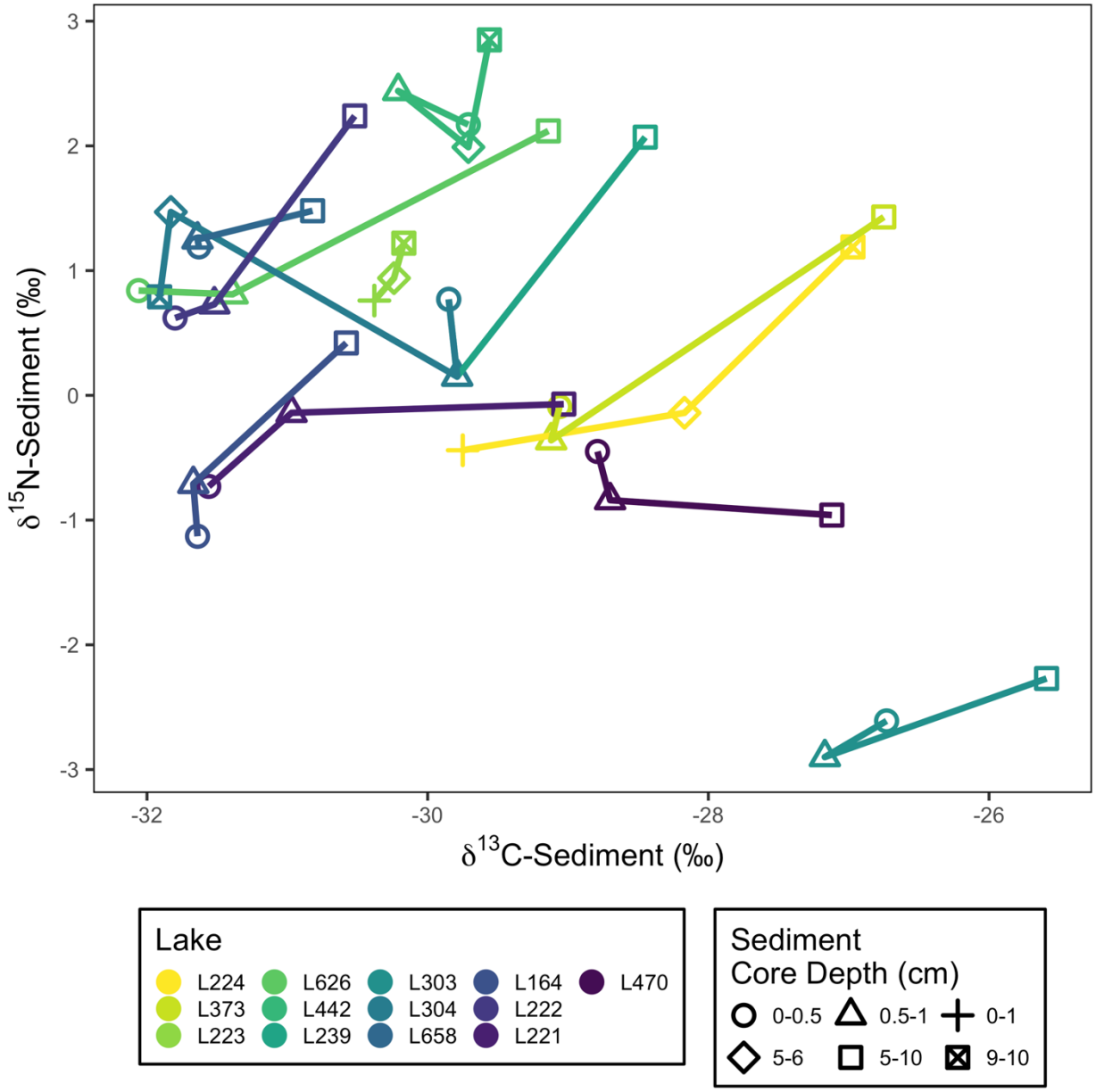

Figure 2.27 Relationship between δ^{15}N-sediment values and δ^{13}C-sediment values.

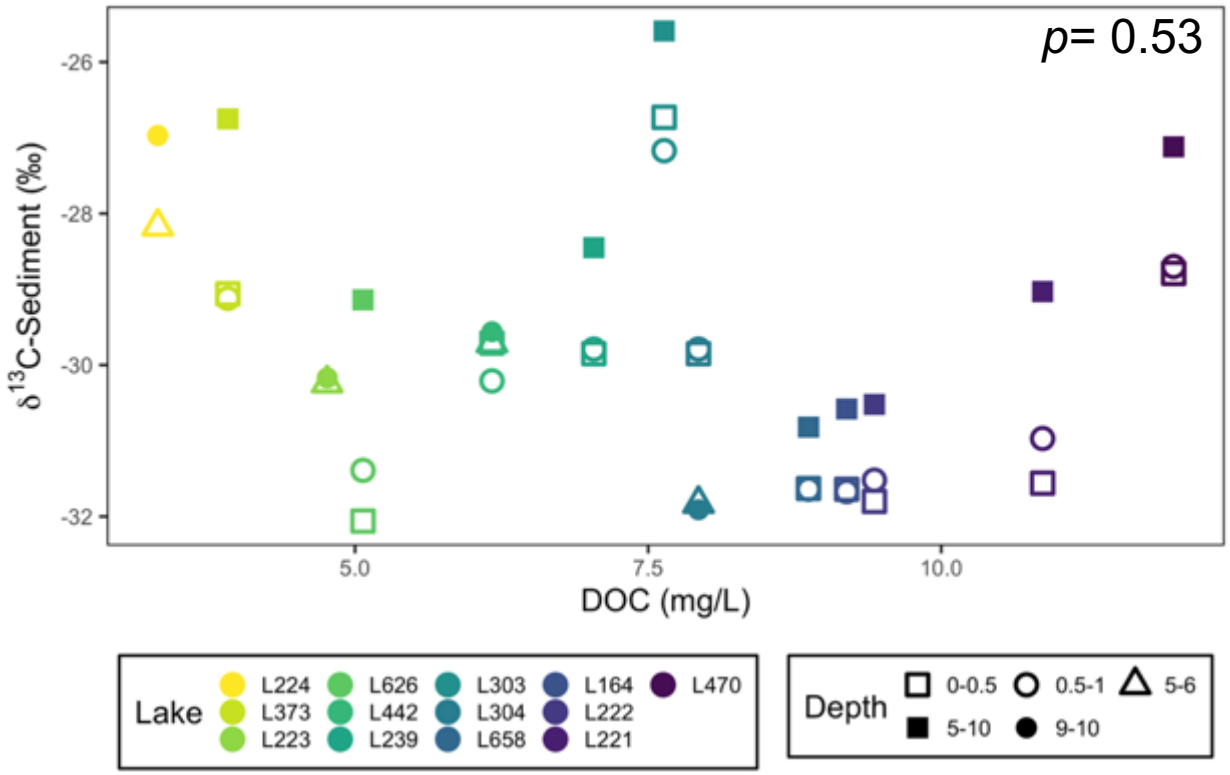

Figure 2.28 Relationship between DOC concentration (mg/L) and δ^{13}C-sediment values. Results of a linear mixed-effects model show that there is no significant the effect of DOC on the δ^{13}C-sediment values at depth within the sediment core.

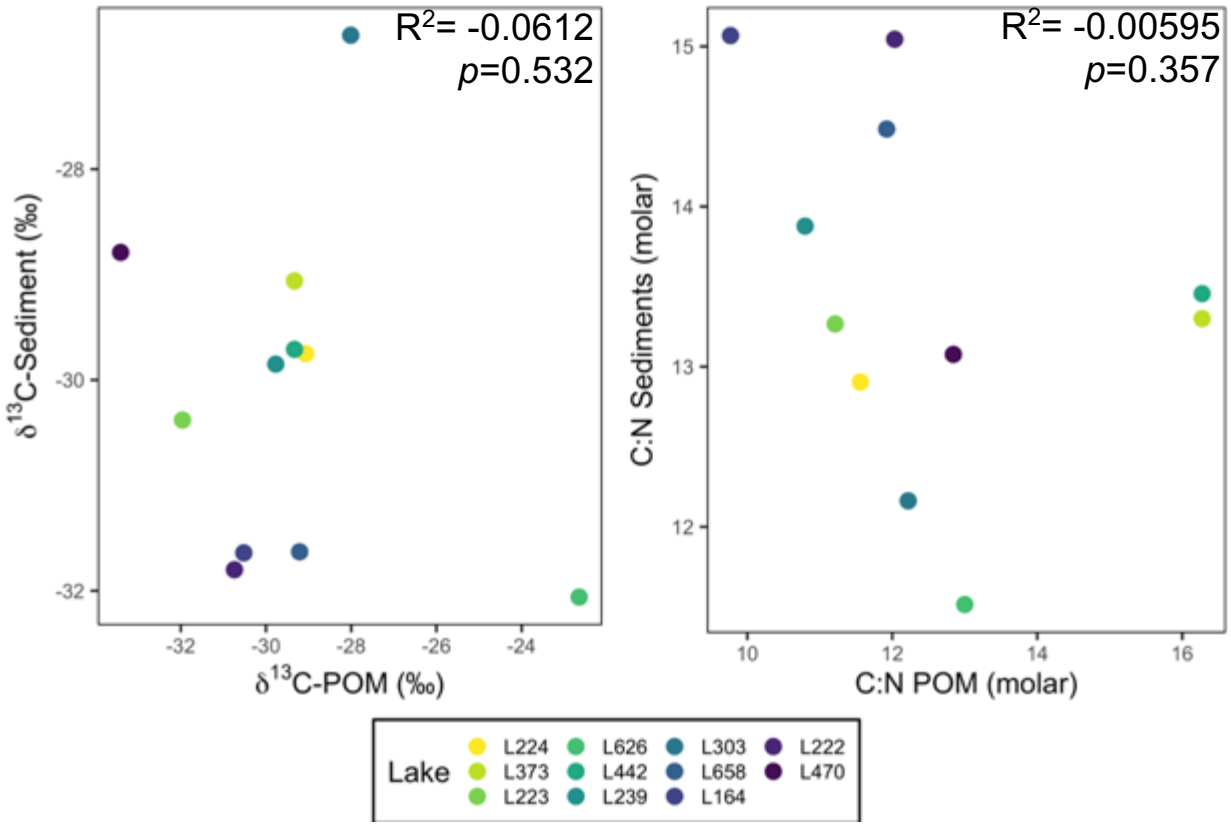

Figure 2.29A. Relationship between δ^{13}C-POM values and surface δ^{13}C-sediment values. **B.** Relationship between the C:N ratio of POM and C:N ratio of surface sediments.

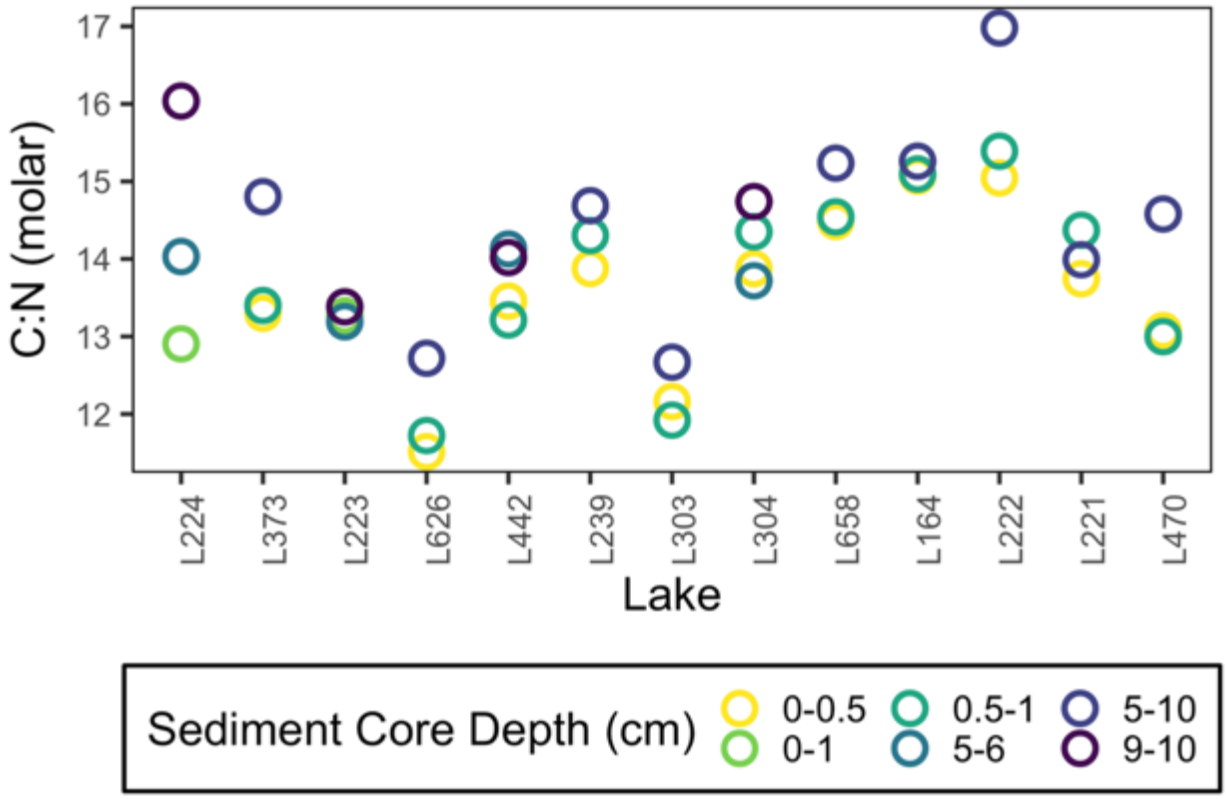

Figure 2.30 Molar C:N ratios for sediment cores.

Chapter 3. Partitioning terrestrial and aquatic energy flows using δ^2H values

3.1 Introduction

Stable carbon isotopes are widely used to provide information on ecosystem processes and dynamics. One such application is examining the use of terrestrially derived (allochthonous) and in-lake derived (autochthonous) carbon. There can be isotopic differences between aquatic and terrestrial vegetation that allow for the use of $\delta^{13}C$ values in order to determine if allochthonous carbon is preferentially used over autochthonous carbon in aquatic ecosystems (Grey et al. 2001). However, there are many cases where the $\delta^{13}C$ values of allochthonous material cannot be distinguished from autochthonous material and/or there are large, seasonal fluctuations in the $\delta^{13}C$ values (Bade et al. 2006, Doucett et al. 2007, Karlsson et al. 2012, Wilkinson et al. 2013b). If lakes are dominated by inputs of allochthonous dissolved organic matter (DOM) from the terrestrial environment, then the $\delta^{13}C$ values of terrestrial material cannot be differentiated from DOM (Wilkinson et al. 2013b, Yang et al. 2014). Another complication is that the $\delta^{13}C$ values of phytoplankton change on seasonal timescales due to changes in pH, dissolved inorganic carbon (DIC) concentration, species composition, and the form of DIC used in photosynthesis (HCO_3^- and $CO_{2\,(aq)}$) (Fry and Sherr 1989, Goericke et al. 1994). Therefore, it is advantageous to use additional stable isotopes, especially in the aforementioned cases where $\delta^{13}C$ values between carbon sources do not differ enough (Hondula et al. 2014, Vander Zanden et al. 2016).

Stable hydrogen isotopes (δ^2H) can provide information regarding allochthonous versus autochthonous energy sources (Doucett et al. 2007, Karlsson et al. 2012), methanogenesis pathways (Whiticar 1999) and CH_4 subsidies in food webs (Deines et al. 2009, Vander Zanden et al. 2016). Measuring δ^2H is advantageous due large δ^2H values in sources generated by the large relative mass difference between ^1H and ^2H (Doucett et al. 2007, Deines et al. 2009).

Allochthonous and autochthonous organic matter (OM) are characterized by two end members: organic matter from phytoplankton and terrestrial sources. The hydrogen incorporated into the organic matter of aquatic vegetation and algae originates from environmental water (i.e. the water surrounding the organism). The water utilized in photosynthesis for aquatic plants and algae originates from environmental water, and

since the lighter isotope (^1H) is preferentially used over the heavier isotope (^2H), the δ^2H value of aquatic plant OM is typically much more negative (160-170 ‰) than the surrounding water (Doucett et al. 2007, Solomon et al. 2011, Hondula et al. 2014). In terrestrial plants, transpiration causes plant matter to retain the heavier isotope (^2H), yielding more positive δ^2H values than aquatic primary producers (Roden and Ehleringer 1999, Doucett et al. 2007, Hondula et al. 2014). The δ^2H values of plants vary, depending on the fractionation during the biosynthesis of different tissues (lipids, proteins etc.) (Smith and Epstein 1970, Sessions et al. 1999, Solomon et al. 2009, Soto et al. 2013). These large differences in δ^2H values between aquatic and terrestrial OM illustrate how hydrogen stable isotopes can circumvent some of the problems that arise with stable carbon isotopes when distinguishing between autochthonous and allochthonous carbon sources (Karlsson et al. 2012, Wilkinson et al. 2013b).

Particulate organic matter (POM) in lakes can be composed of terrestrial material, algal material, bacteria, and detritus (Mostofa et al. 2009). Therefore, POM in lakes naturally has a range in δ^2H values between its terrestrial and aquatic sources illustrating the advantages of the use of δ^2H values. The terrestrial end member is often defined by taking the average of stable isotopic values of vegetation sources from the catchment (Cole et al. 2002, Pace et al. 2004, Caraco et al. 2010, Solomon et al. 2011, Wilkinson et al. 2013a, 2013b, Guillemette et al. 2016); **Table 3.1**, **Table 3.2**)

However, the majority of allochthonous organic carbon that enters lakes is not terrestrial vegetation. POM represents less than 10% of terrestrial organic matter inputs to lakes (Wetzel 2001b, Kortelainen et al. 2006). Literature estimates of allochthony therefore may be overestimated because the δ^2H values of terrestrial vegetation are more positive than aquatic OM.

Most terrestrial organic carbon enters freshwater lakes as DOM (Schindler et al. 1997), and DOM represents the largest portion of organic carbon in most lakes. While allochthonous DOM does originate from the terrestrial environment, it is the result of extensive microbial processing. DOM can be transformed through the various reactions within the lake carbon cycle (i.e. sedimentation, photodegradation, and respiration).

There is a need to define end members in aquatic systems, particularly the terrestrial end member which has previously been misidentified due to overestimating the direct inputs of vegetation (e.g. leaves). In this case, the terrestrial end member can

be defined as the DOC entering lakes via inflow streams- the importance of DOC inputs from streams to boreal lakes have been shown by Hall et al. (2018) where 60-75% of lake water inputs came from three inflow streams. Therefore, the goal of this chapter is to:

1. Examine the δ^2H-DOM values in a series of Canadian Shield lakes and streams in comparison to the allochthonous and autochthonous end members.
2. Evaluate the use of δ^2H-DOM values as a method for separating allochthonous and autochthonous inputs to food webs.

3.2 Methods

3.2.1 Study sites

Six boreal lakes (L373, L239, L222, L221, L470, L227) and four small headwater boreal streams (U8, NWIF, EIF, NEIF) were sampled in the 2018 and 2019 (L227) field seasons at the International Institute for Sustainable Development Experimental Lakes Area (IISD-ELA). These lakes represent a subset of the lake DOC gradient studied in **Chapter 2**. A summary of physical and chemical parameters of the study sites can be found in **Table *3.3***. L227 is an experimentally eutrophied lake, and nutrients have been added in various N:P ratios since 1969 (Hecky et al. 1994).

3.2.2 Field sampling

δ^{13}C-DOM and δ^{15}N-DOM samples were filtered using Whatman 0.45 μm syringe tip filters, collected in 250 mL glass serum bottles with a small headspace, capped with rubber stoppers, and acidified using 6 mol/L HCl at the IISD-ELA field station in order to lower the pH to approximately 3. Water for δ^2H-DOM samples was collected in 2 L Nalgene bottles at surface depths in a subset of lakes along the DOC gradient (L373, L239, L222, L221, L470, L227) and in several streams (U8, NWIF, EIF, NEIF), filtered to 0.45 μm with Whatman membrane filters, frozen, and shipped to the University of Waterloo for analysis.

δ^{13}C-DIC samples were collected in duplicate in 60 mL glass serum bottles with no headspace and rubber stoppers. They were then preserved with approximately 5 μL of 100% v/v $ZnCl_2$/ 1 mL of lake water. δ^2H-H_2O samples were collected in the field to 0.45 μm using Whatman syringe tip filters into 30 mL Nalgene bottles with no headspace to prevent evaporation. Samples were subsequently shipped to the University of Waterloo

for analysis. pH samples were collected in 15 mL PET containers with a Hach HQ40d meter and IntelliCAL™ PH301 probe.

3.2.3 Laboratory and stable isotope analysis

Isotopic analysis for stable C isotopes, as well as analysis for δ^2H-H_2O was conducted at the University of Waterloo Environmental Isotope Laboratory. δ^{13}C-DOM and δ^{15}N-DOM samples were freeze dried and weighed into Elemental Microanalysis D1002 tin sample cup (Elemental Analysis Ltd., UK) and analyzed by EA-CF-IRMS using a Carlo Erba Elemental Analyzer and folding into an Elemental Microanalysis D1002 tin sample cup (Elemental Analysis Ltd., UK) (CHNS-O EA1108) coupled with a Delta Plus (Thermo) IRMS (δ^{13}C precision ± 0.2‰, δ^{15}N precision ± 0.3‰). δ^2H-H_2O samples were analyzed by laser absorption spectrometry (LAS) using a Los Gatos Research (LGR) Liquid Water Isotope Analyser (LWIA), model T-LWIA-45-EP (precision δ^2H = ± 0.8 ‰). DOC concentration analysis was conducted using a Shimadzu Total Organic Carbon (TOC-L) analyzer (precision ± 0.3 mg C/L).

δ^2H-DOM samples were first freeze dried at the University of Waterloo then analyzed at the University of Ottawa Ján Veizer Stable Isotope Laboratory for non-exchangeable H using a Thermo Scientific thermal conversion elemental analyzer (TC/EA) (via a Confo IV) with a Costech Zero-blank autosampler (δ^2H precision ± 2‰), following (Doucett et al. 2007). δ^2H-DOM samples of L373, L239, L222, L221, U8, EIF, NEIF, and NWIF were taken in the 2018 field season and L227 was sampled in July 2019. DIC concentration and stable isotope samples were prepared by acidifying, then equilibrating the headspace. Samples were then analyzed by GC-CF-IRMS using an Agilent 6890 GC coupled to an Isochrom isotope ratio mass spectrometer (IRMS: Micromass UK) (δ^{13}C precision ± 0.3‰). DOC concentration analysis was conducted using a Shimadzu Total Organic Carbon (TOC-L) analyzer (precision ± 0.3 mg C/L).

δ^{13}C-CO_2 values were calculated using the "isocalc" package version 1 using measured values for water temperature, pH, and DIC concentration (Henderson, 2018). The δ^2H value of phytoplankton was estimated similar to Tonin (2019) using δ^2H= 160.9 ‰ ±17 (Wilkinson et al. 2013b). The mean δ^2H-H_2O for lake water at IISD-ELA was calculated by taking the average of δ^2H-H_2O for 28 different IISD-ELA lakes. Precipitation

δ^2H-H_2O values for IISD-ELA were obtained from the International Atomic Energy Agency (IAEA) and World Meteorological Organization (WMO) Global Network of Isotopes in Precipitation (GNIP) database (IAEA and WMO 2020).

3.3 Results

3.3.1 δ^2H-DOM, δ^{13}C-DOM, and δ^{15}N-DOM values of lake and inflow streams

The six lake δ^2H-DOM values ranged between -127 ‰ to -104 ‰ **(Figure 3.1)** and the four stream δ^2H-DOM values ranged between -117.5 ‰ and -94.8 ‰ **(Figure 3.1)**. Lake water δ^2H-H_2O values had a mean value of -70.2 ‰ **(Figure 3.1)**. Stream δ^2H-H_2O values determined using the GMWL for IISD-ELA are approximately -55.1 ‰. Lake δ^{13}C-DOM values ranged between -28.0 ‰ and-27.2 ‰ **(Figure 3.3)**. Stream δ^{13}C-DOM values ranged between -28.7 ‰ and -26.9 ‰ **(Figure 3.3**). δ^{15}N-DOM values for lakes ranged from 0 ‰ to 1.8 ‰ and between -2.12 ‰ and -0.15 ‰ for streams **(Figure 3.5)**.

3.3.2 δ^2H, δ^{13}C, and δ^{15}N values of terrestrial vegetation and phytoplankton

The mean δ^2H and δ^{13}C values of terrestrial vegetation from around the PHISH lakes at IISD-ELA were determined to be -187 ‰ and -29.7 ‰ respectively by Tonin (2019). Lake and stream DOM have more positive δ^2H-DOM values than the pooled terrestrial vegetation δ^2H value of -187.6 ‰ (n = 27), (Tonin 2019) **(Figure 3.1, Figure 3.2)**. The mean δ^{13}C value of terrestrial vegetation at IISD-ELA was found to be -29.7 ‰ (Tonin 2019) was more negative than the δ^{13}C-DOM values, which ranged between -26.9 ‰ **(Figure 3.3)**.

The calculated mean phytoplankton δ^2H value (Tonin 2019) is more negative than surrounding lake water δ^2H-DOM **(Figure 3.1, Figure 3.2)**. Phytoplankton δ^2H values are also more negative than zooplankton δ^2H values, as determined by (Tonin 2019) **(Figure 3.1, Figure 3.3)**.

Plotting δ^{13}C-DOM versus δ^{13}C-CO_2 using three different apparent fractionations (ε_C) reported in Bade et al. 2006 and Mohamed and Taylor 2009) as shown in (Wilkinson et al. 2013b), results in three trend lines. However, δ^{13}C-DOM values of lakes and streams do not vary with δ^{13}C-CO_2 values **(Figure 3.4)**. Lake and stream values are more positive than the δ^{13}C value of terrestrial vegetation at IISD-ELA. The lack of a trend of δ^{13}C-DOM

values with $\delta^{13}C$-CO_2 values is similar to the lack of a trend between δ^2H-DOM values and δ^2H-H_2O values **(Figure 3.2)**. For both lakes and streams, δ^2H-DOM values and $\delta^{13}C$-DOM values are relatively constant along the range in δ^2H-H_2O values and $\delta^{13}C$-CO_2 values respectively.

$\delta^{15}N$-DOM values of lakes and streams are more positive than the mean terrestrial vegetation value (-5.5 ‰, (Tonin 2019)). This is particularly true for lake $\delta^{15}N$-DOM values **(Figure 3.5)**.

3.4 Discussion

3.4.1 Comparing isotopic values of lake and stream DOM, terrestrial vegetation, and phytoplankton

The terrestrial end member is frequently defined by taking the stable isotopic value of vegetation from the catchment, and calculating the mean value (Cole et al. 2002, Pace et al. 2004, Caraco et al. 2010, Solomon et al. 2011, Wilkinson et al. 2013a, 2013b, Guillemette et al. 2016); see **Table 3.1**, **Table 3.2**).

However, this approach ignores the contributions of DOM to lake ecosystems and elicits the question of what should actually be considered terrestrial, when the majority of terrestrial organic carbon enters freshwater lakes as DOC (Schindler et al. 1997).

The key assumption in using δ^2H-DOM to separate allochthonous and autochthonous OM is that the terrestrial end member can be obtained by using vegetation from the catchment, even though most terrestrial inputs to lakes enter as DOM. Thus, determinations of allochthonous OM based on the incorporation of vegetation alone assume that only vegetation is being consumed, not the microbial community that is gaining energy from DOM that may be allochthonous in origin.

Since most of terrestrial organic carbon enters lakes as DOM (Schindler et al. 1997), it is composed of mostly terrestrial material (Jones 1992, Solomon et al. 2015). This is shown in IISD-ELA lakes and streams, because $\delta^{13}C$-DOM values in the studied lakes and streams did not vary with calculated $\delta^{13}C$-CO_2 values **(Figure 3.4)**. If the DOM was autochthonous in origin, it would change with $\delta^{13}C$-CO_2 as DOM from phytoplankton should (Wilkinson et al. 2013b). This also applies to δ^2H-DOM and δ^2H-H_2O values **(Figure 3.2)**, since δ^2H-DOM do not vary along the trendline plotted with ε_H. If DOM was

comprised of phytoplankton, the δ^2H-DOM values would vary in this predictable manner **(Figure 3.2)**.

Additionally, DOM samples from L227, an experimentally eutrophied lake with two annual phytoplankton blooms with high phytoplankton biomass and chlorophyll *a* concentrations (Higgins et al. 2018), should be composed of more autochthonous OM. L227 also has a long residence time **(Figure 3.6)**, which is typically associated with lower terrestrial DOM loading (Zwart et al. 2017). Yet, L227 DOM is similar to the DOM from the oligotrophic lakes, as shown by δ^2H-DOM and δ^{13}C-DOM values **(Figure 3.2**, **Figure 3.4)**. This shows that lake DOM is dominantly comprised of terrestrial OM, even in a eutrophic lake.

Differences between allochthonous and autochthonous OM can also be observed through δ^{15}N values. δ^{15}N-DOM values of lake and stream DOM are more positive than those of terrestrial vegetation **(Figure 3.5)**. The boreal forest is nitrogen limited (Maynard et al. 2014), whereas in aquatic systems, nitrogen limitation can be circumvented due to nitrogen fixating species (Schindler et al. 2008). The nitrogen starved terrestrial environment causes the much more negative δ^{15}N values observed in vegetation. Thus, it is not accurate to equate lake DOM to terrestrial vegetation, as shown through δ^{15}N values **(Figure 3.5)**.

3.4.2 Separating allochthonous and autochthonous inputs to food webs

Once allochthonous DOM reaches lakes, it is further transformed by microbiological (Tranvik 1992) or photodegradation (Findlay and Sinsabaugh 2003) processes. Through extensive abiotic and biotic in-soil and in-lake processing, it is apparent that while DOM is formed in the terrestrial environment, it is altered by the carbon cycle.

This is clear because if no transformation of terrestrial OM occurred, DOM δ^{13}C, δ^2H, and δ^{15}N values would be very similar to vegetation. However, this is not the case. δ^{13}C-DOM values do not vary with δ^{13}C-CO_2 values, indicating that DOM is not autochthonous in origin **(Figure 3.4)**. δ^2H-DOM values show that in addition to not being autochthonous, lake DOM is distinct (i.e. more positive) from terrestrial vegetation **(Figure 3.2)**. δ^{15}N-DOM values further support this finding **(Figure 3.5)**. Using δ^2H values in lake food web studies should then allow for the identification of terrestrial inputs

(Doucett et al. 2007), as long as terrestrial inputs are viewed as DOM rather than vegetation.

3.5 Conclusion

DOM in these boreal lakes and streams does not reflect the autochthonous OM sources (unlike (Wilkinson et al. 2013b)), but is substantially modified from terrestrial vegetation, as shown by δ^2H-DOM values. Therefore, the stable isotopic values for terrestrial vegetation cannot be used to assess terrestrial contribution of lake DOM to food webs. While terrestrial material is the precursor to DOM, they are not the same because of microbial action, photodegradation, and other reactions within the lake carbon cycle.

In conjunction, δ^{13}C, δ^2H, and δ^{15}N values show that lake and stream DOM does not come from an autochthonous source, while at the same time, it is distinct from terrestrial vegetation. It is clear that DOM is not the same as terrestrial vegetation and what is considered the terrestrial end member depends on the context of what the author wants to be considered terrestrial. In boreal systems, it is more accurate to use stable isotopic values of DOM, rather than catchment vegetation, as an allochthonous end member.

Table 3.1 Literature δ^2H values for terrestrial and phytoplankton end members.

δ^2H-terrestrial (‰)	±SD (‰)	δ^2H-H_2O range (‰)	δ^2H-phytoplankton range (‰)	δ^2H-terrestrial source	Reference
-129.8	13.7	-86.7 to -61.7	-254.2 to -224.5	Forest soils (n=5, different depths including litter), peat soils (n=3), Sphagnum plants (n=4), fresh leaf and needle mixes (n=4, several tree species).	(Berggren et al. 2014)
-147.2	4.8	-106.8 to -80.5	-277.3 to 214.3	Grass, mesquite, tamarisk, willow, and leaf litter (n= 31).	(Doucett et al. 2007)
-117.6	12.23	-39.9 to -30.2	-206.9 to -197.2	Fresh leaves from *Acer spp.* and *Liriodendron tulipfera* L. (n=8).	(Emery et al. 2015)
-134.5	11.4	-97.9 to -94.3	-233.7	Humus layer of dominant vegetation (spruce(n=3), pine(n=2), mire (n=3)).	(Karlsson et al. 2012)

-129.5	15.2	-51.6 to -40.1	-204.3 to -194.6	Pooled leaf material (n=18) collected from *Acer saccharum, Acer rubrum, Betula alleghaniensis, Abies balsamea, Picea mariana, Tsuga canadensis, Thuja occidentalis.* Authors note that these values are indistinguishable from lake DOM and groundwater (n=4).	(Solomon et al. 2011, Wilkinson et al. 2013b)
-173.2 to -117.6	0.4 to 15.2	-89.8 to -30.42	-167.9 to -266.9	Leaf litter of dominant terrestrial plants, soil OM, or fresh leaves.	(Tanentzap et al. 2017)
-187.6	11.2	-76.9 to -64.9	-239.9 to -225.0	Pooled leaf material (n = 27) collected from *Pinus banksiana, Picea mariana, Larix laricina, Betula papyrifera.*	(Tonin 2019)

Table 3.2 Literature δ^2H-DOM values in lakes, rivers, reservoirs, and streams, and whether the values were measured directly as DOM or assumed.

Study site type	δ^2H-DOM range (‰)	Measured or Assumed	δ^2H-H_2O range (‰)	n	Reference
Lakes	-154 to -123	Measured	-86.7 to -61.7	18	(Berggren et al. 2014)
Lakes	-130[a]	Assumed	-51.6 to -40.1	4	(Solomon et al. 2011)
Lakes	-173 to -118[b]	Assumed	-89.8 to -30.42	147	(Tanentzap et al. 2017)
Lakes	-127 to 110	Measured	-78.4 to -66.4	6	This study
Lakes	-151 to -102	Measured	-80.0 to -42.0	39	(Wilkinson et al. 2013b)
Reservoirs	-129 to -94.2	Measured	-39.9 to -30.2	10	(Emery et al. 2015)
Streams	-118 to -94.8	Measured	-55.06[c]	4	This study

[a]Pooled leaf material (n=18) collected from *Acer saccharum, Acer rubrum, Betula alleghaniensis, Abies balsamea, Picea mariana, Tsuga canadensis,* and *Thuja occidentalis.* Authors note that these values are indistinguishable from lake DOM and groundwater (n=4).
[b] Leaf litter of dominant terrestrial plants, soil OM, or fresh leaves. Authors note that these values are indistinguishable from lake DOM inputs.
[c] Estimated based off of the GMWL for IISD-ELA (Gibson et al. 2017).

Table 3.3 Summary of physical and chemical parameters of sampled lakes and streams, including lake order, lake area, lake volume, maximum depth (Z_{max}), residence time, and DOC concentration on the sampling day. Residence time calculated as the average theoretical water renewal time (years) by dividing lake volume (m^3) by estimated outflow (m^3).

Lake	DOC (mg/L)	Lake order	Lake Area (ha)	Lake Volume (m^3)	Z_{max} (m)	Estimated Outflow (m^3)	Residence time (years)
L373	4.0	1	27.3	2941000	21	198316	14.8
L239	7.0	1	56.1	5910000	30.4	967813	6.1
L227	15.5	1	34.4	221000	10	84641	2.6
L222	8.7	1	16.4	600000	5.8	502680	1.2
L221	10.9	2	9	189100	5.7	201761	0.9
L470	12.1	4	6	33000	2	412626	0.1
U8	28.3	-	-	-	-	-	-
EIF	26.8	-	-	-	-	-	-
NWIF	32.8	-	-	-	-	-	-
NEIF	59.9	-	-	-	-	-	-

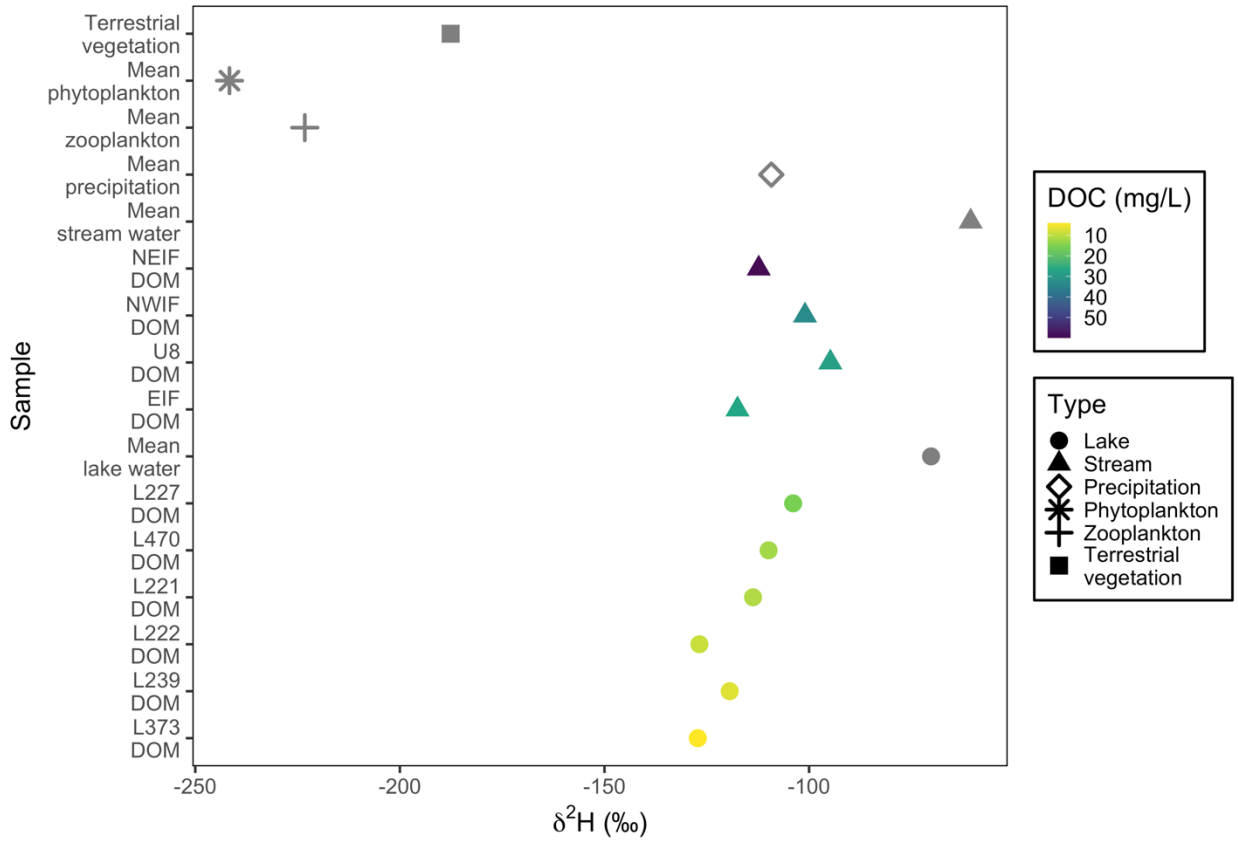

Figure 3.1 δ^2H-DOM values of the sampled set of lakes and streams, and the average pooled δ^2H value of terrestrial vegetation (Tonin 2019). The mean zooplankton and phytoplankton values was taken from the δ^2H values were calculated for 8 IISD-ELA lakes (Tonin 2019). The mean lake water δ^2H-H_2O value is an average of 28 IISD-ELA lakes. Mean stream water δ^2H-H_2O is an average of the 4 IISD-ELA streams measured in this study. Mean precipitation was calculated using historical δ^2H-H_2O values from IISD-ELA from the GNIP database (n= 157) (IAEA and WMO 2020).

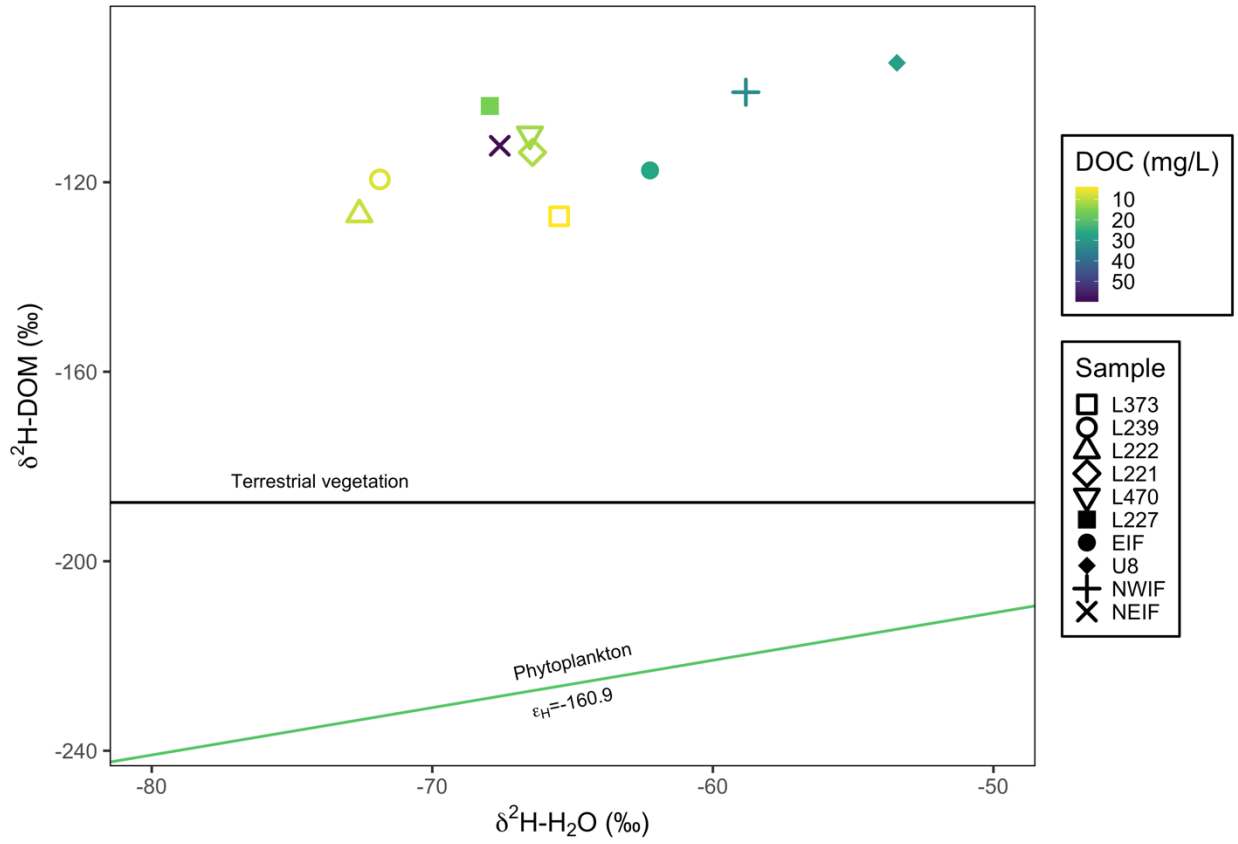

Figure 3.2 δ^2H-DOM values and δ^2H-H_2O values of the sampled set of lakes and streams. The black line represents the mean δ^2H value of terrestrial vegetation at IISD-ELA (Tonin 2019). Phytoplankton δ^2H values are represented by the green line and calculated using ε_H= 160.9, as determined by Wilkinson et al. (2013b).

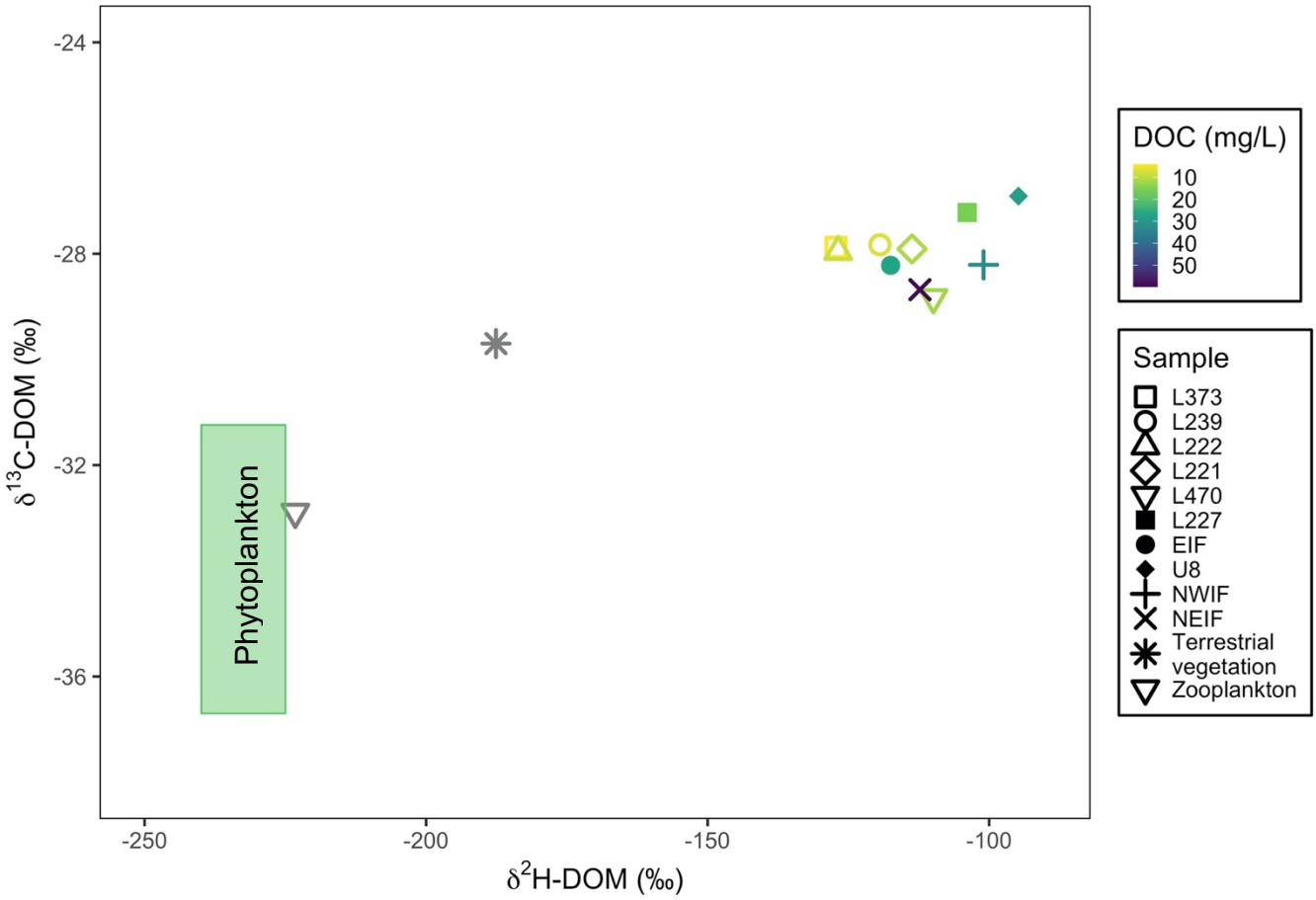

Figure 3.3 δ^2H-DOM and δ^{13}C-DOM values of the sampled set of lakes and streams, as well as the average pooled terrestrial vegetation from the PHISH lakes (Tonin 2019). The mean zooplankton values was taken from the δ^2H values were calculated for 8 IISD-ELA lakes (Tonin 2019). The green box indicates the potential range in δ^{13}C and δ^2H phytoplankton values (Tonin 2019).

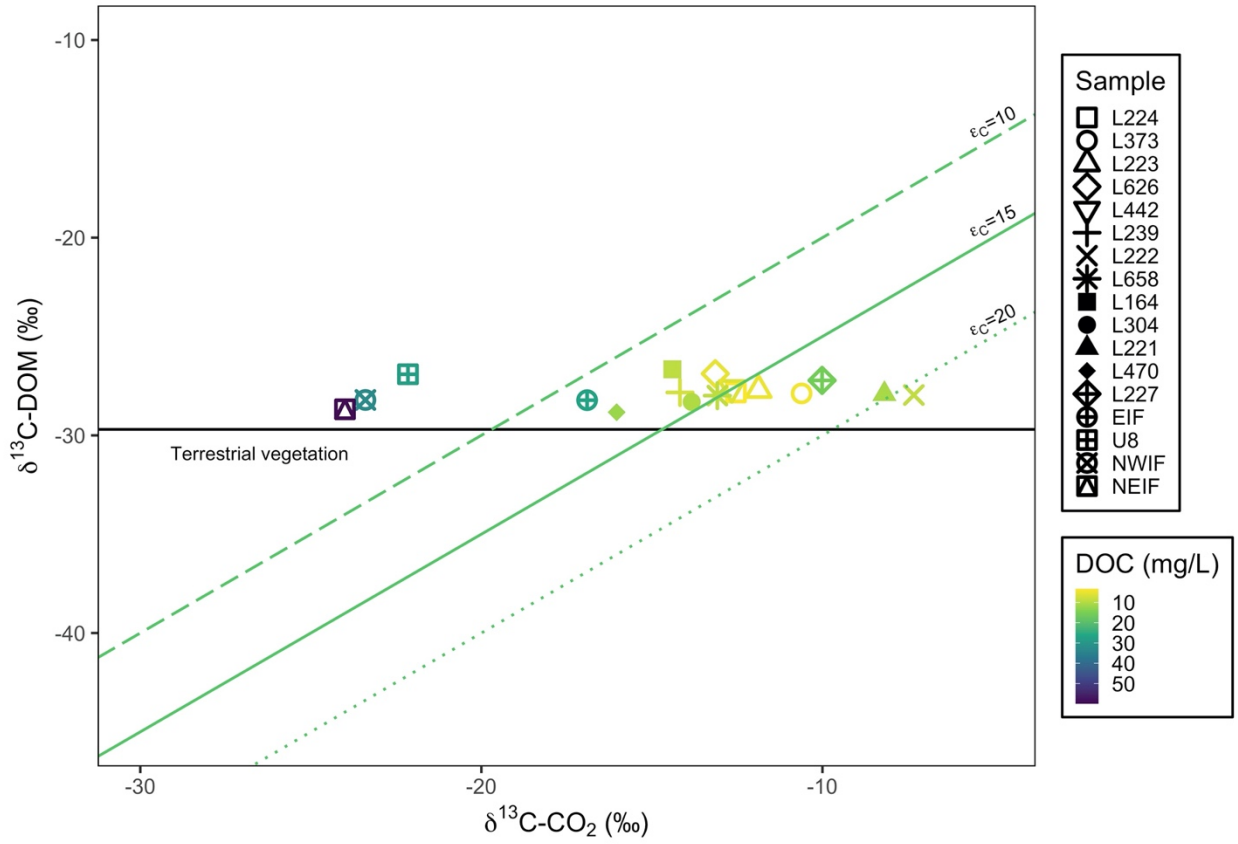

Figure 3.4 δ^{13}C-DOM values and calculated δ^{13}C-CO_2 values of the sampled set of lakes and streams. The black line represents the mean δ^{13}C value of terrestrial vegetation at IISD-ELA (Tonin 2019). Phytoplankton estimated δ^{13}C values estimations are represented by the three green lines. The ε_C values used are the same as those utilized by Wilkinson et al. (2013b) and are based on various reported ε_C in (Bade et al. 2006, Mohamed and Taylor, 2009).

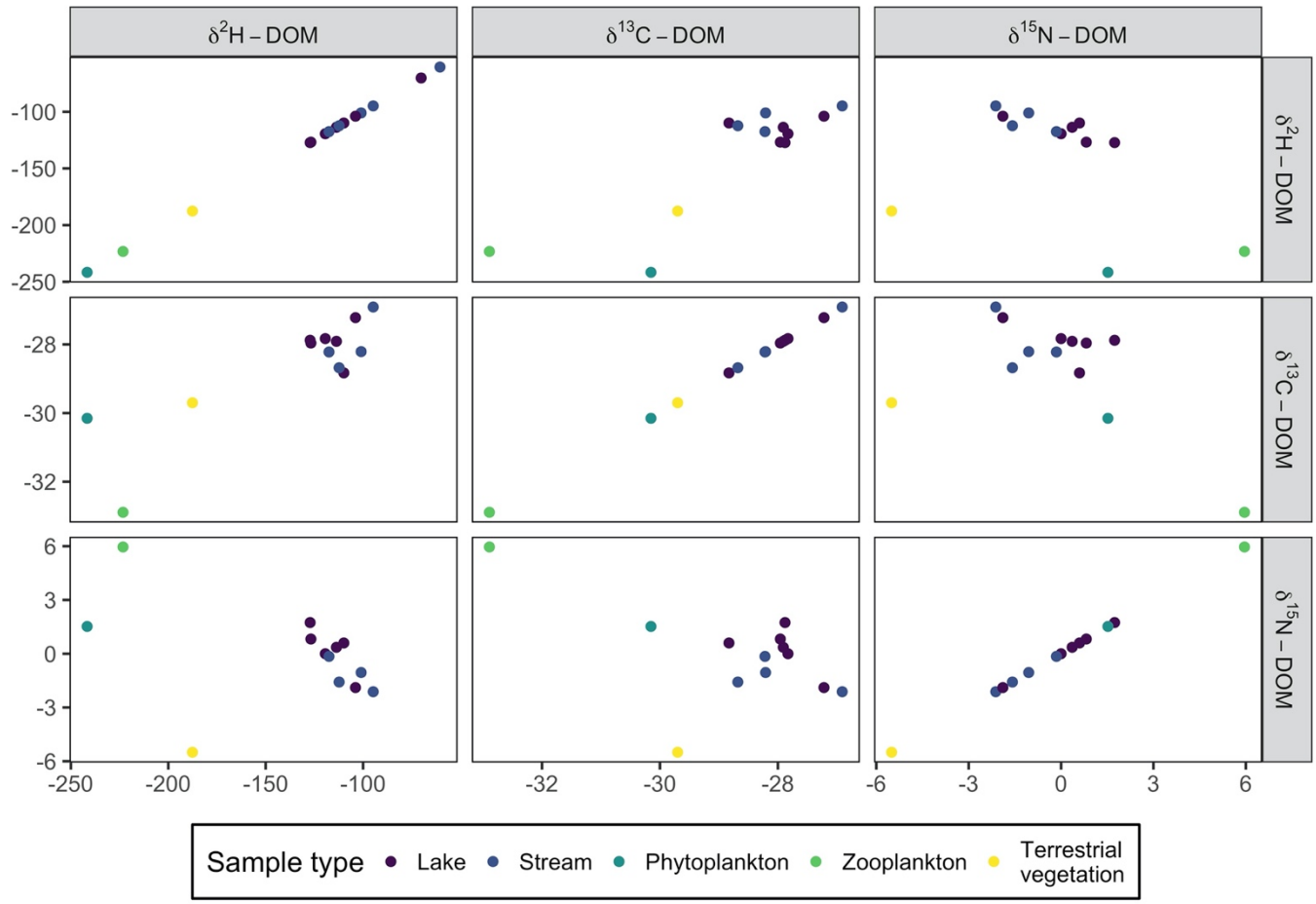

Figure 3.5 Paired plot of δ^2H-DOM, δ^{13}C-DOM, and δ^{15}N-DOM data. Terrestrial vegetation, phytoplankton, and zooplankton values are from (Tonin 2019).

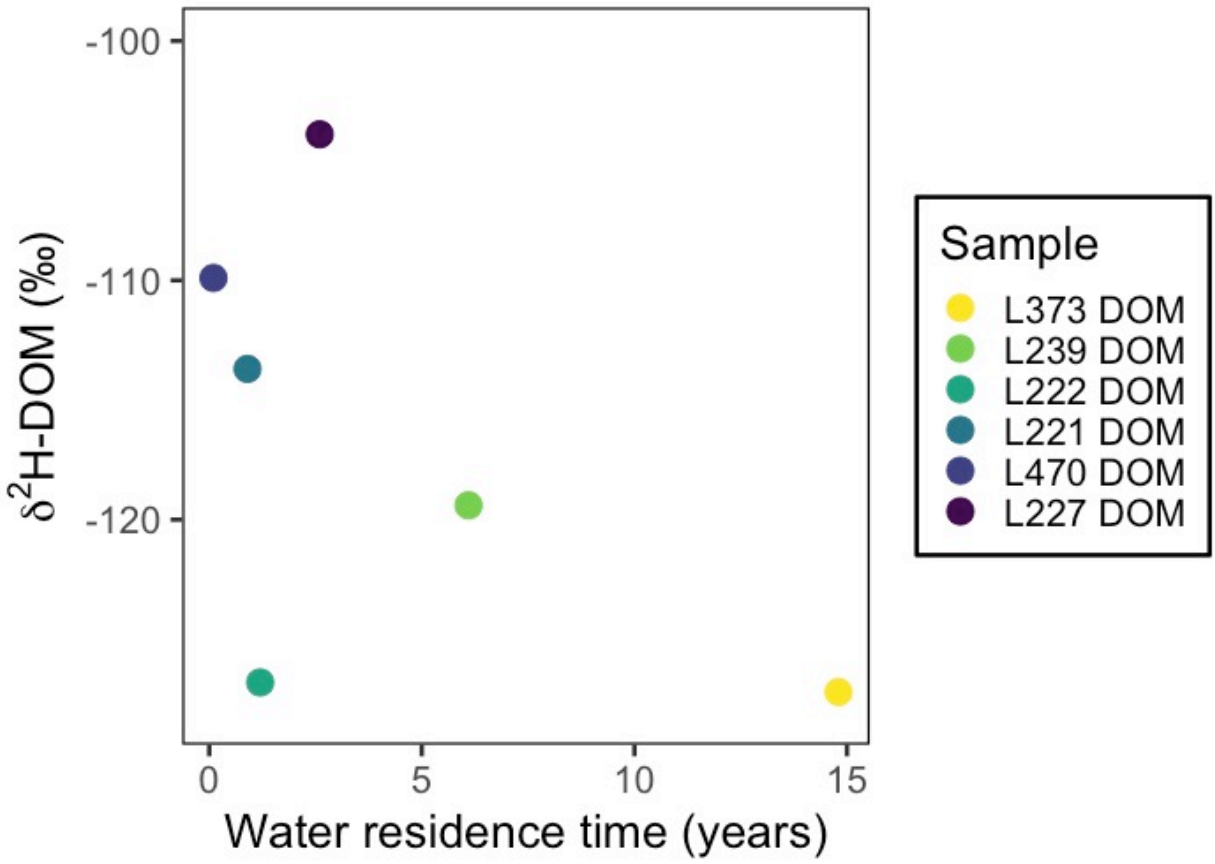

Figure 3.6 Relationship between ^{2}H-DOM and water residence time in the lake DOM samples.

Chapter 4. Determining CH_4 dynamics using $\delta^{13}C$-CH_4 and $\delta^{2}H$-CH_4 values in Canadian Shield lakes

4.1 Introduction

Methane (CH_4) is a key player in global greenhouse gas (GHG) budgets with 25 times greater warming potential than carbon dioxide (CO_2) on a 100-year time scale (Battin et al. 2009, Lehours et al. 2016). Although CH_4 is naturally produced, emissions have dramatically increased in the past century. Atmospheric CH_4 concentrations have risen from 0.72 ppm in preindustrial times to 1.86 ppm today (May 1, 2019) (Intergovernmental Panel on Climate Change 2014, National Oceanic and Atmospheric Administration 2019b), attributed to enhanced anthropogenic activities such as fossil fuel combustion, agriculture, waste management, and land use change (Walter et al. 2007, Kirschke et al. 2013, Saunois et al. 2016). To estimate these anthropogenic effects, it is important to investigate the processes responsible for CH_4 production and consumption in the natural environment.

CH_4 production, or methanogenesis, is conducted by archaea. Methanogenesis is the terminal degradation process of organic matter in anoxic freshwater (Biagini et al. 1998). Methanogens are typically obligate anaerobes meaning that most cannot withstand high oxygen (O_2) concentrations and live under reducing conditions (E_h < -200 mV) (Whiticar 1999, Venkiteswaran and Schiff 2005). This is because methanogenesis is dependent on the F_{420}-hydrogenase enzyme complex, which is unstable at high concentrations of O_2, nitrate (NO_3^-), or nitrite (NO_2^-) (Schönheit et al. 1981). However, production of CH_4 has recently been observed in the oxic zone by cyanobacteria and as a result of other unknown processes (Donis et al. 2017, Bižić et al. 2020)

There are two main biogenic pathways of methanogenesis: acetate fermentation and carbonate reduction. Generally, methanogens are classified by their respective pathway of methanogenesis and carbon substrate. Acetate fermentation, or acetoclastic methanogenesis, **(Equation *4.1*)** utilizes non-competitive substrates. Non-competitive substrates are those that not energetically favourable for other microbes (Whiticar 1999). Acetate fermentation has been thought to be the dominant methanogenesis pathway in freshwater sediments (Whiticar et al. 1986).

Equation 4.1 $$CH_3COOH \rightarrow CH_4 + CO_2$$

In contrast, carbonate reduction **(Equation *4.2*)** utilizes competitive substrates, or substrates more effectively used by other microbes. Carbonate reduction is the dominant methanogenesis pathway in marine sediments with low sulfate (SO_4^{2-}) concentrations. In these environments, SO_4^{2-} reducing bacteria (SRB) become less active and cannot outcompete methanogens (Whiticar 1999). Carbonate reduction can occur in freshwater environments when other substrates are depleted and thus the bicarbonate pool can be used as a substrate for methanogens (Whiticar 1999).

Equation 4.2 $CO_2 + 8H^+ + 8e^- \rightarrow CH_4 + 2H_2O$

Once CH_4 is produced, it can be used as an energy source for methanotrophs in CH_4 oxidation or can be emitted to the atmosphere (Bastviken et al. 2003). CH_4 oxidation can occur aerobically, whereby energy is generated from the oxidation of CH_4 by O_2 to produce CO_2 and H_2O. CH_4 oxidation can also occur anaerobically where SO_4^{2-} is the final electron acceptor. More recently, anaerobic oxidation of CH_4 has been found in other environments, but the electron acceptors and pathways remain unknown (Martinez-Cruz et al. 2018).

Globally, oxidation is a sink for CH_4 (Kirschke et al. 2013), however, many natural aquatic ecosystems are sources of CH_4 to the atmosphere (Kirschke et al. 2013). For instance, it is estimated that freshwater lakes are the second largest natural source of CH_4 to the atmosphere (Sieczko et al. 2020). Lakes emit CH_4 via diffusion, ebullition, and flux from emergent vegetation (Sanches et al. 2019). Small lakes, such as the boreal lakes examined in this study, store large amounts of carbon and therefore are important in the carbon cycle and in terms of regional carbon fluxes (Cole et al. 2007). Small lakes have been shown to have high rates of CH_4 and CO_2 emissions per unit area (Bastviken et al. 2004, DelSontro et al. 2018).

Lake surface CH_4 is a source of CH_4 to the atmosphere (Bastviken et al. 2004). Therefore, if the source of lake CH_4 cannot be identified, the source of a portion of atmospheric CH_4 cannot be identified. In a mixed or poorly stratified lake, the majority of CH_4 that reaches the sediment-water interface is oxidized by aerobic methanotrophs and can be subsequently incorporated into the food web (Grey 2016). In stratified lakes with anoxic bottom waters, CH_4 reaches the oxic-anoxic boundary in the water column where it is mostly consumed by aerobic methanotrophs, which can be consumed by

zooplankton and feed higher trophic levels (Grey 2016). However, it is important to note that not all CH_4 is consumed, as a portion of lake CH_4 flux can be lost to the atmosphere through ebullition and diffusion (DelSontro et al. 2016).

CH_4 concentration in surface water is a function of methanogenesis, methanotrophy, rates of methane fluxes within the lake, and rates of fluxes between the lake and the atmosphere (Bastviken et al. 2004). CH_4 concentrations are so low in the mixed water column because methanogenesis is an anoxic process (Whiticar 1999). In order for methane production to occur, low O_2 concentrations are imperative because methanogens are obligate anaerobes (Whiticar 1999, Venkiteswaran and Schiff 2005). Therefore, in order for high rates of methane production, low oxygen concentrations are necessary. It has been shown that low CH_4 concentrations are observed in conjunction with high O_2 saturation in a variety of lake types (Juutinen et al. 2009). Any CH_4 has diffused from anoxic waters below or from anoxic sediment and will be diffused to the atmosphere.

Zooplankton have been shown to consume methanotrophic, or CH_4-oxidizing bacteria and archaea (Taipale et al. 2008, Schilder et al. 2015). In the past, it was thought that CH_4 did not escape to the oxic zone and remained in anoxic sediments and in the bottom, anoxic waters of lakes. Recent work has shown that CH_4 can be produced in the oxic water column (Bogard et al. 2014) and that CH_4 can also be consumed in the anoxic zone. CH_4 provides a connection between the benthic and pelagic zones of lakes and can potentially play an important role in the overall lake food web (Deines et al. 2009, Grey 2016). CH_4 derived carbon in lake food webs can be reflected at all trophic levels, from the base (e.g. algae) to higher consumers (e.g. fish). The stable isotopic values of CH_4 can illustrate the importance of CH_4 to the lake carbon cycle and potentially to lake food webs **(Figure 4.1)**.

CH_4 produced by methanogens has lower $\delta^{13}C$ and lower $\delta^{2}H$ values with respect to CO_2, plant material, and surrounding lake water (Woltemate et al. 1984, Peterson and Fry 1987). These negative values are characteristic of biogenic CH_4, and therefore can be used to determine if CH_4 has been consumed and thus if methanotrophs contribute to aquatic food webs (Deines et al. 2009, Jones and Grey 2011, Grey 2016).

The two main pathways of methanogenesis have characteristic ranges in $\delta^{13}C$ and $\delta^{2}H$ values. Typically, CH_4 produced by acetate fermentation **(Equation 4.1)** has $\delta^{13}C$

values of -70 ‰ to -50 ‰ whereas CH_4 produced by carbonate reduction **(Equation *4.2*)** has $\delta^{13}C$ values of -110 to -60 ‰ (Whiticar 1999). CH_4 produced by acetate fermentation typically has δ^2H values of -400 ‰ to -250 ‰, and CH_4 produced by carbonate reduction has δ^2H values of -250 ‰ to -150 ‰ (Whiticar et al. 1986, Schoell 1988, Whiticar 1999). These notably low δ^2H values are due to large fractionation of hydrogen during CH_4 production, especially via acetate fermentation (Whiticar 1999).

The δ^2H-CH_4 values may be dependent on the isotopic composition (δ^2H-H_2O) of environmental water (Waldron et al. 1999). The hydrogen in CH_4 is derived from formation water for the carbonate reduction formation pathway **(Equation *4.2*)** (Pine and Barker 1956, Daniels et al. 1980). Similarly, it has been shown that in shallow, low sulfate environments, that the isotopic values of hydrogen incorporated into CH_4 produced from acetate fermentation also depends on the isotopic values of the formation water (Waldron et al. 1999). Laboratory incubation experiments by Waldren et al. (1999) approximated that 50% of variation in δ^2H-CH_4 values in shallow, subsurface, freshwater could be explained by δ^2H-H_2O values.

In CH_4 oxidation, the residual CH_4 pool more positive in $\delta^{13}C$-CH_4 and δ^2H-CH_4 because ^{12}C is used preferentially over ^{13}C. Fractionation factors for CH_4 oxidation are ε_C= 4-30 ‰ and ε_H= 95-285 ‰ (Whiticar 1999). Fractionation factors in boreal reservoirs for $\delta^{13}C$-CH_4 have been reported in a much tighter range of 18.6 to 21.4 ‰ (Venkiteswaran and Schiff 2005).

It is common to measure only $\delta^{13}C$-CH_4, however measuring δ^2H-CH_4 can provide information pertaining to the biogenic production pathway, and can further separate oxidation from a change in methane formation pathway (Whiticar 1999). Most work utilizing δ^2H values of CH_4 in aquatic ecosystems focuses on large, deep, and permanently anoxic tropical lakes (Pasche et al. 2011); large, deep, and permanently ice covered lakes (Wand et al. 2006); arctic lakes (Cadieux et al. 2016); temperate wetlands (Hornibrook et al. 1997, Sugimoto and Fujita 2006, Alstad and Whiticar 2011); and northern terrestrial wetlands (Chasar et al. 2000, Chanton et al. 2006) **(Table *4.1*)**. These environments are markedly different from the small, soft water, and oligotrophic lakes characteristic of the Canadian Shield. These small boreal lakes are important to the global carbon cycle due to the large amount of carbon they store and high rates of both CH_4 and

CO_2 emissions (Bastviken et al. 2004, Cole et al. 2007, DelSontro et al. 2018). Further, large datasets including δ^2H-CH_4 values are lacking in current literature (Conrad 2005), and there is a lack of information particularly on the δ^2H values of methanotrophs themselves (Grey 2016), as well as fractionation factors for δ^2H-CH_4 in methanogenesis and CH_4 oxidation.

To study the use of δ^{13}C-CH_4 and δ^2H-CH_4 in understanding CH_4 dynamics in small boreal lakes, fourteen lakes were selected at the International Institute for Sustainable Development – Experimental Lakes Area (IISD-ELA). These fourteen lakes span a dissolved organic carbon (DOC) gradient of 3.3 mg/L – 12 mg/L and represent varying mixing regimes.

In Chapter 4, I aim to:

1. Examine and define the range of δ^{13}C-CH_4 and δ^2H-CH_4 values in fourteen boreal lakes, over four broad categories: deep anoxic bottom lakes, shallow anoxic bottom lakes, majority oxic lakes, and polymictic lakes.
2. Compare the observed δ^{13}C-CH_4 and δ^2H-CH_4 values to atmospheric values and predictions of sources based on literature values for both surface and deeper water column CH_4
3. Assess the potential roles of methanogenic pathway and CH_4 oxidation in controlling CH_4 isotopes.

4.2 Material and methods

4.2.1 Study Sites

The fourteen selected lakes **(Table 4.2)** are located at the IISD-ELA, a research station located on the Canadian shield in northwestern Ontario (49°40`N, 93°44`W) (Figure 1). The lakes were sorted into groups based on if their water columns were deep and anoxic at the bottom, shallow and anoxic at the bottom, oxic, or polymictic.

Four different lakes fall into the deep lakes with anoxic bottoms group: L223, L224, L227, and L442, characterized by being greater than 6 m in depth and having anoxia develop in their bottom depths ("anoxic deep lakes": L223, L224, L227, L442). Similarly, three lakes are characterized by being shallower than 6 m in depth and having anoxia develop in their bottom depths ("shallow lakes": L221, L222, L304). The remaining lakes

are termed "oxic" (L164, L239, L373, L626, and L658) and are characterized by having a water column that is mostly oxic with the exception of the bottom one or two depths and are not stratified. Lastly, two polymictic lakes were examined in this study (L303 and L470; permanently mixed and has no hypolimnion).

4.2.2 Field sampling

Each lake was sampled midsummer in 2018 for a suite of water chemistry and stable isotope parameters. Full lake water column profiles were sampled at the maximum depth using a gear pump. Depending on the depth of the lake, samples were taken at 2-5 m intervals throughout the water column.

As part of IISD-ELA's long term ecological research (LTER) program, temperature profiles were taken biweekly for L239, L373, L442, and L224 using an RBR sonde. As such, LTER temperature profiles were used for these lakes. For PHISH project lakes, monthly temperature profiles were taken using an EXO II water-quality sonde. For lakes not sampled as part of the LTER program or the PHISH project, separate temperature profiles were taken during sampling.

L227 is an experimentally eutrophied lake, and nutrients have been added in various N:P ratios since 1969 (Hecky et al. 1994). Sonde profiles were taken biweekly in L227 using an RBR sonde.

Samples for CH_4 concentration and CH_4 stable isotope analysis were collected in 60 mL glass serum bottles with no headspace, then preserved by injecting a saturated solution of $ZnCl_2$. Samples for DOC concentration analysis were collected in 40 mL amber glass vials. Using Whatman QM-A quartz filters with a nominal pore size of 2.2 μm, particulate organic matter (POM) isotope samples were collected, frozen, and shipped back to the University of Waterloo. pH samples were collected in 15 mL PET containers with a Hach HQ40d meter and IntelliCAL™ PH301 probe.

4.2.3 Stable isotope analysis and calculations

$\delta^{13}C\text{-}CH_4$ and $\delta^{2}H\text{-}CH_4$ analysis was undertaken at the Environmental Isotope Laboratory at the University of Waterloo. Samples were prepared by using the headspace equilibrium method, where serum bottles were injected with helium simultaneously as water was removed, then gently shaken to ensure equilibration between the gas and liquid phase. Concentrations could then be calculated using Henry's

Law. The headspace was analyzed by GC-CF-IRMS using an Agilent 6890 GC coupled to an Isochrom isotope ratio mass spectrometer (IRMS: Micromass UK) ($\delta^{13}C$ precision ± 0.3 ‰, $\delta^{2}H$ precision ± 5 ‰, detection limit 1 ppm CH_4). $\delta^{2}H$-H_2O samples were analyzed by laser absorption spectrometry (LAS) using a Los Gatos Research (LGR) Liquid Water Isotope Analyser (LWIA), model T-LWIA-45-EP (precision $\delta^{2}H$ precision ± 0.8 ‰). DOC concentration analysis was conducted using a Shimadzu Total Organic Carbon (TOC-L) analyzer (precision ± 0.3 mg C/L). $\delta^{13}C$-POM analysis was conducted by drying frozen Whatman QM-A quartz filters and analyzed by EA-CF-IRMS using a Carlo Erba Elemental Analyzer (CHNS-O EA1108) coupled with a Delta Plus (Thermo) IRMS ($\delta^{13}C$ precision ± 0.2‰). $\delta^{13}C$-POM values are not available for the L221 and L304 profiles. $\delta^{13}C$-DIC samples were prepared by acidifying, then equilibrating the headspace. Samples were then analyzed by GC-CF-IRMS using an Agilent 6890 GC coupled to an Isochrom isotope ratio mass spectrometer (IRMS: Micromass UK) ($\delta^{13}C$ precision ± 0.3‰).

$\delta^{2}H$-DOM samples were first freeze dried at the University of Waterloo then analyzed at the University of Ottawa Ján Veizer Stable Isotope Laboratory for non-exchangeable H using a Thermo Scientific thermal conversion elemental analyzer (TC/EA) (via a Confo IV) with a Costech Zero-blank autosampler ($\delta^{2}H$ precision ± 2‰), following (Doucett et al. 2007). $\delta^{2}H$-DOM samples of L373, L239, L222, and L221 were taken in the 2018 field season and L227 was sampled in July 2019. DIC concentration and stable isotope samples were prepared by acidifying, then equilibrating the headspace. Samples were then analyzed by GC-CF-IRMS using an Agilent 6890 GC coupled to an Isochrom isotope ratio mass spectrometer (IRMS: Micromass UK) ($\delta^{13}C$ precision ± 0.3‰).

$\delta^{13}C$-CO_2 values were calculated using the "isocalc" package (version 1) using measured values for water temperature, pH, and DIC concentration, and measured $\delta^{13}C$-DIC (Henderson, 2018). $\delta^{13}C$-CO_2 values could not be calculated for L304, L470 2m, L442 15m, and L164 6 m.

Thermocline depths were calculated using the R package "rLakeAnalyzer" version 1.11.4.1 (Winslow et al. 2019). In order to assess the potential role of CH_4 oxidation in controlling CH_4 isotopes, the R package "rayleigh" version 0.1.3 was used (Venkiteswaran 2019). A set of seven calculated carbon fractionation factors (ε) ranging

from -21.4 ‰ to -14.0 ‰ were used to estimate the δ^2H-CH_4 and δ^{13}C-CH_4 values of oxidized CH_4 produced from hypolimnion values (Venkiteswaran and Schiff 2005). A ε= -190 ‰ for hydrogen was estimated from the mean of the range of suggested values in Whiticar (1999).

Keeling plots are often used to examine the diffusion fluxes between the atmospheric concentration of a gas and a source (Pataki et al. 2003, Nickerson and Risk 2009). Keeling plots are underpinned by two assumptions; (1) only two gas components are examined and (2) the isotopic values of the two gas components does not change over the course of the observation (Pataki et al. 2003). Keeling plots also assume linearity, however, these diffusive processes are non-linear processes in non-steady state environments (Nickerson and Risk 2009). In this thesis, a Keeling plot were used to identify difference between lake CH_4 and atmospheric CH_4.

4.3 Results

4.3.1 CH_4 Concentrations

The mean concentration of CH_4 in the well mixed water column is 0.76 μM, compared to the atmospheric value of 0.077 μM, or ten times supersaturated. At this level of supersaturation, isotopic exchange with the atmosphere is a very small effect (Thuss 2008). Lakes that developed anoxia in their hypolimnia had the highest CH_4 concentrations **(Figure 4.7)**.

4.3.2 Epilimnion CH_4 isotopes

Surface δ^{13}C-CH_4 values for all lakes ranged between -67.2 ‰ and -39.4 ‰, while δ^2H-CH_4 ranged between -323 ‰ and -121 ‰ **(Figure 4.3, Figure 4.4)**. Atmospheric δ^{13}C-CH_4 has a value of -47.2 ‰ (Rice et al. 2016), which falls within this range. In comparison, δ^2H-CH_4 values in the well mixed water column are much more negative than the atmosphere (-95.0 ‰; (Rice et al. 2016)), ranging between -323 ‰ and -121 ‰. These isotopic values are accompanied by low CH_4 concentrations (<2 μM CH_4 with the exception of one outlier) **(Figure 4.9)**.

4.3.3 Metalimnion CH_4 isotopes

In most lakes across the oxic, and deep and shallow anoxic bottom lakes the δ^2H-CH_4 and δ^{13}C-CH_4 values in the middle of the water column are more positive than the surface or bottom depths **(Figure 4.3, Figure 4.4)**. This is not the case for the two polymictic lakes **(Figure 4.3, Figure 4.4)**.

4.3.4 Hypolimnion CH_4 isotopes

The δ^2H-CH_4 values at the bottom depths of each lake that develops an anoxic hypolimnion ranged between approximately -350 ‰ and -300 ‰ **(Figure 4.3)**. Anoxic hypolimnion δ^{13}C-CH_4 values ranged between approximately -76.6 ‰ and -41.9 ‰ **(Figure 4.4)**. The most negative δ^2H-CH_4 and δ^{13}C-CH_4 values were also found where the CH_4 concentrations were highest **(Figure 4.11)**. In lakes with oxic bottoms, δ^{13}C-CH_4 and δ^2H-CH_4 values were similar to the surface values **(Figure 4.3, Figure 4.4)**.

In the shallow lakes with anoxic bottoms, the δ^{13}C-CH_4 values stay relatively consistent throughout the water column, in the -50 ‰ range **(Figure 4.4)**. However, these values decrease compared to the surface, reaching up to -76.6 ‰ at the bottom of L442 and -74.4 ‰ at the bottom of L221 **(Figure 4.4)**.

Lakes with an oxic water column and an oxic hypolimnion have extremely low CH_4 concentrations throughout their water columns, with the exception of the bottom the L658 **(Figure 4.7)**. At the bottom of L658, where the δ^{13}C of CH_4 is -70.5 ‰. This value is accompanied with high CH_4 concentrations **(Figure 4.7)** low O_2 concentrations **(Figure 4.8)**, indicating that there is CH_4 production occurring.

4.3.5 Lake δ^2H-H_2O and δ^2H-DOM values

Lake δ^2H-H_2O values in this study ranged between -72.6 ‰ and -63.7 ‰. Where δ^2H-CH_4 values are available, literature values of δ^2H-H_2O values for environmental water range from -282 ‰ to -36.7 ‰ **(Table 4.1)**. There is not a strong relationship between the lake δ^2H-H_2O values and δ^2H-CH_4 values in the studied lakes or in the literature values **(Figure 4.13, Table 4.1)**. The δ^2H-DOM values in a subset of lakes exhibit a small range, varying from -127.2‰ to -103.9 ‰. There is also not a strong relationship between δ^2H-DOM and δ^2H-CH_4 values **(Figure 4.13)**.

4.3.6 δ^{13}C-DIC, δ^{13}C-CO_2 and δ^{13}C-POM values

δ^{13}C-DIC values ranged from -24.53 ‰ to 1.17 ‰ **(Figure 4.5)**. Calculated δ^{13}C-CO_2 values ranged from -28.5 ‰ to -8.55 ‰ **(Figure 4.11)**. δ^{13}C-POM values ranged from **(Figure 4.6)**.

More negative values for both δ^{13}C-CO_2 and δ^{13}C-CH_4 can be found at deeper depths **(Figure 4.11A)**. At higher CH_4 concentrations, more negative δ^{13}C-CO_2 values are observed, however, the highest CH_4 concentration (987 μM, L227 10 m) has a δ^{13}C-CO_2 value of -14.0 ‰ **(Figure 4.11B)**. Low CH_4 concentrations exhibit a large range of δ^{13}C-CO_2 values **(Figure 4.11B)**. The calculated δ^{13}C-CO_2 values do not fit the range of fractionation factors (ε= 4, ε= 17, ε= 30) suggested by Whiticar (1999) **(Figure 4.11A)**.

Surface δ^{13}C-DIC values are approximately the same for each lake **(Figure 4.5)**. Surface δ^{13}C-POM values are approximately – 30 ‰ for most lakes **(Figure 4.6).** This is shown in **Figure 4.12**, where negative δ^{13}C-POM values are associated with negative δ^{13}C-CH_4. There is a relationship between δ^{13}C-DIC and δ^{13}C-POM values in the lakes (p= $7.27*10^{-3}$, R^2= 0.336) **(Figure 4.10)**.

4.3.7 Seasonal CH_4 dynamics and CH_4 isotopes in L227 and L442

CH_4 concentrations are low in the surface for each month, then much higher in the hypolimnion **(Figure 4.16E)**. The highest hypolimnion CH_4 concentrations were found in September 2018 **(Figure 4.16E)**. The hypolimnion is anoxic for May, July, and September of 2018 **(Figure 4.16F)**.

Most negative δ^{2}H-CH_4 values in L227 occur in September, rather than earlier in the ice-free season **(Figure 4.15A)**. This is also the case for δ^{13}C-CH_4 values In May and June at 4 m, the δ^{13}C of CH_4 is approximately -20 ‰, whereas in September the 4 m δ^{13}C-CH_4 values reaches -66.9 ‰. (**Figure 4.15B)**. δ^{13}C- DIC values follow roughly the same trend for each month, however, September appears to have more positive values than May and June **(Figure 4.15C)**. Surface δ^{13}C-POM values are approximately -23 ‰ in June and September, but more negative (approximately -29 ‰) in May **(Figure 4.15D)**.

Surface CH_4 concentrations are identical in all three months, and concentrations increase deeper in the water column **(Figure 4.15E)**. The highest CH_4 concentrations were

observed in September **(Figure 4.15E)**. For June and September, L227 is anoxic below the thermocline, whereas the water column is oxic in May **(Figure 4.15F)**.

The seasonal changes in δ^2H-CH_4, δ^{13}C-CH_4, δ^{13}C-DIC, δ^{13}C-POM, CH_4 concentration, and O_2 concentration in L442 were also explored in May, July, and September 2018. The most negative values for δ^2H of CH_4 are at 17 m of L442 at approximately -300 ‰ in each month **(Figure 4.16A)**. Surface δ^2H-CH_4 is also approximately -300 ‰ in July and September, however, the surface value in May is -237.4 ‰ **(Figure 4.16A)**. A δ^2H-CH_4 value outlier is observed for September at 9 m, where the δ^2H-CH_4 value is -39.7 ‰. A similar pattern can be observed in δ^{13}C-CH_4 values for L442 in the ice-free season **(Figure 4.16B)**. July and September δ^{13}C-DIC values are very similar to each other **(Figure 4.16C)**. In contrast, the May δ^{13}C-DIC values are more negative in the surface **(Figure 4.16C)**. δ^{13}C-POM values for July and September are very similar in the surface (approximately -30 ‰) and follow the same relative trend deeper in the water column, with the July values being more negative compared to the September values. May δ^{13}C-POM values are more negative in the surface (-35 ‰) and are generally more positive at deeper depths **(Figure 4.16D)**.

4.3.8 Theoretical Rayleigh fractionation of hypolimnion CH_4 and determination of methanogenesis pathway

The CH_4 in this suite of lakes is not atmospheric **(Figure 4.18, Figure 4.19)**. The high concentration, hypolimnion CH_4 for the most part does not fall within the acetate fermentation or carbonate reduction pathway **(Figure 4.19)**. While these values are within range for the acetate fermentation pathway in terms of their δ^2H-CH_4 values, this is not the case for their δ^{13}C-CH_4 values, which are more negative (approaching -80 ‰).

Above the thermocline, select CH_4 samples fell within the range of acetate fermentation **(Figure 4.18)**, while no samples were found in the range of carbonate reduction methanogenesis given by Whiticar (1999) **(Figure 4.18)** .

When examining all CH_4 data, only two samples fall within the diagnostic range for carbonate reduction methanogenesis, L223 9 m and L227 6 m **(Figure 4.19)**. In contrast, some of the CH_4 for the whole water column falls within the range for acetate fermentation methanogenesis.

The relationship between calculated $\delta^{13}C\text{-}CO_2$ values and $\delta^{13}C\text{-}CH_4$ values show that most CH_4 falls above the range of ε for CH_4 oxidation suggested by Whiticar (1999).

4.4 Discussion

4.4.1 Epilimnion CH_4 isotopes and CH_4 processes

Although the data do not represent a true mixing scenario between atmospheric CH_4 and lake CH_4, Keeling plots can still show fundamental differences between these two CH_4 pools. There are two important source values for biogenically produced CH_4-environmental water and atmospheric CH_4. Atmospheric CH_4 has a $\delta^2H\text{-}CH_4$ value and a $\delta^{13}C\text{-}CH_4$ value of -95.0 ‰ and -47.2 ‰ respectively (Rice et al. 2016). Particularly in the case of $\delta^2H\text{-}CH_4$ values, it is apparent that atmospheric CH_4 is not consistent with lake surface CH_4 and that it is not a CH_4 source to lake surface water. Atmospheric CH_4 has a more positive $\delta^2H\text{-}CH_4$ value than the values observed above lake thermoclines **(Figure 4.9D)**. While surface water $\delta^{13}C\text{-}CH_4$ values may be similar to atmospheric CH_4, the concentration of surface water is 1-2 orders of magnitude higher than the atmosphere and the $\delta^2H\text{-}CH_4$ values are much more negative. Therefore, lake CH_4 is distinct from atmospheric CH_4.

Since lakes are supersaturated in CH_4 during the ice-free season, and the $\delta^{13}C\text{-}CH_4$ and $\delta^2H\text{-}CH_4$ values show that lake CH_4 does not originate from the atmosphere, the source of epilimnion CH_4 are called into question. Epilimnion $\delta^{13}C\text{-}CH_4$ values are quite similar across lake groups **(Figure 4.18)**. This is because above the thermocline, CH_4 fluxes from the sediment are well mixed with surface water in the ice free season (Bastviken et al. 2008, Juutinen et al. 2009). CH_4 is either consumed by methanotrophs at the sediment water interface (Bastviken et al. 2002) or released to the atmosphere via diffusion (Bastviken et al. 2004). However, $\delta^{13}C\text{-}CH_4$ values are more positive than one would expect from oxidized hypolimnion CH_4 **(Figure 4.18)**.

The range in epilimnion $\delta^2H\text{-}CH_4$ values **(Figure 4.18)** indicate that oxidation is not the only potential process responsible for CH_4 concentrations in the epilimnion. For instance, oxic water column methanogenesis (Bogard et al. 2014, Khatun et al. 2019). However, Bogard et al. (2014) posit that their sampled CH_4 originated from the acetate fermentation pathway, whereas the CH_4 sampled in this thesis do not clearly fall within

this diagnostic range. In three Arctic lakes, extremely positive δ^2H-CH_4 and δ^{13}C-CH_4 values (>0 ‰) were found under ice and in open water (Cadieux et al. 2016a). These values indicate very efficient methanotrophs that can fractionate C and H to a very high degree and were also associated with low CH_4 concentrations (Cadieux et al. 2016a). Epilimnion CH_4 from the IISD-ELA lakes studied does not show this degree of oxidation. Therefore, there is a large range of CH_4 isotopic values possible in freshwater environments.

During the midsummer, the surface layer would be well mixed and at relative equilibrium with the atmosphere. This is because phytoplankton are taking up DIC from the surface of the lake, and as shown by the δ^{13}C-DIC values, the DIC in each lake is fairly similar.

4.4.2 Hypolimnion CH_4 isotopes and processes

Hypolimnion δ^{13}C-CH_4 and δ^2H-CH_4 values are similar across lakes **(Figure 4.3, Figure 4.4;** δ^{13}C-CH_4 within 32.7 ‰, δ^2H-CH_4 within 250.6‰**)**, and suggests that that across lake groups, CH_4 processes in the hypolimnion are similar, likely due to CH_4 escaping from anoxic sediments. In terms of δ^{13}C-DIC values, there are more negative values in the hypolimnion **(Figure 4.5)** because of organic matter (OM) degradation (Herczeg 1987). This was also the case in 32 small European lakes (Rinta et al. 2015). When stratified, the hypolimnion is essentially isolated from the rest of the lake, building up the products of OM degradation (Herczeg 1987). In addition, CH_4 oxidation will produce negative δ^{13}C-DIC values (Whiticar et al. 1986, Whiticar 1999).

The hydrogen atoms of CH_4 originate from either water or acetate (organic matter) (Woltemate et al. 1984, Whiticar 1999, Chanton et al. 2006). During carbonate reduction methanogenesis, all four hydrogen atoms come from water, whereas during acetate fermentation methanogenesis, three hydrogen atoms come from a methyl (CH_3) group, with the remaining hydrogen atom supplied by water (Whiticar et al. 1986). This is what causes the large ranges in possible δ^2H-CH_4 values for biogenic CH_4. Therefore, the δ^2H-H_2O values of formation water are one controlling factor that determines the δ^2H-CH_4 values of CH_4.

δ^2H-H_2O values are important for CH_4 isotopes because they dictate the δ^2H-CH_4 value, especially in the case of carbonate reduction. δ^2H-H_2O values for IISD-ELA lakes

are at the higher end of the range of observed values in literature **(Table *4.1*)**. These more negative δ^2H-CH_4 values compared to formation water are characteristic to biogenic CH_4 (Woltemate et al. 1984). However, only two hypolimnion samples fell within the suggested ranges for carbonate reduction **(Figure 4.19)** and there was no strong relationship found between δ^2H-H_2O values and δ^2H-CH_4 values **(Figure *4.13*)**. Therefore, in the case of the IISD-ELA lakes studied, δ^2H-H_2O values do not play a large role in dictating δ^2H-CH_4 values.

δ^2H-CH_4 values from Lake Kivu, a meromictic African Rift lake (maximum depth of 485 m) has a large portion of its CH_4 produced via carbonate reduction below 260 m, whereas in shallower depths acetate fermentation is more dominant (Pasche et al. 2011), based on δ^{13}C-CH_4 values. This was also found in Lake Untersee, where carbonate reduction accounts for 90-100 % of methanogenesis (Wand et al. 2006). In these lakes, δ^2H-H_2O values play a larger role in determining δ^2H-CH_4 values as they are meromictic, meaning that they are permanently stratified. This is in direct contrast to the suite of IISD-ELA lakes sampled for this study in which only a subset seasonally stratify. However, studies have shown that when stratified, IISD-ELA lakes can be compared to large meromictic systems such as Lake Kivu (Schiff et al. 2017). Studies of peat porewaters (Hornibrook et al. 1997, Chasar et al. 2000, Chanton et al. 2006, Alstad and Whiticar 2011) show that at depth, carbonate reduction methanogenesis is dominant, compared to acetate fermentation in the surface. The above studies outline the reason for the change of pathway with depth as deeper peat is differences in the type of organic matter substrates for methanogenesis. Therefore, the lake values in this study do not show the transition between methanogenesis pathway at depth.

Although DOM could provide a substrate in the anoxic, DOM rich hypolimnion at IISD-ELA, there is no clear relationship between δ^2H-DOM and δ^2H-CH_4 **(Figure *4.14*)**. The δ^2H-H_2O values are not highly variable for these lakes **(Figure *4.13*)** and therefore do not account for the variation in δ^2H-CH_4. It has previously been established that there is a need for additional research on the fractionation of hydrogen isotopes between organic matter, acetate, CH_4, H_2, and H_2O (Chanton et al. 2006). Without estimates of the fractionation factor between organic matter and CH_4 in acetate fermentation, it is hard to determine the role of δ^2H-DOM values on δ^2H-CH_4 values. It is also important to note that

many hypolimnion CH_4 samples fall outside of the suggested diagnostic range for acetate fermentation **(Figure 4.19)**.

4.4.3 Examination of isotopic values of CH_4 oxidation

A theoretical, closed system, Rayleigh fractionation was assumed using a range of ε_C values (Venkiteswaran and Schiff 2005) and the mean ε_H found in Whiticar (1999) to calculate δ^2H-CH_4 and δ^{13}C-CH_4 values of residual CH_4 after oxidation. The mean δ^{13}C-CH_4 value of metalimnion/hypolimnion source CH_4 in 14 Canadian Shield lakes in Quebec was found to be -72.5 ‰ (Thottathil et al. 2018), compared to -72.3 ‰ in this study. Most low concentration CH_4 samples fall above the line for ε_C= 21.4. This may suggest that the ε_C value in these systems may be >21.4. CH_4 oxidation is limited by CH_4 concentration (i.e. methanogenesis) (Thottathil et al. 2019), illustrating that CH_4 oxidation is accompanied by low CH_4 concentrations. These more positive values of CH_4 can be found in the middle of the water column, at the anoxic/oxic boundary, as this is where CH_4 oxidation occurs (Rudd et al. 1974, Kankaala et al. 2013, Blees et al. 2014, Oswald et al. 2015, Zigah et al. 2015) **(Figure 4.3, Figure 4.4).**

Evidence of methanotrophy at intermediate depths in lakes with anoxic bottoms is also shown by δ^{13}C-CH_4 values. For instance, at L227 4m the δ^{13}C-CH_4 value is -17.9 ‰ alongside relatively low CH_4 and O_2 concentrations. There are several samples which may be the residual CH_4 from CH_4 that has been highly oxidized, with δ^2H-CH_4 values >-100 ‰, the highest being at L442 9m, with δ^2H-CH_4 = -39.0 ‰. This indicates that between 75 % and 90 % of that CH_4 has been oxidized (f= 0.25 to 0.1) **(Figure 4.17)**. CH_4 oxidation often takes place in the middle of the water column, near the thermocline, and thus may be the cause of the more positive values **(Figure 4.3, Figure 4.4)**. This means that in the case of the stratified lakes studied in this thesis, it is likely that the CH_4 produced in the hypolimnion diffuses to the anoxic/oxic boundary, and is oxidized by methanotrophs (Blees et al. 2014, Vachon et al. 2019).

4.4.4 Seasonal progression of ^{13}C-CH_4 and δ^2H-CH_4 values in two stratified boreal lakes

The seasonal progression of two deep boreal lakes that develop anoxia, L227 and L442, was examined. Through the ice-free season, as the lake becomes more and more stratified, the thermocline deepens. Summer stratification of boreal lakes causes distinct

chemical gradients, for instance CH_4 concentrations are higher later in the ice free season and O_2 is lower later in the season for both L227 and L442 deeper in the water column **(Figure 4.15**, **Figure 4.16)**. Juutinen et al. (2009) showed that in a suite of 207 Finnish lakes, lake CH_4 storage was higher during stratification, and variations in DIC and $\delta^{13}C$-CH_4 values have been found to have been a consequence of stratification in 32 European lakes (Rinta et al. 2015). When lakes are strongly stratified, there is higher CH_4 storage (Vachon et al. 2019). Therefore, not only can methanogenesis take place in lake sediment, but also in the anoxic hypolimnion of lakes such as L227 and L442. This results in the seasonal trends present in the lakes.

The seasonal progression of these two lakes shows that the $\delta^{2}H$-CH_4 and $\delta^{13}C$-CH_4 values are more negative in September **(Figure 4.15**, **Figure 4.16)**. More negative $\delta^{13}C$-CH_4 values were found with high CH_4 concentrations, while more positive $\delta^{13}C$-CH_4 values were found with lower CH_4 concentrations (Rinta et al. 2015). These highly negative values observed in L227 and L442 may be due to the timing of high CH_4 concentrations. Higher in the water column in L227, less negative $\delta^{13}C$-CH_4 values are observed in May and June **(Figure 4.18B)** as methanotrophs use ^{12}C over ^{13}C during CH_4 oxidation (Barker and Fritz 1981). In two northern temperate stratified lakes, Paul and Peter Lake, these increases in $\delta^{13}C$-CH_4 in the middle of the water column can also be observed over the ice free season between May and September (Bastviken et al. 2008). Similarly, more positive $\delta^{2}H$-CH_4 values in L227 and L442 are likely from residual CH_4 after CH_4 oxidation occurring at the anoxic/oxic boundary, as exhibited by the O_2 profile **(Figure 4.16)**. Along the sediment water interface, the anoxic/oxic boundary is typically where CH_4 oxidation occurs due to low O_2 concentrations and high CH_4 concentrations (Rudd et al. 1974, Kankaala et al. 2013, Blees et al. 2014, Oswald et al. 2015, Zigah et al. 2015). In addition, L227 is eutrophic, and therefore high CH_4 concentrations are likely due to the large availability of OM (Jones and Grey 2011). In one study, it was estimated that 90 % of the CH_4 produced in the summer in L227 did not leave the anoxic hypolimnion (Rudd and Hamilton 1978).

4.4.5 Potential incorporation of CH_4 in the food web shown through $\delta^{13}C$-POM values

Many studies have shown that through CH_4 oxidation metabolism, CH_4 can be incorporated into lake food webs (Bastviken et al. 2003, Kankaala et al. 2006b, 2006a,

Deines et al. 2007, Jones et al. 2008, Rask et al. 2010, Jones and Grey 2011, Sanseverino et al. 2012, van Duinen et al. 2013, Agasild et al. 2014, 2018, Schilder et al. 2015, Grey 2016). This process is traced through the distinctive negative $\delta^{13}C$ values from biogenic CH_4. In short, methanotrophs are consumed by benthic macroinvertebrates or zooplankton, and this CH_4 derived carbon is incorporated into the food web (Grey 2016) **(Figure 4.1)**. Additionally, the CO_2 produced in CH_4 oxidation may be utilized by phytoplankton, which are then consumed by zooplankton (Grey 2016). The latter of these two routes may explain the more negative $\delta^{13}C$-POM values observed at intermediate depths in L227 and L222, where CH_4 oxidation would be occurring. Another example of the potential incorporation of the CH_4 signal is in hypolimnion POM in L224 **(Figure 4.6)**.

4.5 Conclusions

This chapter provides baseline data of $\delta^{13}C$-CH_4 and $\delta^{2}H$-CH_4 values in small, oligotrophic, Canadian Shield lakes. While $\delta^{13}C$-CH_4 values for similar environments are quite abundant in the literature, this is not the case for $\delta^{2}H$-CH_4 values.

The CH_4 in the well mixed water column, above the thermocline, is distinct from atmospheric CH_4. Particularly, the $\delta^{2}H$-CH_4 values of lake CH_4 are much more negative compared to those of atmospheric CH_4, indicating in-lake processes dictate the CH_4 balance. In general, quantifying processes that control CH_4 production and consumption can provide information about diagenesis in environments, such as lakes (Whiticar 1999). Since CH_4 is an important GHG, it is critical that it is understood, particularly in environments such as boreal lakes. Indeed, it has been shown that small, boreal lakes, have larger CH_4 fluxes per unit area compared to large lakes (Juutinen et al. 2009).

Upon examination of the four, broad lake groups, it is clear that each group has unique characteristics in terms of CH_4 dynamics. Both the deep anoxic and shallow anoxic lake groups behaved similarly, with high concentrations of CH_4 in the anoxic hypolimnion with similar and very negative $\delta^{13}C$-CH_4 and $\delta^{2}H$-CH_4 values. The lakes with a majority oxic water column had for the most part consistent isotopic values throughout the water column, as well as low CH_4 concentrations and high O_2 concentrations. Comparably, the polymictic lakes also had consistent values across variables throughout the water column. Most lakes, with the exception of the polymictic group, showed some evidence in the isotopic values of CH_4 oxidation occurring at the anoxic/oxic boundary.

Two seasonally stratified lakes were studied throughout the ice-free season. CH_4 dynamics in L227 and L442 showed that later in the season, CH_4 concentrations increased. Broadly, this was accompanied by more negative $\delta^{13}C$-CH_4 and $\delta^{2}H$-CH_4 values.

In assessing the potential roles of methanogenic pathway and CH_4 oxidation in controlling CH_4 isotopes, it became clear that the sampled CH_4 does not fall clearly into either the acetate fermentation or carbonate reduction pathway as described in the literature. Further, oxidation does not appear to be the only factor at work, particularly in the epilimnion. This is evidenced by the highly variable range in epilimnion $\delta^{2}H$-CH_4 values.

The consumption of CH_4 through oxidation by methanotrophs decreases the amount of CH_4 that is emitted to the atmosphere (Bastviken et al. 2008) and as such the CH_4 dynamics of boreal lakes are compelling with respect to global climate change. It is important to note that aerobic methane oxidation is not only controlled by CH_4 concentration, but by many factors that can vary within lakes (Thottathil et al. 2019) that were not explored in this thesis. It is also important to note that this thesis only discussed diffusive CH_4 flux.

To continue this work, the role of anaerobic methane oxidation in boreal lakes should be examined, as this process is currently not well known. However, this has recently been found to be wide spread in lake sediments (Martinez-Cruz et al. 2018) and in boreal lakes (Schiff et al. 2017). Further, these lakes presented data from midsummer, representing only a snapshot in time in terms of the biogeochemical processing that occurs all year in lakes, including under ice.

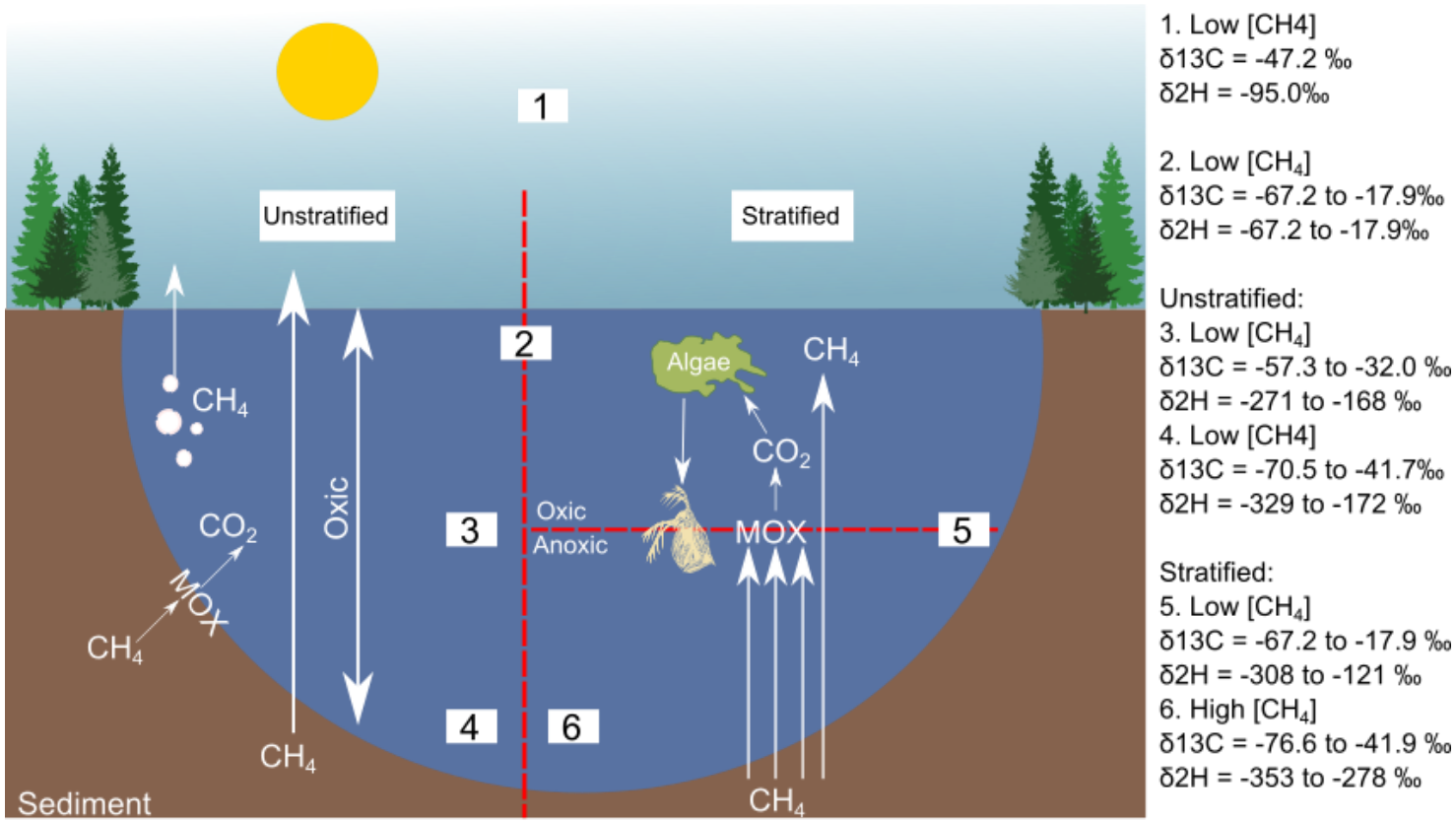

Figure 4.1 Simplified diagram of CH_4 dynamics in two types of lakes, unstratified (representing the oxic and polymictic lakes in this study) and stratified (representing the deep and shallow lakes with anoxic bottoms in this study) adapted from (Grey, 2016). MOX = CH_4 oxidation. This also shows how CH_4 derived carbon can enter the food web through CH_4 oxidation.

Table 4.1 Literature values of $\delta^{13}C\text{-}CH_4$ and $\delta^{2}H\text{-}CH_4$ for various ecosystems. – indicates that mean $\delta^{2}H\text{-}H_2O$ values were not given.

Sample name (location)	Sample type	$\delta^{13}C\text{-}CH_4$ range (‰)	$\delta^{2}H\text{-}CH_4$ range (‰)	$\delta^{2}H\text{-}H_2O$ mean (‰)	n	Reference
Ombrotrophic bog (Northern Alberta, Canada)	Porewater	-78 to -68	-348 to -248	-80.4	17	(Alstad and Whiticar 2011)
Minerotrophic Fen (Southeastern Ontario, Canada)	Porewater	-75 to -66	-375 to -275	-134	27	(Alstad and Whiticar 2011)
EVV Upper Lake (Eastern Greenland)	Water column	-69.0 to -50	-370 to -150	-91.5	8	(Cadieux et al. 2016b)
Teardrop Lake (Eastern Greenland)	Water column	-35.0 to 7.40	-325 to 250	-96.5	9	(Cadieux et al. 2016b)
Pontentilla Lake (Eastern Greenland)	Water column (under ice)	-65.0 to -34.0	-375 to 2.00	-97.4	10	(Cadieux et al. 2016b)
EVV Upper Lake (Eastern Greenland)	Water column (under ice)	-72.2 to -71.3	-385 to -350	-	6	(Cadieux et al. 2016)
Teardrop Lake (Eastern Greenland)	Water column (under ice)	-59.1 to -56.3	-350 to -305	-	6	(Cadieux et al. 2016)
Pontentilla Lake (Eastern Greenland)	Water column (under ice)	-38.4 to -69.4	-388 to 29	-	16	(Cadieux et al. 2016)
Turnagain Bog (Alaska, USA)	Porewater	-75.0 to -62.9	-351 to -308	-122	9	(Chanton et al. 2006)
Fen 62 (Alaska, USA)	Porewater	-86.0 to -82.2	-330 to -346	-132	2	(Chanton et al. 2006)
Bonanza Mix (Alaska, USA)	Porewater	-55.1	-390	-138	1	(Chanton et al. 2006)
Beaver Sports Hallow (Alaska, USA)	Porewater	-56.9 to -56.6	-394 to -365	-145	2	(Chanton et al. 2006)
Smith Lake Carex (Alaska, USA)	Porewater	-50.5	-362	-136	1	(Chanton et al. 2006)

UAF Bog (Alaska, USA)	Porewater	-52.3	-377	-145	1	(Chanton et al. 2006)
Discontinuous permafrost (Alaska, USA)	Porewater	-66.2 to -65.5	-384 to -393	-157	2	(Chanton et al. 2006)
Fen 67 (Alaska, USA)	Porewater	-66.2	-394	-161	1	(Chanton et al. 2006)
Galbraith Lake (Alaska, USA)	Porewater	-67.2 to -62.9	-388 to -372	-146	2	(Chanton et al. 2006)
Imnavaiat Creek (Alaska, USA)	Porewater	-65.9 to -63	-379 to -367	-152	2	(Chanton et al. 2006)
Pipeline 70 Fen (Alaska, USA)	Porewater	-57.8	-363	-148	1	(Chanton et al. 2006)
Franklin Bluff Fen (Alaska, USA)	Porewater	-62.8 to -58.1	-369 to -366	-135	2	(Chanton et al. 2006)
Fen (Northern Minnesota, USA)	Porewater	-67.9 to -58.8	-302 to-276	-	7	(Chasar et al. 2000)
Bog crest (Northern Minnesota, USA)	Porewater	-67.6 to -66.1	-263 to -287	-	10	(Chasar et al. 2000)
Point Pelee Marsh (Southern Ontario, Canada)	Porewater	-72.3 to -48.2	-320 to -183	-43.3	17	(Hornibrook et al. 1997)
Sifton Bog (Southern Ontario, Canada)	Porewater	-72.3 to -48.2	-67.5 to -49.6	-66.6	20	(Hornibrook et al. 1997)
Radar Lake (Western Alaska, USA)	Ebullitive flux	-60.3 to -55.2	-381 to -360	-	6	(Martens et al. 1992)
Tundra Lake Ridge (Western Alaska, USA)	Ebullitive flux	-62.9 to -57.4	-383 to -361	-	6	(Martens et al. 1992)
Pingo Pond (Western Alaska, USA)	Ebullitive flux	-63.5 to -58.0	-371to -326	-	7	(Martens et al. 1992)

Lake ABLE (Western Alaska, USA)	Ebullitive flux	-61.6 to -58.4	-361 to -323	-	5	(Martens et al. 1992)
Lake Kivu (Republic of Rwanda and the Democratic Republic of the Congo)	Water column (anoxic hypolimnion only)	-61.0 to -32.0	-225 to -190	-	12	(Pasche et al. 2011)
Mizorogaike Pond (Kyoto, Japan)	Ebullitive flux	-76.2 to -52.8	-371 to -254	-36.7	24	(Sugimoto and Fujita 2006)
Lake Untersee (Eastern Antarctica)	Water column (under ice)	-51.5 to -31.0	-409 to -164	-282	6	(Wand et al. 2006)
IISD-ELA Lakes (Northwestern Ontario, Canada)	Water column	-76.6 to -10	-353 to -39.1	-68.3	94	This study

Table 4.2 Summary of mean physical and chemical parameters of sampled lakes including lake order, lake area, lake volume, maximum depth (Z_{max}), residence time, DOC concentration, whether the lake is sampled as part of the PHISH project, and lake group. Residence time calculated as the average theoretical water renewal time (years) by dividing lake volume (m^3) by estimated outflow (m^3).

Lake	DOC (mg/L)	Lake order	Lake Area (ha)	Lake Volume (m^3)	Z_{max} (m)	Estimated Outflow (m^3)	Residence time (years)	PHISH lake?	Group
L224	3.3	2	25.9	3005000	27.4	239899	12.5	Yes	Anoxic bottom deep
L373	3.9	1	27.3	2941000	21	198316	14.8	Yes	Oxic
L223	4.7	3	27.3	1951000	14.4	639730	3.0	Yes	Anoxic bottom deep
L626	5.1	4	25.9	1772000	11.3	954674	1.9	Yes	Oxic
L442	6.2	2	16	1303000	16	396141	3.3	Yes	Anoxic bottom deep
L239	7.0	1	56.1	5910000	30.4	967813	6.1	Yes	Oxic
L303	7.6	1	9.9	150000	2.5	133113	1.1	No	Polymictic
L304	7.9	1	3.6	115000	6.7	64957	1.8	No	Anoxic bottom shallow
L227	8.3	1	34.4	221000	10	84641	2.6	No	Anoxic bottom deep
L658	8.9	1	8.4	546473	13.5	140249	3.9	Yes	Oxic
L222	9.4	1	16.4	600000	5.8	502680	1.2	No	Anoxic bottom shallow
L164	9.2	32	20.3	1002000	7	12174554	0.2	Yes	Oxic
L221	11	2	9	189100	5.7	201761	0.9	No	Anoxic bottom shallow
L470	12	4	6	33000	2	412626	0.1	Yes	Polymictic

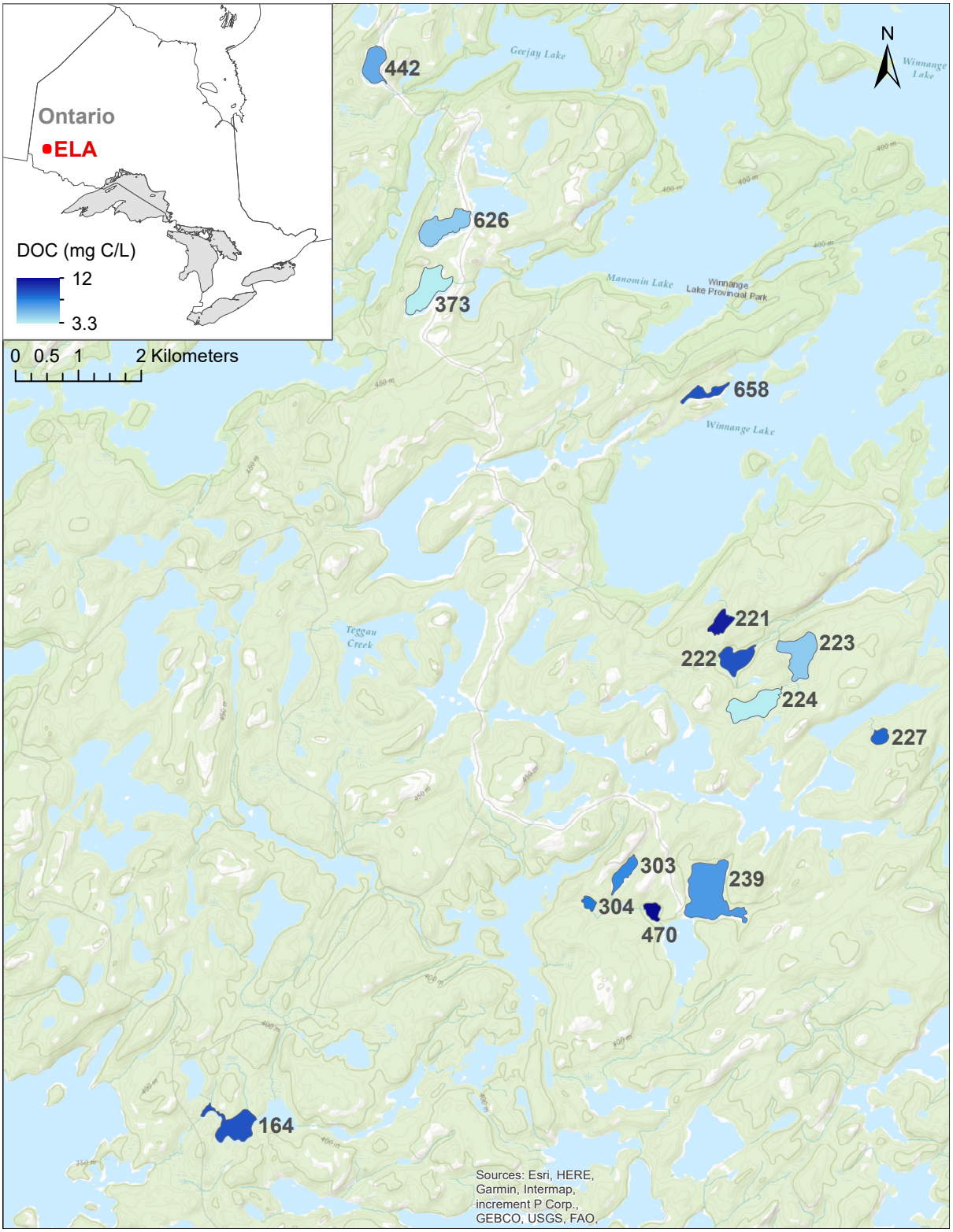

Figure 4.2 Map of IISD-ELA showing the fourteen lakes sampled as part of this research project.

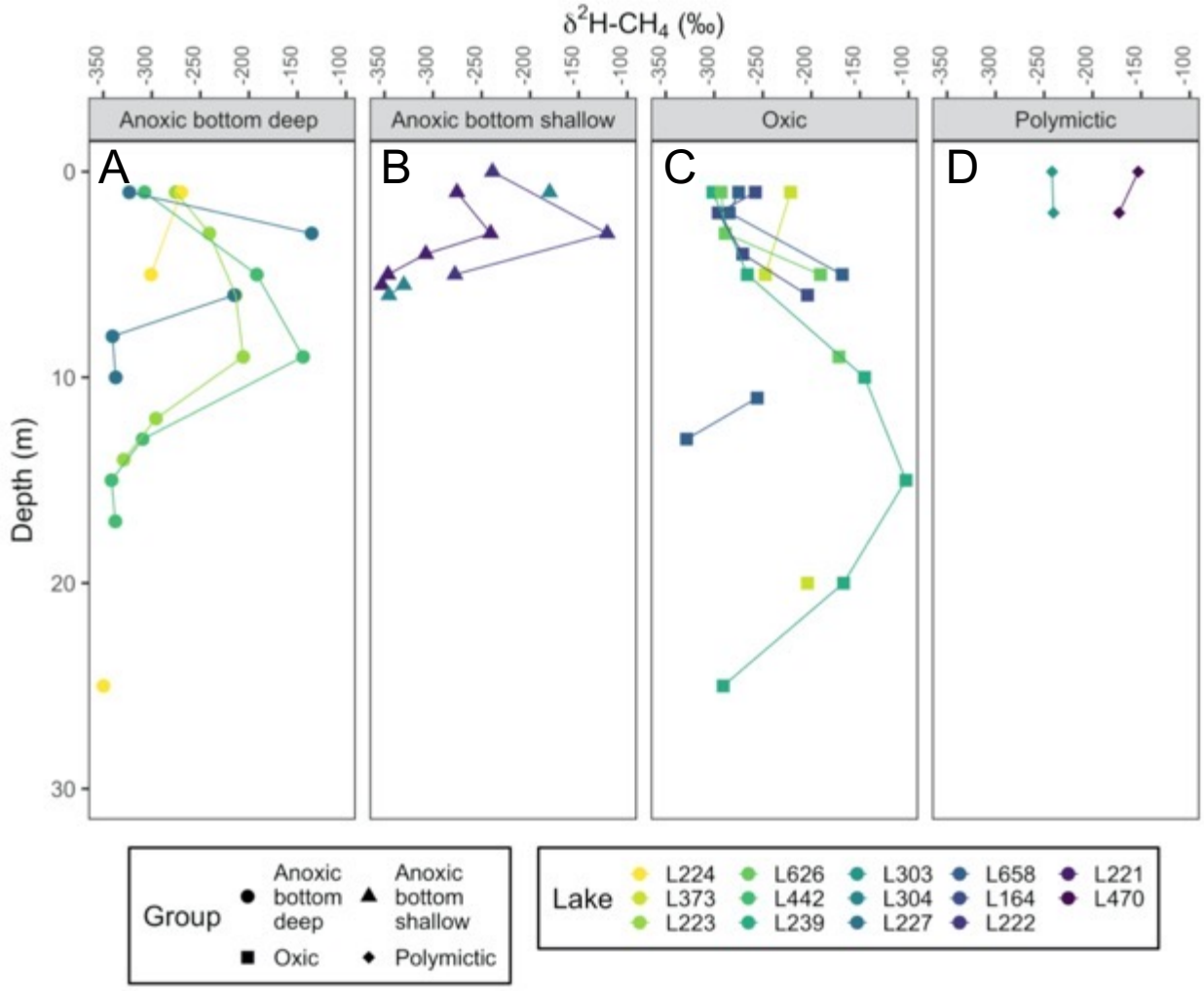

Figure 4.3 Midsummer δ^2H-CH_4 values of sampled lakes by group; **A.** Anoxic deep lakes, **B.** Anoxic shallow lakes, **C.** Majority oxic lakes, **D.** Polymictic lakes. Missing values indicate that samples were below CH_4 concentration detection limit.

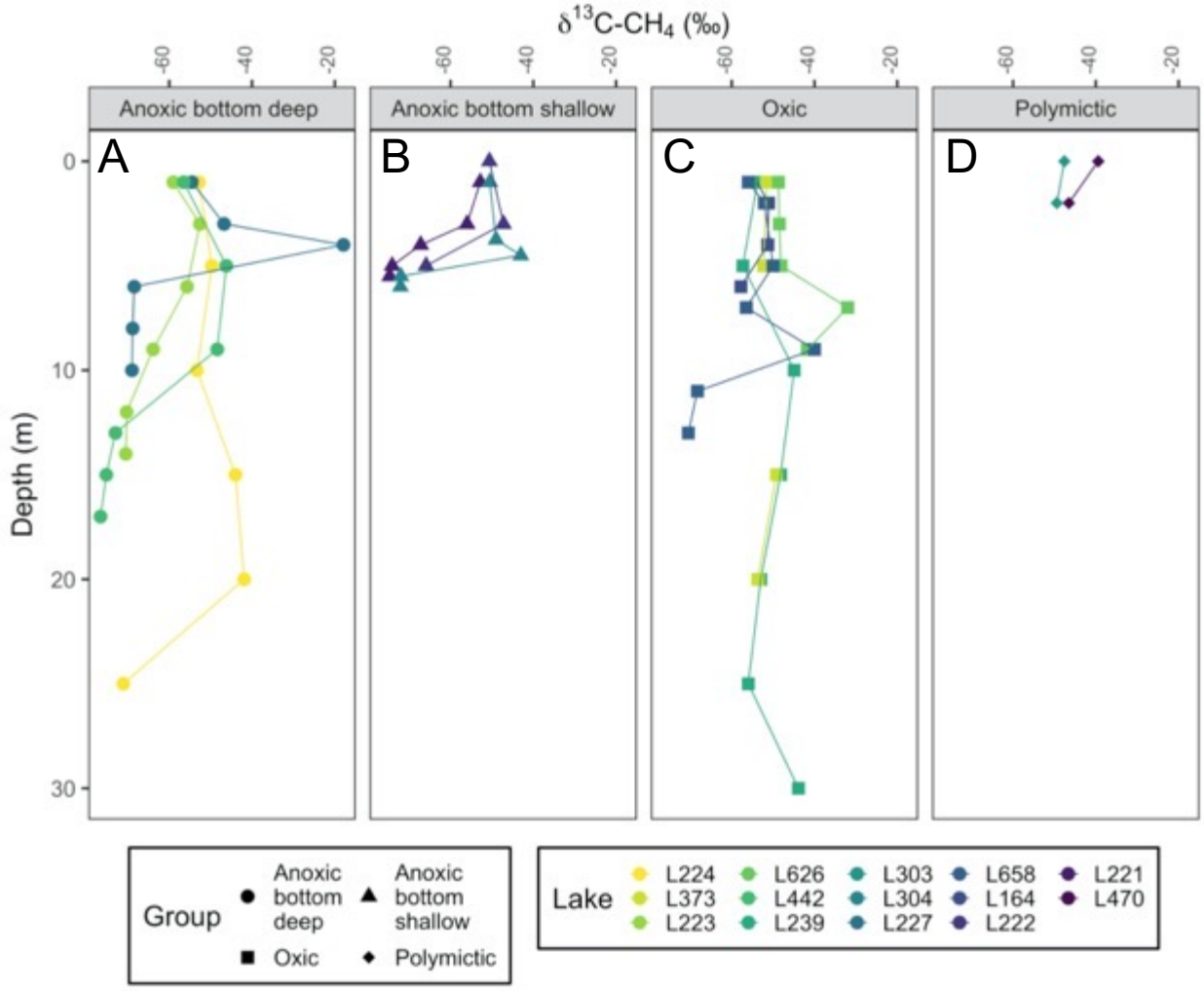

Figure 4.4 Midsummer $\delta^{13}C\text{-}CH_4$ values of sampled lakes by group; **A.** Anoxic deep lakes, **B.** Anoxic shallow lakes, **C.** Majority oxic lakes, **D.** Polymictic lakes.

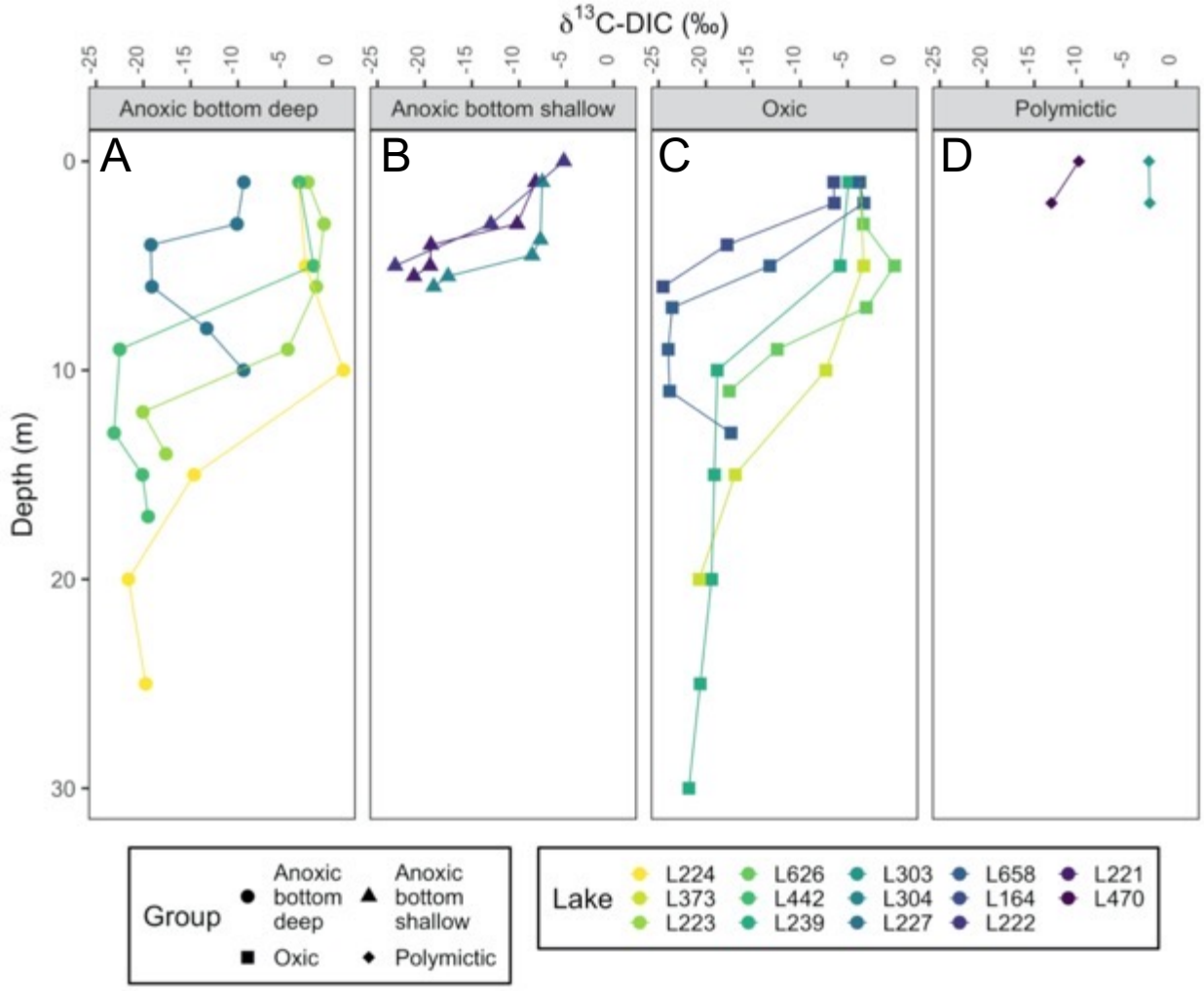

Figure 4.5 Midsummer δ^{13}C-DIC values of sampled lakes by group; **A.** Anoxic deep lakes, **B.** Anoxic shallow lakes, **C.** Majority oxic lakes, **D.** Polymictic lakes.

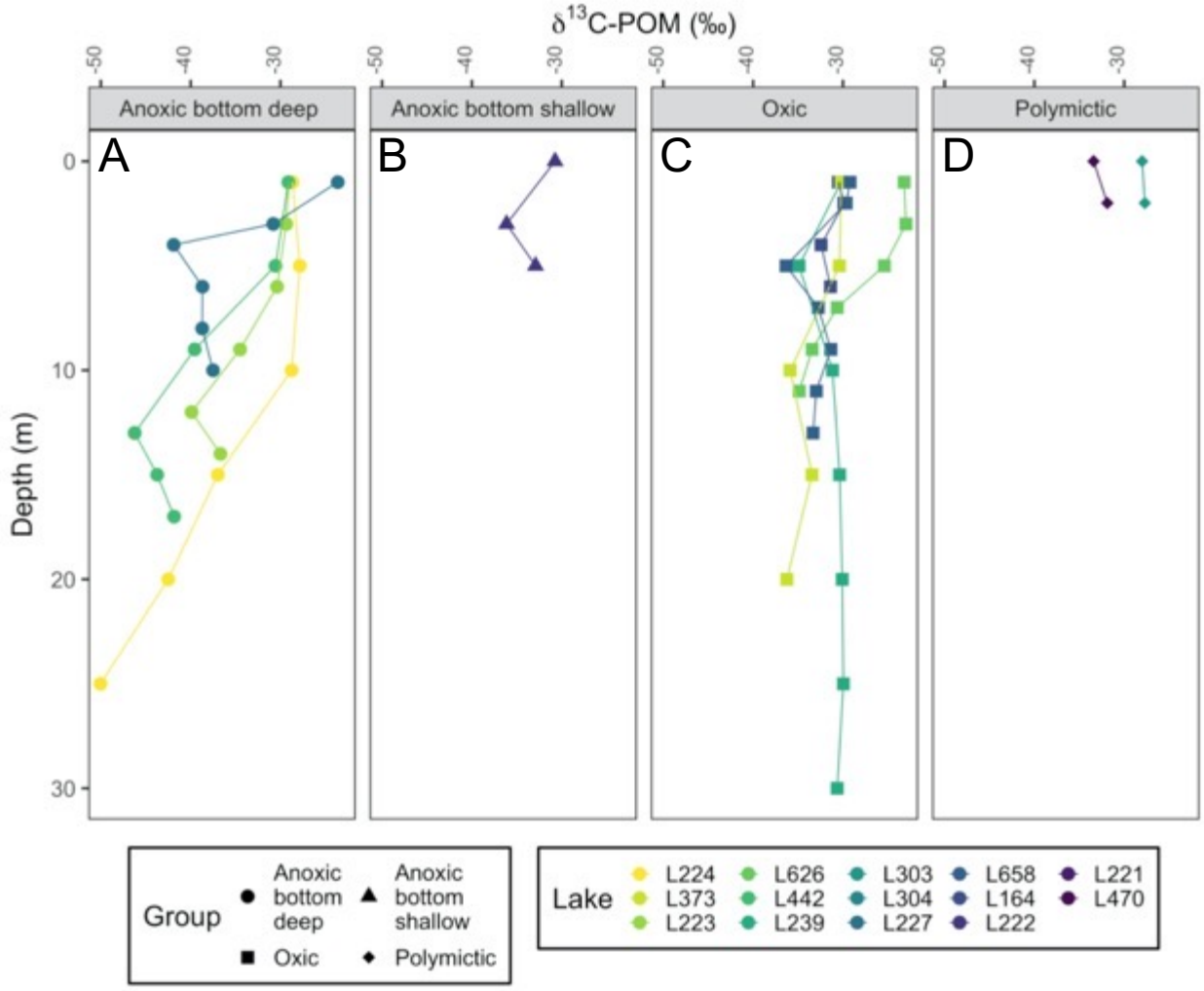

Figure 4.6 Midsummer δ^{13}C-POM values of sampled lakes by group; **A.** Anoxic deep lakes, **B.** Anoxic shallow lakes, **C.** Majority oxic lakes, **D.** Polymictic lakes. δ^{13}C-POM values are not available for L304 and L221.

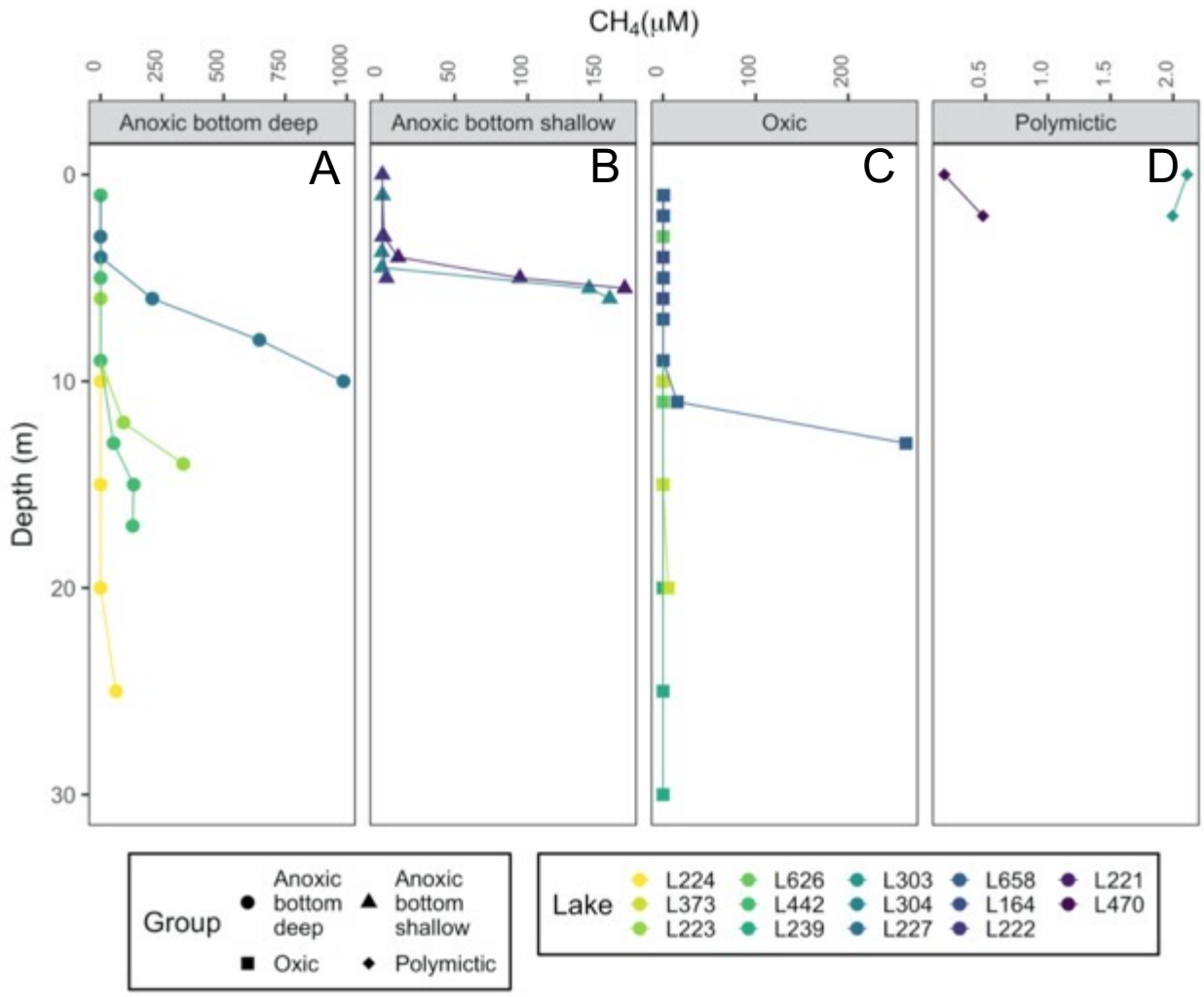

Figure 4.7 Midsummer CH_4 concentrations of sampled lakes by group; **A.** Anoxic deep lakes, **B.** Anoxic shallow lakes, **C.** Majority oxic lakes, **D.** Polymictic lakes.

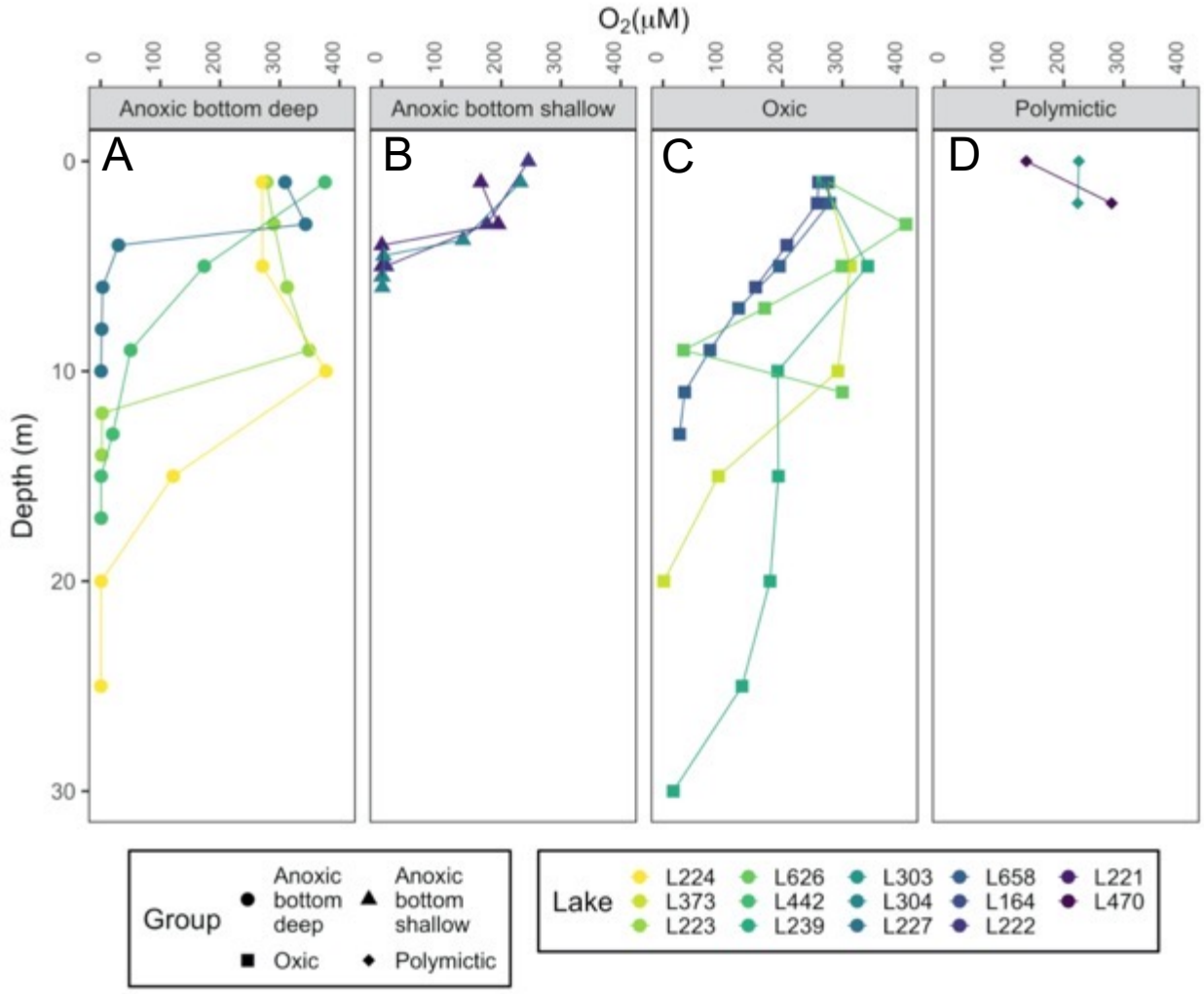

Figure 4.8 Midsummer O_2 concentrations of sampled lakes by group; **A.** Anoxic deep lakes, **B.** Anoxic shallow lakes, **C.** Majority oxic lakes, **D.** Polymictic lakes.

Table 4.3 Summary of general results of 2018 midsummer δ^2H-CH_4 values, $\delta^{13}C$-CH_4 values, $\delta^{13}C$-DIC values, $\delta^{13}C$-POM values, CH_4 concentration (μM), and O_2 concentration (μM) for the sampled suite of lakes.

Group	Lakes	δ^2H-CH_4	$\delta^{13}C$-CH_4	$\delta^{13}C$-DIC	$\delta^{13}C$-POM	CH_4 (μM)	O_2 (μM)
Anoxic bottom deep	L223, L224, L227, L442	More positive values in metalimnion (meta), most negative values in hypolimnion (hypo)	Most negative values in hypo	Epilimnion (epi) values approximately the same for each lake, most negative values in hypo	Most negative values in hypo	<1 ppm in epi, ≥50 ppm in hypo	Anoxic in hypo
Anoxic bottom shallow	L221, L222, L304	More positive values in meta, most negative values in hypo	Most negative values in hypo	Epi values approximately the same for each lake, most negative values in hypo	Consistent throughout water column*	<1 ppm in epi, ≥3 ppm in hypo	Anoxic in hypo
Oxic	L164, L239, L373, L626, L658	Most negative values in hypo	Relatively consistent throughout water column	Epi values approximately the same for each lake, most negative values in hypo	Relatively consistent throughout water column	<1 ppm throughout water column, except L658 with ≥15 ppm in hypo	Oxic for most of water column
Polymictic	L303, L470	Consistent throughout water column	Consistent throughout water column	Consistent throughout water column	Consistent throughout water column	≤2 ppm	Oxic water column

* $\delta^{13}C$-POM values not available for L221 and L304

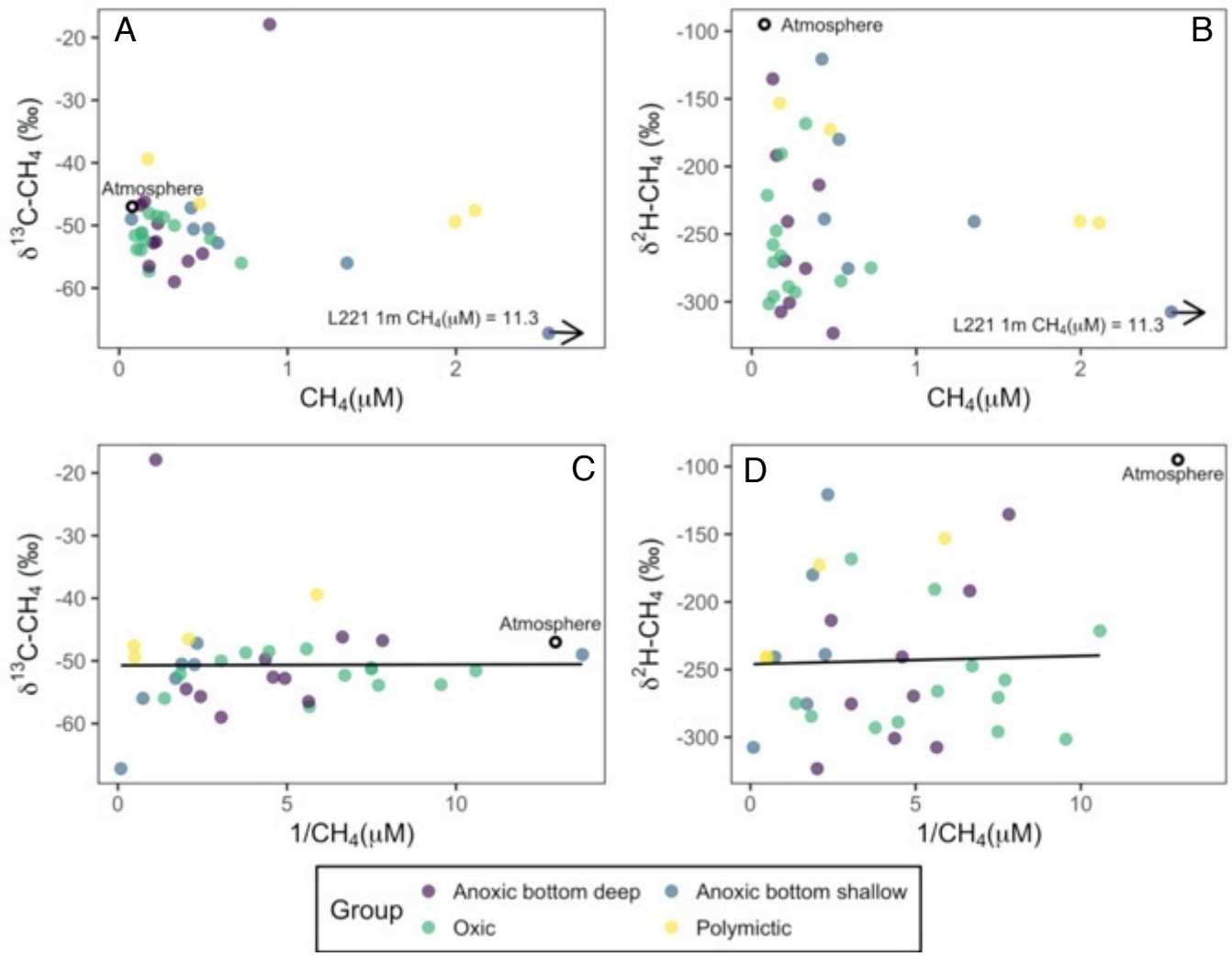

Figure 4.9A. Relationship between δ^{13}C-CH_4 values and CH_4 concentration in the well mixed water column above the thermocline. **B.** Relationship between δ^2H-CH_4 values and CH_4 concentration in the well mixed water column above the thermocline. **C.** Keeling plot of δ^{13}C-CH_4 values and the inverse of CH_4 concentration in the well mixed water column above the thermocline (y= 0.014x-50.7, R^2= -0.3121). **D.** Keeling plot of δ^2H-CH_4 values and the inverse of CH_4 concentration in the well mixed water column above the thermocline (y= 0.606x -246, R^2= -0.0323).

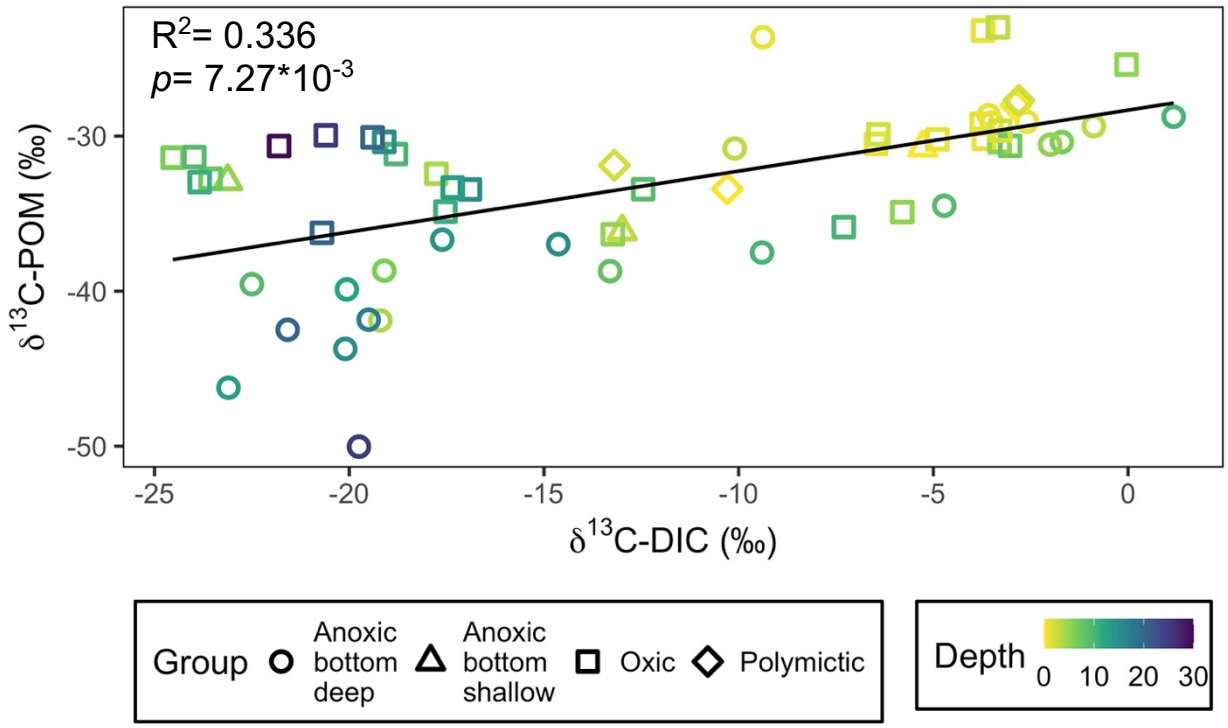

Figure 4.10 Relationship between δ^{13}C-DIC values and δ^{13}C-POM values in the suite of samples lakes.

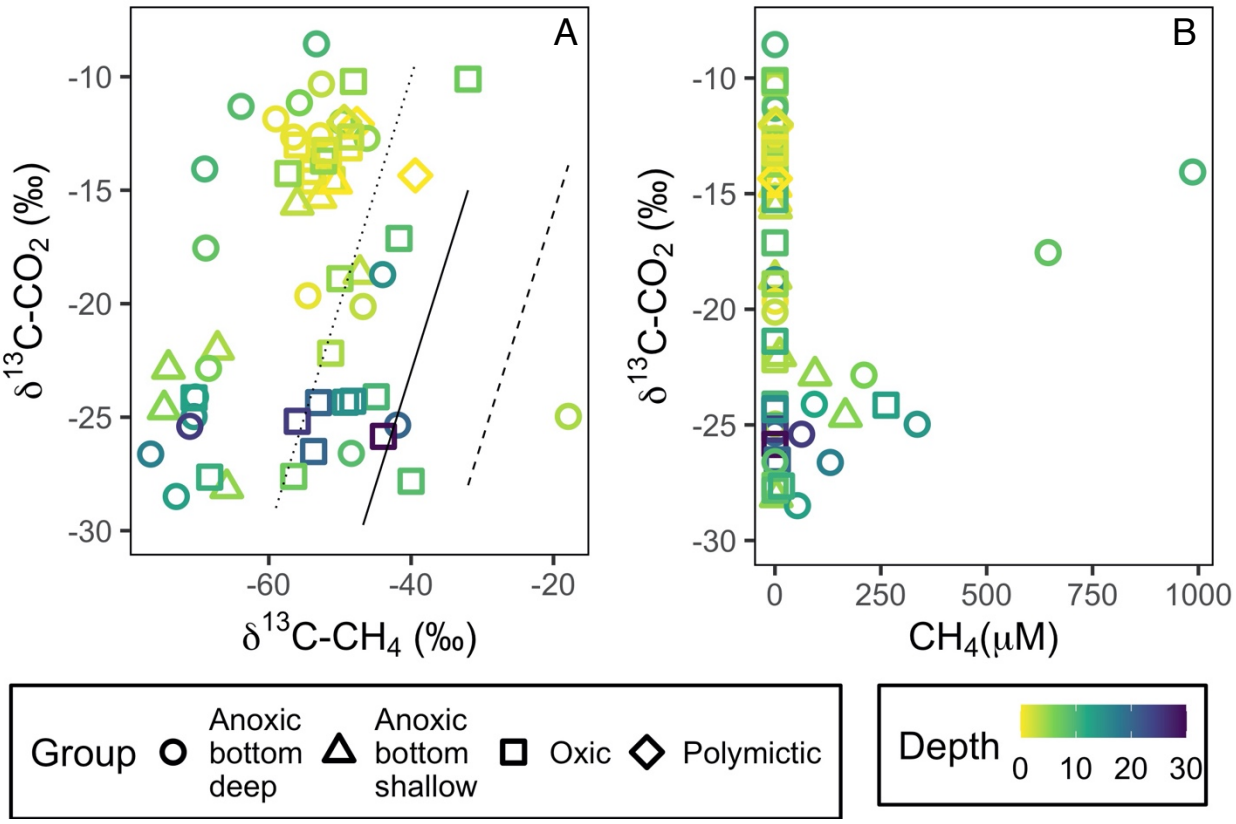

Figure 4.11A. Relationship between calculated $\delta^{13}C\text{-}CO_2$ values and $\delta^{13}C\text{-}CH_4$ values. Dashed line represents ε= 4, solid line represents ε= 17, dotted line represents ε=30. ε values based on the range for methanotrophy published in Whiticar (1999). **B.** Relationship between calculated $\delta^{13}C\text{-}CO_2$ values and CH_4 concentration.

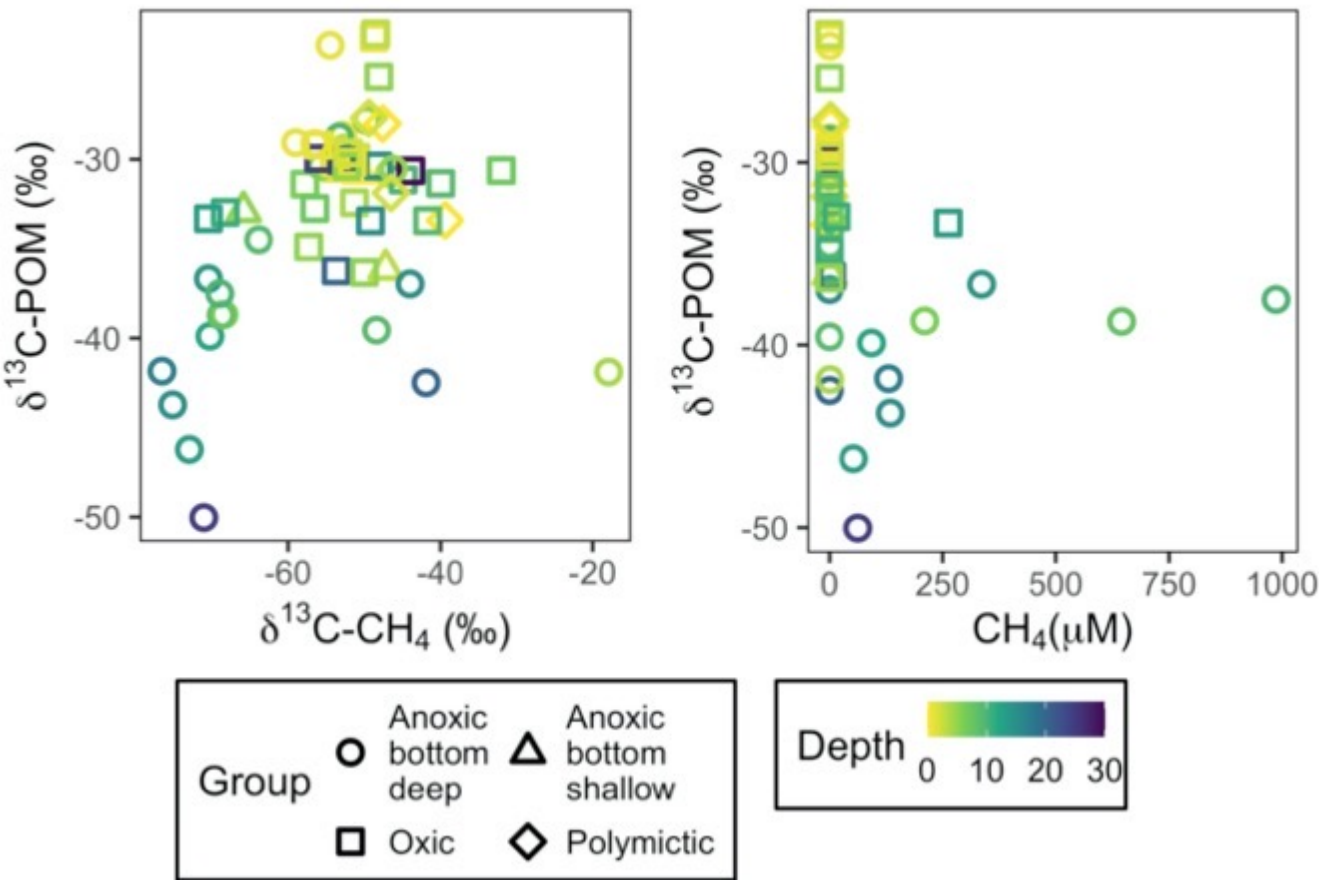

Figure 4.12A. Relationship between midsummer δ^{13}C-CH_4 and δ^{13}C-POM values. **B.** Relationship between midsummer CH_4 concentrations and δ^{13}C-POM values.

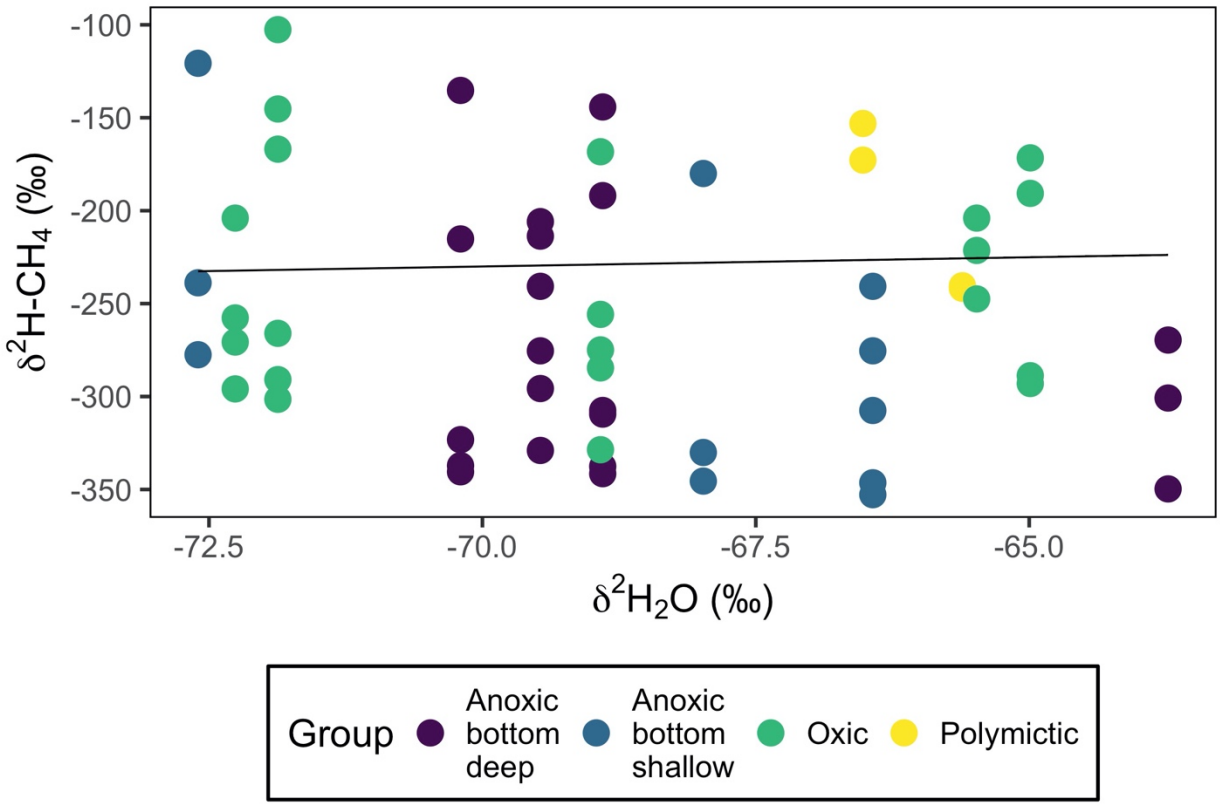

Figure 4.13 Relationship between δ^2H-H_2O values and δ^2H-CH_4 values. The line represents ε= 160, the direct use of water-hydrogen in the carbonate reduction pathway (Whiticar 1999). Note that the surface δ^2H-H_2O value for each lake was assumed to remain constant for the whole water column.

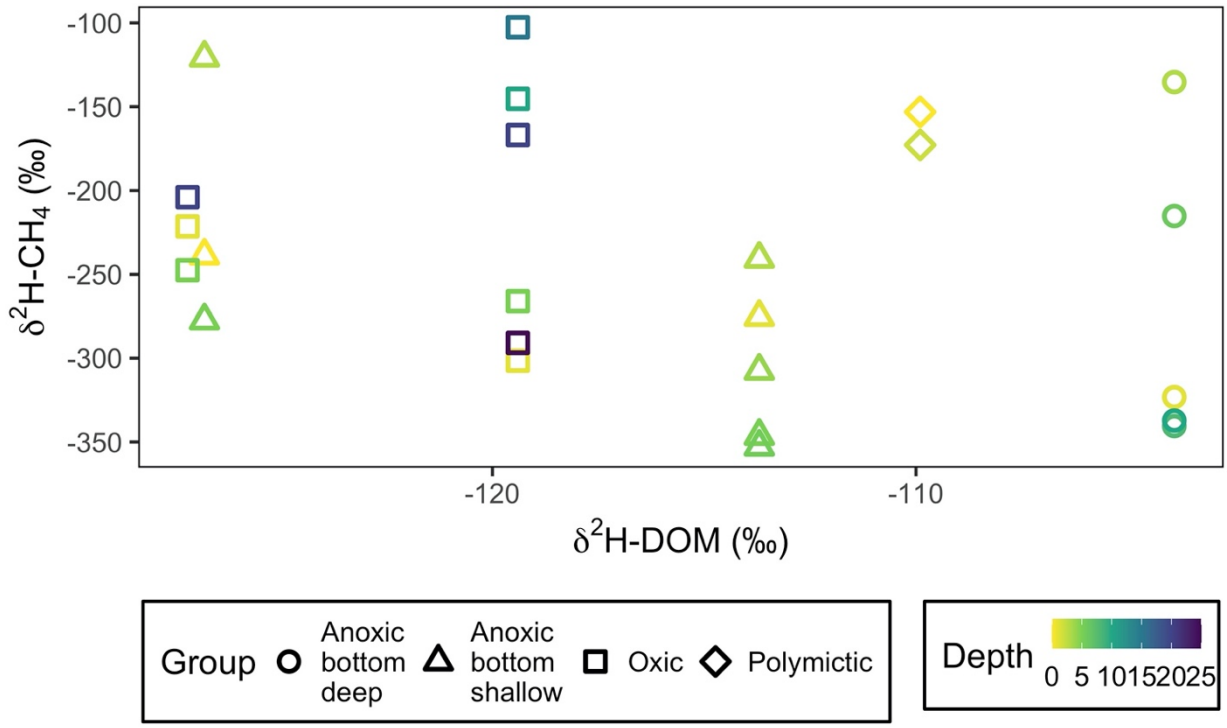

Figure 4.14 Relationship between δ^2H-DOM values and δ^2H-CH_4 values in a subset of the sampled lakes. δ^2H-DOM values were taken at the surface and assumed for the entire water column.

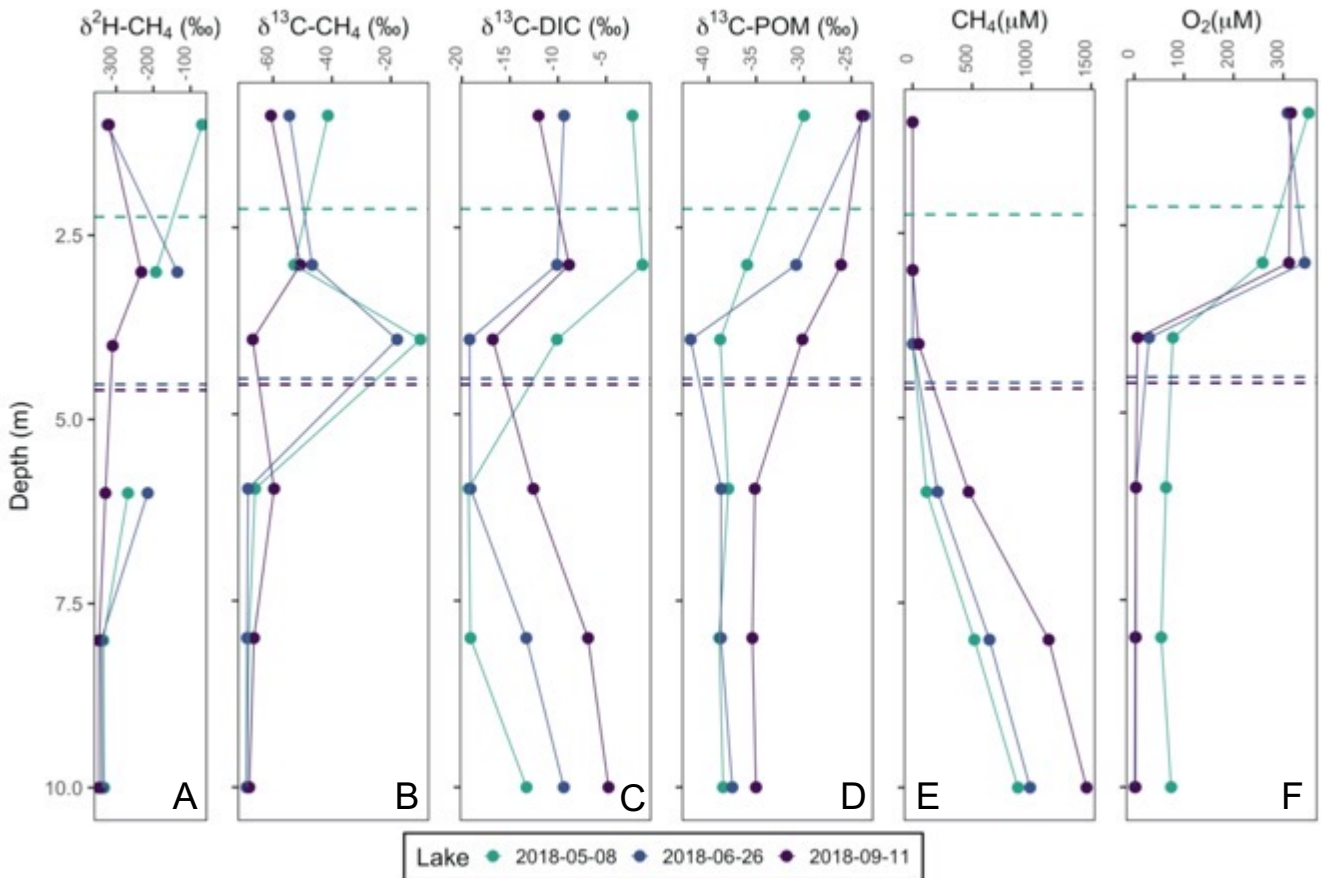

Figure 4.15 Seasonal progression of **A.** δ^2H-CH_4, **B.** δ^{13}C-CH_4, **C.** δ^{13}C-DIC, **D.** δ^{13}C-POM, **E.** CH_4 concentration, and **F.** O_2 concentration for L227. Dashed lines indicate thermocline depth for each month and the colour of each line corresponds with its respective month.

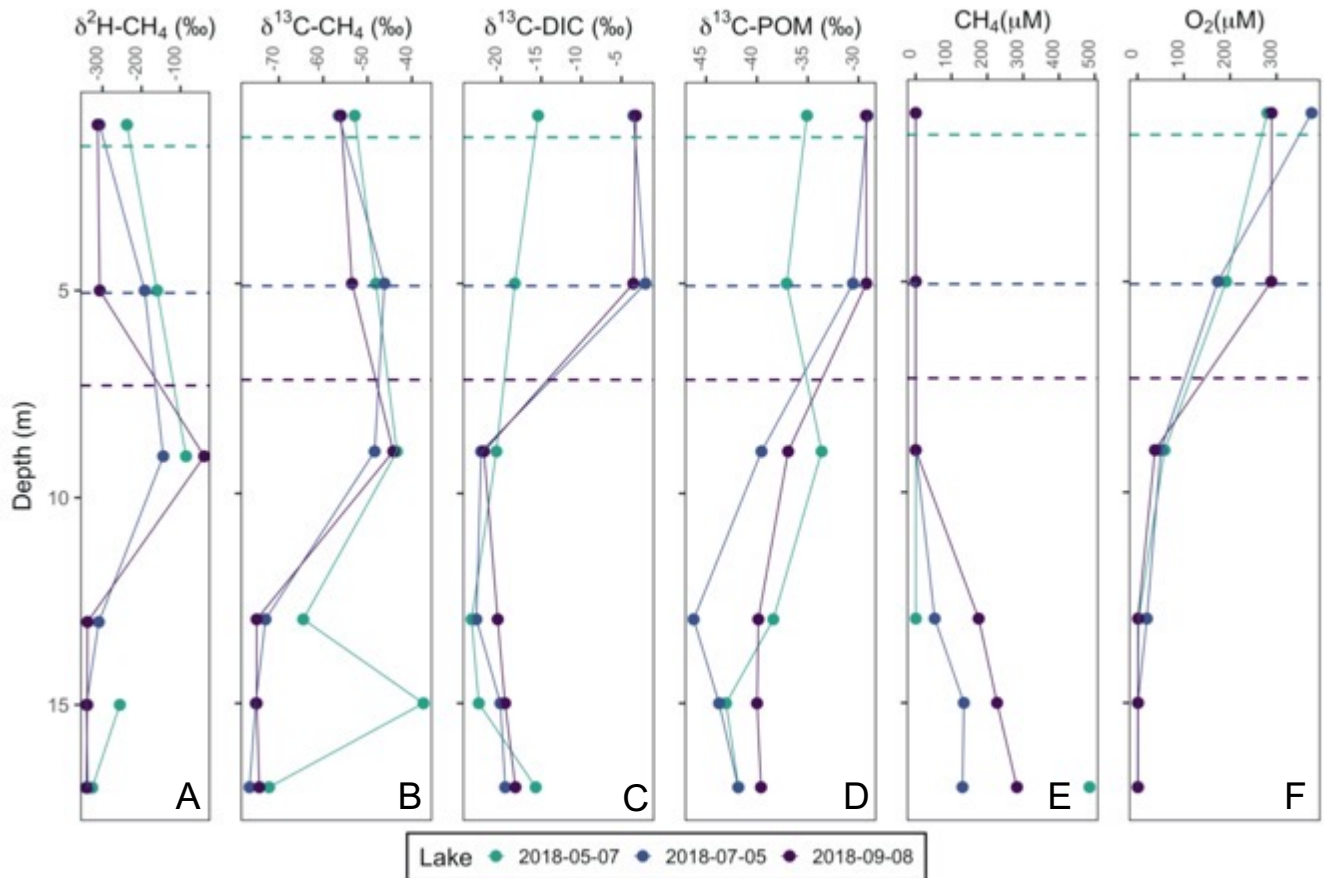

Figure 4.16 Seasonal progression of **A.** δ^2H-CH_4, **B.** δ^{13}C-CH_4, **C.** δ^{13}C-DIC, **D.** δ^{13}C-POM, **E.** CH_4 concentration, and **F.** O_2 concentration for L442. Dashed lines indicate thermocline depth for each month and the colour of each line corresponds with its respective month.

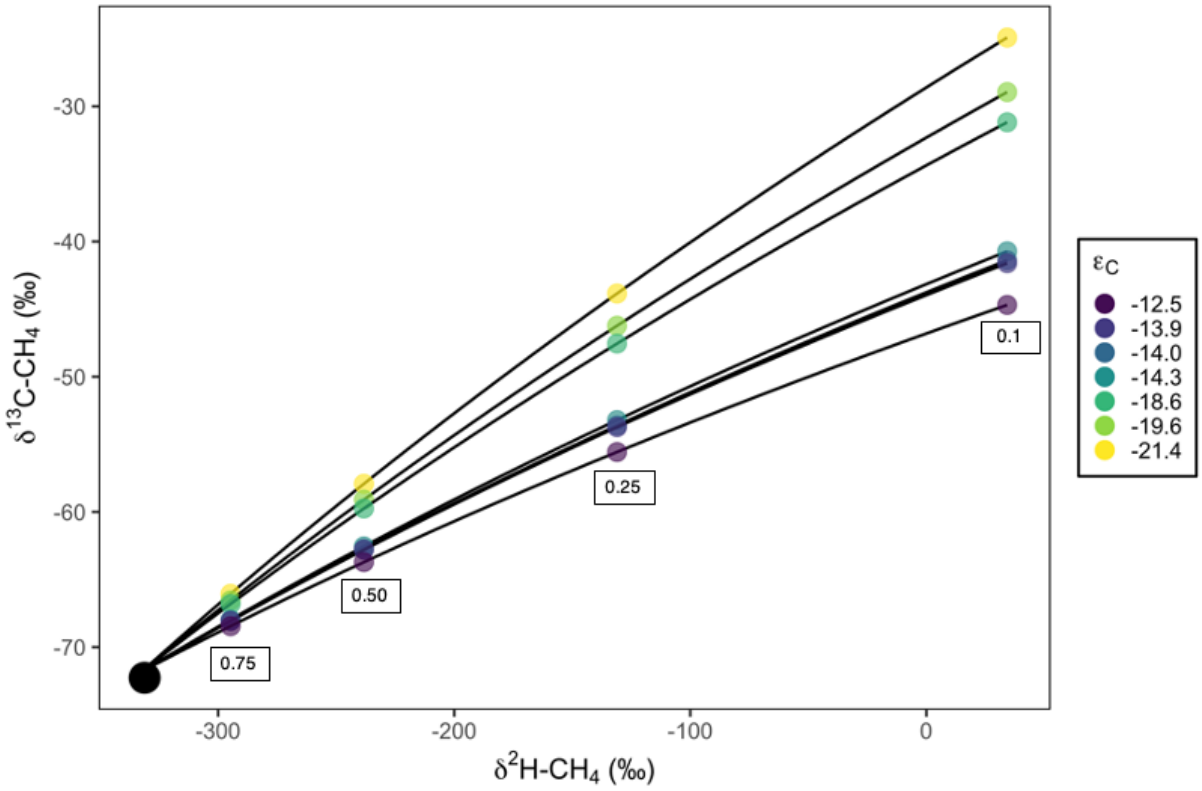

Figure 4.17 Rayleigh fractionation plot of theoretical CH_4 oxidation of initial δ^2H-CH_4 and δ^{13}C-CH_4 values. Residual δ^2H-CH_4 and δ^{13}C-CH_4 values after CH_4 oxidation were calculated assuming a closed system Rayleigh fractionation. Values in boxes represent the fraction (f) of CH_4 remaining after oxidization.

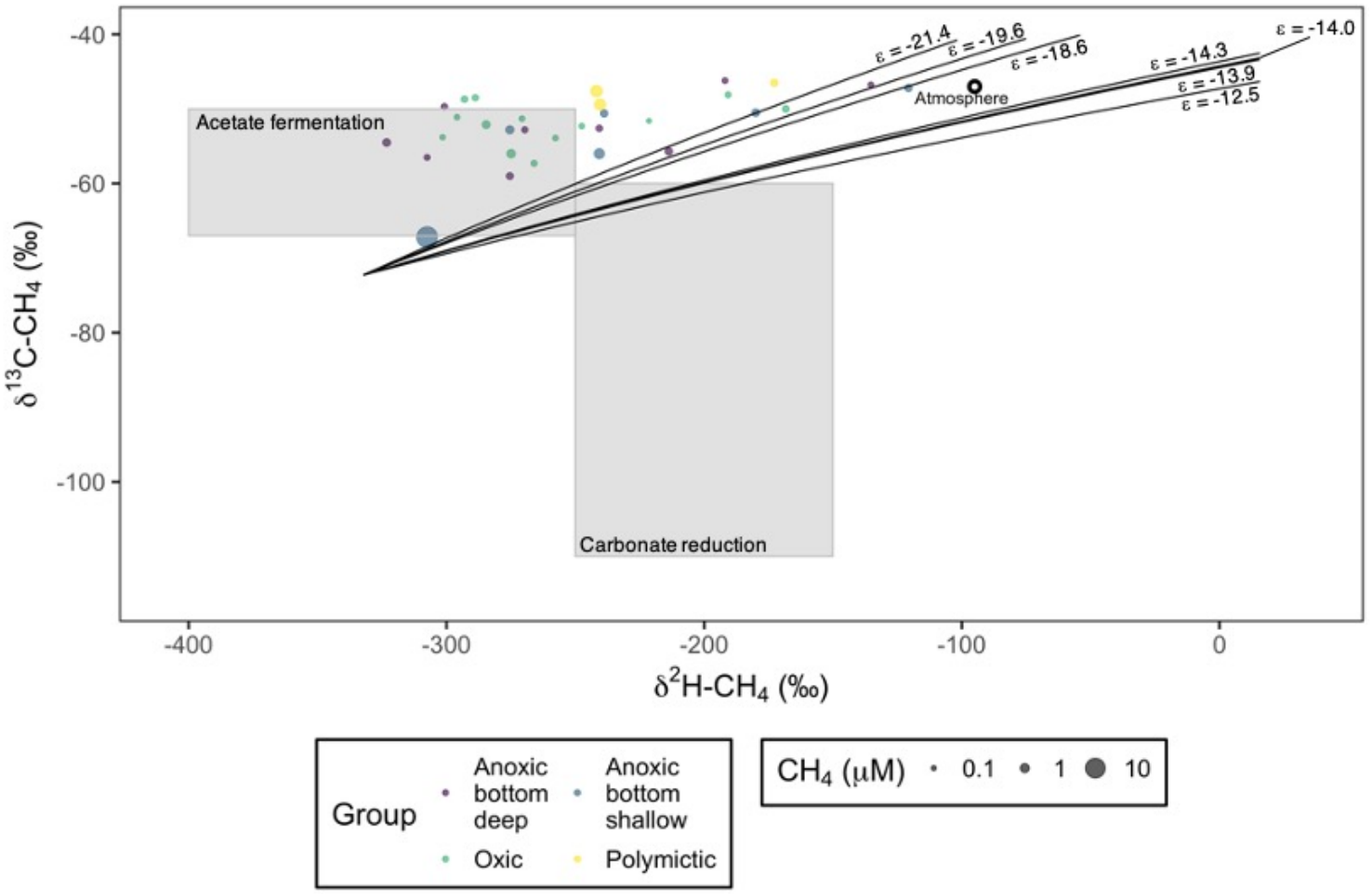

Figure 4.18 Crossplot of $\delta^{2}H\text{-}CH_4$ and $\delta^{13}C\text{-}CH_4$ values above the thermocline for all lakes. Size represents CH_4 concentration throughout the water column. Diagnostic ranges of the acetate fermentation and carbonate reduction methanogenesis pathway from (Whiticar 1999).

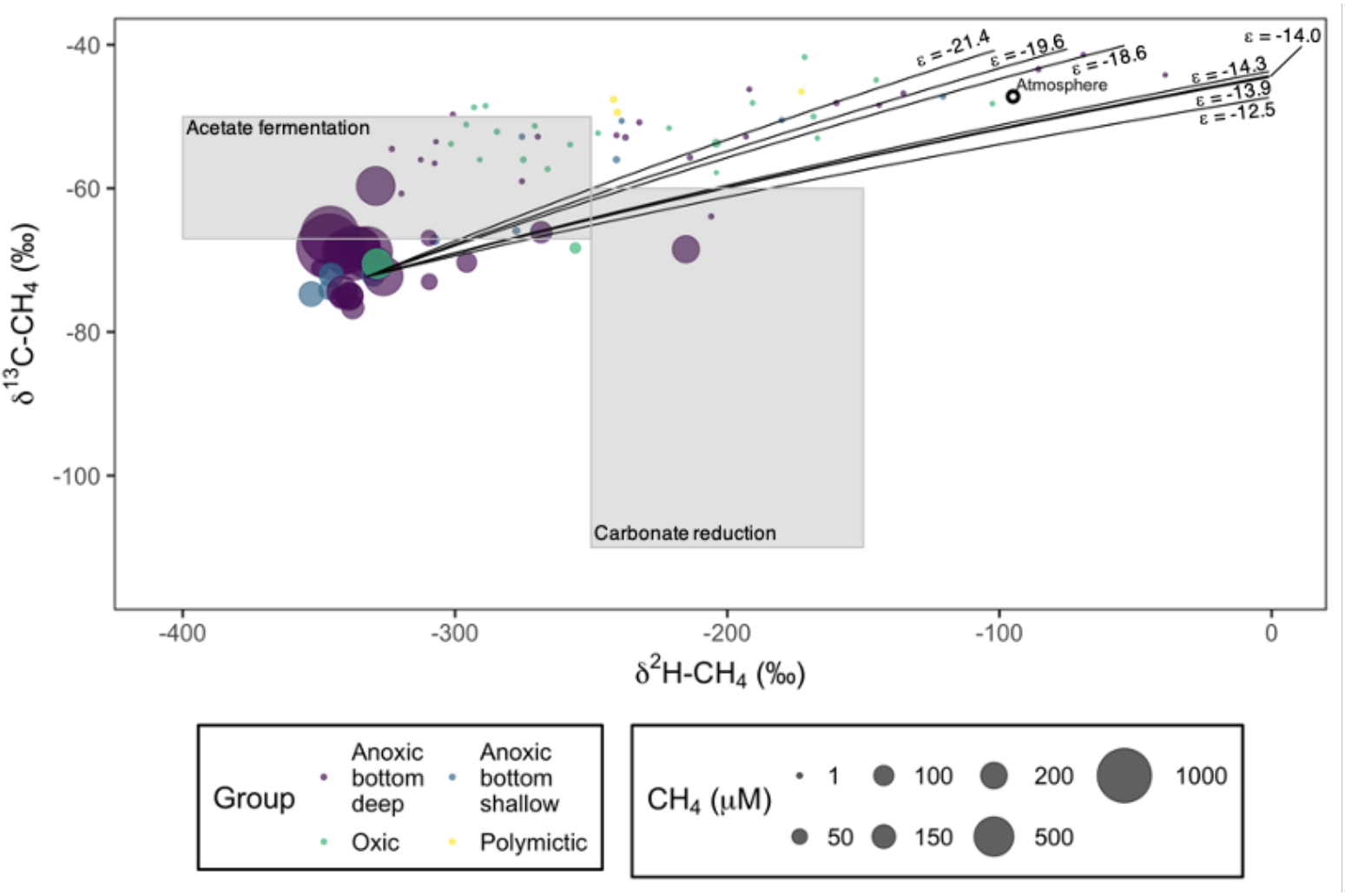

Figure 4.19 Crossplot of δ^2H-CH_4 and δ^{13}C-CH_4 values throughout the water column for all lakes. Size represents CH_4 concentration throughout the water column. Diagnostic ranges of the acetate fermentation and carbonate reduction methanogenesis pathway from (Whiticar 1999).

5. Conclusions, Implications, and Future Research

5.1 The control of terrestrial organic matter on lake carbon cycling along a DOC gradient

Over the summer of 2018, surface samples of DIC concentration, pH, POC, PON, δ^{13}C-DIC, δ^{13}C-POM and δ^{15}N-POM were taken on a monthly basis for each of the PHISH lakes. Using this data, C:N ratios of POM, pCO_2 and δ^{13}C-CO_2 values were also calculated.

Surface DIC concentrations were higher earlier in the year because decomposition and respiration cause accumulation under ice (Striegl et al. 2001). After ice-off, the lakes can then equilibrate with the atmosphere. Similarly, surface pCO_2 were higher earlier in the season. The PHISH lakes were above atmospheric saturation after ice-off, perhaps indicating a high rate of respiration of allochthonous carbon by bacteria (Jansson et al. 2012). No significant relationship was found between DOC concentration and pCO_2 values. However, there is a significant relationship between DOC concentration and δ^{13}C-DIC values. This is likely due to the production of more negative δ^{13}C-CO_2 during the respiration of DOC.

Both δ^{13}C-POM and δ^{15}N-POM values varied throughout the ice-free season. The C:N ratios of POM in the PHISH lakes also varied seasonally, with values indicating a mix between allochthonous and autochthonous material. In lakes with higher DOC concentrations, POM C:N ratios were found to be lower. This is unexpected, because terrestrial material has a higher C:N ratio (Meyers 1994). In lakes with higher DOC concentrations, there are more terrestrial inputs and therefore POM C:N ratios should increase with DOC concentrations. One potential reason for this is as DOC is photolyzed, the C:N ratio decreases (Chomicki 2009).

To more closely examine the control of terrestrial OM on the carbon cycle in the PHISH lakes, three approaches were taken: (1) the physical size separation of POM, (2) estimating the δ^{13}C and δ^{15}N values ($\delta^{13}C_A$, $\delta^{15}N_A$) of phytoplankton by correcting for terrestrial fraction of POM, (3) calculating the percentage of DOC composed of algal material.

POM samples were not only collected in bulk, but also collected along a series of size fractions in order to physically separate different components of POM and obtain a more "algal" sample. No significant differences were found between the δ^{13}C and δ^{15}N values of each size fraction, perhaps due to detrital particles attaching themselves to

algae. However, significant differences were found between the molar C:N ratios of the size fractions (one-way ANOVA, p= 1.62 x 10^{-5}, F= 13.99), and a post-hoc Tukey test showed that the 10<x<20 μm size fraction is significantly different from all other fractions. This may be because of the deposition of airborne particulate organic carbon, such as pollen.

Before estimating $\delta^{13}C_A$ and $\delta^{15}N_A$ values, the terrestrial fraction (ϕ_T) of POM was calculated using two different commonly used terrestrial end members: DOC and terrestrial vegetation. These calculations show that when DOC is used as the end member, ϕ_T is higher than when terrestrial vegetation is used. $\delta^{13}C_A$ values are therefore calculated to be more negative than bulk values when DOC is used to correct for ϕ_T, with the exception of L626. On average, using DOC to correct for ϕ_T decreased $\delta^{13}C_A$ values by 0.489 ‰, compared to a decrease of 0.0497 ‰ when using terrestrial vegetation. δ^{13}C-DOC values are more positive than those of phytoplankton, so when removing the influence of DOC, the resulting $\delta^{13}C_A$ values are more negative than bulk POM.

These calculations were also undertaken using the results from the size separation experiment. Similarly, using DOC as an end member to estimate ϕ_T for size separated POM also showed higher ϕ_T values than when terrestrial vegetation was used. The 10<x<20 μm size fraction had the highest estimated ϕ_T values for all lakes and both possible end members. It is conceivable that some terrestrial material was captured in this size fraction, causing higher ϕ_T values. This is also supported by the results of the C:N ratio of this size fraction. When correcting the size separated POM using the terrestrial end members, the $\delta^{13}C_A$ and $\delta^{15}N_A$ values are not changed drastically.

Lastly, the algal percentage of DOC was estimated using lake colour and chlorophyll *a* (chl *a*) concentrations, following the methodology and empirical relationship outlined in Bade et. al (2007). The PHISH lakes with higher DOC concentrations are estimated to have a much lower calculated percentage of algal material than lakes with lower DOC concentrations. This is because allochthonous carbon likely represents a larger portion of DOC in high DOC lakes than in low DOC lakes, which may have DOC comprised of more algal material. The calculated percent algal DOC had no relationship with δ^{13}C-DOM values, but had a slight, positive relationship with δ^{13}C-POM values.

Another approach that would help clarify the role of DOC on basal carbon resources would be to combine stable isotope data with methods to investigate DOC composition (e.g. fluorescence, absorbance, LC-OCD) to provide more insight into terrestrial versus aquatic origin of OM.

Sediment cores were taken at the deepest depth of each of the lakes. Since terrestrial OM is the main source of OM to lake sediments (Meyers and Ishiwatari 1993, Hall et al. 2018), it was expected that there would be relationships between sediment and the OM that is deposited there. However, no significant relationships were found between surficial sediments and epilimnetic δ^{13}C-POM values or C:N ratios. The effect of DOC concentration on δ^{13}C values of sediment with depth was tested using a linear mixed-effects model, and no significant relationship was found across the DOC gradient. One reason for the lack of relationships between OM and sediments is alterations on OM both in the water column (Teranes and Bernasconi 2000) and in the sediments (Meyers and Ishiwatari 1993).

This thesis examined only the pelagic zone of small, oligotrophic, soft water Canadian Shield lakes, therefore excluding the contributions of benthic primary production (i.e. periphyton) to the lake carbon cycle.

5.2 Partitioning terrestrial and aquatic energy flows using δ^2H values

For this chapter, the δ^2H values of DOM were measured in a subset of six lakes, as well as four small headwater boreal streams. δ^{13}C-DOM and δ^{15}N-DOM values were also measured. These values were compared to the average pooled δ^2H value of dominant vegetation at IISD-ELA, measured by Tonin (2019). The studied lakes have varying degrees of terrestrial OM inputs. δ^2H-DOM values did not vary with δ^2H-H_2O values along the ε_H trendline, as it would if comprised of autochthonous (i.e. phytoplankton) OM. In addition, δ^{13}C-DOM values did not fluctuate alongside calculated δ^{13}C-CO_2 values. This also shows that DOM is not made up of autochthonous OM, as the δ^{13}C values of phytoplankton would vary with ε_C.

To further show this, δ^2H-DOM values in L227 were measured. L227 is a lake that has been experimentally eutrophied in various nutrient regimes since 1969 and has two annual phytoplankton blooms (Higgins et al. 2018). L227 also has a long residence, which

is typically associated with lower amounts of DOM loading (Zwart et al. 2017). Therefore, it was expected that L227 should have DOM samples that appear to be more autochthonous. δ^{2}H-DOM and δ^{13}C-DOM values show that the DOM in L227 is similar to the DOM from the oligotrophic lakes sampled.

δ^{15}N-DOM values can also aid in separating allochthonous and autochthonous inputs to food webs. The δ^{15}N-DOM values of lakes and streams are more positive than the mean terrestrial vegetation value. The discrepancy between the terrestrial vegetation value and the lake and stream values is because of differences in the nitrogen cycling of the terrestrial versus the aquatic environment.

By using δ^{2}H-DOM values with δ^{13}C-DOM and δ^{15}N-DOM values, it is clear that the DOM in these IISD-ELA lakes and streams is neither strictly autochthonous or allochthonous in origin. However, while DOM may originate from the terrestrial environment, it is heavily processed and thus not identical to terrestrial vegetation. Therefore, while the terrestrial end member is typically defined as the average of stable isotopic values of vegetation sources from the catchment (Cole et al. 2002, Pace et al. 2004, Caraco et al. 2010, Solomon et al. 2011, Wilkinson et al. 2013a, 2013b, Guillemette et al. 2016), this is not entirely accurate. In boreal systems, choosing DOM as the terrestrial end member is more appropriate. To further expand on this research, examining how terrestrial and aquatic energy flow is partitioned using δ^{2}H values should be undertaken across different aquatic ecosystems and at different times of year.

5.3 Determining CH_4 dynamics using δ^{13}C-CH_4 and δ^{2}H-CH_4 values in Canadian Shield lakes

Fourteen lakes were sampled once throughout the water column, midsummer during the 2018 field season. Both the shallow and deep lakes with anoxic bottoms had similar characteristics, with high concentrations of CH_4 in the anoxic hypolimnion alongside negative δ^{13}C-CH_4 and δ^{2}H-CH_4 values. The polymictic and oxic lakes had fairly consistent values throughout the water column.

The water column above the thermocline across all lakes was quite similar, due to the fact that it is well mixed. In some lakes that developed anoxic hypolimnia, more positive isotopic values were observed in the middle of the water column, which is indicative of CH_4 oxidation (Whiticar 1999).

In two lakes, L227 and L442, full water column profiles were taken three times in the ice-free season. Later in the 2018 field season, CH_4 concentrations increased. These higher CH_4 concentrations were associated with more negative δ^2H-CH_4 and $\delta^{13}C$-CH_4 values at deeper depths. In the future, lake sampling under ice could aid in further understanding CH_4 dynamics and emissions. A of lack CH_4 data in northern, ice covered lakes has been identified in the literature (Denfeld et al. 2018).

By examining the well mixed water column, above the thermocline, it is clear that surface water CH_4 is different from atmospheric CH_4. While surface CH_4 concentrations are low and the $\delta^{13}C$-CH_4 values are similar to atmospheric CH_4, the δ^2H-CH_4 values are much more negative. Keeling plots of surface CH_4 data show that this CH_4 does not originate from the atmosphere.

Other aquatic systems in the literature are quite different in terms of CH_4 dynamics compared to the studied lakes. Only two CH_4 samples fell within the diagnostic ranges for the carbonate reduction methanogenesis pathway (Whiticar 1999), whereas this pathway was shown to be more dominant in meromictic lakes (Wand et al. 2006, Pasche et al. 2011). Acetate fermentation appeared to be the more dominant pathway of CH_4 production, likely due to the abundance of organic matter in the hypolimnion that could be used as a substrate. Since acetate fermentation is the more prevalent methanogenesis pathway, the isotopic values of organic matter are a key control on the isotopic values of CH_4.

A portion of CH_4 found in the studied lakes appears to be oxidized at the anoxic/oxic boundary. A theoretical Rayleigh fractionation was assumed to examine what the potential isotopic values of oxidized hypolimnion CH_4. With oxidation, residual CH_4 has increasingly positive δ^2H-CH_4 and $\delta^{13}C$-CH_4 values. These more positive values were associated with low CH_4 concentrations. However, epilimnion CH_4 was shown to be distinct from residual oxidized CH_4, and therefore has a distinct source.

Climate change is increasing DOC loading to fresh waters in Europe and North America (Evans et al. 2005, Monteith et al. 2007, Clark et al. 2010). This has many consequences, one being changes in lake thermal structure (Solomon et al. 2015). Changes in thermocline depth have been shown to alter access by organisms to CH_4 derived carbon (Rask et al. 2010). Further, as it has been established that CH_4 contributes to lake food webs (Bastviken et al. 2003, Kankaala et al. 2006a, 2006b, Deines et al. 2007, Jones et

al. 2008, Rask et al. 2010, Jones and Grey 2011, Sanseverino et al. 2012, van Duinen et al. 2013, Agasild et al. 2014, 2018, Schilder et al. 2015, Grey 2016), $\delta^{13}C\text{-}CH_4$ and $\delta^{2}H\text{-}CH_4$ values provide a valuable tool to understand how CH_4 dynamics can affect food webs.

In order to better assess and quantify methanogenesis pathway, it would be advantageous to conduct incubation experiments to determine a more accurate range of possible fractionation factors for $\delta^{2}H$ in CH_4 oxidation. Pairing stable isotope data for CH_4 with metagenomic data would also be beneficial in better defining CH_4 dynamics in Canadian Shield lakes by shedding light on the mechanisms associated with aerobic methane oxidation (Tsuji 2020).

Other important factors on the control of CH_4 in lake ecosystems are piston velocity and temperature (Bastviken et al. 2004), thus examining lake morphometry may help explain patterns in CH_4 production, consumption, and diffusion to the atmosphere.

References

Agasild, H., Kisand, A., Ainelo, E., Feldmann, T., Timm, H., Karus, K., Kisand, V., Jones, R.I., and Nõges, T. 2018. Chironomid incorporation of methane-derived carbon in plankton- and macrophyte-dominated habitats in a large shallow lake. Freshw. Biol. **63**(11): 1433–1445. doi:10.1111/fwb.13170.

Agasild, H., Zingel, P., Tuvikene, L., Tuvikene, A., Timm, H., Feldmann, T., Salujõe, J., Toming, K., Jones, R.I., and Nõges, T. 2014. Biogenic methane contributes to the food web of a large, shallow lake. Freshw. Biol. **59**(2): 272–285. doi:10.1111/fwb.12263.

Alstad, K.P., and Whiticar, M.J. 2011. Carbon and hydrogen isotope ratio characterization of methane dynamics for Fluxnet Peatland Ecosystems. Org. Geochem. **42**(5): 548–558. Elsevier Ltd. doi:10.1016/j.orggeochem.2011.03.004.

Ask, J., Karlsson, J., and Jansson, M. 2012. Net ecosystem production in clear-water and brown-water lakes. Global Biogeochem. Cycles **26**(1): 1–7. doi:10.1029/2010GB003951.

Bade, D.L., Carpenter, S.R., Cole, J.J., Pace, M.L., Kritzberg, E., Van De Bogert, M.C., Cory, R.M., and McKnight, D.M. 2007. Sources and fates of dissolved organic carbon in lakes as determined by whole-lake carbon isotope additions. Biogeochemistry **84**(2): 115–129. doi:10.1007/s10533-006-9013-y.

Bade, D.L., Cole, J.J., Hanson, P.C., and Hesslein, R.H. 2004. Controls of 13C-DIC in lakes: Geochemestry, lake metabolism, and morphometry. Limnol. Oceanogr. **49**(4): 1160–1172. doi:10.4319/lo.2004.49.4.1160.

Bade, D.L., Pace, M.L., Cole, J.J., and Carpenter, S.R. 2006. Can algal photosynthetic inorganic carbon isotope fractionation be predicted in lakes using existing models? Aquat. Sci. **68**(2): 142–153. doi:10.1007/s00027-006-0818-5.

Baril, M. 2001. Dissolved inorganic carbon from the decomposition of vegetation and soils of flooded reservoirs: Stable carbon isotope ratios. University of Waterloo.

Barker, J.F., and Fritz, P. 1981. Carbon isotope fractionation during microbial methane oxidation. doi:10.1038/293289a0.

Bartels, P., Cucherousset, J., Gudasz, C., Jansson, M., Karlsson, J., Persson, L., Premke, K., Rubach, A., Steger, K., Tranvik, L.J., and Eklöv, P. 2012. Terrestrial subsidies to lake food webs: An experimental approach. Oecologia **168**(3): 807–818. doi:10.1007/s00442-011-2141-7.

Bassett, I.J., Crompton, C.W., and Parmelee, J.A. 1978. An Atlas of Airborne Pollen and Common Fungus Spores of Canada. Ottawa, Ontario. Available from http://biblio.uqar.ca/archives/30426283.pdf.

Bastviken, D., Cole, J., Pace, M., and Tranvik, L. 2004. Methane emissions from lakes: Dependence of lake characteristics, two regional assessments, and a global estimate. Global Biogeochem. Cycles **18**(4): 1–12. doi:10.1029/2004GB002238.

Bastviken, D., Cole, J.J., Pace, M.L., and Van de-Bogert, M.C. 2008. Fates of methane from different lake habitats: Connecting whole-lake budgets and CH4emissions. J. Geophys. Res. Biogeosciences **113**(2): 1–13. doi:10.1029/2007JG000608.

Bastviken, D., Ejlertsson, J., Sundh, I., and Tranvik, L. 2003. Methane As a Source of Carbon and Energy for Lake Pelagic Food Webs. **84**(4): 969–981.

Bastviken, D., Ejlertsson, J., and Tranvik, L. 2002. Measurement of methane oxidation in lakes: A comparison of methods. Environ. Sci. Technol. **36**(15): 3354–3361. doi:10.1021/es010311p.

Bates, D., Maechler, M., Bolker, B., and Walker, S. 2015. Fitting Linear Mixed-Effects Models using lme4. J. Stat. Softw. **67**(1): 1–49. doi:doi:10.18637/jss.v067.i01.
Battin, T.J., Luyssaert, S., Kaplan, L.A., Aufdenkampe, A.K., Richter, A., and Tranvik, L.J. 2009. The boundless carbon cycle. Nat. Geosci. **2**(9): 598–600. Nature Publishing Group. doi:10.1038/ngeo618.
Berggren, M., Ziegler, S.E., St-Gelais, N.F., Beisner, B.E., and Del Giorgio, P.A. 2014. Contrasting patterns of allochthony among three major groups of crustacean zooplankton in boreal and temperate lakes. Ecology **95**(11): 3230.
Biagini, G. a, Finlay, B.J., and Lloyd, D. 1998. Protozoan stimulation of anaerobic microbial activity: enhancement of. FEMS Microbiol. Ecol. **27**: 1–8. doi:10.1111/j.1574-6941.1998.tb00520.x.
Bižić, M., Klintzsch, T., Ionescu, D., Hindiyeh, M.Y., Günthel, M., Muro-Pastor, A.M., Eckert, W., Urich, T., Keppler, F., and Grossart, H.P. 2020. Aquatic and terrestrial cyanobacteria produce methane. Sci. Adv. **6**(3): 1–10. doi:10.1126/sciadv.aax5343.
Blees, J., Niemann, H., Wenk, C.B., Zopfi, J., Schubert, C.J., Kirf, M.K., Veronesi, M.L., Hitz, C., and Lehmann, M.F. 2014. Micro-aerobic bacterial methane oxidation in the chemocline and anoxic water column of deep south-Alpine Lake Lugano (Switzerland). Limnol. Oceanogr. **59**(2): 311–324. doi:10.4319/lo.2014.59.2.0311.
Bogard, M.J., Del Giorgio, P.A., Boutet, L., Chaves, M.C.G., Prairie, Y.T., Merante, A., and Derry, A.M. 2014. Oxic water column methanogenesis as a major component of aquatic CH4 fluxes. Nat. Commun. **5**(May): 1–9. Nature Publishing Group. doi:10.1038/ncomms6350.
Borrel, G., Jézéquel, D., Biderre-Petit, C., Morel-Desrosiers, N., Morel, J.P., Peyret, P., Fonty, G., and Lehours, A.C. 2011. Production and consumption of methane in freshwater lake ecosystems. Res. Microbiol. **162**(9): 833–847. doi:10.1016/j.resmic.2011.06.004.
Boudreau, N.M. 2000. Soil Carbon, Carbon Dioxide, and Methane in Three Experimentally Flooded Upland Boreal Forest Reservoirs: a δ13C Inventory of Sources and Processes. University of Waterloo.
Brett, M.T., Bunn, S.E., Chandra, S., Galloway, A.W.E., Guo, F., Kainz, M.J., Kankaala, P., Lau, D.C.P., Moulton, T.P., Power, M.E., Rasmussen, J.B., Taipale, S.J., Thorp, J.H., and Wehr, J.D. 2017. How important are terrestrial organic carbon inputs for secondary production in freshwater ecosystems? Freshw. Biol. **62**(5): 833–853. doi:10.1111/fwb.12909.
Brett, M.T., Kainz, M.J., Taipale, S.J., and Seshan, H. 2009. Phytoplankton, not allochthonous carbon, sustains herbivorous zooplankton production. Proc. Natl. Acad. Sci. **106**(50): 21197–21201. doi:10.1073/pnas.0904129106.
Brunskill, G.J., and Schindler, D.W. 1971. Geography and Bathymetry of Selected Lake Basins, Experimental Lakes Area, Northwestern Ontario. J. Fish. Res. Board Canada **28**(2): 139–155. doi:10.1139/f71-028.
Cabana, G., and Rasmussen, J.B. 1996. Comparison of aquatic food chains using nitrogen isotopes. **93**(October): 10844–10847.
Cadieux, S.B., White, J.R., Sauer, P.E., Peng, Y., Goldman, A.E., and Pratt, L.M. 2016a. Large fractionations of C and H isotopes related to methane oxidation in Arctic lakes. Geochim. Cosmochim. Acta **187**: 141–155. Elsevier Ltd. doi:10.1016/j.gca.2016.05.004.
Cadieux, S.B., White, J.R., Sauer, P.E., Peng, Y., Goldman, A.E., and Pratt, L.M. 2016b. Large fractionations of C and H isotopes related to methane oxidation in Arctic lakes. Geochim. Cosmochim. Acta **187**: 141–155. Elsevier Ltd.

doi:10.1016/j.gca.2016.05.004.
Caraco, N., Bauer, J.E., Cole, J.J., Petsch, S., and Raymond, P. 2010. Millennial-aged organic carbon subsidies to a modern river food web. Ecology **91**(8): 2385–2393. doi:10.1890/09-0330.1.
Carpenter, S.R., Cole, J.J., Pace, M.L., Bogert, M. Van De, Bade, D.L., Bastviken, D., Gille, C.M., Hodgson, J.R., Kitchell, J.F., and Kritzberg, S. 2005. Ecosystem Subsidies: Terrestrial Support of Aquatic Food Webs from 13C Addition to Contrasting Lakes. Ecology **86**(10): 2737–2750. doi:10.1890/04-1282.
Chanton, J.P., Fields, D., and Hines, M.E. 2006. Controls on the hydrogen isotopic composition of biogenic methane from high-latitude terrestrial wetlands. J. Geophys. Res. Biogeosciences **111**(4): 1–9. doi:10.1029/2005JG000134.
Chasar, L.S., Chanton, J.P., Glaser, P.H., Siegel, D.I., and Rivers, J.S. 2000. Radiocarbon and stable carbon isotopic evidence for transport and transformation of dissolved organic carbon, dissolved inorganic carbon, and CH4in a northern Minnesota Peatland. Global Biogeochem. Cycles **14**(4): 1095–1108. doi:10.1029/1999GB001221.
Chmiel, H.E., Kokic, J., Denfeld, B.A., Einarsdóttir, K., Wallin, M.B., Koehler, B., Isidorova, A., Bastviken, D., Ferland, M.È., and Sobek, S. 2016. The role of sediments in the carbon budget of a small boreal lake. Limnol. Oceanogr. **61**(5): 1814–1825. doi:10.1002/lno.10336.
Chomicki, K. 2009. The use of stable carbon and oxygen isotopes to examine the fate of dissolved organic matter in two small, oligotrophic Canadian Shield lakes. University of Waterloo. Available from http://hdl.handle.net/10012/5016.
Clark, J.M., Bottrell, S.H., Evans, C.D., Monteith, D.T., Bartlett, R., Rose, R., Newton, R.J., and Chapman, P.J. 2010. The importance of the relationship between scale and process in understanding long-term DOC dynamics. Sci. Total Environ. **408**(13): 2768–2775. Elsevier B.V. doi:10.1016/j.scitotenv.2010.02.046.
Cole, J.J. 2013a. Chapter 6. The Carbon Cycle. *In* Fundamentals of Ecosystem Science, First Edit. *Edited by* K.C. Weathers, D. Strayer, and G.E. Likens. Academic Press. pp. 109–136. doi:10.1016/B978-0-08-091680-4.00006-8.
Cole, J.J. 2013b. Freshwater in flux. Nat. Geosci. **6**(1): 13–14. Nature Publishing Group. doi:10.1038/ngeo1696.
Cole, J.J., Caraco, N.F., Kling, G.W., and Kratz, T.K. 1994. Carbon Dioxide Supersaturation in the Surface Waters of Lakes. Science (80-.). **265**(5178): 1568–1570. doi:10.1126/science.265.5178.1568.
Cole, J.J., Carpenter, S.R., Kitchell, J., Pace, M.L., Solomon, C.T., and Weidel, B. 2011. Strong evidence for terrestrial support of zooplankton in small lakes based on stable isotopes of carbon, nitrogen, and hydrogen. Proc. Natl. Acad. Sci. **108**(5): 1975–1980. doi:10.1073/pnas.1012807108.
Cole, J.J., Carpenter, S.R., Kitchell, J.F., and Pace, M.L. 2002. Pathways of organic carbon utilization in small lakes: Results from a whole-lake 13C addition and coupled model. Limnol. Oceanogr. **47**(6): 1664–1675. doi:10.4319/lo.2002.47.6.1664.
Cole, J.J., Carpenter, S.R., Pace, M.L., Van De Bogert, M.C., Kitchell, J.L., and Hodgson, J.R. 2006. Differential support of lake food webs by three types of terrestrial organic carbon. Ecol. Lett. **9**(5): 558–568. doi:10.1111/j.1461-0248.2006.00898.x.
Cole, J.J., Prairie, Y.T., Caraco, N.F., McDowell, W.H., Tranvik, L.J., Striegl, R.G., Duarte, C.M., Kortelainen, P., Downing, J.A., Middelburg, J.J., and Melack, J. 2007. Plumbing the global carbon cycle: Integrating inland waters into the terrestrial carbon budget. Ecosystems **10**(1): 171–184. doi:10.1007/s10021-006-9013-8.
Conrad, R. 2005. Quantification of methanogenic pathways using stable carbon isotopic

signatures: A review and a proposal. Org. Geochem. **36**(5): 739–752. doi:10.1016/j.orggeochem.2004.09.006.
Craig, N., Jones, S.E., Weidel, B.C., and Solomon, C.T. 2017. Life history constraints explain negative relationship between fish productivity and dissolved organic carbon in lakes. Ecol. Evol. (May): 6201–6209. doi:10.1002/ece3.3108.
Creed, I.F., Bergström, A.K., Trick, C.G., Grimm, N.B., Hessen, D.O., Karlsson, J., Kidd, K.A., Kritzberg, E., McKnight, D.M., Freeman, E.C., Senar, O.E., Andersson, A., Ask, J., Berggren, M., Cherif, M., Giesler, R., Hotchkiss, E.R., Kortelainen, P., Palta, M.M., Vrede, T., and Weyhenmeyer, G.A. 2018. Global change-driven effects on dissolved organic matter composition: Implications for food webs of northern lakes. Glob. Chang. Biol. **24**(8): 3692–3714. doi:10.1111/gcb.14129.
Crompton, C.W., and Wojtas, W.A. 1993. Pollen grains of Canadian honey plants. Ottawa, Ontario. Available from http://publications.gc.ca/site/eng/9.644658/publication.html.
Cuthbert, I.D., and del Giorgio, P. 1992. Toward a standard method of measuring color in freshwater. Limnol. Oceanogr. **37**(6): 1319–1326. doi:10.4319/lo.1992.37.6.1319.
Daniels, L., Fulton, G., Spencer, R.W., and Orme-Johnson, W.H. 1980. Origin of hydrogen in methane produced by Methanobacterium thermoautotrophicum. J. Bacteriol. **141**(2): 694–698. doi:10.1128/jb.141.2.694-698.1980.
Danielsson, L.G. 1982. On the use of filters for distinguishing between dissolved and particulate fractions in natural waters. Water Res. **16**(2): 179–182. doi:10.1016/0043-1354(82)90108-7.
Deines, P., Bodelier, P.L.E., and Eller, G. 2007. Methane-derived carbon flows through methane-oxidizing bacteria to higher trophic levels in aquatic systems. Environ. Microbiol. **9**(5): 1126–1134. doi:10.1111/j.1462-2920.2006.01235.x.
Deines, P., Wooller, M.J., and Grey, J. 2009. Unravelling complexities in benthic food webs using a dual stable isotope (hydrogen and carbon) approach. Freshw. Biol. **54**(11): 2243–2251. doi:10.1111/j.1365-2427.2009.02259.x.
DelSontro, T., Beaulieu, J.J., and Downing, J.A. 2018. Greenhouse gas emissions from lakes and impoundments: Upscaling in the face of global change. Limnol. Oceanogr. Lett. **3**(3): 64–75. doi:10.1002/lol2.10073.
DelSontro, T., Boutet, L., St-Pierre, A., del Giorgio, P.A., and Prairie, Y.T. 2016. Methane ebullition and diffusion from northern ponds and lakes regulated by the interaction between temperature and system productivity. Limnol. Oceanogr. **61**. doi:10.1002/lno.10335.
Denfeld, B.A., Baulch, H.M., del Giorgio, P.A., Hampton, S.E., and Karlsson, J. 2018. A synthesis of carbon dioxide and methane dynamics during the ice-covered period of northern lakes. Limnol. Oceanogr. Lett. **3**(3): 117–131. doi:10.1002/lol2.10079.
DeNiro, M., and Epstein, S. 1981. Influence of diet on the distribution of nitrogen isotopes in animals. Geochim. Cosmochim. Acta **45**(3): 495–506. doi:10.1016/0016-7037(81)90244-1.
DeNiro, M.J., and Epstein, S. 1978. Influence of diet on the distribution of carbon isotopes in animals. Geochim. Cosmochim. Acta **42**: 495–506. doi:10.1016/0016-7037(78)90199-0.
Dlugokencky, E.J., Lang, P.M., and Masade, K.A. 1994. The growth rate and distribution of atmospheric methane. J. Geophys. Res. Atmos. **99**: 17021–17043. doi:10.1029/94JD01245.
Donis, D., Flury, S., Stöckli, A., Spangenberg, J.E., Vachon, D., and McGinnis, D.F. 2017. Full-scale evaluation of methane production under oxic conditions in a

mesotrophic lake. Nat. Commun. **8**(1): 1–11. Springer US. doi:10.1038/s41467-017-01648-4.
Doucett, R.R., Marks, J.C., Blinn, D.W., Caron, M., and Hungate, B.A. 2007. Measuring Terrestrial Subsidies To Aquatic Food Webs Using Stable Isotopes of Hydrogen. Ecology **88**(6): 1587–1592. doi:10.1890/06-1184.
Downing, J.A. 2010. Emerging global role of small lakes and ponds: Little things mean a lot. Limnetica **29**(1): 9–24. doi:10.4103/0019-5359.100336.
van Duinen, G.A., Vermonden, K., Bodelier, P.L.E., Hendriks, A.J., Leuven, R.S.E.W., Middelburg, J.J., van der Velde, G., and Verberk, W.C.E.P. 2013. Methane as a carbon source for the food web in raised bog pools. Freshw. Sci. **32**(4): 1260–1272. doi:10.1899/12-121.1.
Elser, J.J., Fagan, W.F., Denno, R.F., Dobberfuhl, D.R., Folarin, A., Huberty, A., Interlandi, S., Kilham, S.S., McCauley, E., Schulz, K.L., Siemann, E.H., and Sterner, R.W. 2000. Nutritional constraints in terrestrial and freshwater food webs. Nature **408**(6812): 578–580. doi:10.1038/35046058.
Emery, K.A., Wilkinson, G.M., Ballard, F.G., and Pace, M.L. 2015. Use of allochthonous resources by zooplankton in reservoirs. Hydrobiologia **758**(1): 257–269. Springer International Publishing. doi:10.1007/s10750-015-2338-6.
Evans, C.D., Monteith, D.T., and Cooper, D.M. 2005. Long-term increases in surface water dissolved organic carbon: Observations, possible causes and environmental impacts. Environ. Pollut. **137**(1): 55–71. doi:10.1016/j.envpol.2004.12.031.
Falkowski, P., Scholes, R.J., Boyle, E., Canadell, J., Canfield, D., Elser, J., Gruber, N., Hibbard, K., Hogberg, P., Linder, S., Mackenzie, F.T., Moore, B., Pedersen, T., Rosenthal, Y., Seitzinger, S., Smetacek, V., and Steffen, W. 2000. The global carbon cycle: A test of our knowledge of earth as a system. Science (80-.). **290**(5490): 291–296. doi:10.1126/science.290.5490.291.
Farquhar, G., Ehleringer, J., and Hubick, K. 1989. Carbon Isotope Discrimination and Photosynthesis. Annu. Rev. Plant Physiol. Plant Mol. Biol. doi:1040-2519/89/0601-503.
Fee, E.J., Hecky, R.E., Kasian, S.E.M., and Cruikshank, D.R. 1996. Effects of lake size, water clarity, and climatic variability on mixing depths in Canadian Shield lakes. Limnol. Oceanogr. **41**(5): 912–920. doi:10.4319/lo.1996.41.5.0912.
Fellman, J.B., Hood, E., and Spencer, R.G.M. 2010. Fluorescence spectroscopy opens new windows into dissolved organic matter dynamics in freshwater ecosystems: A review. Limnol. Oceanogr. **55**(6): 2452–2462. doi:10.4319/lo.2010.55.6.2452.
Ferguson, G. 2000. Sources of dissolved organic carbon in flooded uplands. University of Waterloo.
Findlay, S., and Sinsabaugh, R.L. 2003. Aquatic Ecosystems Interactivity of Dissolved Organic Matter. *In* Aquatic Ecology Series. *Edited By*S. Findlay and R.L. Sinsabaugh. Academic Press, San Diego. doi:10.1016/B978-012256371-3/50020-2.
Finstad, A.G., Helland, I.P., Ugedal, O., Hesthagen, T., and Hessen, D.O. 2014. Unimodal response of fish yield to dissolved organic carbon. (0316): 36–43. doi:10.1111/ele.12201.
Flinn, N.A.P. 2012. The use of stable nitrogen and carbon isotopes to examine the sources, sinks and cycling of nitrogen in a small, artificially eutrophic Boreal lake. University of Waterloo. Available from https://uwspace.uwaterloo.ca/bitstream/handle/10012/6763/Flinn_Nicholas.pdf?sequence=1%0Ahttp://hdl.handle.net/10012/6763.
Francis, T.B., Schindler, D.E., Holtgrieve, G.W., Larson, E.R., Scheuerell, M.D.,

Semmens, B.X.., and Ward, E.J. 2011. Habitat structure determines resource use by zooplankton in temperate lakes. Ecol. Lett. **14**: 364–372. doi:10.1111/j.1461-0248.2011.01597.x.
Fry, B., and Sherr, E.B. 1989. 13C Measurements as Indicators of Carbon Flow in Marine and Freshwater Ecosystems. *In* Stable Isotopes in Ecological Research. Ecological Studies (Analysis and Synthesis). *Edited by* P.W. Rundel, J.R. Ehleringer, and K.A. Nagy. New York. pp. 196–229. doi:https://doi.org/10.1007/978-1-4612-3498-2_12.
Gälman, V., Rydberg, J., and Bigler, C. 2009. Decadal diagenetic effects on δ13C and δ15N studied in varved lake sediment. Limnol. Oceanogr. **54**(3): 917–924. doi:10.4319/lo.2009.54.3.0917.
Gibson, J.J., Birks, S.J., Jeffries, D., and Yi, Y. 2017. Regional trends in evaporation loss and water yield based on stable isotope mass balance of lakes: The Ontario Precambrian Shield surveys. J. Hydrol. **544**: 500–510. doi:10.1016/j.jhydrol.2016.11.016.
del Giorgio, P., and Williams, P. 2007. Respiration in Aquatic Ecosystems. *In* Respiration in Aquatic Ecosystems. doi:10.1093/acprof:oso/9780198527084.001.0001.
Goericke, R., Montoya, J.P., and Fry, B. 1994. Physiology of isotope fractionation in algae and cyanobacteria. *In* Stable isototopes in ecology and environmental science. *Edited by* K. Lajtha and R.H. Michener. Blackwell Scientific Publications, Oxford. pp. 187–221.
Grey, J. 2016. The Incredible Lightness of Being Methane-Fuelled: Stable Isotopes Reveal Alternative Energy Pathways in Aquatic Ecosystems and Beyond. Front. Ecol. Evol. **4**(February): 1–14. doi:10.3389/fevo.2016.00008.
Grey, J., Jones, R.I., and Sleep, D. 2000. Stable isotope analysis of the origins of zooplankton carbon in lake of differing trophic state. Oecologia **123**: 232–240. doi:10.1007/s004420051010.
Grey, J., Jones, R.I., and Sleep, D. 2001. Seasonal changes in the importance of the source of organic matter to the diet of zooplankton in Loch Ness, as indicated by stable isotope analysis. Limnol. Oceanogr. **46**(3): 505–513. doi:10.4319/lo.2001.46.3.0505.
Grosbois, G., Vachon, D., del Giorgio, P.A., and Rautio, M. 2020. Efficiency of crustacean zooplankton in transferring allochthonous carbon in a boreal lake. Ecology **0**(0). doi:10.1002/ecy.3013.
Gu, B. 2009. Variations and controls of nitrogen stable isotopes in particulate organic matter of lakes. Oecologia **160**(3): 421–431. doi:10.1007/s00442-009-1323-z.
Gu, B., Schelske, C.L., and Brenner, M. 1996. Relationship between sediment and plankton isotope ratios (δ13C and δ15N) and primary productivity in Florida lakes. Can. J. Fish. Aquat. Sci. **53**(4): 875–883. doi:10.1139/cjfas-53-4-875.
Gu, B., Schelske, C.L., and Waters, M.N. 2011. Patterns and controls of seasonal variability of carbon stable isotopes of particulate organic matter in lakes. Oecologia **165**: 1083–1094. doi:10.1007/s00442-010-1888-6.
Guillemette, F., and del Giorgio, P.A. 2012. Simultaneous consumption and production of fluorescent dissolved organic matter by lake bacterioplankton. Environ. Microbiol. **14**(6): 1432–1443. doi:10.1111/j.1462-2920.2012.02728.x.
Guillemette, F., Leigh Mccallister, S., and Del Giorgio, P.A. 2016. Selective consumption and metabolic allocation of terrestrial and algal carbon determine allochthony in lake bacteria. ISME J. **10**(6): 1373–1382. doi:10.1038/ismej.2015.215.
Guillemette, F., von Wachenfeldt, E., Kothawala, D.N., Bastviken, D., and Tranvik, L.J. 2017. Preferential sequestration of terrestrial organic matter in boreal lake sediments. J. Geophys. Res. Biogeosciences **122**(4): 863–874.

doi:10.1002/2016JG003735.
Hall, B.D., Hesslein, R.H., Emmerton, C.A., Higgins, S.N., Ramlal, P., and Paterson, M.J. 2018. Multidecadal carbon sequestration in a headwater boreal lake. Limnol. Oceanogr. **64**: 1–16. doi:10.1002/lno.11060.
Hanson, P.C., Hamilton, D.P., Stanley, E.H., Preston, N., Langman, O.C., and Kara, E.L. 2011. Fate of allochthonous dissolved organic carbon in lakes: A quantitative approach. PLoS One **6**(7). doi:10.1371/journal.pone.0021884.
Hecky, R.E., Campbell, P., and Hendzel, L.L. 1993. The stoichiometry of carbon, nitrogen, and phosphorus in particulate matter of lakes and oceans. Limnol. Oceanogr. **38**(4): 709–724.
Hecky, R.E., Rosenberg, D.M., and Campbell, P. 1994. The 25th anniversary of the Experimental Lakes Area and the history of Lake 227. Can. J. Fish. Aquat. Sci. **51**(10): 2243–2246. doi:10.1139/f94-227.
Herczeg, A.L. 1987. A Stable Carbon Isotope Study of Dissolved Inorganic Carbon Cycling in A Softwater Lake. Biogeochemistry **4**(3): 231–263. doi:10.1007/BF02187369.
Herczeg, A.L. 1988. Early diagenesis of organic matter in lake sediments: a stable carbon isotope study of pore waters. Chem. Geol. Isot. Geosci. Sect. **72**(3): 199–209. doi:10.1016/0168-9622(88)90025-5.
Higgins, S.N., Paterson, M.J., Hecky, R.E., Schindler, D.W., Venkiteswaran, J.J., and Findlay, D.L. 2018. Biological Nitrogen Fixation Prevents the Response of a Eutrophic Lake to Reduced Loading of Nitrogen: Evidence from a 46-Year Whole-Lake Experiment. Ecosystems **21**(6): 1088–1100. Springer US. doi:10.1007/s10021-017-0204-2.
Hondula, K.L., Pace, M.L., Cole, J.J., and Batt, R.D. 2014. Hydrogen isotope discrimination in aquatic primary producers: Implications for aquatic food web studies. Aquat. Sci. **76**(2): 217–229. doi:10.1007/s00027-013-0331-6.
Hornibrook, E.R.C., Longstaffe, F.J., and Fyfe, W.S. 1997. Spatial distribution wetland of microbial methane production pathways in temperate soils : Stable carbon and hydrogen isotope evidence zone. **61**(4): 745–753.
Imberger, J. 1998. Flux paths in a stratified lake: A review. *In* Physical Processes in Lakes and Oceans. *Edited by* J. Imberger. American Geophysical Union, Washington, D.C. pp. 1–18. doi:https://doi.org/10.1029/CE054p0001.
Intergovernmental Panel on Climate Change. 2014. Anthropogenic and Natural Radiative Forcing. *In* Climate Change 2013 - The Physical Science Basis. *Edited by* Intergovernmental Panel on Climate Change. Cambridge University Press, Cambridge. pp. 659–740. doi:10.1017/CBO9781107415324.018.
International Atomic Energy Association, and World Meterorological Organization. 2020. Global Network of Isotopes in Precipitation. Available from https://nucleus.iaea.org/wiser.
Jansson, M., Karlsson, J., and Jonsson, A. 2012. Carbon dioxide supersaturation promotes primary production in lakes. Ecol. Lett. **15**(6): 527–532. doi:10.1111/j.1461-0248.2012.01762.x.
Jansson, M., Persson, L., De Roos, A.M., Jones, R.I., and Tranvik, L.J. 2007. Terrestrial carbon and intraspecific size-variation shape lake ecosystems. Trends Ecol. Evol. **22**(6): 316–322. doi:10.1016/j.tree.2007.02.015.
Johnson, W., and Vallentyne, J. 1971. Rationale, Background, and Development of Experimental Lake Studies in Northwestern Ontario. J. Fish. Res. Board Canada **28**:

123–128. doi:https://doi.org/10.1139/f71-026.
Jones, R.I. 1992. The influence of humic substances on lacustrine planktonic food chains. Hydrobiologia **229**: 73–91. Available from http://www.springerlink.com/index/10.1007/978-94-011-2474-4_6%5Cnpapers3://publication/doi/10.1007/978-94-011-2474-4_6.
Jones, R.I., Carter, C.E., Kelly, A., Ward, S., Kelly, D.J., and Grey, J. 2008. Widespread contribution of methane-cycle bacteria to the diets of Lake Profundal chironomid larvae. Ecology **89**(3): 857–864. doi:https://doi.org/10.1890/06-2010.1.
Jones, R.I., and Grey, J. 2011. Biogenic methane in freshwater food webs. Freshw. Biol. **56**(2): 213–229. doi:10.1111/j.1365-2427.2010.02494.x.
Jones, R.I., Grey, J., Sleep, D., and Arvola, L. 1999. Stable Isotope Analysis of Zooplankton Carbon Nutrition in Humic Lakes Author. Oikos **86**(1): 97–104. Available from http://www.jstor.org/stable/3546573.
Jones, R.I., Kankaala, P., Nykänen, H., Peura, S., Rask, M., and Vesala, S. 2018. Whole-Lake Sugar Addition Demonstrates Trophic Transfer of Dissolved Organic Carbon to Top Consumers. Ecosystems **21**(3): 495–506. doi:10.1007/s10021-017-0164-6.
Jones, S.E., Solomon, C.T., and Weidel, B.C. 2012. Subsidy or Subtraction: How Do Terrestrial Inputs Influence Consumer Production in Lakes? Freshw. Rev. **5**(1): 37–49. doi:10.1608/FRJ-5.1.475.
Juutinen, S., Rantakari, M., Kortelainen, P., Huttunen, J.T., Larmola, T., Alm, J., Silvola, J., and Martikainen, P.J. 2009. Methane dynamics in different boreal lake types. Biogeosciences **6**: 209–223. doi:10.5194/bgd-5-3457-2008.
Kankaala, P., Grey, J., Arvola, L., and Jones, R.I. 2006a. Experimental d 13 C evidence for a contribution of methane to pelagic food webs in lakes. Limnol. Ocean. **51**(6): 2821–2827.
Kankaala, P., Huotari, J., Peltomaa, E., Saloranta, T., and Ojala, A. 2006b. Methanotrophic activity in relation to methane efflux and total heterotrophic bacterial production in a stratified, humic, boreal lake. Limnol. Oceanogr. **51**(2): 1195–1204. doi:10.4319/lo.2006.51.2.1195.
Kankaala, P., Lopez Bellido, J., Ojala, A., Tulonen, T., and Jones, R.I. 2013. Variable Production by Different Pelagic Energy Mobilizers in Boreal Lakes. Ecosystems **16**(6): 1152–1164. doi:10.1007/s10021-013-9674-z.
Karlsson, J., Berggren, M., Ask, J., Byström, P., Jonsson, A., Laudon, H., and Jansson, M. 2012. Terrestrial organic matter support of lake food webs: Evidence from lake metabolism and stable hydrogen isotopes of consumers. Limnol. Oceanogr. **57**(4): 1042–1048. doi:10.4319/lo.2012.57.4.1042.
Karlsson, J., Bergström, A.K., Byström, P., Gudasz, C., Rodríguez, P., and Hein, C. 2015. Terrestrial organic matter input suppresses biomass production in lake ecosystems. Ecology **96**(11): 2870–2876. doi:10.1890/15-0515.1.sm.
Karlsson, J., Bystrom, P., Ask, J., and Jansson, M. 2009. Light limitation of nutrient-poor lake ecosystems. Nature **460**(7254): 506–509. Nature Publishing Group. doi:10.1038/nature08179.
Keeling, R.F., Graven, H.D., Welp, L.R., Resplandy, L., Bi, J., Piper, S.C., Sun, Y., Bollenbacher, A., and Meijer, H.A.J. 2017. Atmospheric evidence for a global secular increase in carbon isotopic discrimination of land photosynthesis. Proc. Natl. Acad. Sci. U. S. A. **114**(39): 10361–10366. doi:10.1073/pnas.1619240114.
Kennedy, C., Zellweger, G.W., and Jones, B.F. 1974. Filter Pore-Size Effects on the Analysis of. Water Resour. Res. **10**(4): 785–790. doi:https://doi.org/10.1029/WR010i004p00785.

Khatun, S., Iwata, T., Kojima, H., Fukui, M., Aoki, T., Mochizuki, S., Naito, A., Kobayashi, A., and Uzawa, R. 2019. Aerobic methane production by planktonic microbes in lakes. Sci. Total Environ. **696**: 133916. Elsevier B.V. doi:10.1016/j.scitotenv.2019.133916.

Kirschke, S., Bousquet, P., Ciais, P., Saunois, M., Canadell, J.G., Dlugokencky, E.J., Bergamaschi, P., Bergmann, D., Blake, D.R., Bruhwiler, L., Cameron-Smith, P., Castaldi, S., Chevallier, F., Feng, L., Fraser, A., Heimann, M., Hodson, E.L., Houweling, S., Josse, B., Fraser, P.J., Krummel, P.B., Lamarque, J.F., Langenfelds, R.L., Le Quéré, C., Naik, V., O'doherty, S., Palmer, P.I., Pison, I., Plummer, D., Poulter, B., Prinn, R.G., Rigby, M., Ringeval, B., Santini, M., Schmidt, M., Shindell, D.T., Simpson, I.J., Spahni, R., Steele, L.P., Strode, S.A., Sudo, K., Szopa, S., Van Der Werf, G.R., Voulgarakis, A., Van Weele, M., Weiss, R.F., Williams, J.E., and Zeng, G. 2013. Three decades of global methane sources and sinks. Nat. Geosci. **6**(10): 813–823. doi:10.1038/ngeo1955.

De Kluijver, A., Schoon, P.L., Downing, J.A., Schouten, S., and Middelburg, J.J. 2014. Stable carbon isotope biogeochemistry of lakes along a trophic gradient. Biogeosciences **11**(22): 6265–6276. doi:10.5194/bg-11-6265-2014.

Kortelainen, P. 1993. Content of Total Organic Carbon in Finnish Lakes and its Relationship to Catchment Characteristics.

Kortelainen, P., Mattsson, T., Finér, L., Ahtiainen, M., Saukkonen, S., and Sallantaus, T. 2006. Controls on the export of C, N, P and Fe from undisturbed boreal catchments, Finland. Aquat. Sci. **68**(4): 453–468. doi:10.1007/s00027-006-0833-6.

Kortelainen, P., Pajunen, H., Rantakari, M., and Saarnisto, M. 2004. A large carbon pool and small sink in boreal Holocene lake sediments. Glob. Chang. Biol. **10**(10): 1648–1653. doi:10.1111/j.1365-2486.2004.00848.x.

Kritzberg, E.S., Cole, J.J., Pace, M.L., Granéli, W., and Bade, D.L. 2004. Autochthonous versus allochthonous carbon sources of bacteria: Results from whole-lake 13C addition experiments. Limnol. Oceanogr. **49**(2): 588–596. doi:10.4319/lo.2004.49.2.0588.

Lamontagne, S., Schiff, S.L., and Elgood, R.J. 2000. Recovery of 15N-labelled nitrate applied to a small upland boreal forest catchment. Can. J. For. Res. **30**(7): 1165–1177. doi:10.1139/cjfr-30-7-1165.

Lehmann, M., Bernasconi, S., Barbieri, A., McKenzie, J., Ambientali, L.S., Pradiso, R., Lehmann, M., Bernasconi, S., Barbieri, A., and McKenzie, J. 2002. Preservation of organic matter and alteration of its carbon and nitrogen isotope composition during …. Geochim. Cosmochim. Acta **66**(20): 3573–3584. doi:10.1016/S0016-7037(02)00968-7.

Lehours, A.-C., Borrel, G., Morel-Desrosiers, N., Bardot, C., Grossi, V., Keraval, B., Attard, E., Morel, J.-P., Amblard, C., and Fonty, G. 2016. Anaerobic Microbial Communities and Processes Involved in the Methane Cycle in Freshwater Lakes-a Focus on Lake Pavin. *In* Lake Pavin: History, geology, biogeochemistry, and sedimentology of a deep meromictic maar lake. *Edited by* T. Sime-Ngando, P. Boivin, E. Chapron, D. Jezequel, and M. Meybeck. Springer International Publishing, Cham. pp. 255–284. doi:10.1007/978-3-319-39961-4_16.

Liikanen, A., Huttunen, J.T., Murtoneimi, T., Tanskanen, H., Väisänen, T., Silvola, J., Alm, J., and Martikainen, P.J. 2003. Spatial and seasonal variation in greenhouse gas and nutrient dynamics and their interactions in the sediments of a boreal eutrophic lake. Biogeochemistry **65**(1): 83–103. doi:10.1023/A:1026070209387.

Likens, G.E. 1975. Primary Production of Inland Aquatic Ecosystems. *In* Primary

Productivity of the Biosphere. *Edited by* H. Leith and R.H. Whittaker. Springer-Verlag, New York. pp. 185–202. doi:10.1007/978-3-642-80913-2_9.
Lindeman, R.L. 1942. The trophic-dynamic aspect of ecology. Bull. Math. Biol. **53**(1–2): 167–191. doi:10.1007/BF02464428.
Liu, R., Lead, J.R., and Baker, A. 2007. Fluorescence characterization of cross flow ultrafiltration derived freshwater colloidal and dissolved organic matter. Chemosphere **68**(7): 1304–1311. doi:10.1016/j.chemosphere.2007.01.048.
MacIntyre, S., Sickman, J.O., Goldthwait, S.A., and Kling, G.W. 2006. Physical pathways of nutrient supply in a small, ultraoligotrphic arctic lake. Limnol. Oceanogr. **51**(2): 1107–1124. doi:https://doi.org/10.4319/lo.2006.51.2.1107.
Marshall, J.D., Brooks, J.R., and Lajtha, K. 2008. Sources of Variation in the Stable Isotopic Composition of Plants. *In* Stable Isotopes in Ecology and Environmental Science: Second Edition. doi:10.1002/9780470691854.ch2.
Martens, C.S., Kelley, C.A., Chanton, J.P., and Showers, W.J. 1992. Carbon and Hydrogen Isotopic Characterization of Methane from Wetlands and Lakes of the Yukon-Kuskokwim Delta, Western Alaska. J. Geophys. Res. **97**: 16689–16701. doi:10.1029/91JD02885.
Martinez-Cruz, K., Sepulveda-Jauregui, A., Casper, P., Anthony, K.W., Smemo, K.A., and Thalasso, F. 2018. Ubiquitous and significant anaerobic oxidation of methane in freshwater lake sediments. Water Res. **144**(2): 332–340. Elsevier Ltd. doi:10.1016/j.watres.2018.07.053.
Marty, J., and Planas, D. 2008. Comparison of methods to determine algal δ 13 C in freshwater. Limnol. Oceanogr. Methods **6**: 51–63. doi:https://doi.org/10.4319/lom.2008.6.51.
Mattsson, T., Kortelainen, P., and Räike, A. 2005. Export of DOM from boreal catchments: Impacts of land use cover and climate. Biogeochemistry **76**(2): 373–394. doi:10.1007/s10533-005-6897-x.
Maynard, D.G., Paré, D., Thiffault, E., Lafleur, B., Hogg, K.E., and Kishchuk, B. 2014. How do natural disturbances and human activities affect soils and tree nutrition and growth in the Canadian boreal forest? Environ. Rev. **22**(2): 161–178. doi:10.1139/er-2013-0057.
McCullough, G.K., and Campbell, P. 1993. Lake variation and climate change study: ELA lakes, 1986-1990: II. Watershed geography and lake morphology. Available from N/A.
Mead, J. 2017. The Control of Fe and pH on the Photodegradation and Characterization of Dissolved Organic Matter in Small, Oligotrophic Canadian Shield Freshwaters. University of Waterloo. Available from https://uwspace.uwaterloo.ca/handle/10012/11942.
Meili, M. 1992. Sources, concentrations and characteristics of organic matter in softwater lakes and streams of the Swedish forest region. Hydrobiologia **229**(1): 23–41. doi:10.1007/BF00006988.
Mendonça, R., Müller, R.A., Clow, D., Verpoorter, C., Raymond, P., Tranvik, L.J., and Sobek, S. 2017. Organic carbon burial in global lakes and reservoirs. Nat. Commun. **8**(1): 1–6. Springer US. doi:10.1038/s41467-017-01789-6.
Meyers, P.A. 1994. Preservation of elemental and isotopic source identification of sedimentary organic matter. Chem. Geol. **114**(3–4): 289–302. doi:10.1016/0009-2541(94)90059-0.
Meyers, P.A., and Ishiwatari, R. 1993. Lacustrine organic geochemistry- an overview of indicators of organic matter sources and diagenesis in lake sediments. **20**(7): 867–

900. doi:10.1016/0146-6380(93)90100-P.
Meyers, P.A., Leenheer, M.J., and Bourbonniere, R.A. 1995. Diagenesis of vascular plant organic matter components during burial in lake sediments. Aquat. Geochemistry **1**(1): 35–52. doi:10.1007/BF01025230.
Meyers, P.A., and Teranes, J.L. 2001. Sediment Organic Matter. *In* Tracking Environmental Change Using Lake Sediments Volume 2 Physical and Geochemical Methods. *Edited by* W.M. Last and J.P. Smol. Kluwer Academic Publishers, Boston. pp. 239–269. doi:10.1007/0-306-47670-3_9.
Middelburg, J.J. 2014. Stable isotopes dissect aquatic food webs from the top to the bottom. Biogeosciences **11**(8): 2357–2371. doi:10.5194/bg-11-2357-2014.
Mohamed, M.N., and Taylor, W.D. 2009. Relative contribution of autochthonous and allochthonous carbon to limnetic zooplankton: A new cross-system approach. Fundam. Appl. Limnol. **175**(2): 113–124. doi:10.1127/1863-9135/2009/0175-0113.
Monteith, D.T., Stoddard, J.L., Evans, C.D., de Wit, H.A., Forsius, M., Høgåsen, T., Wilander, A., Skjelkvåle, B.L., Jeffries, D.S., Vuorenmaa, J., Keller, B., Kopácek, J., and Vesely, J. 2007. Dissolved organic carbon trends resulting from changes in atmospheric deposition chemistry. Nature **450**(7169): 537–540. doi:10.1038/nature06316.
Mostofa, K.M.G., Liu, C., Mottaleb, M.A., and Wan, G. 2013. Photobiogeochemistry of Organic Matter. doi:10.1007/978-3-642-32223-5.
Mostofa, K.M.G., Wu, F.C., Yoshioka, T., Sakugawa, H., and Tanoue, E. 2009. Dissolved organic matter in aquatic environments. *In* Natural organic matter and its significance in the environment. *Edited by* F. Wu and B. Xing. Science Press, Bejing. pp. 3–66.
National Oceanic and Atmospheric Administration. 2019a. Full Mauna Loa CO2 Record. Available from https://www.esrl.noaa.gov/gmd/ccgg/trends/full.html [accessed 1 May 2019].
National Oceanic and Atmospheric Administration. 2019b. Recent Global CH4. Available from www.esrl.noaa.gov/gmd/ccgg/trends_ch4/ [accessed 1 May 2019].
Natural Resources Canada. 2005. Land and freshwater area, by province and territory. Available from http://www.statcan.gc.ca/tables-tableaux/sum-som/l01/cst01/phys01-eng.htm.
Nickerson, N., and Risk, D. 2009. Keeling plots are non-linear in non-steady state diffusive environments. Geophys. Res. Lett. **36**(8): 6–9. doi:10.1029/2008GL036945.
O'Leary, M.H. 1988. Carbon Dynamics in Plants. Bioscience **38**(5): 328–336.
Oswald, K., Milucka, J., Brand, A., Littmann, S., Wehrli, B., Kuypers, M.M.M., and Schubert, C.J. 2015. Light-dependent aerobic methane oxidation reduces methane emissions from seasonally stratified lakes. PLoS One **10**(7): 1–22. doi:10.1371/journal.pone.0132574.
Pace, M.L., Carpenter, S.R., Cole, J.J., Coloso, J.J., James, F., Hodgson, J.R., Middelburg, J.J., Preston, N.D., Christopher, T., Weidel, B.C., Pace, L., Carpenter, R., Cole, J., Coloso, J., Kitchell, F., Hodgson, R., Middelburg, J.J., Preston, D., Weidel, B.C., and Solomon, T. 2011. Does terrestrial organic carbon subsidize the planktonic food web in a clear-water lake? Limnol. Oceanogr. **52**(5): 2177–2189.
Pace, M.L., Cole, J.J., Carpenter, S.R., Kitchell, J.F., Hodgson, J.R., Van De Bogert, M.C., Bade, D.L., Kritzberg, E.S., and Bastviken, D. 2004. Whole lake carbon-13 additions reveal terrestrial support of aquatic food webs. Nature **427**: 240–243. doi:10.1038/nature02215.1.

Palmer, M.E., Yan, N.D., and Somers, K.M. 2014. Climate change drives coherent trends in physics and oxygen content in North American lakes. Clim. Change **124**(1–2): 285–299. doi:10.1007/s10584-014-1085-4.
Pasche, N., Schmid, M., Vazquez, F., Schubert, C.J., Wüest, A., Kessler, J.D., Pack, M.A., Reeburgh, W.S., and Bürgmann, H. 2011. Methane sources and sinks in Lake Kivu. J. Geophys. Res. Biogeosciences **116**(3): 1–16. doi:10.1029/2011JG001690.
Pataki, D.E., Ehleringer, J.R., Flanagan, L.B., Yakir, D., Bowling, D.R., Still, C.J., Buchmann, N., Kaplan, J.O., and Berry, J.A. 2003. The application and interpretation of Keeling plots in terrestrial carbon cycle research. Global Biogeochem. Cycles **17**(1). doi:10.1029/2001GB001850.
Perkins, M.J., McDonald, R.A., van Veen, F.J.F., Kelly, S.D., Rees, G., and Bearhop, S. 2014. Application of Nitrogen and Carbon Stable Isotopes (δ15N and δ13C) to Quantify Food Chain Length and Trophic Structure. PLoS One **9**(3): e93281. doi:10.1371/journal.pone.0093281.
Peterson, B.J., and Fry, B. 1987. Stable Isotopes in Ecosystem Studies. Annu. Rev. Ecol. Syst. **18**(1): 293–320. doi:10.1146/annurev.es.18.110187.001453.
Pine, M.J., and Barker, H.. 1956. Studies on the methane fermentation. XII. The pathway of hydrogen in the acetate fermentation. J. Bacteriol. **71**(6): 644–648. doi:10.1128/jb.71.6.644-648.1956.
Polis, G.A., Anderson, W.B., and Holt, R.D. 1997. Toward an integration of landscape and food web ecology:The Dynamics of Spatially Subsidized Food Webs. Annu. Rev. Ecol. Syst. **28**(1): 289–316. doi:10.1146/annurev.ecolsys.28.1.289.
Post, D.M. 2002. Using stable isotopes to estimate trophic position: Models, methods, and assumptions. Ecology **83**(3): 703–718. doi:10.2307/3071875.
Preston, N.D., Carpenter, S.R., Cole, J.J., and Pace, M.L. 2008. Airborne carbon deposition on a remote forested lake. Aquat. Sci. **70**(3): 213–224. doi:10.1007/s00027-008-8074-5.
Rantakari, M., and Kortelainen, P. 2008. Controls of organic and inorganic carbon in randomly selected Boreal lakes in varied catchments. Biogeochemistry **91**(2–3): 151–162. doi:10.1007/s10533-008-9266-8.
Rask, M., Verta, M., Korhonen, M., Salo, S., Forsius, M., Arvola, L., Jones, R.I., and Kiljunen, M. 2010. Does lake thermocline depth affect methyl mercury concentrations in fish? Biogeochemistry **101**(1): 311–322. doi:10.1007/s10533-010-9487-5.
Rasmussen, J.B., Godbout, L., and Schallenberg, M. 1989. The humic content of lake water and its relationship to watershed and lake morphometry. Limnol. Oceanogr. **34**(7): 1336–1343. doi:10.4319/lo.1989.34.7.1336.
Read, J.S., and Rose, K.C. 2013. Physical responses of small temperate lakes to variation in dissolved organic carbon concentrations. Limnol. Oceanogr. **58**(3): 921–931. doi:10.4319/lo.2013.58.3.0921.
Renwick, W.H. 2009. Lakes and Reservoirs of North America. *In* Encyclopedia of Inland Waters. *Edited by* G.E. Likens. Academic Press, Oxford. pp. 524–532. doi:https://doi.org/10.1016/B978-012370626-3.00033-8.
Rice, A.L., Butenhoff, C.L., Teama, D.G., Röger, F.H., Khalil, M.A.K., and Rasmussen, R.A. 2016. Atmospheric methane isotopic record favors fossil sources flat in 1980s and 1990s with recent increase. Proc. Natl. Acad. Sci. U. S. A. **113**(39): 10791–10796. doi:10.1073/pnas.1522923113.
Rinta, P., Bastviken, D., van Hardenbroek, M., Kankaala, P., Leuenberger, M., Schilder, J., Stötter, T., and Heiri, O. 2015. An inter-regional assessment of concentrations

and δ13C values of methane and dissolved inorganic carbon in small European lakes. Aquat. Sci. **77**(4): 667–680. doi:10.1007/s00027-015-0410-y.
Roden, J.S., and Ehleringer, J.R. 1999. Observations of Hydrogen and Oxygen Isotopes in Leaf Water Confirm the Craig-Gordon Model under Wide-Ranging Environmental Conditions. Plant Physiol. **120**: 1165–1173. doi:https://doi.org/10.1104/pp.120.4.1165.
Rudd, J.W.M., and Hamilton, R.D. 1978. Methane cycling in a eutrophic shield lake and its effects on whole lake metabolism. Limnol. Oceanogr. **23**(2): 337–348.
Rudd, J.W.M., Hamilton, R.D., and Campbell, N.E.R. 1974. Measurement of microbial oxidation of methane in lake water. Limnol. Oceanogr. **19**: 519–524. doi:https://doi.org/10.4319/lo.1974.19.3.0519.
Sanches, L.F., Guenet, B., Marinho, C.C., Barros, N., and de Assis Esteves, F. 2019. Global regulation of methane emission from natural lakes. Sci. Rep. **9**(1): 1–10. doi:10.1038/s41598-018-36519-5.
Sanseverino, A.M., Bastviken, D., Sundh, I., Pickova, J., and Enrich-Prast, A. 2012. Methane carbon supports aquatic food webs to the fish level. PLoS One **7**(8). doi:10.1371/journal.pone.0042723.
Saunois, M., Bousquet, P., Poulter, B., Peregon, A., Ciais, P., Canadell, J.G., Dlugokencky, E.J., Etiope, G., Bastviken, D., Houweling, S., Janssens-Maenhout, G., Tubiello, F.N., Castaldi, S., Jackson, R.B., Alexe, M., Arora, V.K., Beerling, D.J., Bergamaschi, P., Blake, D.R., Brailsford, G., Brovkin, V., Bruhwiler, L., Crevoisier, C., Crill, P., Covey, K., Curry, C., Frankenberg, C., Gedney, N., Höglund-Isaksson, L., Ishizawa, M., Ito, A., Joos, F., Kim, H.S., Kleinen, T., Krummel, P., Lamarque, J.F., Langenfelds, R., Locatelli, R., Machida, T., Maksyutov, S., McDonald, K.C., Marshall, J., Melton, J.R., Morino, I., Naik, V., O'Doherty, S., Parmentier, F.J.W., Patra, P.K., Peng, C., Peng, S., Peters, G.P., Pison, I., Prigent, C., Prinn, R., Ramonet, M., Riley, W.J., Saito, M., Santini, M., Schroeder, R., Simpson, I.J., Spahni, R., Steele, P., Takizawa, A., Thornton, B.F., Tian, H., Tohjima, Y., Viovy, N., Voulgarakis, A., Van Weele, M., Van Der Werf, G.R., Weiss, R., Wiedinmyer, C., Wilton, D.J., Wiltshire, A., Worthy, D., Wunch, D., Xu, X., Yoshida, Y., Zhang, B., Zhang, Z., and Zhu, Q. 2016. The global methane budget 2000-2012. Earth Syst. Sci. Data **8**(2): 697–751. doi:10.5194/essd-8-697-2016.
Sawara, A.K.M.G. 2007. Pollen Morphology and Its Systematic Significance in the Ericaceae. Hokkaido University. Available from http://eprints.lib.hokudai.ac.jp/dspace/handle/2115/46925.
Schiff, S.L., Tsuji, J.M., Wu, L., Venkiteswaran, J.J., Molot, L.A., Elgood, R.J., Paterson, M.J., and Neufeld, J.D. 2017. Millions of Boreal Shield Lakes can be used to Probe Archaean Ocean Biogeochemistry. Sci. Rep. **7**: 46708. doi:10.1038/srep46708.
Schilder, J., Bastviken, D., van Hardenbroek, M., Leuenberger, M., Rinta, P., Stötter, T., and Heiri, O. 2015. The stable carbon isotopic composition of Daphnia ephippia in small, temperate lakes reflects in-lake methane availability. Limnol. Oceanogr. **60**(3): 1064–1075. doi:10.1002/lno.10079.
Schindler, D.W. 1971. A Hypothesis to Explain Differences and Similarities Among Lakes in the Experimental Lakes Area, Northwestern Ontario. J. Fish. Res. Board Canada **28**(2): 295–301. doi:10.1139/f71-039.
Schindler, D.W., Bayley, S.E., Parker, B.R., Beaty, K.G., R, D., Fee, E.J., Schindler, E.U., Stainton, M.P., Fee, J., and Cruikshank, D.R. 1996. The effects of climatic warming on the properties of boreal lakes and streams at the Experimental Lakes Area. Limnology **41**(5): 1004–1017. doi:https://doi.org/10.4319/lo.1996.41.5.1004.

Schindler, D.W., Curtis, P.J., Bayley, S.E., Parker, B.R., Beaty, K.G., and Stainton, M.P. 1997. Climate-induced changes in the dissolved organic carbon budgets of boreal lakes. Biogeochemistry **36**: 9–28. doi:10.1023/A:1005792014547.
Schindler, D.W., Hecky, R.E., Findlay, D.L., Stainton, M.P., Parker, B.R., Paterson, M.J., Beaty, K.G., Lyng, M., and Kasian, S.E.M. 2008. Eutrophication of lakes cannot be controlled by reducing nitrogen input: Results of a 37-year whole-ecosystem experiment. Proc. Natl. Acad. Sci. U. S. A. **105**(32): 11254–11258. doi:10.1073/pnas.0805108105.
Schoell, M. 1988. Multiple origins of methane in the Earth. Chem. Geol. **71**(1–3): 1–10. doi:10.1016/0009-2541(88)90101-5.
Schönheit, P., Keweloh, H., and Thauer, R.. 1981. Factor F420 degradatio in Methanobacterium thermoautotrophicum during exopsure to oxygen. FEMS Microbiol. Lett. **12**: 347–349. doi:10.1007/978-1-4615-6369-3_67.
Seekell, D.A., Lapierre, J.-F., Ask, J., Bergström, A.-K., Deininger, A., Rodríguez, P., and Karlsson, J. 2015. The influence of dissolved organic carbon on primary production in northern lakes. Limnol. Oceanogr. **60**(4): 1276–1285. doi:10.1002/lno.10096.
Sessions, A.L., Burgoyne, T.W., Schimmelmann, A., and Hayes, J.M. 1999. Fractionation of hydrogen isotopes in lipid biosynthesis. Org. Geochem. **30**(9): 1193–1200. doi:10.1016/S0146-6380(99)00094-7.
Sieczko, A.K., Thanh Duc, N., Schenk, J., Pajala, G., Rudberg, D., Sawakuchi, H.O., and Bastviken, D. 2020. Diel variability of methane emissions from lakes. Proc. Natl. Acad. Sci. U. S. A. **117**(35): 21488–21494. doi:10.1073/pnas.2006024117.
Smith, B.N., and Epstein, S. 1970. Biogeochemistry of the Stable Isotopes of Hydrogen and Carbon in Salt Marsh Biota. Plant Physiol. **46**(5): 738–742. doi:10.1104/pp.46.5.738.
Sobek, S., Durisch-Kaiser, E., Zurbrügg, R., Wongfun, N., Wessels, M., Pasche, N., and Wehrli, B. 2009. Organic carbon burial efficiency in lake sediments controlled by oxygen exposure time and sediment cores. Limnol. Oceanogr. **54**(6): 2243–2254. doi:https://doi.org/10.4319/lo.2009.54.6.2243.
Sobek, S., Tranvik, L.J., and Cole, J.J. 2005. Temperature independence of carbon dioxide supersaturation in global lakes. Global Biogeochem. Cycles **19**(2): 1–10. doi:10.1029/2004GB002264.
Sobek, S., Tranvik, L.J., Prairie, Y.T., Kortelainen, P., and Cole, J.J. 2007. Patterns and regulation of dissolved organic carbon: An analysis of 7,500 widely distributed lakes. Limnol. Oceanogr. **52**(3): 1208–1219. doi:10.4319/lo.2007.52.3.1208.
Solomon, C.T., Carpenter, S.R., Clayton, M.K., Cole, J.J., Coloso, J.J., Pace, M.L., Vander Zanden, M.J., and Weidel, B.C. 2011. Terrestrial, benthic, and pelagic resource use in lakes: Results from a three-isotope Bayesian mixing model. Ecology **92**(5): 1115–1125. doi:10.1890/10-1185.1.
Solomon, C.T., Cole, J.J., Doucett, R.R., Pace, M.L., Preston, N.D., Smith, L.E., and Weidel, B.C. 2009. The influence of environmental water on the hydrogen stable isotope ratio in aquatic consumers. **161**: 313–324. doi:10.1007/s00442-009-1370-5.
Solomon, C.T., Jones, S.E., Weidel, B.C., Buffam, I., Fork, M.L., Karlsson, J., Larsen, S., Lennon, J.T., Read, J.S., Sadro, S., and Saros, J.E. 2015. Ecosystem Consequences of Changing Inputs of Terrestrial Dissolved Organic Matter to Lakes : Current Knowledge and Future Challenges. Ecosystems. doi:10.1007/s10021-015-9848-y.
Soto, D.X., Wassenaar, L.I., and Hobson, K.A. 2013. Stable hydrogen and oxygen isotopes in aquatic food webs are tracers of diet and provenance. Funct. Ecol. **27**(2):

535–543. doi:10.1111/1365-2435.12054.
Steinberg, C.E.W., Kamara, S., Prokhotskaya, V.Y., Manusadžianas, L., Karasyova, T.A., Timofeyev, M.A., Jie, Z., Paul, A., Meinelt, T., Farjalla, V.F., Matsuo, A.Y.O., Burnison, B.K., and Menzel, R. 2006. Dissolved humic substances - Ecological driving forces from the individual to the ecosystem level? Freshw. Biol. **51**(7): 1189–1210. doi:10.1111/j.1365-2427.2006.01571.x.
Strayer, R.F., and Tiedje, J.M. 1978. In situ methane production in a small, hypereutrophic, hard-water lake: Loss of methane from sediments by vertical diffusion and ebullition. Limnol. Oceanogr. **23**(6): 1201–1206. doi:10.4319/lo.1978.23.6.1201.
Striegl, R.G., Kortelainen, P., Chanton, J.P., Wickland, K.P., Bugna, G.C., and Rantakari, M. 2001. Carbon dioxide partial and 13C content of north and boreal lakes at pressure temperate ice melt spring. Limnol. Oceanogr. **46**(4): 941–945. doi:10.4319/lo.2001.46.4.0941.
Stubbins, A., Lapierre, J.F., Berggren, M., Prairie, Y.T., Dittmar, T., and Del Giorgio, P.A. 2014. What's in an EEM? Molecular signatures associated with dissolved organic fluorescence in boreal Canada. Environ. Sci. Technol. **48**(18). doi:10.1021/es502086e.
Sugimoto, A., and Fujita, N. 2006. Hydrogen concentration and stable isotopic composition of methane in bubble gas observed in a natural wetland. Biogeochemistry **81**(1): 33–44. doi:10.1007/s10533-006-9028-4.
Sulzman, E.W. 2020. Stable isotope chemistry and measurement: a primer. *In* Stable isotopes in ecology and environmental Science, 2nd edition. *Edited by* R.H. Michener and K. Lajtha. Blackwell Publishing. pp. 1–21.
Syväranta, J., Tiirola, M., and Jones, R.I. 2008. Seasonality in lake pelagic δ15N values: patterns, possible explanations, and implications for food web baselines. Fundam. Appl. Limnol. / Arch. für Hydrobiol. **172**(3): 255–262. doi:10.1127/1863-9135/2008/0172-0255.
Taipale, S., Kankaala, P., Tiirola, M., and Jones, R.I. 2008. Whole-Lake Dissolved Inorganic 13C Additions Reveal Seasonal Shifts in Zooplankton Diet. Ecology **89**(2): 463–474. doi:10.1890/07-0702.1.
Tanentzap, A.J., Kielstra, B.W., Wilkinson, G.M., Berggren, M., Craig, N., Del Giorgio, P.A., Grey, J., Gunn, J.M., Jones, S.E., Karlsson, J., Solomon, C.T., and Pace, M.L. 2017. Terrestrial support of lake food webs: Synthesis reveals controls over cross-ecosystem resource use. Sci. Adv. **3**(3): 1–11. doi:10.1126/sciadv.1601765.
Teranes, J.L., and Bernasconi, S.M. 2000. The record of nitrate utilization and productivity limitation provided by δ15N values in lake organic matter - A study of sediment trap and core sediments from Baldeggersee, Switzerland. Limnol. Oceanogr. **45**(4): 801–813. doi:10.4319/lo.2000.45.4.0801.
Thottathil, S.D., Reis, P.C.J., del Giorgio, P.A., and Prairie, Y.T. 2018. The Extent and Regulation of Summer Methane Oxidation in Northern Lakes. J. Geophys. Res. Biogeosciences **123**(10): 3216–3230. doi:10.1029/2018JG004464.
Thottathil, S.D., Reis, P.C.J., and Prairie, Y.T. 2019. Methane oxidation kinetics in northern freshwater lakes. Biogeochemistry **143**(1): 105–116. Springer International Publishing. doi:10.1007/s10533-019-00552-x.
Thurman, E.M. 1985. Organic Geochemistry of Natural Waters. *In* Organic Geochemistry of Natural Waters. Martinus Nijhoff/Dr. W. Junk Publishers, Dordrecht. p. 497. doi:10.1007/978-94-009-5095-5.

Thuss, S.J. 2008. Nitrous oxide production in the Grand RIver, Ontario, Canada: New insights from stable isotope analysis of dissolved nitrous oxide. University of Waterloo. Available from http://hdl.handle.net/10012/4086.
Tonin, J. 2019. The effects of dissolved organic carbon on pathways of energy flow , resource availability , and consumer biomass in nutrient-poor boreal lakes. University of Manitoba. Available from https://mspace.lib.umanitoba.ca/handle/1993/34267.
Tranvik, L.J. 1992. Allochthonous dissolved organic matter as an energy source for pelagic bacteria and the concept of the microbial loop. Hydrobiologia **229**(1): 107–114. doi:10.1007/BF00006994.
Tranvik, L.J., Downing, J.A., Cotner, J.B., Loiselle, S.A., Striegl, R.G., Ballatore, T.J., Dillon, P., Finlay, K., Fortino, K., Knoll, L.B., Kortelainen, P.L., Kutser, T., Larsen, S., Laurion, I., Leech, D.M., McCallister, S.L., McKnight, D.M., Melack, J.M., Overholt, E., Porter, J.A., Prairie, Y., Renwick, W.H., Roland, F., Sherman, B.S., Schindler, D.W., Sobek, S., Tremblay, A., Vanni, M.J., Verschoor, A.M., von Wachenfeldt, E., and Weyhenmeyer, G.A. 2009. Lakes and reservoirs as regulators of carbon cycling and climate. Limnol. Oceanogr. **54**(6 Part 2): 2298–2314. doi:10.4319/lo.2009.54.6_part_2.2298.
Tsuji, J.M. 2020. Microbial Ecology of Phototrophs in Iron-rich Boreal Shield Lakes. University of Waterloo. Available from http://hdl.handle.net/10012/16362.
Turner, M.A., Howell, E.T., Robinson, G.G.C., Campbell, P., Hecky, R.E., and Schindler, E.U. 1994. Roles of Nutrients in Controlling Growth in Epilithon in Oligotrohpic Lakes of Low Alkalinity. Can. J. Fish. Aquat. Sci. **51**: 2784–2793. doi:https://doi.org/10.1139/f94-278.
Vachon, D., Langenegger, T., Donis, D., and McGinnis, D.F. 2019. Influence of water column stratification and mixing patterns on the fate of methane produced in deep sediments of a small eutrophic lake. Limnol. Oceanogr. **64**(5): 2114–2128. doi:10.1002/lno.11172.
Venkiteswaran, J.J. 2008. Greenhouse gas cycling in experimental boreal reservoirs. University of Waterloo. Available from https://uwspace.uwaterloo.ca/handle/10012/4168.
Venkiteswaran, J.J. 2019. rayleigh: Calculates and Plotes isotope Rayleigh curves. R package version 0.1.3.
Venkiteswaran, J.J., and Schiff, S.L. 2005. Methane oxidation: isotopic enrichment factors in freshwater boreal reservoirs. Appl. Geochemistry **20**: 683–690. doi:10.1016/j.apgeochem.2004.11.007.
Vuorio, K., Meili, M., and Sarvala, J. 2006. Taxon-specific variation in the stable isotopic signatures (δ13C and δ15N) of lake phytoplankton. Freshw. Biol. **51**(5): 807–822. doi:10.1111/j.1365-2427.2006.01529.x.
Waldron, S., Lansdown, J.M., Scott, E.M., Fallick, A.E., and Hall, A.J. 1999. The global influence of the hydrogen isotope composition of water on that of bacteriogenic methane from shallow freshwater environments. Geochim. Cosmochim. Acta **63**(15): 2237–2245. doi:10.1016/S0016-7037(99)00192-1.
Walter, K.M., Smith, L.C., and Chapin, F.S. 2007. Methane bubbling from northern lakes: Present and future contributions to the global methane budget. Philos. Trans. R. Soc. A Math. Phys. Eng. Sci. **365**(1856): 1657–1676. doi:10.1098/rsta.2007.2036.
Wand, U., Samarkin, V.A., Nitzsche, H.-M., and Hubberten, H.-W. 2006. Biogeochemistry of methane in the permanently ice-covered Lake Untersee, central Dronning Maud Land, East Antarctica. **51**(2): 1180–1194.

Wetzel, R.G. 1995. Death, detritus, and energy flow in aquatic ecosystems. Freshw. Biol. **33**(1): 83–89. doi:10.1111/j.1365-2427.1995.tb00388.x.
Wetzel, R.G. 2001a. The Inorganic Carbon Complex. *In* Limnology, Third edit. Academic Press. pp. 187–204. doi:10.1016/b978-0-08-057439-4.50015-0.
Wetzel, R.G. 2001b. Detritus: Organic Carbon Cycling and Ecosystem Metabolism. *In* Limnology, Third edit. Academic Press. pp. 731–783. doi:10.1016/b978-0-08-057439-4.50027-7.
Whitfield, C., Aherne, J., and Watmough, S. 2009. Predicting the Partial Pressure of Carbon Dioxide in Boreal Lakes. Can. Water Resour. J. **34**(4): 415–426. doi:10.4296/cwrj3404415.
Whiticar, M.J. 1999. Carbon and hydrogen isotope systematics of bacterial formation and oxidation of methane. Chem. Geol. **161**(1–3): 291–314. doi:10.1016/s0009-2541(99)00092-3.
Whiticar, M.J., Faber, E., and Schoell, M. 1986. Biogenic methane formation in marine and freshwater environments: CO2 reduction vs. acetate fermentation-Isotope evidence. Geochim. Cosmochim. Acta **50**(5): 693–709. doi:10.1016/0016-7037(86)90346-7.
Wilkinson, G.M., Carpenter, S.R., Cole, J.J., Pace, M.L., and Yang, C. 2013a. Terrestrial support of pelagic consumers: Patterns and variability revealed by a multilake study. Freshw. Biol. **58**(10): 2037–2049. doi:10.1111/fwb.12189.
Wilkinson, G.M., Pace, M.L., and Cole, J.J. 2013b. Terrestrial dominance of organic matter in north temperate lakes. Global Biogeochem. Cycles **27**(1): 43–51. doi:10.1029/2012GB004453.
Winslow, L., Read, J., Woolway, R., Brentrup, J., Leach, T., Zwart, J., Alberts, S., and Collinge, D. 2019. rLakeAnalyzer: Lake Physics Tools. R package version 1.11.4.1.
Woltemate, I., Whiticar, M., and Schoell, M. 1984. Carbon and hydrogen isotopic composition of bacterial methane in a shallow freshwater lake. Limnol. Oceanogr. **29**(5): 985–992. doi:10.4319/lo.1984.29.5.0985.
Woodland, R.J., Magnan, P., Glémet, H., Rodríguez, M.A., and Cabana, G. 2012. Variability and directionality of temporal changes in 13C and 15N of aquatic invertebrate primary consumers. **169**: 199–209. doi:10.1007/s00442-011-2178-7.
Xenopoulos, M.A., Lodge, D.M., Frentress, J., Kreps, T.A., Bridgham, S.D., Grossman, E., and Jackson, C.J. 2003. Regional comparisons of watershed determinants of dissolved organic carbon in temperate lakes from the Upper Great Lakes region and selected regions globally. Limnol. Oceanogr. **48**(6): 2321–2334. doi:10.4319/lo.2003.48.6.2321.
Xiao, Y.H., Sara-Aho, T., Hartikainen, H., and Vähätalo, A. V. 2013. Contribution of ferric iron to light absorption by chromophoric dissolved organic matter. Limnol. Oceanogr. **58**(2): 653–662. doi:10.4319/lo.2013.58.2.0653.
Yang, C., Wilkinson, G.M., Cole, J.J., Macko, S.A., and Pace, M.L. 2014. Assigning hydrogen, carbon, and nitrogen isotope values for phytoplankton and terrestrial detritus in aquatic food web studies. Inl. Waters **4**(2): 233–242. doi:10.5268/IW-4.2.700.
Vander Zanden, H.B., Soto, D.X., Bowen, G.J., and Hobson, K.A. 2016. Expanding the Isotopic Toolbox: Applications of Hydrogen and Oxygen Stable Isotope Ratios to Food Web Studies. Front. Ecol. Evol. **4**(March): 1–19. doi:10.3389/fevo.2016.00020.
Zigah, P.K., Oswald, K., Brand, A., Dinkel, C., Wehrli, B., and Schubert, C.J. 2015. Methane oxidation pathways and associated methanotrophic communities in the water column of a tropical lake. Limnol. Oceanogr. **60**(2): 553–572.

doi:10.1002/lno.10035.
Zohary, T., Erez, J., Gophen, M., Berman-Frank, I., and Stiller, M. 1994. Seasonality of stable carbon isotopes within the pelagic food web of Lake Kinneret. Limnol. Oceanogr. **39**(5): 1030–1043. doi:10.4319/lo.1994.39.5.1030.
Zwart, J.A., Sebestyen, S.D., Solomon, C.T., and Jones, S.E. 2017. The Influence of Hydrologic Residence Time on Lake Carbon Cycling Dynamics Following Extreme Precipitation Events. Ecosystems **20**(5): 1000–1014. Springer US. doi:10.1007/s10021-016-0088-6.

Appendix A. Individual midsummer lake profiles for δ^2H-CH_4, δ^{13}C-CH_4, δ^{13}C-DIC, δ^{13}C-POM, CH_4 concentration, and oxygen concentration.

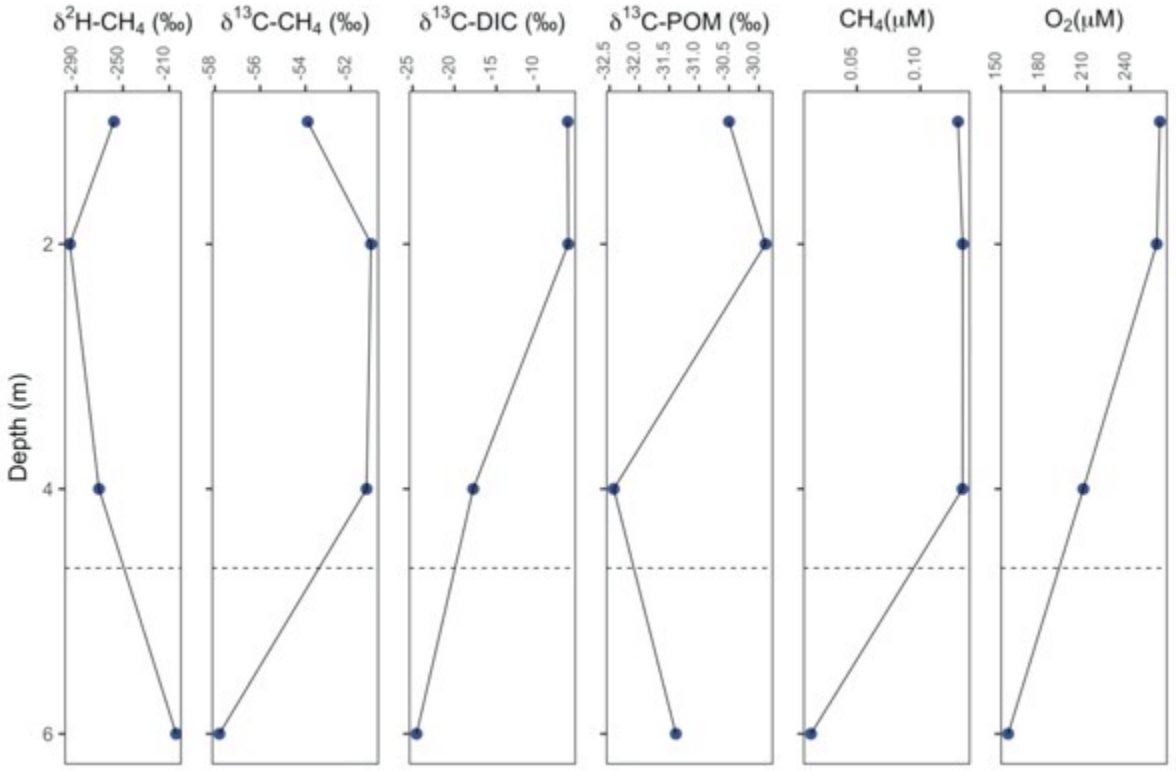

Figure A1. δ^2H-CH_4, δ^{13}C-CH_4, δ^{13}C-DIC, δ^{13}C-POM, CH_4 concentration, and O_2 concentration profiles for L164, midsummer 2018. Dashed line indicates thermocline depth.

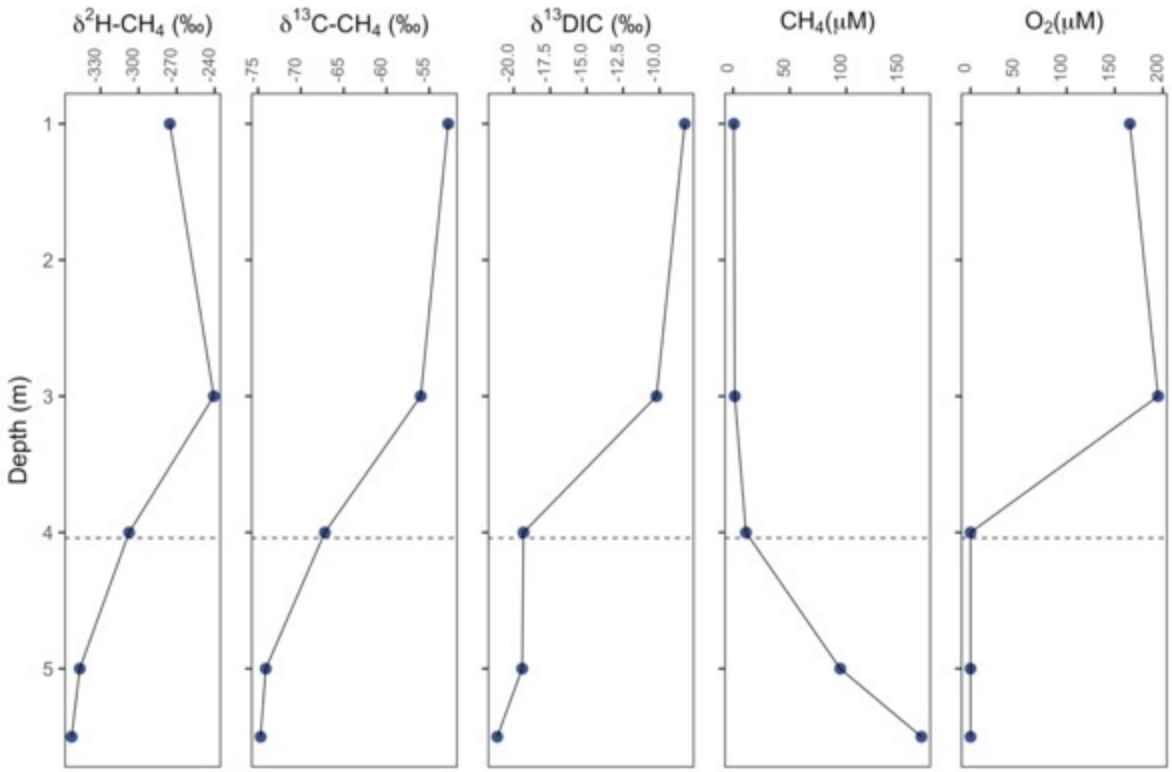

Figure A2. δ^2H-CH_4, δ^{13}C-CH_4, δ^{13}C-DIC, CH_4 concentration, and O_2 concentration profiles for L221, midsummer 2018. Dashed line indicates thermocline depth.

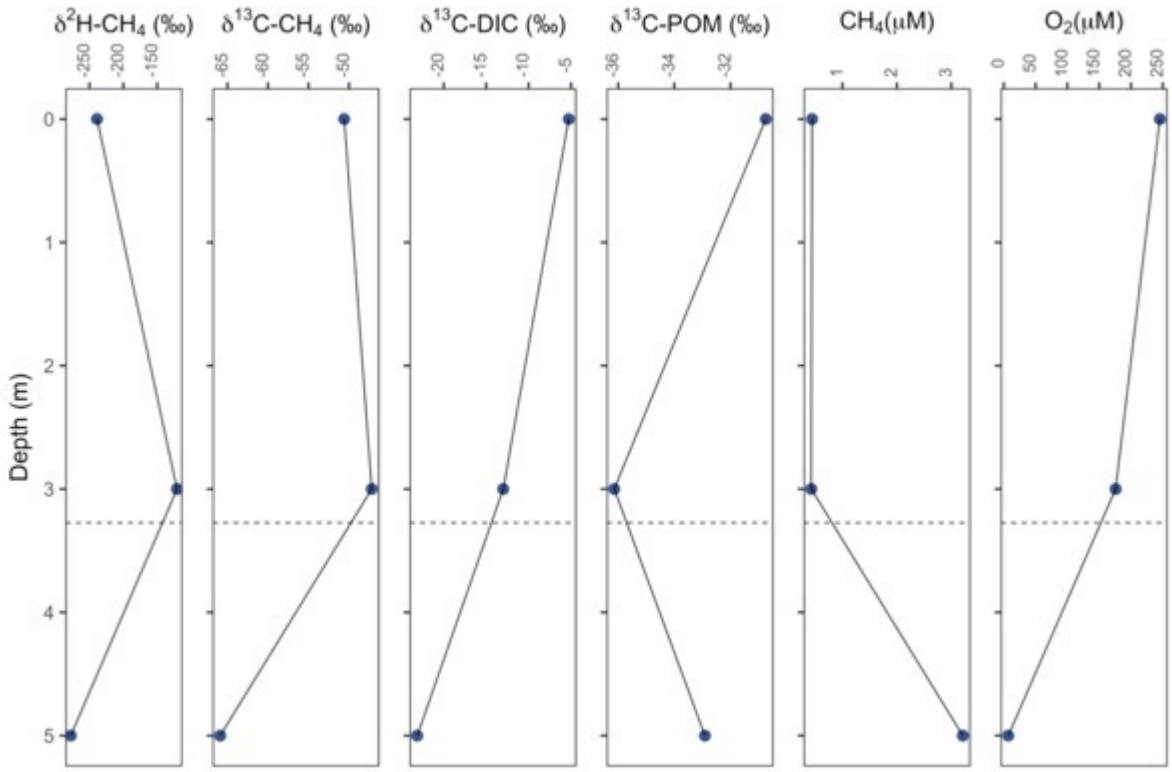

Figure A3. δ^2H-CH_4, δ^{13}C-CH_4, δ^{13}C-POM, CH_4 concentration, and O_2 concentration profiles for L222, midsummer 2018. Dashed line indicates thermocline depth.

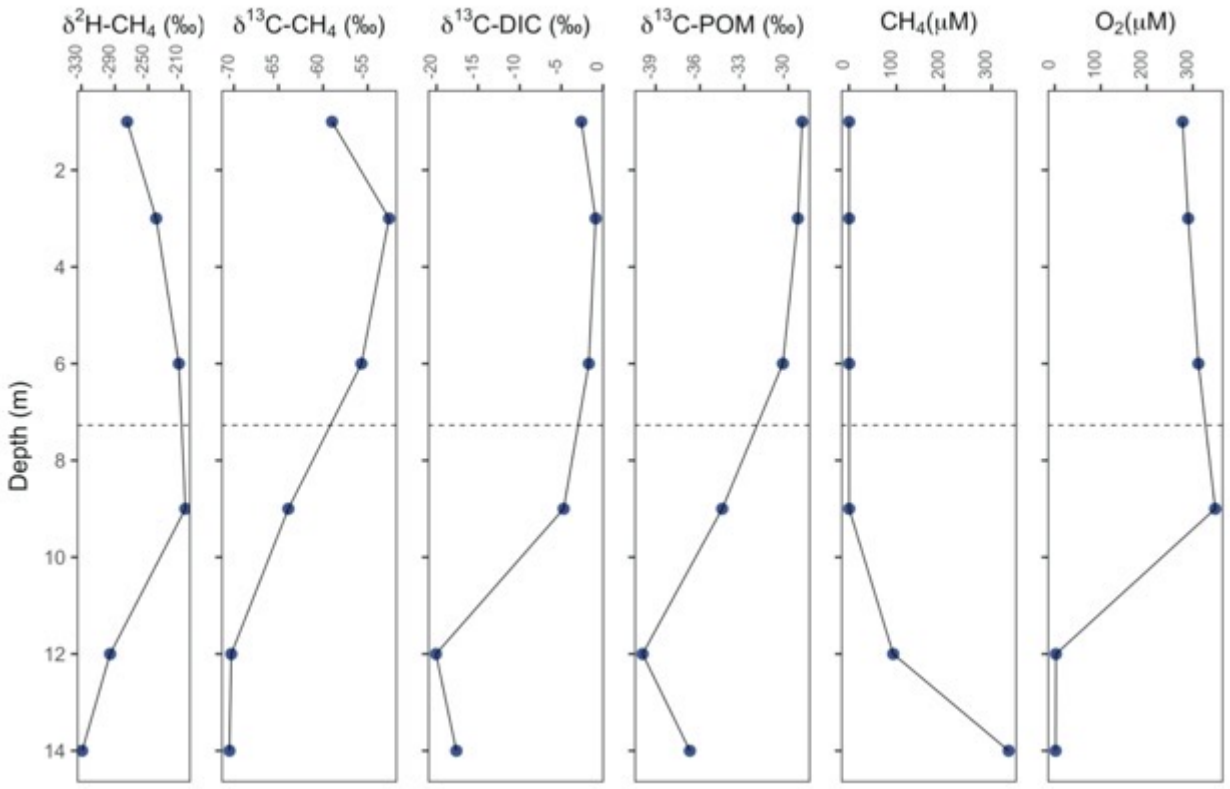

Figure A4. δ^2H-CH_4, δ^{13}C-CH_4, δ^{13}C-POM, CH_4 concentration, and O_2 concentration profiles for L223, midsummer 2018. Dashed line indicates thermocline depth.

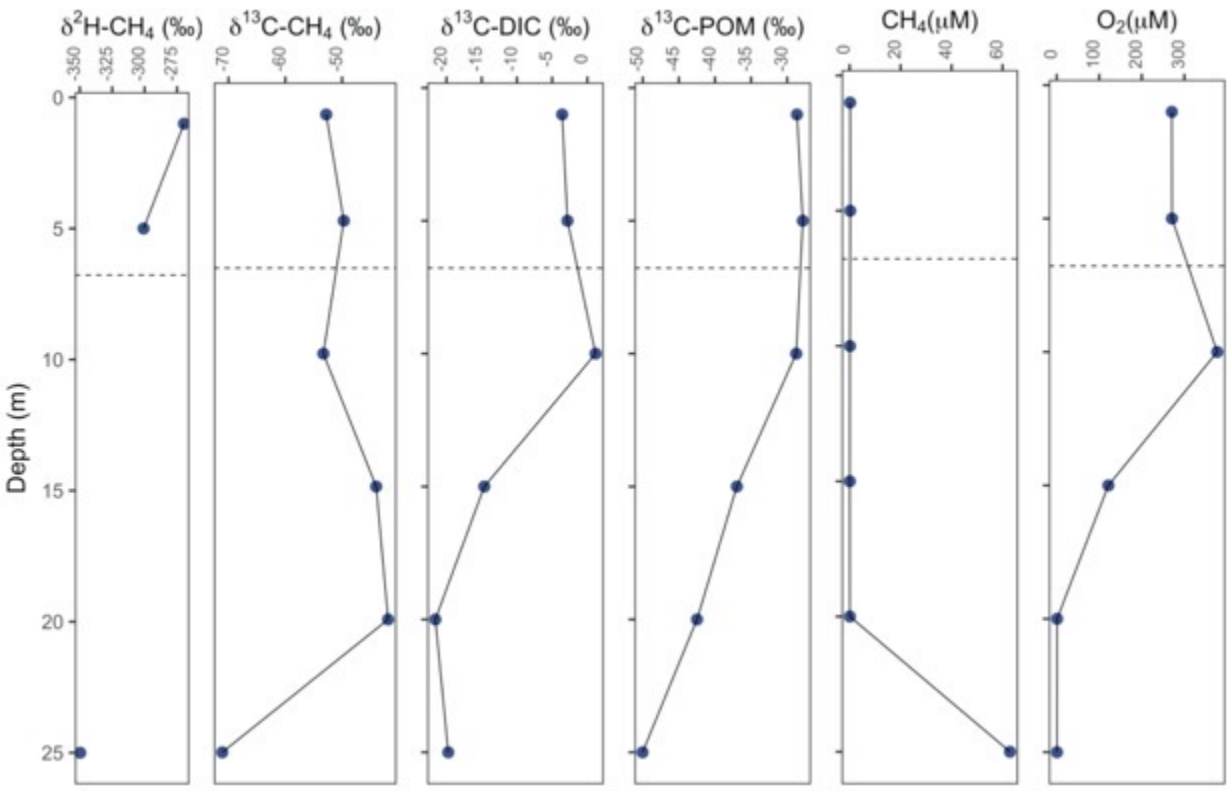

Figure A5. δ^2H-CH_4, δ^{13}C-CH_4, δ^{13}C-POM, CH_4 concentration, and O_2 concentration profiles for L224, midsummer 2018. Dashed line indicates thermocline depth. Missing values indicate that samples were below CH_4 concentration detection limit.

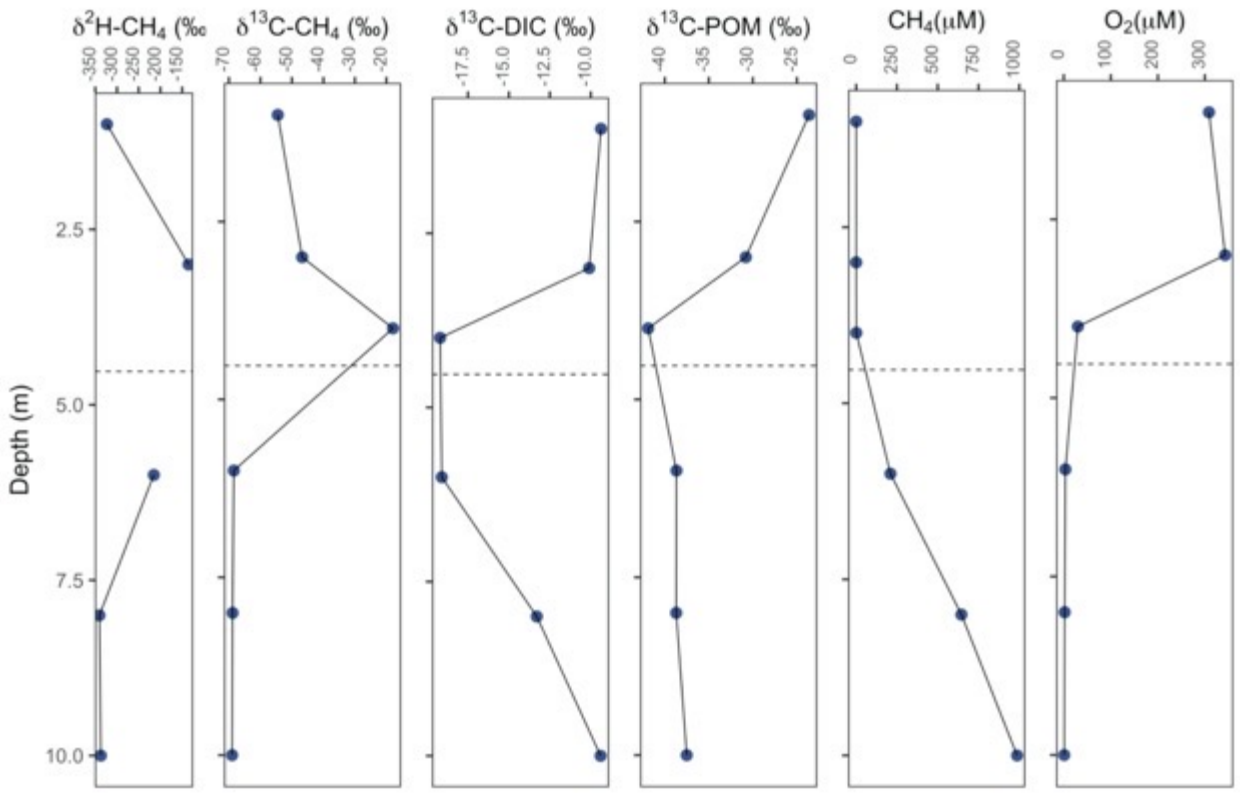

Figure A6. δ^2H-CH_4, δ^{13}C-CH_4, δ^{13}C-POM, CH_4 concentration, and O_2 concentration profiles for L227, midsummer 2018. Dashed line indicates thermocline depth. Missing values indicate that samples were below CH_4 concentration detection limit.

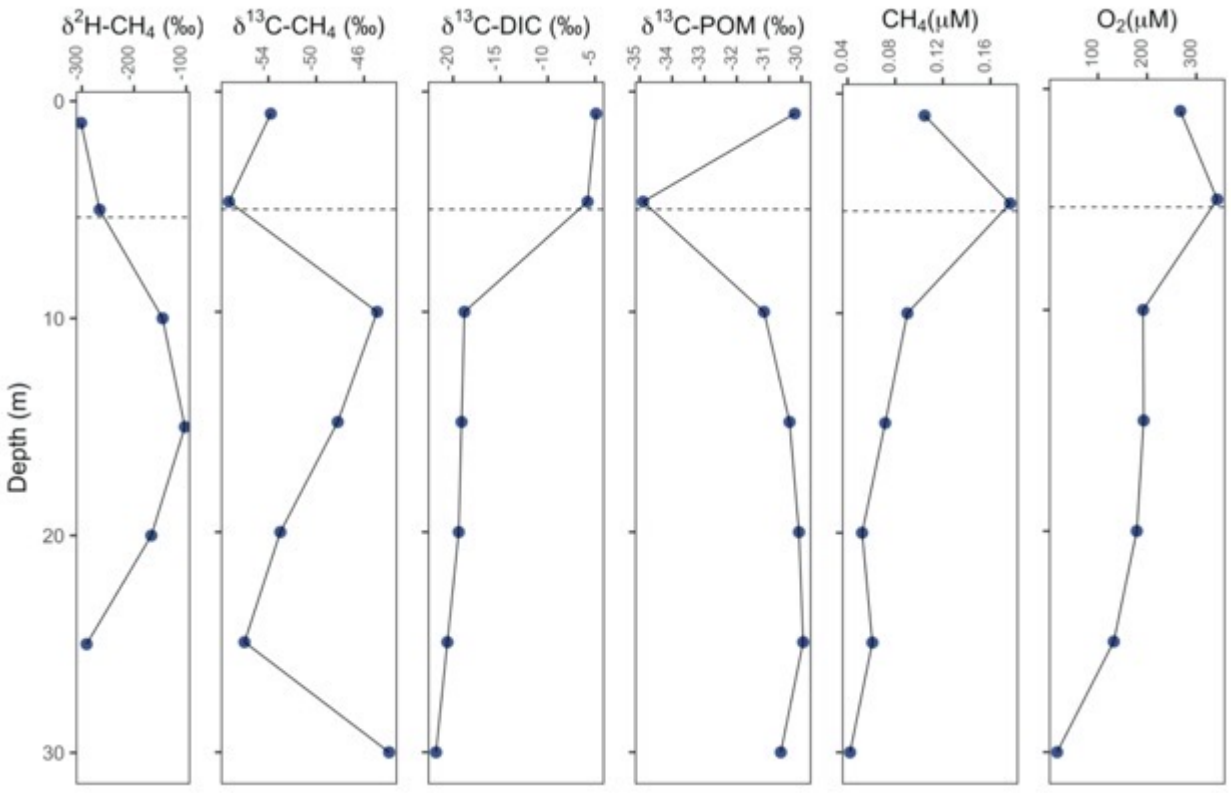

Figure A7. δ^2H-CH_4, δ^{13}C-CH_4, δ^{13}C-POM, CH_4 concentration, and O_2 concentration profiles for L239, midsummer 2018. Dashed line indicates thermocline depth.

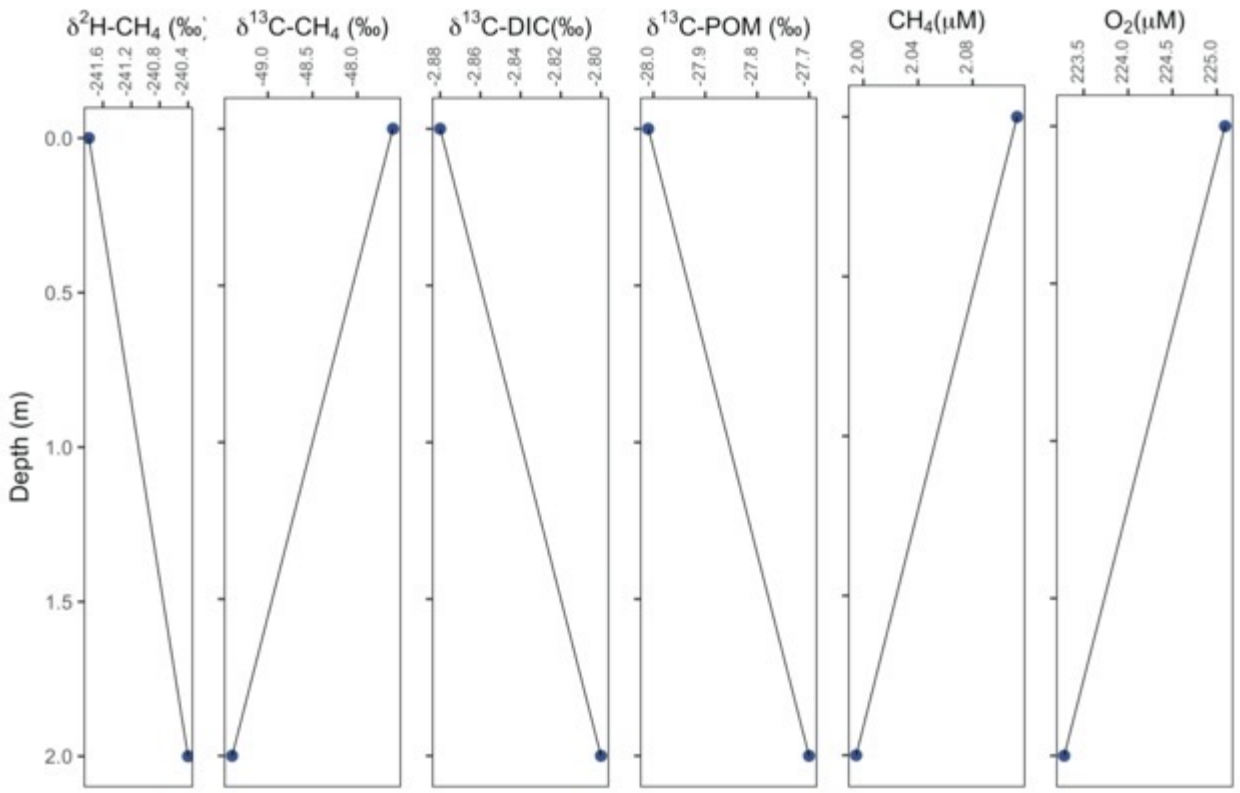

Figure A8. δ^2H-CH_4, δ^{13}C-CH_4, δ^{13}C-POM, CH_4 concentration, and O_2 concentration profiles for L303, midsummer 2018. L303 is a polymictic lake and therefore does not have a thermocline.

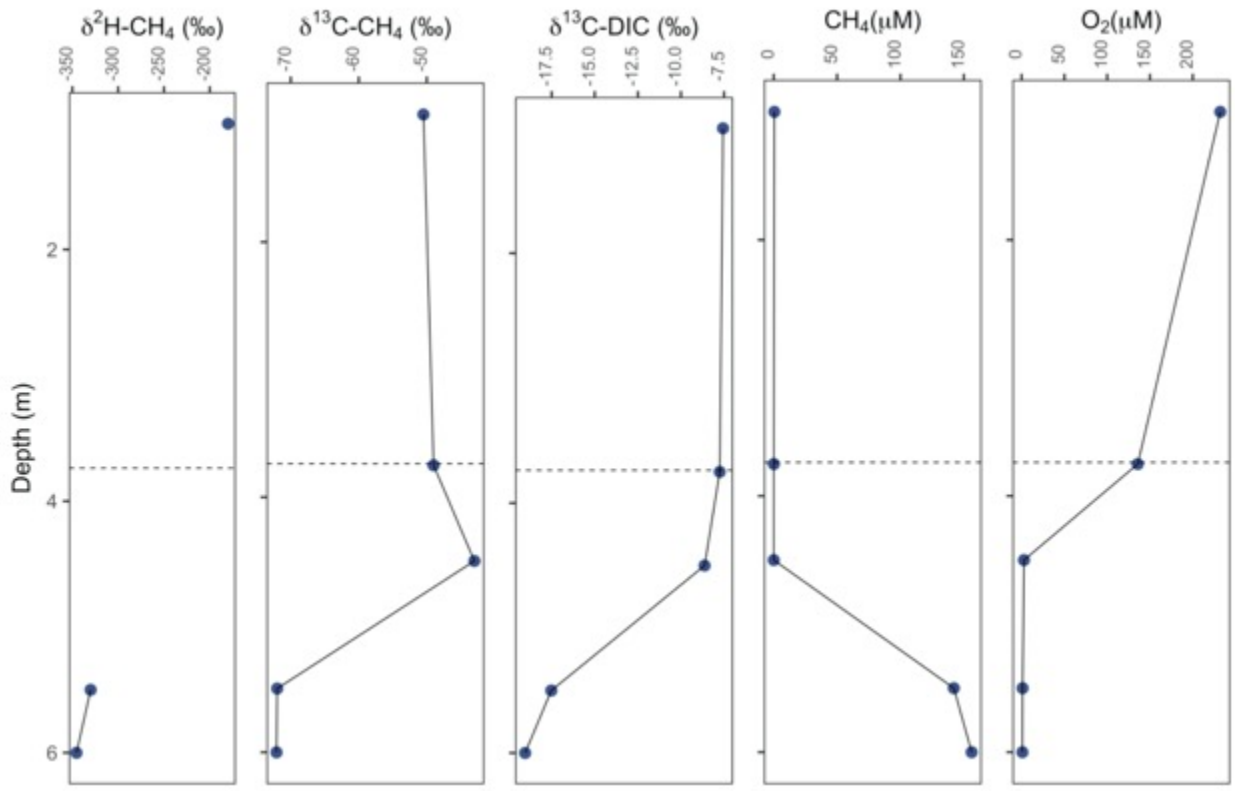

Figure A9. δ^2H-CH_4, δ^{13}C-CH_4, CH_4 concentration, and O_2 concentration profiles for L304, midsummer 2018. Dashed line indicates thermocline depth. Missing values indicate that samples were below CH_4 concentration detection limit.

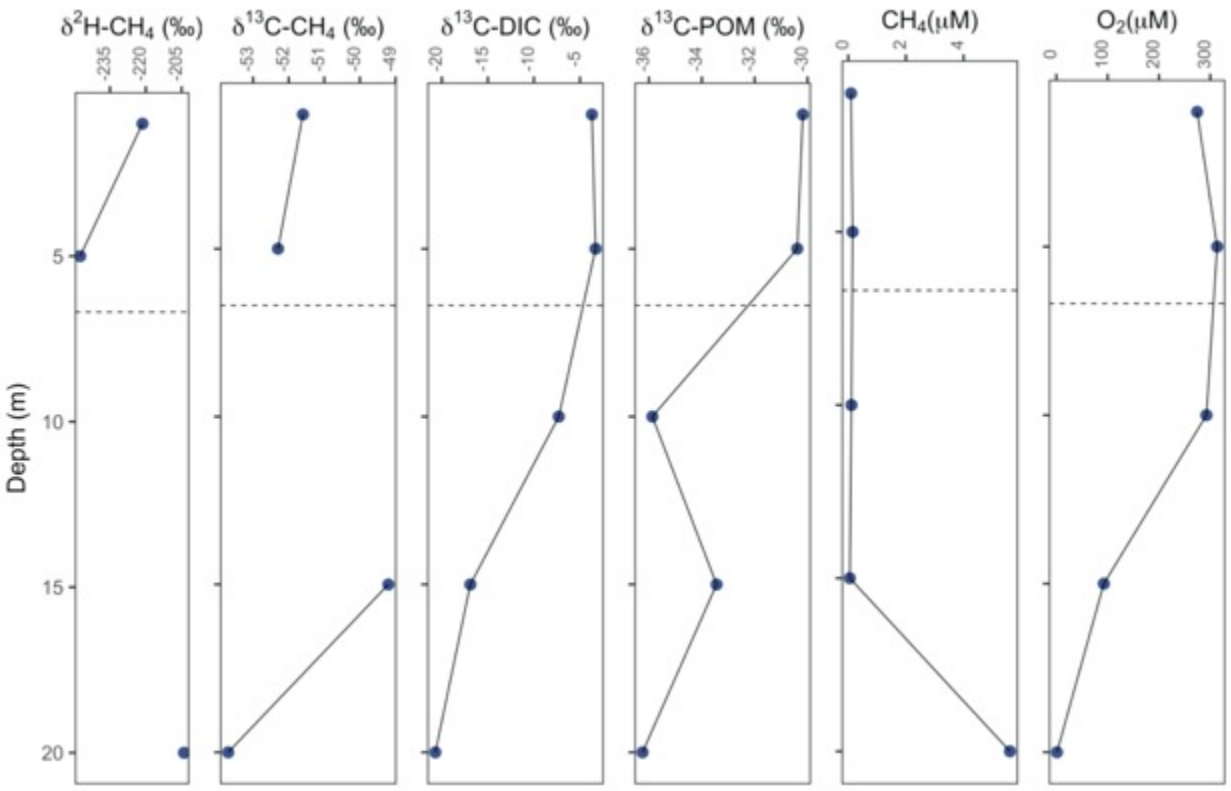

Figure A10. δ^2H-CH_4, δ^{13}C-CH_4, δ^{13}C-POM, CH_4 concentration, and O_2 concentration profiles for L373, midsummer 2018. Dashed line indicates thermocline depth. Missing values indicate that samples were below CH_4 concentration detection limit.

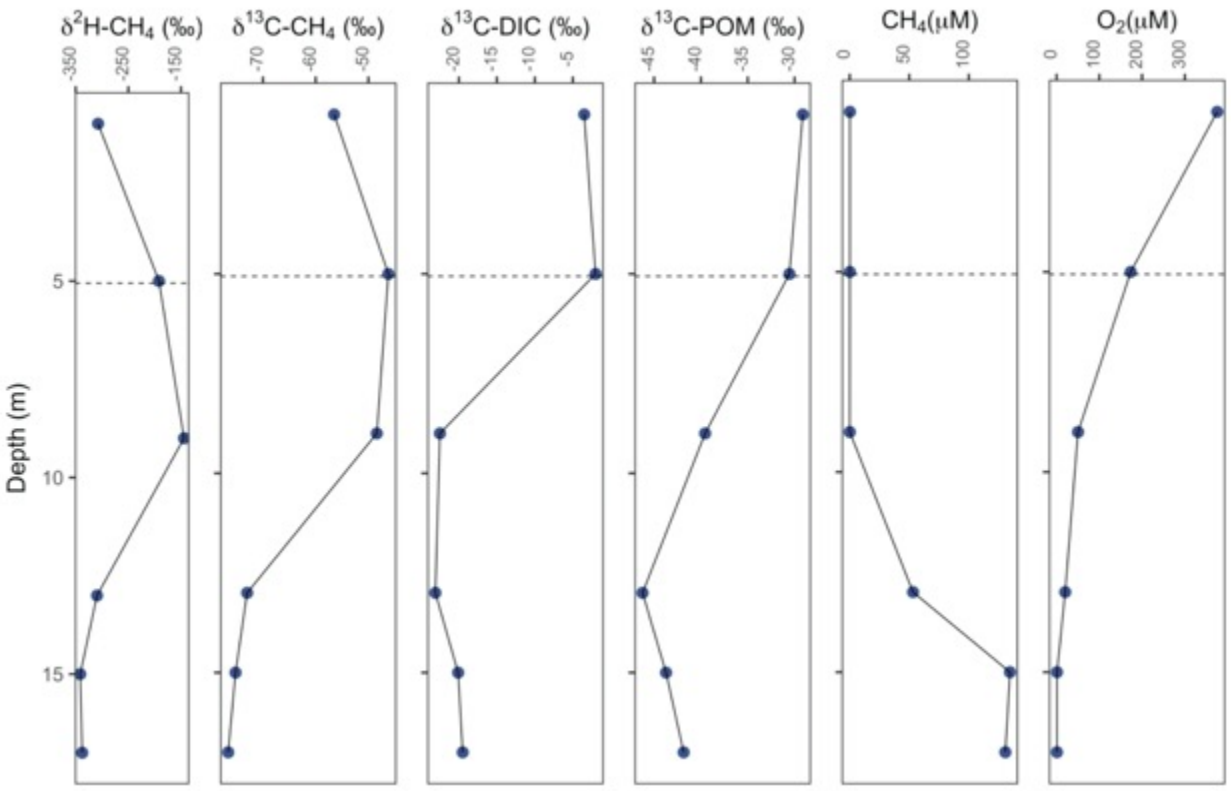

Figure A11. δ^2H-CH_4, δ^{13}C-CH_4, δ^{13}C-POM, CH_4 concentration, and O_2 concentration profiles for L442, midsummer 2018. Dashed line indicates thermocline depth.

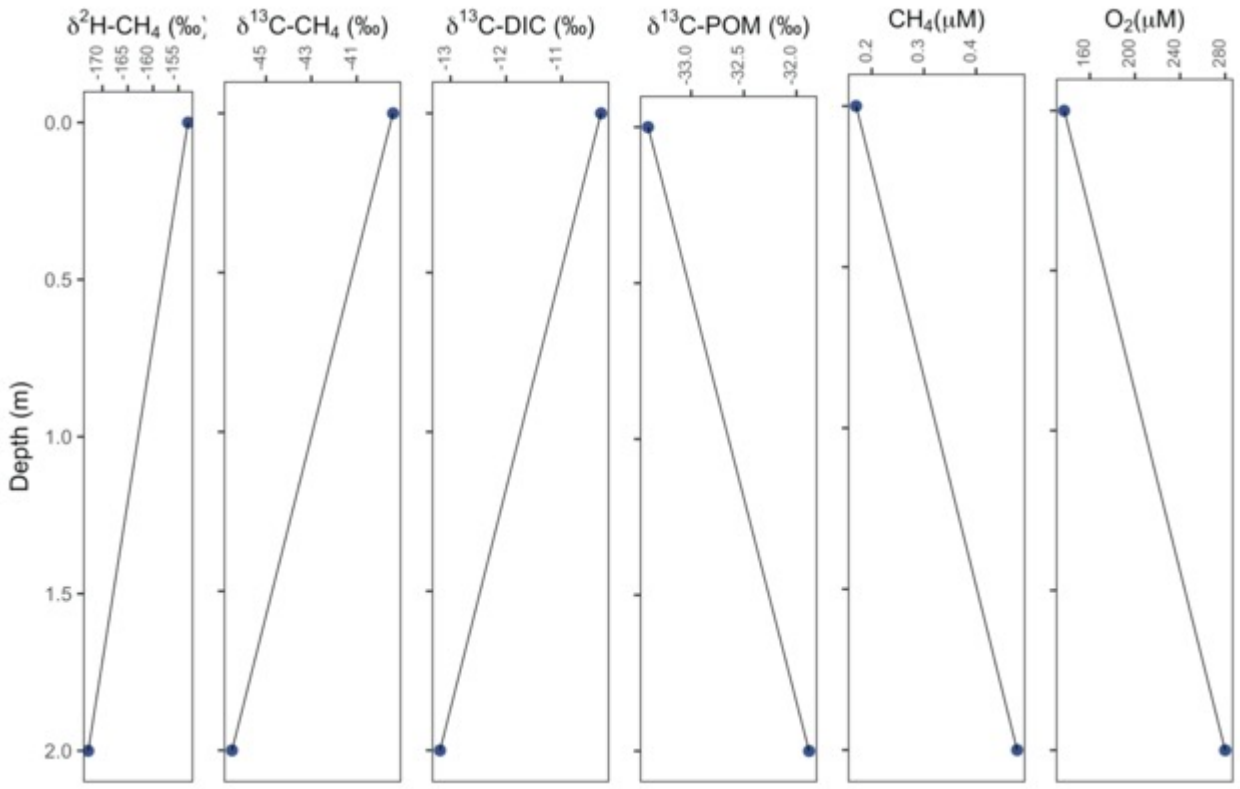

Figure A12. δ^2H-CH_4, δ^{13}C-CH_4, δ^{13}C-POM, CH_4 concentration, and O_2 concentration profiles for L470, midsummer 2018. L470 is a polymictic lake and therefore does not have a thermocline.

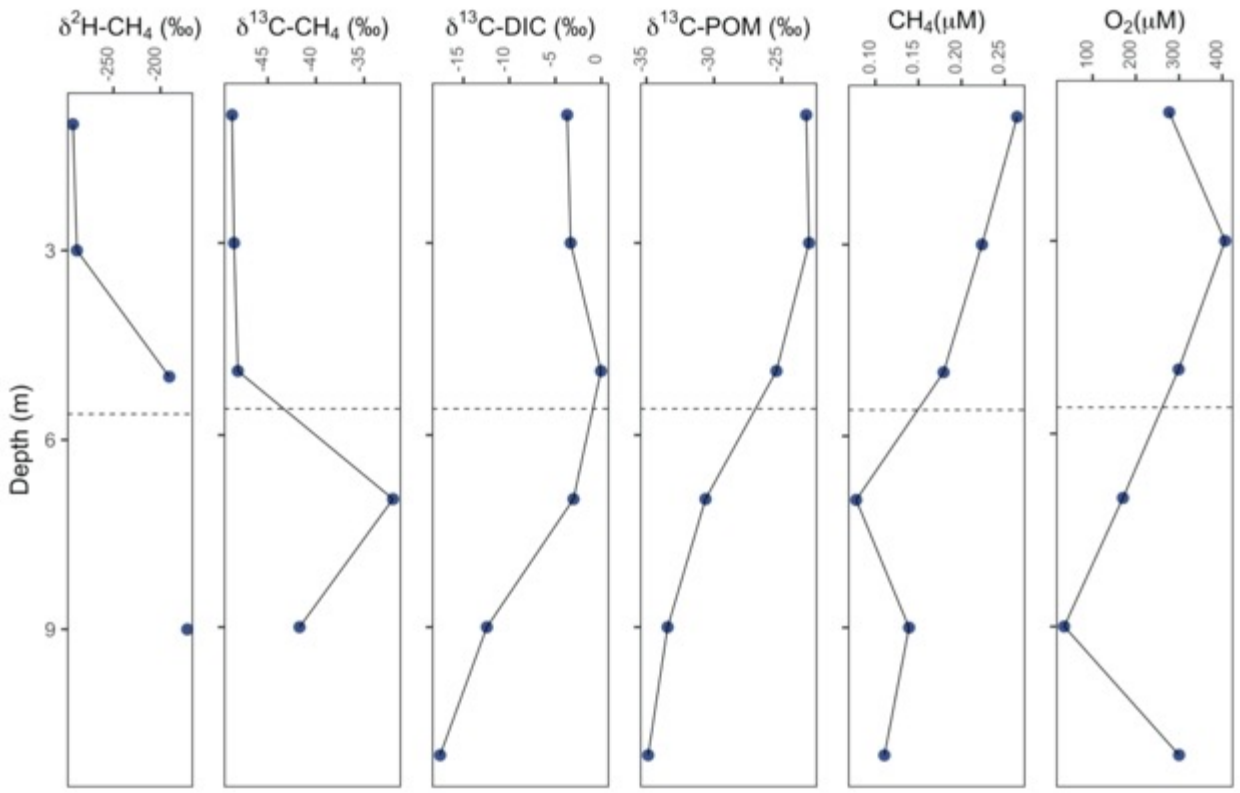

Figure A13. δ^2H-CH_4, δ^{13}C-CH_4, δ^{13}C-POM, CH_4 concentration, and O_2 concentration profiles for L626, midsummer 2018. Missing values indicate that samples were below CH_4 concentration detection limit. Dashed line indicates thermocline depth.

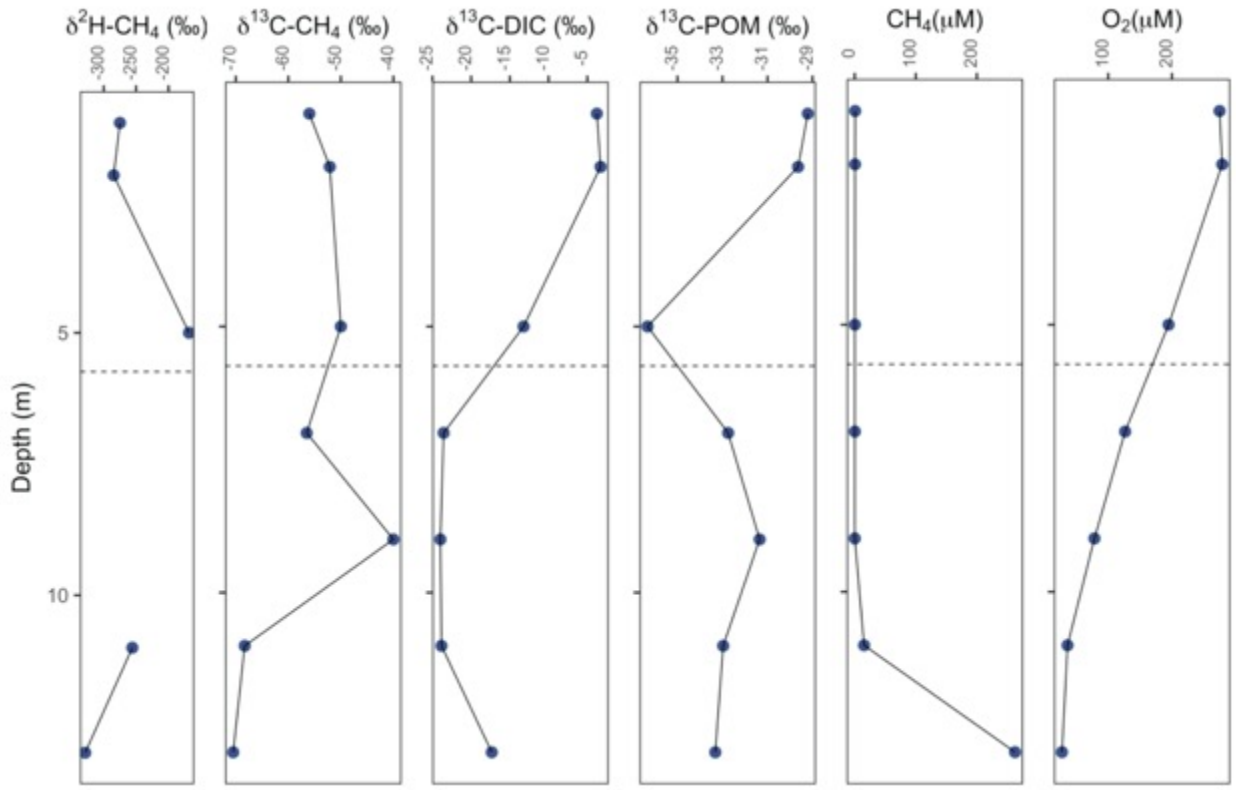

Figure A14. δ^2H-CH_4, δ^{13}C-CH_4, δ^{13}C-POM, CH_4 concentration, and O_2 concentration profiles for L658, midsummer 2018. Dashed line indicates thermocline depth. Missing values indicate that samples were below CH_4 concentration detection limit.